OPEN ACCESS

University of BRISTOL

This electronic thesis or dissertation has been downloaded from Explore Bristol Research, http://research-information.bristol.ac.uk

Author:
Thomas, Amy C

Title:
Carriage of Bacterial Pathogens in the Bovine Upper Respiratory Tract

Effects of Respiratory Virus Vaccination

General rights
Access to the thesis is subject to the Creative Commons Attribution - NonCommercial-No Derivatives 4.0 International Public License. A copy of this may be found at https://creativecommons.org/licenses/by-nc-nd/4.0/legalcode This license sets out your rights and the restrictions that apply to your access to the thesis so it is important you read this before proceeding.

Take down policy
Some pages of this thesis may have been removed for copyright restrictions prior to having it been deposited in Explore Bristol Research. However, if you have discovered material within the thesis that you consider to be unlawful e.g. breaches of copyright (either yours or that of a third party) or any other law, including but not limited to those relating to patent, trademark, confidentiality, data protection, obscenity, defamation, libel, then please contact collections-metadata@bristol.ac.uk and include the following information in your message:

• Your contact details
• Bibliographic details for the item, including a URL
• An outline nature of the complaint

Your claim will be investigated and, where appropriate, the item in question will be removed from public view as soon as possible.

Carriage of Bacterial Pathogens in the Bovine Upper Respiratory Tract: Effects of Respiratory Virus Vaccination

Submitted by
Amy Carolyn Thomas BSc (Hons)

A dissertation submitted to the University of Bristol in accordance with the requirements for award of the degree of Doctor of Philosophy in the Faculty of Health Sciences

Bristol Veterinary School
June 2019

Word count: 58,305

Abstract

Despite the major welfare and economic burdens of bovine respiratory disease worldwide, *Pasteurellaceae* carriage in cattle has been relatively unexplored. To address this, molecular techniques and epidemiological studies were employed to investigate upper respiratory tract carriage of three important respiratory pathobionts, *Histophilus somni*, *Mannheimia haemolytica* and *Pasteurella multocida*, in cattle in an experimental beef production setting.

Real-time PCR assays were optimised and validated to detect and quantify these three bacterial species. These assays were deployed to investigate pathobiont carriage in a longitudinal study of weaned cattle (n=90) during 2015-2016 winter housing. A separate cohort (n=30) was followed from birth in spring 2016 to just after weaning in November 2016. Carriage was shown to be highly dynamic; different organisms predominated as calves aged, and during housing, carriage patterns were distinct among pathobiont species. Interval-censored exponential survival models estimated the median duration of *H. somni* and *P. multocida* carriage at 14.8 ($CI_{95\%}$: 10.6–20.9) and 55.5 ($CI_{95\%}$: 43.3–71.3) days respectively; higher density *P. multocida* carriage was associated with slower clearance ($p = 0.036$).

A double-blind cluster randomised controlled trial was conducted in housed cattle (n=87) over winter 2016-2017 to investigate the effect of bovine respiratory syncytial virus and parainfluenza-3 virus on respiratory bacterial carriage. Viral infection used a bivalent intranasal live-attenuated vaccine following a stepped wedge design. Mixed effect models showed that the *M. haemolytica* carriage rate declined significantly following respiratory viral infection (odds ratio: 0.48; $CI_{95\%}$: 0.27–0.85). Carriage of *H. somni* and *P. multocida*, declined similarly although these trends were not statistically significant. There were no consistent effects of viral infection on pathobiont carriage density.

This research showed that improved molecular techniques can provide valuable novel insights into the carriage and biology of *Pasteurellaceae* and lays the foundation for further detailed investigations and modelling studies into the epidemiology of bovine respiratory disease.

Acknowledgements

I would like to say a huge thank you to my supervisors, Prof Mark Eisler, Prof Adam Finn, Prof Michael Bailey and Prof Michael Lee, throughout every moment of this work you have provided me with guidance, inspiration and encouragement. It has been such a pleasure to work with you all - thank you for making my PhD so enjoyable.

I am grateful for receiving financial support from the Biotechnology and Biological Sciences Research Council and Zoetis. I have been fortunate to work within a number of groups and thank you all for warmly welcoming me and ensuring I could complete my scheduled work: Bristol Children's Vaccine Centre, Zoetis Research and Development at Louvain la Neuve, and Grazing Livestock Systems at Rothamsted Research. Special thanks are given to Begonia Morales-Aza for continued support throughout laboratory investigations, to Dr Barry Vipond for help designing PCR assays, and to Andrew Mead and Dr Rosy Reynolds for invaluable statistical support. The animal work in this thesis could not have been possible without the wonderful team of farm staff and animal technicians at Rothamsted Research: Hannah Fleming, Simon White, Bruce Griffith, Melanie Mills, Richard Brook, John Hunt and Karen Saunders, thank you for supporting me so adeptly. I also extend my gratitude to the late Robert Orr who was instrumental in initiating this project. I am thankful to fellow students for our discussions over many cups of tea (and cake) and making this journey so enjoyable, special thanks go to Dr Emily Porter, Dr Ore Francis, Dr Thomas Chisnell and Serina Filler.

Finally, thank you to my friends and family for your forbearance during what has been a long four years, you never complained about me (well less than I complained about things not working) and have helped me develop into the person I am now. I suppose these acknowledgements would not be complete if I did not mention my cat, Kevin, who always managed to keep me entertained, provide companionship and gave me something different to talk about - much to everyone's delight.

Author’s Declaration

I declare that the work in this dissertation was carried out in accordance with the requirements of the University's *Regulations and Code of Practice for Research Degree Programmes* and that it has not been submitted for any other academic award. Except where indicated by specific reference in the text, the work is the candidate's own work. Work done in collaboration with, or with the assistance of, others, is indicated as such. Any views expressed in the dissertation are those of the author.

SIGNED: ..... DATE: .....

Table of Contents

Table of Tables

Table of Figures

Abbreviations

ADS	Acid Detergent Solution
AIC	Akaike Information Criterion
ANOVA	Analysis of Variance
APHA	Animal and Plant Health Agency
ATCC	American Type Culture Collection
BAL	Bronchoalveolar Lavage
BAV	Bovine Adenovirus
BBSRC	Biotechnology and Biological Sciences Research Council
bcb	Gene encoding *Pasteurella multocida* serogroup B capsule
BCV	Bovine Corona Virus
BHV-1	Bovine Herpesvirus-1
BLAST	Basic Local Alignment Search Tool
bp	Base Pair
BPIV-3	Bovine Parainfluenza Virus-3
BHI	Brain Heart Infusion
BRD	Bovine Respiratory Disease
BRSV	Bovine Respiratory Syncytial Virus
BVD	Bovine Viral Diarrhoea
BVDV	Bovine Viral Diarrhoea Virus
CA	California
CBA	Columbia Blood Agar
$CCID_{50}$	Cell Culture 50% Infective Dose
CCUG	Culture Collection University of Gothenburg
CD11a	Integrin α-light chain
CD18	Integrin β2 chain
CEESA	Executive Animal Health Study Centre
CFU	Colony Forming Unit
ChoP	Phosphorylcholine
CHX	Charolais Cross
$CI_{95\%}$	95% Confidence Interval
CO_2	Carbon Dioxide
CP	Crude Protein

C_q	Cycle Quantification
CRT	Cluster Randomised Trial
CTAB	Hexadecyl Trimethyl Ammonium Bromide
CV	Coefficient of Variation
DART	Depression, Appetite, Respiration and Temperature
dcbF	Gene encoding *Pasteurella multocida* serogroup D capsule
DNA	Deoxyribonucleic Acid
DOMD	Digestible Organic Dry Matter
dPCR	Digital Polymerase Chain Reaction
dsDNA	Double Stranded Deoxyribonucleic Acid
ecbJ	Gene encoding to *Pasteurella multocida* serogroup E capsule
ELISA	Enzyme-linked Immunosorbent Assay
FAM™	6-Carboxyfluorescein
FASTA	FAST-All
fcbD	Gene encoding to *Pasteurella multocida* serogroup F capsule
FRET	Fluorescence Resonance Energy Transfer
GAPDH	Glyceraldehyde 3-Phosphate Dehydrogenase
GAS	Group A *Streptococcus*
Hs	*Histophilus somni*
hyaD-hyaC	Gene encoding *Pasteurella multocida* serogroup A capsule
IBR	Infectious Bovine Rhinotracheitis
ICC	Intracluster Correlation Coefficient
ID	Calf Identification Number
IgA	Immunoglobulin A
IgG	Immunoglobulin G
IgG1	Immunoglobulin G1
IgG2	Immunoglobulin G2
IgM	Immunoglobulin M
IL-17	Interleukin 17
IL-8	Interleukin 8
kmt1	Gene encoding outer membrane protein for all *P. multocida* serogroups
LAIV	Live Attenuated Influenza Vaccine
LIMX	Limousin Cross

Lkt	Leukotoxin
lktC-artJ	Leukotoxin Acyl Transferase Gene
lktCABD	Leukotoxin Operon
LOD	Limit of Detection
LOS	Lipooligosachharide
Lpp1	Lipoprotein 1
LPS	Lipopolysaccharide
LRT	Likelihood Ratio Test
MADF	Modified Acid Detergent Fibre
MADS	Modified Acid Detergent Solution
ME	Metabolisable Energy
Mh	*Mannheimia haemolytica*
Mn-SOD	Manganese-dependent Superoxide Dismutase
MyD88	Myeloid Differentiation Primary Response 88
NA	Not Applicable
NCBI	National Center for Biotechnology Information
NCTC	National Collection of Type Cultures
NIO	Named Information Officer
NOAH	National Office of Animal Health
NWFP	North Wyke Farm Platform
OD	Optical Density
OmpA	Outer Membrane Protein A
OR	Odds Ratio
PAMP	Pathogen Associated Molecular Pattern
PCR	Polymerase Chain Reaction
Pm	*Pasteurella multocida*
pm0762	Putative transcriptional regulator gene of *Pasteurella multocida*
pm1231	Putative transcriptional regulator gene of *Pasteurella multocida*
PP	Primer and Probe
PRR	Pattern Recognition Receptor
qPCR	Real-time Polymerase Chain Reaction
r^2	Coefficient of Determination
RCT	Randomised Controlled Trial

rpoB	Gene encoding DNA-directed RNA polymerase
rRNA	Ribosomal Ribonucleic Acid
RSV	Respiratory Syncytial Virus
RTX	Repeats in Toxin
SIR	Susceptible-Infectious-Recovered
SIS	Susceptible-Infectious-Susceptible
sodA	Gene encoding manganese-dependent superoxide dismutase
SRUC	Scotland's Rural College
ST	Stabiliser
STGG	Skim milk, Tryptone, Glucose, Glycerol
SYBR®	Commerical Cyanine Dye
TAMRA™	Tetramethylrhodamine
TLR	Toll-like Receptor
toxA	Gene encoding the *Pasteurella multocida* dermonecrotic toxin
TRAF	Tumour Necrosis Factor Receptor-associated Factor
TRIF	Toll/interleukin-1 Receptor Domain-containing Adapter-inducing Interferon-β
UN	Undetermined
URT	Upper Respiratory Tract
UV	Ultraviolet
VIC™	2′-chloro-7′phenyl-1,4-dichloro-6-carboxy-fluorescein
VIDA	Veterinary Investigation Diagnosis Analysis
ΔRn	Adjusted Absorbance
16S rRNA	16S Ribosomal Ribonucleic Acid

Chapter 1 Introduction

1.1 Cattle production and its importance

Livestock are a key component of global agriculture, providing meat, milk, draught power, manure and acting as an important source of income, investment and insurance for rural and poor families [1]. In 2013, the worldwide cattle population was estimated at 1.5 billion animals. The Americas, closely followed by Asia and Africa have the largest populations, with Europe contributing 10.6% of the total [2]. Amongst these continents distinct and dynamic farming systems exist, such as, smallholder, pastoralist, extensive commercial and intensive commercial. As our global population continues to increase, farming dynamics become increasingly unstable. Intensive systems in northern, temperate climates often depend on permanent housing, high-stocking densities and mainly cereal-based diets; conditions exacerbating disease transmission, with associated costs to animal and public health, and environmental preservation [3].

1.2 Beef production and bovine respiratory disease

Bovine respiratory disease (BRD) is a global problem causing severe economic losses to the cattle farming industry and is a major welfare concern. It is the single most important disease syndrome affecting the beef industry; with high mortality and morbidity rates, particularly within 'feedlot' systems. Beef feedlots refer to the finishing (fattening) of vast numbers of cattle on grains and concentrates; commonly, feedlots are located in the grain producing regions of the United States and Canada [4]. In the 1970s feedlots had a one-time capacity of 1000 head or more, operations have since become more specialised and numbers have increased (>32,000 head capacity in 2002) [5]. Typically, beef feedlots are stocked with mainly steer calves purchased from either 'cow-calf' or dairy operations [4] [6]. Cow-calf operations rely on beef cows to raise calves at pasture until weaning, when they are sold [4]. Calves from multiple sources are transported to 'order-buyer' barns where they are auctioned and then transported to feedlots [7]. The travel to feedlots is often long, with reports of up to 3,500 km in Canada [6]. Travel is commonly by truck [6] [8] or even train [9]. On arrival to the feedlot animals from these multiple sources have comingled [10], and having had opportunities to exchange pathogens disease is commonly seen within days of arrival [11].

In the UK, beef production occurs on a smaller scale with the average herd size in 2015 at 88 [12]. Typically, beef production is seasonal and the majority of calvings occur between March to May [13]. Calves suckle with their dams during spring and summer, then at the start of winter are weaned and housed, the following spring they are turned out for grazing: farms commonly operate as closed herds. Dairy bull calves may also be raised for beef and in these circumstances mixing of bull calves from multiple farms can occur [14]. During winter housing either conserved forage, concentrates, or a combination of feeds are fed, but there is growing interest in raising animals from pasture-based diets as a step towards sustainable agriculture [15].

BRD is estimated to cost the UK cattle industry £80 million per annum [16]. However, this cost was estimated approximately 20 years ago and is barely reflective of costs incurred today, yet despite the impact of the disease a more recent analysis has not been carried out. Total costs can be assessed in terms of: prevention and treatment with vaccines and medicines; veterinary professional fees and medical costs; increased husbandry; mortality (replacement costs); decreased production efficiency and reduced live-weight gain [17].

The clinical syndromes defining BRD complex include beef cattle pneumonia and enzootic (calf) pneumonia. Pneumonic pasteurellosis and shipping fever (or undifferentiated shipping fever) are also terms used, and relate to the diseases' multifactorial aetiology, namely bacteria and viruses in combination with predisposing stress factors and management [18] [19]. Shipment or transport of cattle in North American feedlot operations often results in occurrence of respiratory disease shortly after transport. This has been termed shipping fever and can involve large numbers of animals, with disease usually occurring 7 to 10 days after transport [20]. The major cause of death is pneumonic pasteurellosis, an acute fibrinous pneumonia. In young calves suffering with BRD, commonly <6 months of age, suppurative bronchopneumonia is the most common pneumonia seen, largely associated with the bacterium *Pasteurella multocida* [18].

1.3 Aetiological agents and predisposition to disease occurrence

A number of viruses are associated with respiratory disease in calves and are ubiquitous in the cattle population: bovine respiratory syncytial virus (BRSV); bovine parainfluenza virus-3 (BPIV-3); bovine herpesvirus-1 (BHV-1); bovine viral diarrhoea virus (BVDV); bovine corona virus (BCV) and bovine adenovirus (BAV) [21]. Infection with viruses is usually transient and less frequent compared with carriage of the main commensal bacteria. Infection with respiratory viruses alone are generally not fatal, except some instances of BRSV. Rather, viral infection alters the respiratory environment to allow for colonisation and proliferation of opportunistic bacterial pathogens frequently implicated in BRD [19].

Several consequences of viral infection could affect bacterial carriage either through evasion of adaptive and modification of innate immune responses, or physiological disruption to respiratory mucosa. For example, BPIV-3 can inhibit the bactericidal function of alveolar macrophages and enhance secondary bacterial infections through impaired phagocytosis and antigen presentation [22]. Disruption to epithelium through viral infection can also compromise mucociliary responses, in turn favouring bacterial colonisation and migration to the lower respiratory tract [17] [19]. Under healthy respiratory conditions these bacterial organisms reside as common commensals of the nasopharynx [19] [20] but at what density they colonise has been rarely explored, therefore they could exist at lower densities in the healthy nasopharynx but higher in animals suffering respiratory virus infection. Members of the *Pasteurellaceae* most frequently implicated in BRD include: *Pasteurella multocida*, *Mannheimia haemolytica, Histophilus somni,* and *Bibersteinia trehalosi* [19] [23] [24]. *Mycoplasma bovis*, *Mycoplasma dispar*, *Arcanobacterium pyogenes*, *Ureaplasma* spp., *Fusobacterium* spp., and *Chlamydia* spp. have also been associated with BRD [19] [21].

1.4 Epidemiology of bovine respiratory disease

1.4.1 Risk factors

Reducing the risk of BRD may be achieved through good management practices that decrease stress. Various predisposing risk factors have been identified for BRD, including: transport, housing (ventilation, dust particles and humidity), diet change, increased stocking densities, surgical procedures, sex, breed and genetics [23].

Transportation is considered as one of the most important risk factors, where longer transport distances have been found to be associated with increased morbidity incidence [25], and it is likely stress may increase as transport time increases. Transportation has been shown to activate the hypothalamic-pituitary-adrenal axis, resulting in increased plasma glucocorticoid and altered immune function [26]. Taylor et al. confirmed the role of *M. haemolytica* in BRD associated with transportation by isolating increased densities of *M. haemolytica* in calves after shipment; in addition the nasopharyngeal presence of *M. haemolytica* was more common in calves suffering with BRD, implying that this bacterium has a role within the disease complex [27].

Mixing of cattle from multiple sources increases stress due to establishing social hierarchy and can provide exposure of naïve to infected individuals, subsequently initiating a disease outbreak. Youngstock may be more predisposed to stress from transport and weaning, and have less immunity to common pathogens compared to older cattle, hence their association with increased morbidity at feedlot entry [28]. As a result of the syndesmochorial character of the ruminant placenta prepartum transfer of immunoglobulins from cow to calf *in utero* is prevented [29]. Colostrum which is rich in IgG, particularly IgG1, is essential during the first 24 hours of life in order to acquire passive immunity [29]. Therefore, failure of passive transfer in bovine neonates can compromise a calves ability to mount adaptive immune responses, where inadequate levels of maternal IgG and other immunoglobulins can increase risk of respiratory infection [30]. Interestingly, a greater incidence of BRD has been reported in male calves than in female calves during both pre-weaning and feedlot periods [28]. Figure 1.1 illustrates the major stressors that young cattle may experience.

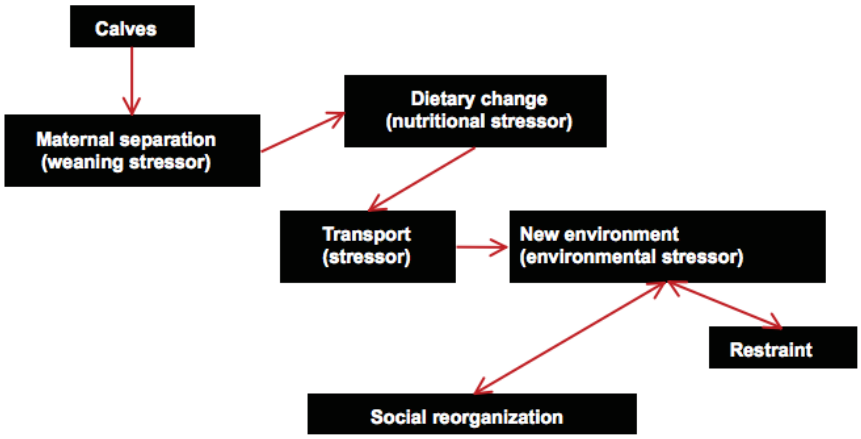

Figure 1.1: Schematic illustrating important stressors of feedlot cattle. Figure unedited from Aich et al. [31]

1.4.2 Seasonality of respiratory disease

BRD is usually seasonal with the highest deaths occurring in autumn and winter, particularly within feedlot systems [32]. Cyclical variation of *M. haemolytica* has also been observed in sheep; with the first peak occurring in late autumn, and the second in late spring to early summer, with this high carrier rate coinciding with enzootic pneumonia. Furthermore, disease attributable *B. trehalosi* in sheep generally occurs from August to November [33]. Submissions for necropsy examinations from 297 bovine carcasses with naturally occurring disease caused by *H. somni* between 1970–1990 in Saskatchewan, Canada demonstrated a strong seasonality: disease occurred frequently between late October to January [34]. However, this study, conducted some time ago only reflects a small number of the cattle population in Canada and gave no details on the farms where cattle came from.

1.5 Clinical signs

Clinical signs include increased respiratory rate and body temperature, the presence and character of nasal discharge (varies from serous to mucopurulent), coughing and/or increased respiratory sounds [21]. Lethargy, depression, ear/head tilt and reduced food intake may also be present [35]. Observations for signs of respiratory disease may be quantified to give a clinical score, for example using the Wisconsin scoring system for calf respiratory health (Figure 1.2) or the DART score (Depression, Appetite, Respiration and Temperature) developed for beef cattle in feedlots [36] [37] [19].

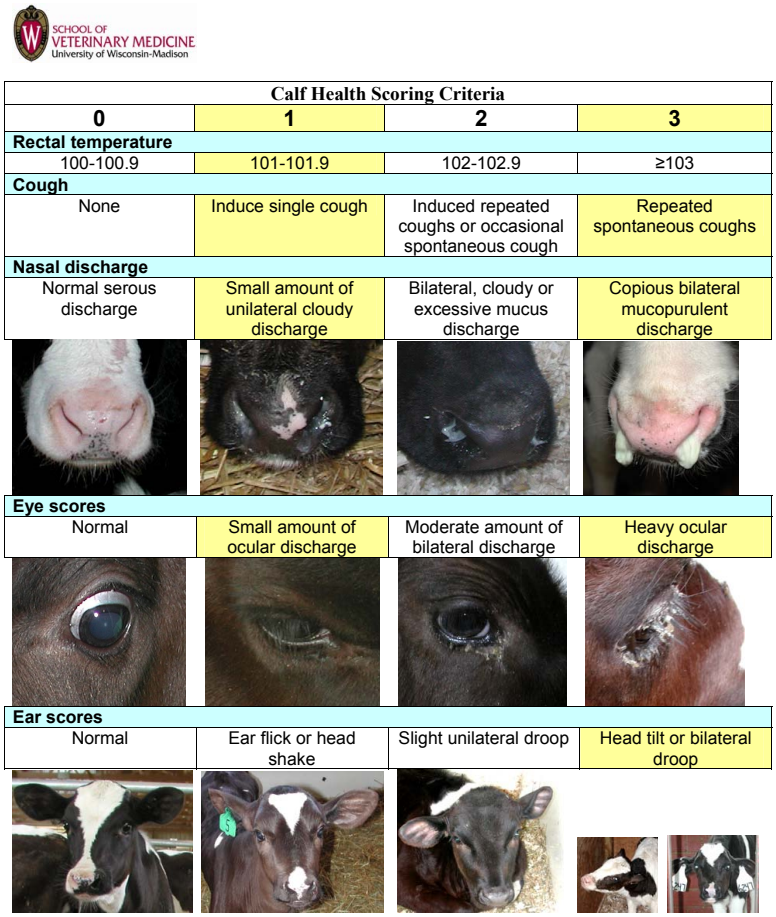

Figure 1.2: Scoring system for calf respiratory health designed by researchers at the University of Wisconsin at Madison. Figure unedited [36].

Often, there will be no clinical signs i.e. subclinical. In these instances, decreased average daily gain (poor growth) can be observed and may act as a clue to subclinical infection. One study reported South African feedlot calves treated for BRD had increased growth compared to those with subclinical BRD [38], suggesting that treatment was effective and that animals suffering with BRD may have decreased growth rates. This observation is strengthened by that of Griffin et al. who also reported the average daily gain of feedlot cattle which received treatment for BRD to be increased compared to those that did not receive treatment [39]. These observations are further supported by reports of decreased average daily gain associated with lung lesions at slaughter in cattle [40] [41].

1.6 Diagnosis

Clinical diagnosis can be made without any attempt to identify the aetiological agents involved [35] and instead, observations for signs of respiratory disease (e.g. those

introduced above) are used. However, often a combination of clinical signs and diagnostic laboratory testing is used. If animals have not received anthelminthic treatment, then lungworm may be involved, providing treatment is effective/no resistance. A faecal sample can be collected to confirm lungworm infection through detecting larvae using the Baermann technique [42], or exposure can be confirmed using serology, which is useful for herd diagnosis [43].

Bacterial and/or viral agents can be detected from samples collected from live animals: nasal or nasopharyngeal swabs, transtracheal wash or bronchoalveolar lavage (BAL). Bacterial culture or virus isolation from collected specimens can be used to detect viable bacteria and viruses respectively. Ideally, cultured bacterial species should be tested for susceptibility to antimicrobials to inform treatment practices [44]. If respiratory bacteria known to be involved in BRD are cultured it does not immediately imply they are of disease significance given carriage in healthy animals [45]. However, both of these culture-based techniques require skilled personnel, can take several days to weeks, and for virus isolation, may require specific cell lines not readily available [46]. Alternatively, bacterial or viral nucleic acid can be detected rapidly using PCR, often with increased specificity to culture. Multiplex PCR formats exist which allow simultaneous detection of multiple viruses and/or bacteria in the same assay, increasing throughput even further than conventional PCR [47] [48]. However, PCR does not give evidence for an active infection by detecting the presence of viable organisms, rather a recent footprint of colonisation/infection.

Serology can be performed on paired blood samples to detect evidence of rising titres to viruses, or less commonly, bacteria using either virus neutralisation tests or enzyme-linked immunosorbent assay (ELISA) [46]. The disadvantage to this approach is that two samples are collected, usually 2–3 weeks apart, increasing the time to result. In addition, an increase in antibody titre (seroconversion) does not necessarily indicate clinical disease when viral infections are suspected to be common [45], nor does seroconversion discriminate between vaccinal or natural exposure [46]. Furthermore, maternal antibody may be involved in animals under 6 months [49]. Serological results can be relevant to the herd if multiple animals are tested and are useful for informing future herd health plans.

Diagnosis can also be made at post-mortem following gross and histopathologic examination. In addition, samples can be collected from affected tissues for laboratory diagnosis [45]. In conclusion, a combination of clinical, pathologic and microbiologic approaches can be used to diagnose cases of BRD.

1.7 Control of bovine respiratory disease

Control of BRD is through improving environmental and management conditions, and prevention of viral and secondary bacterial infections through vaccination and/or treatment with antimicrobial therapy [50] [51]. Metaphylactic administration of antimicrobials is often advocated for calves which may not have had time to mount an effective immune response to respiratory virus vaccination, or otherwise deemed to be at 'high risk'. However, this kind of mass medication of animals before development of signs of disease may promote selective antimicrobial resistance, and if live bacterial vaccines are being used, can compromise their efficacy [51] through inhibiting bacterial replication of vaccine organisms [52]. Resistance to antimicrobial drugs once used effectively in BRD treatment such as ampicillin, amoxicillin and oxytetracycline is now common. Newer compounds are available, such as long-acting macrolides (e.g. tulathromycin) and fluoroquinolones (e.g. danofloxacin), but a decline in BRD isolates susceptible even to these newer antimicrobials has been reported: antimicrobial stewardship is essential to preserve drug effectiveness for the future [53].

1.8 Vaccination of cattle in the UK

In the UK, more than 40 vaccines are authorised for use in cattle [54]. Legally, farmers are required to record vaccine administration in a Medicines Book, available for inspection upon request [55]. Currently, there is no national recording system for data on vaccination use in animals. Therefore, sales data represent the best available approximation for vaccine coverage of cattle in the UK [56].

The National Office of Animal Health (NOAH) and Executive Animal Health Study Centre (CEESA) conduct an independent sales survey to assess UK sales of authorised veterinary medicines. Many UK NOAH member companies participate, and a smaller number of companies independently provide sales data; together, data are estimated to represent around 95% of the total UK animal medicine market [57]. In 2017,

NOAH/CEESA sales survey data estimated 39% of medicine sales were for food producing animals, 58% for companion animals, and 3% for others and multi-species. Vaccines and antimicrobials accounted for 24.6% and 10.6% of the overall UK animal medicine market respectively [57]. Compared to the 2015/2016 annual review, vaccine use is increasing (2015/2016: 22%) and antimicrobial use decreasing (2015/2016: 16%). In addition, the relative proportion of sales to food producing animals is decreasing (2015/2016: 42%), while sales to companion animals are increasing (2015/2016: 55%) [56].

1.9 Vaccines for respiratory disease in cattle

Between 2011 and 2017, twelve vaccines for the control of respiratory disease in cattle were marketed in the UK (Table 1.1) [54]. In 2011, a questionnaire aimed to estimate usage and uptake of cattle vaccines by UK farmers [58]. From 266 respondents, motivations to vaccinate were grouped following responses to open questions. These motivations were due to losses (49%), on the basis of veterinary advice (26%), disease control (15%) and testing/monitoring (12%). Unfortunately, no further specific details to motivations were given. Sixty-five percent of farmers did not vaccinate because they did not perceive there to be a problem. To assess the uptake of vaccines used by respondents they were broadly categorised by disease. For respiratory disease, vaccine use was greater in beef (~35%) than in dairy (~18%) cattle. Rispoval 4 (BPIV-3, BRSV, BVDV, BHV-1) was the most widely used respiratory vaccine in both sectors. Rispoval 3, Rispoval RS, Bovipast RSP and Imuresp RP were only used in beef cattle. Interestingly, for 6 of the 8 disease categories surveyed, the beef sector used a greater number of different vaccines compared to dairy. It is not clear whether increased variety of vaccines represents increased diversity of respiratory agents in beef systems, differences in advice given to sectors, or farm experiences. A limitation to this survey is that it captures only a small proportion of farmers and relies on recall of information, moreover the categorisation of data resulted in loss of study detail, but it did capture motivation for vaccination, and attempted to compare coverage between beef and dairy.

Table 1.1: Vaccines licensed for use in cattle in the UK for respiratory disease.

Target Pathogen(s)	Company	Product Name	Formulation	Dosage and administration
Mannheimia haemolytica type A1	Boehringer Ingelheim Animal Health UK Ltd	Bovalto Pastobov	Inactivated, aluminium adjuvant	Two injections, 3–4 weeks apart, calves over 12 weeks of age. Re-vaccination recommended before each risk period, no later than 1 year after previous vaccination.
Mannheimia haemolytica type A1, BRSV, BPIV-3	Boehringer Ingelheim Animal Health UK Ltd	Bovalto Respi 3	Inactivated: Aluminium hydroxide and Quillaja saponin adjuvants	Two injections, 3 weeks apart. Re-vaccination recommended 6 months post primary vaccination.
Mannheimia haemolytica type A1, BRSV, BPIV-3, BVDV	Boehringer Ingelheim Animal Health UK Ltd	Bovalto Respi 4	Inactivated: Aluminium hydroxide and Quillaja saponin adjuvants	Two injections, 3 weeks apart. Re-vaccination recommended 6 months post primary vaccination.
BRSV, BPIV-3	Boehringer Ingelheim Animal Health UK Ltd	Bovalto Respi Intranasal	Live - attenuated	One dose, intranasally, calves from 10 days of age. Re-vaccination recommended 10 days before each risk period. Duration of immunity 12 weeks.
Mannheimia haemolytica type A1, BRSV, BPIV-3	MSD Animal Health	Bovilis Bovipast RSP	Inactivated: Aluminium hydroxide and Quillaja saponin adjuvants	Two injections, ~4 weeks apart, calves from 2 weeks of age. Re-vaccination recommended 2 weeks before each risk period with a single dose.
Mannheimia haemolytica type A1, *Histophilus somni*	Hipra UK & Ireland Ltd	Hiprabovis SOMNI/Lkt	Inactivated: Liquid paraffin adjuvant	Two injections, 3 weeks apart, calves from 2 months of age. Vaccination recommended 3 weeks prior to risk period.
BPIV-3, IBR	Zoetis UK Ltd	Imuresp RP	Live - attenuated	Single dose, intranasally, calves from 10 weeks of age. Re-vaccination recommended every 6 months.
BRSV, BPIV-3	Zoetis UK Ltd	Rispoval® 3	Live - attenuated, alhydrogel adjuvant	Two injections, 3–4 weeks apart, calves over 12 weeks of age. Re-vaccination recommended every 6 months.

Table 1.1 continued

Target Pathogen(s)	Company	Product Name	Preparation	Course
BRSV, BPIV-3	Zoetis UK Ltd	Rispoval® 4	Attenuated	Two injections, 3–4 weeks apart, calves over 12 weeks of age. Re-vaccination recommended 2 weeks before each risk period. Calves can be vaccinated from 3 weeks of age but re-vaccination at 12 weeks is recommended.
BHV-1, BVDV (cytopathic and non-cytopathic type 1)			Inactivated: Aluminium hydroxide adjuvant	
Mannheimia haemolytica A1	Zoetis UK Ltd	Rispoval® Pasteurella	Inactivated: Aluminium hydroxide and liquid paraffin adjuvants	Single injection, calves over 12 weeks of age. Re-vaccination necessary 7 days prior to next risk period, if risk is 17 weeks after previous dose.
BRSV	Zoetis UK Ltd	Rispoval® RS	Live - attenuated	Two injections, 3–4 weeks apart, calves over 16 weeks of age. For calves from 7 days to 15 weeks: 2 doses, 3–4 weeks apart, a third dose at 16 weeks.
BRSV, BPIV-3	Zoetis UK Ltd	Rispoval® RS + PI3 Intranasal	Live - attenuated	One dose, intranasally, calves from 9 days of age. Duration of immunity 12 weeks.

Data compiled from the AHDB report 'Use of vaccines and vaccination in dairy and beef cattle production 2011–2017'

This list is non-exhaustive, and there are further vaccines for BVD and BHV-1 (both inactivated and live-attenuated) given in the report online [54].

1.10 Surveillance of bovine respiratory disease in UK cattle

The cattle dashboard is an online tool maintained by the Animal & Plant Health Agency (APHA) for sharing surveillance data collected from submissions to the GB veterinary diagnostic network: Veterinary Investigation Centres (England & Wales), SRUC (Scotland's Rural College, Scotland), APHA's network of universities and other partners providing post mortem services [59]. Similarly, the Veterinary Investigation Diagnosis Analysis database (VIDA) shares surveillance data recorded from diagnostic submissions from livestock and wildlife to the Great Britain veterinary diagnostic network and has been operating since 1975 [60]. There are limitations to these data, mainly concerning selection bias: higher counts could be due to increased submissions, maybe as a consequence of increased vigilance of farmers and vets; some diseases may not require laboratory testing, or veterinary practices may have private facilities; or submissions to aid in the epidemiology of certain diseases may be encouraged e.g. Schmallenberg. Further recognised bias includes submissions recorded that represent only the clinical material submitted to centres with no denominator data available. Clinical samples are of different types (blood, faeces, tissue) and carcasses (post-mortem examination). Samples submitted do not capture all cases of disease and factors affecting submission may vary over time due to the *ad hoc* submission of material for investigation. Nevertheless, the cattle dashboard and VIDA provides an approximate overview of diseases affecting livestock or wildlife in the UK.

The number of cases of pneumonia in cattle and agents relating to the BRD complex were extracted from the cattle dashboard. The count of diagnoses made for each sector category (beef, dairy, calf rearing, other/unknown) for all ages between 2012–2017 were considered. The number of diagnoses for pneumonia by sector showed beef, in general, to contribute a greater number of diagnoses for each condition (9/14) compared to dairy, calf rearing and other/unknown sectors (Figure 1.3). BVD (bovine viral diarrhoea), persistent infection with BVD, infectious bovine rhinotracheitis (IBR), parasitic pneumonia and *T. pyogenes* diagnoses were more prevalent in dairy cattle. Of the various bacterial agents identified, *M. haemolytica* was the one most frequently detected in beef, dairy, and calf rearing sectors (Figure 1.3). For respiratory viruses, BHV-1 (IBR) was most frequently detected, followed by BRSV and BPIV-3. Interstitial pneumonia, BVD (post-natal infection) and fog fever were rarely diagnosed.

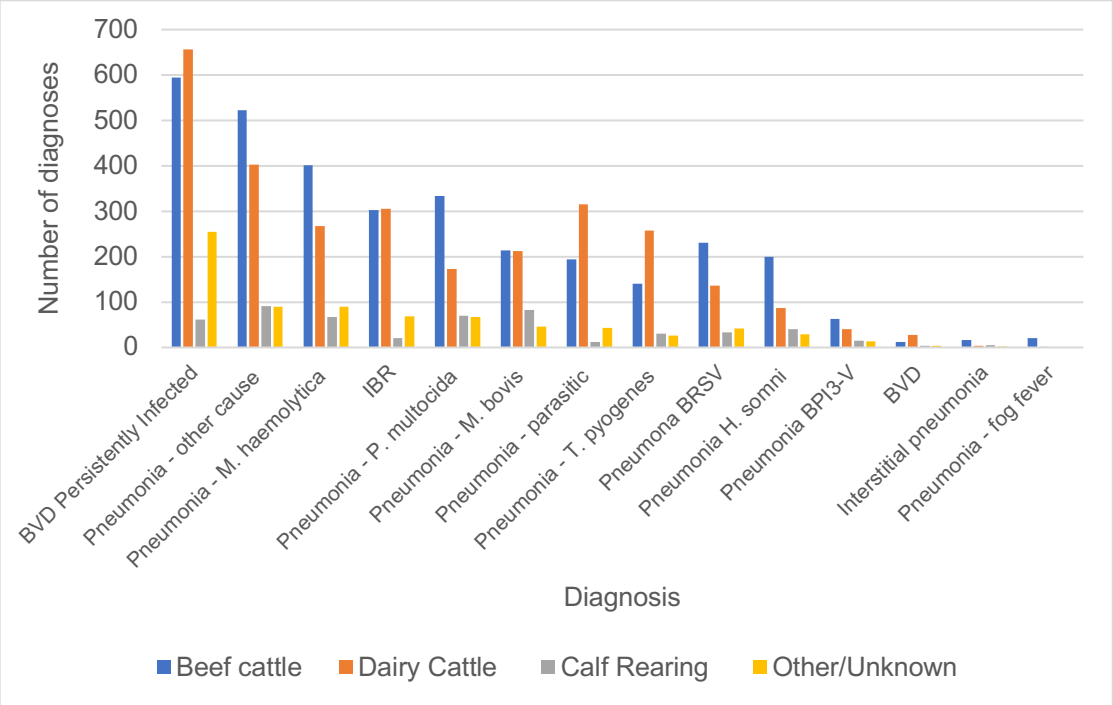

Figure 1.3: Number of diagnoses for pneumonia and agent's related to the bovine respiratory disease complex by cattle production system between 2012–2017. Cattle dashboard data.

Trends in the UK beef sector as reported in the cattle dashboard between 2012–2017 show that diagnoses due to pneumonia have been slowly decreasing or remaining constant. *M. haemoytica,* BHV-1 and *P. multocida* were the most commonly detected organisms during this period (Figure 1.4). Interestingly, persistently infected BVD cases have sharply declined across this period (80% decrease). This decline could be due to uptake of vaccination and/or BVD eradication programs which aim to identify and remove all BVD persistently infected cattle in England, North Ireland, Scotland and Wales [61]. For example, in May 2017, 7 years since the introduction of the scheme into Scotland, herds testing 'not negative' (i.e. where an animal has tested positive for BVD virus) decreased from 40% to 10% [62]. In addition to the general decline in pneumonia diagnoses, the number of submissions from the beef and dairy sectors between 2012–2016 has been decreasing and this could be reflected in the apparent decrease in pneumonia diagnoses. Declines in submissions could occur due to economic pressures on farmers, veterinarians utilising alternatives to veterinary investigation centres, or changes to the surveillance structure [63]. Therefore, the apparent downward trend in pneumonia is confounded by submissions and the lack of denominator data.

Consequently, efficiently evaluating the true impact of respiratory disease on the UK cattle sectors using the VIDA and cattle dashboard is troublesome.

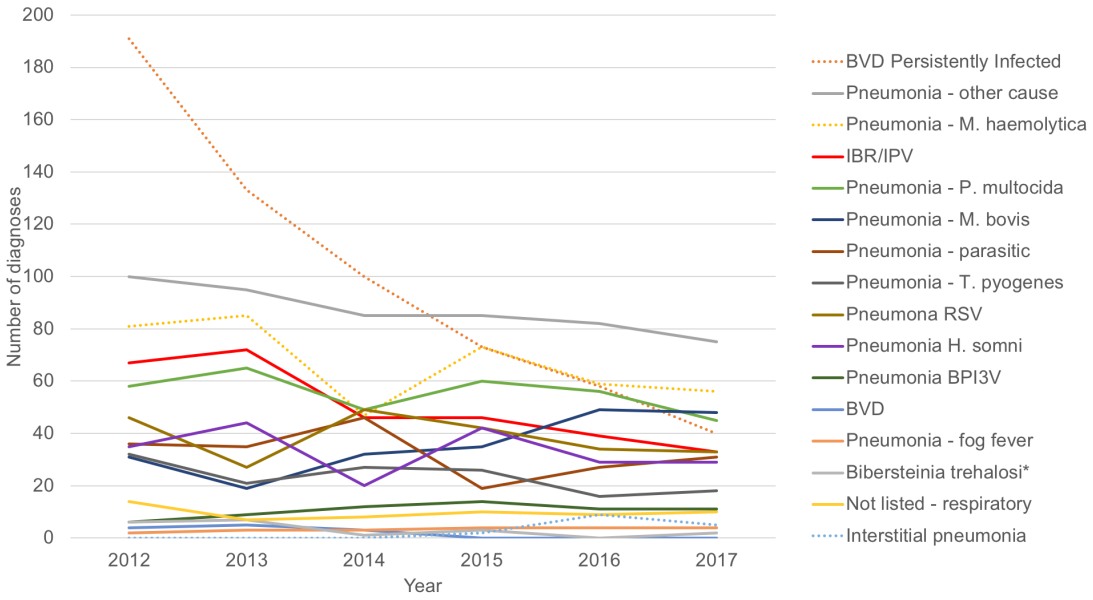

Figure 1.4: Diagnosis of pneumonia and agents relating to pneumonia of beef cattle between 2012 to 2017. Cattle dashboard data. *Isolation of *Bibersteinia trehalosi* in association with respiratory disease.

1.11 *Pasteurellaceae*

Bacterial pneumonia in cattle is commonly attributed to members of the *Pasteurellaceae* family. The genus *Pasteurella* was named after Louis Pasteur, who was one of the early investigators involved in identifying the bacterium as the causative agent of fowl cholera [64]. It was Toussaint in 1879 that first isolated *P. multocida* [65] but Pasteur attenuated the bacterium (at first by accident) and thereby claimed the first production of an attenuated vaccine [66] (Jenner's having been obtained from a milk maid's hand).

Pasteurellaceae have been classified and described based on common phenotypic criteria and biochemical features, supported by genetic studies such as extended deoxyribonucleic acid (DNA) DNA-DNA, or DNA – ribosomal ribonucleic acid (rRNA) hybridisation studies [65]. With respect to phenotype, members of the family may be defined as small facultatively anaerobic or microaerophilic, Gram-negative rods or coccobacilli, usually 0.2–0.4 x 0.4–2.0 µm in size [67]. *Pasteurellaceae* grow between 30°C and 40°C [65], optimally at 37°C [68] and are opportunistic pathogens of

vertebrates, primarily birds and mammals, but also reptiles. They normally inhabit the mucous membranes of the alimentary, genital and respiratory tracts [67].

Since the first isolation of *P. multocida* the family has undergone extensive reorganisation and classification. More recently, novel molecular techniques have been used to revise the taxonomy of these closely related organisms and to resolve misidentification based on phenotypic characterisation [68] [69]. Using 16S rRNA gene sequence comparisons, *Pasteurellaceae* is the only family of the order Pasteurellales, included within the class Gammaproteobacteria of the phylum Proteobacteria [67]. Examples of changes to nomenclature include renaming *Haemophilus somnus* and the ovine isolates *Histophilus ovis* and *Histophilus agnis* to *Histophilus somni* (*H. somni* is the only species of the genus *Histophilus*) [70]. There is a long history of reorganisation and naming within the *Mannheimia* genus, where *M. haemolytica* was first named *Bacterium bipolare multocidum* (1885) and later renamed *Pasteurella haemolytica* (for its weak haemolytic activity on sheep blood agar, 1932) and classified into 16 serotypes [51]. The species was then divided into biotypes based on the ability to ferment arabinose (biotype A) or trehalose (biotype T) [71]. However, following DNA-DNA hybridization studies and 16S rRNA sequencing T biotypes were renamed *Pasteurella trehalosi*, and then *Bibersteinia trehalosi*. A new genus, *Mannheimia* was proposed for the trehalose negative (biotype A) *P. haemolytica* complex, this involved renaming two species and describing three new species, resulting in at least five species that we know today: *P. haemolytica* was reclassified as *M. haemolytica*; *P. granulomatis*, Bisgaard taxon 20 and *P. haemolytica* biovar 3J were combined and reclassified to *M. granulomatis*; *P. haemolytica* biogroups 3A-3H and the beta-glucosidase and meso-inositol-positive strains of *P. haemolytica* biogroup 9 were combined and reclassified as *M. glucocida*; Bisgaard taxon 18 and *P. haemolytica* biogroup 8D strains were combined and reclassified as *M. ruminalis* and finally, *P. haemolytica* biogroup 6, Bisgaard taxon 15 and Bisgaard taxon 36 were combined and reclassified as *M. varigena* [72].

P. multocida has undergone similarly lengthy changes: first, organisms with similar phenotypic characteristics to that of the agent causing fowl cholera were grouped and originally named as *P. septica*, prior to naming as *P. multocida*. The *Pasteurella* genus was then reclassified into 11 species, with four subspecies of *P. multocida*: *multocida*, *septica, gallicida* (based on sugar fermentation) [73] and more recently *tigris* (based on

16S rRNA sequencing) following isolation from a wound infection from a tiger bite [74]. *P. multocida* strains are classified into 5 serotypes (A, B, D, E and F) based on capsule antigens and further classified into 16 Heddleston serovars based on lipopolysaccharide antigens [75] [76]. Of note, *P. multocida* serotypes were previously referred to as serogroups, similarly serovars were referred to as serotypes. The serotypes B:2 and E:2 are most commonly responsible for epidemics of haemorrhagic septicaemia in cattle and buffalo in Asia (B:2) and Africa (E:2) [64] [77]. Elucidation of the *Pasteurellaceae* family continues and genome sequencing can now assist in phylogenetic rearrangement [78].

1.12 Bacterial colonisation and carriage

Bacterial colonisation refers to 'establishment and proliferation' of bacteria at specific sites in the host [9] and differs to 'infection' by not causing disease [79]. The Oxford dictionary defines carriage as 'the harbouring of a potentially disease-causing organism by a person or animal that does not contract the disease' [80]. Thus, carriage describes the occurrence of a given organism. Carriage is frequently reported as a rate to describe the proportion of individuals within a population, at a given point, who are harbouring the organism of interest (point-prevalence carriage rate) [81] [82] [83]. However, 'carrier' and 'colonised' are often used interchangeably to denote that an organism has been detected from an asymptomatic individual. Carriage can imply a temporal association with carrier status through categorisation into 'carrier types' such as, 'persistent' or 'intermittent', which imply either uninterrupted/continuous or interrupted/non-continuous carriage respectively [84].

1.13 Factors that influence *Pasteurellaceae* colonisation

Bacteria may reside within the mucus layer but are subjected to mucociliary clearance and removal through local innate and adaptive immune responses [85]. Adhesive interactions between respiratory bacteria and epithelial cell surfaces can help prevent clearance and enable colonisation via specific or non-specific adhesins, but adhesion can also initiate invasion [86]. Using PCR, several genes encoding for adhesins have been identified for *P. multocida* isolated from the lungs of pneumonic cattle, these include type IV fimbriae (*ptfA*), fimbriae (*fimA*), haemagglutinin (*pfhA*), autotransporter proteins (*hsf-1, hsf-2*) and a putative non-specific tight adherence protein (*tadD*) [87]. *In vitro*,

adherence of *M. haemolytica* to bovine bronchial epithelial cells has been demonstrated to occur through outer membrane protein A (OmpA) and lipoprotein 1 (Lpp1) [88]. In competition assays, binding of *H. somni* to bovine pulmonary artery [89] and brain [90] endothelial cells has been demonstrated to occur through heparin binding proteins. Bacterial flora may also protect the host from colonisation, either through competition for receptor binding sites or nutrients, therefore from an ecological perspective the hosts' niche could be unfavourable for colonisation [91].

1.14 *Pasteurellaceae* virulence factors

Pulmonary damage caused by bacteria results from invasion and production of virulence factors, facilitating colonisation of the lower respiratory tract [92]. A signature of acute pulmonary infection in cattle is fibrinosuppurative and necrotizing inflammatory responses [51]. Various virulence factors have been shown to enhance the ability of *M. haemolytica*, *P. multocida* and *H. somni* to colonise tissues and cause disease. For example: capsule, adhesin, fimbriae, ruminant-specific leukotoxin (Lkt) of *M. haemolytica*, lipopolysaccharide (LPS), outer membrane proteins and colonisation factors [51] [93] [18].

1.15 Bovine respiratory disease associated with *H. somni*

Respiratory disease due to *H. somni* is seen in young calves but commonly feedlot cattle [93] [94]. This bacterium causes histophilosis which manifests as several clinical syndromes: bronchopneumonia, thrombotic meningoencephalitis, pleuritis, polysynovitis, septicaemia, myocarditis, infertility, abortion and mastitis [94] [95]. However, in the 1950s the pathogenic potential of *H. somni* was not first recognised for involvement with respiratory disease, but for causing thrombotic meningoencephalitis in US feedlot cattle [96] originally described as a haemophilus-like organism [97]. This disease was initially called sleeper syndrome [98] due to the appearance of affected cattle: partially closed eyes and severe depression, resulting from *H. somni* binding to endothelial cells, invading to cause septicaemia, followed by vasculitis and thrombosis in the brain [34] [99].

H. somni commonly exists as a commensal at reproductive and respiratory mucosa [93]. However, this bacterium has several potential virulence factors: immunoglobulin-

binding proteins on the cell surface; the ability to survive phagocytosis by bovine alveolar macrophages; lipopolysaccharide with endotoxic activity; and the ability to undergo phase and antigenic variation [100]. This ability to undergo phase and antigenic variation suggests that there are immunological pressures resulting from the host's attempts to control colonisation. *H. somni* can incorporate phosphorylcholine (ChoP) into the lipooligosachharide (LOS) molecule, however ChoP was not found to augment adherence of *H. somni* to bovine nasal turbinate cells but may play a role in pathogenesis through binding to the platelet activating factor receptor on epithelial cells [101] [102]. Naturally occurring respiratory disease due to *H. somni* is characterised by consolidation of the cranioventral lung. Histologically, there is bronchopneumonia with fibrinocellular thrombosis of septal lymphatics, neutrophilic, necrotising bronchiolitis and multifocal haemorrhage [103]. In calves suffering chronic respiratory disease after deliberate infection with *H. somni* coughing was rarely observed and severe clinical signs were only observed for a few days when calves experienced chronic infection [104], leading Corbeil et al. to suggest that chronic *H. somni* infection can be subclinical for weeks [93]. As with human respiratory disease, nasal colonisation is recognised as an important first step for invasion [86] [105]. Given the mobility of this pathobiont to cause a spectrum of diseases understanding asymptomatic carriage in the nasal passages of cattle is of interest.

1.16 Bovine respiratory disease associated with *M. haemolytica*

M. haemolytica is frequently associated with shipping fever, i.e. following transport (shipping) of calves, namely from several sources to feedlot operations and has commonly been isolated from severe fibrinous pneumonia cases [106] [51]. Several virulence factors have been described, these include: adhesin protein, fimbriae, outer membrane proteins and lipopolysaccharide [51]. A major virulence factor of *M. haemolytica* is the ruminant-specific Lkt. Lkt is an exotoxin and member of the repeats in toxin (RTX) family. Lkt shares homology with exotoxins produced by other Gram-negative bacteria, for example *Escherichia coli* and *Actinobacillus pleuropneumoniae*: however, there are differences among the family with respect to the toxin's target cell type [107]. All serotypes of *M. haemolytica* secrete Lkt during logarithmic growth *in vitro*, with different serotypes shown to produce different Lkt types [108]. Lkt can passively adsorb onto the surface of bovine leukocytes or bind through

surface receptors, namely β_2-integrins (amino acids 5–17 of CD18) [109]. Lkt acts on bovine leukocytes in a dose dependent manner: at low concentrations it activates neutrophils and macrophages, stimulating respiratory burst and degranulation [110]; at higher concentrations target cells are triggered to undergo apoptosis [111] [112] and necrosis occurs as a result of pore-like structures forming in the plasma membrane of target cells [113]. In the lower respiratory tract, Lkt is responsible for major lung injury and as β_2-integrins are present on leukocytes, damage to these cells from Lkt could allow the bacterium to evade phagocytosis [85]. In one study, six 10-month-old beef calves were infected with BHV-1 by intranasal inoculation. Blood and BAL was collected from both infected and control (n = 4) calves. Expression of the β_2-integrin CD11a/CD18 was comparable between groups on BAL but slightly increased on mononuclear cells in BHV-1 infected calves 3, 5, and 7 days post infection, and significantly increased on granulocytes 5 and 7-days post infection. In addition, increased binding of Lkt to BAL cells of BHV-1 infected calves was observed, as well as increased cytotoxicity [114]. Therefore, respiratory viral infection may increase susceptibility of cattle to pasteurellosis.

1.17 Bovine respiratory disease associated with *P. multocida*

Pulmonary lesions attributable to infection with *P. multocida* have been characterised as bronchopneumonia. Typically, bronchi and bronchioles are filled with neutrophils, macrophages and necrotic epithelium [18] [115]. *P. multocida* is organised into 5 capsular serotypes: A, B, D, E and F. Serotype A is mainly associated with respiratory disease in cattle [116], mostly A:3 and A:1 [18] [76] [117]. Serotypes B and E cause haemorrhagic septicaemia in cattle [64] [77]. Serotype D causes atrophic rhinitis in pigs but has been isolated from pneumonic sheep and cattle lungs [18]. Serotype F strains are predominately associated with diseased poultry [118] but have been isolated from fatal cases of fibrinous peritonitis in calves [18]. The polysaccharide capsule is an important virulence factor, for example through antiphagocytic activity [119] and molecular mimicry - some strains express hyaluronic acid which is often found naturally in the host and therefore prevents strong antibody responses [76]. Loss of virulence has been reported for an acapsular mutant strain in mice and chickens [120]. Interestingly, vaccination against fowl cholera with acapsular *P. multocida* serotype A:1 was found to stimulate immunity against wild-type challenge [121]. LPS is also a major virulence

factor of *P. multocida* - it is highly antigenic but poorly immunogenic unless complexed with proteins [18]. The lipid A component of LPS is responsible for inducing endotoxic shock [122], and it has also been demonstrated *in vitro* to have a role in neutrophil adhesion and migration through bovine aortic endothelial cell monolayers [123]. Despite its similarity to LPS of other Gram-negative bacteria (*Haemophilus influenzae*, *Campylobacter jejuni* and *Neisseria* spp.) there is no evidence to suggest that LPS genes found in the *P. multocida* genome are capable of phase-variation [124].

1.18 Immune responses against bovine respiratory bacteria

Microorganisms produce conserved molecular patterns: pathogen associated molecular patterns (PAMPs), for example LPS from Gram-negative *Pasteurellaceae*. These PAMPs are recognised by epithelia, alveolar macrophages and pulmonary intravascular macrophages, and in acute inflammation neutrophils recognise PAMPs. Recognition of PAMPs occurs via Pattern Recognition Receptors (PRR), of which Toll-like receptors (TLR) are transmembrane PRR on respiratory epithelia. LPS from *H. somni*, *M. haemolytica* and *P. multocida* binds to TLR4 which can signal through MyD88 or TRIF/TRAF leading to inflammatory reactions [30].

Neutrophil influx to the lung is common in calves suffering with pasteurellosis [125] [85]. *M. haemolytica* has been reported to upregulate production of the chemokine IL-8 by alveolar macrophages, in turn increasing the migration of neutrophils to sites of infection [125] [126]. In cattle, γδ T-cells represent between 15–20% of the circulating lymphocytes, a comparatively higher number than in mice and humans [127]. The pro-inflammatory cytokine IL-17 is primarily produced by activated γδ T-cells and CD4+ T-cells. Expression of IL-17 stimulates stromal and epithelial cells to produce chemokines, one of which is IL-8, resulting in neutrophil recruitment. In an *in vitro* co-infection model, expression of IL-17 was induced by BRSV and significantly increased with co-infection of *M. haemolytica*; production of IL-17 was primarily mediated by γδ T-cells [128].

Colostrum from dairy cows previously exposed to *M. haemolytica* and *P. multocida* contains antibodies to both bacterial species, these bacteria-specific antibodies are then transferred to the calf during suckling [129]. In neonatal beef calves, passively acquired anti-*P. multocida* and anti-*M. haemolytica* antibodies have been detected by ELISA: by

60–90 days of age passively acquired IgG1 antibodies have waned, with autogenous production of anti-bacterial IgG1 and IgG2 starting between 90-120 days of age [106]. Specific antibodies may facilitate phagocytosis of bacteria through the process of opsonisation, whereby phagocyte cell receptors bind to the antibodies' Fc-region. Antibodies (IgG and IgM) can trigger the complement system and opsonise bacteria, leading to enhanced phagocytic action of macrophages and neutrophils [130]. In the bovine respiratory tract IgG1 and to a lesser extent IgG2 are major secretory immunoglobins [131]. Bovine alveolar macrophages have a greater affinity for IgG1 compared to IgG2, with IgA potentially having a secondary role in opsonisation [132]. IgG2 has been shown to be protective against *H. somni* [93]. Exposure to live *M. haemolytica* through deliberate infection results in production of antibodies to antigens on the surface of the bacterium and leukotoxin-specific neutralizing antibodies [133]; anti-leukotoxin antibodies can prevent impairment of phagocyte function [130]. Interestingly, *in vitro M. haemolytica* has demonstrated the ability to secrete proteases which have activity against IgG1 but the presence of IgG2 specific proteases could not be confirmed [131]. This observation has not been confirmed *in vivo* but genome sequence analysis of *M. haemolytica* A1 has identified two autotransporters (MHA_0563 and MHA_2800) which are orthologs to *H. influenzae* and *N. meningitidis* IgA, an IgA peptidase/adhesin. These autotransporters may cleave secreted IgG in the bovine respiratory tract and play a role in adhesion to host receptors on epithelial cells [134].

1.19 Colonisation locations

Despite several authors attempting to characterise and compare colonisation between the upper and lower respiratory tract, exact colonisation locations of pathogens involved in BRD have not been described in detail. These efforts have been directed at ascertaining whether sampling the URT through nasopharyngeal swabs is indicative of the organisms eliciting disease in the lung and hence of diagnostic value, rather than increasing understanding of the biology of carriage. In one study, DeRosa et al. investigated the distribution of *P. multocida, M. haemolytica* and *H. somni* in the respiratory tracts of calves showing clinical signs of respiratory disease after shipment. Bacterial pathogens recovered from both nasal and transtracheal swabs were the same 68.4% of the time, with nasal swab culture giving ribotype profiles genetically identical to the organisms causing disease in the lung for 70% of the calves [135]. Other studies showed lower levels of

concordance, demonstrating greater differences both between the bacterial species isolated and their density between the different respiratory tract locations [136] [137]. In one study, intrabronchial inoculation of cattle with *H. somni* resulted in an increased isolation from bronchoalveolar lavage fluid compared to nasal swabs collected from calves with chronic disease [104]. This observation led authors to suggest that *H. somni* preferentially colonises the lower respiratory tract. However, this is unsurprising given the route of inoculation. Pass et al. investigated the location and extent of colonisation by *M. haemolytica* in the nasal cavity of fifteen beef calves. They considered right and left nasal cavities separately, finding little or no difference between them. Results did not consistently define areas of high and low density colonisation [9].

The bovine palatine tonsil is believed to be a colonisation site for *Pasteurellaceae*. Frank et al. also showed the tonsil to be a site for *M. haemolytica* [138] [139], contrasting with the previously held view that it is a commensal of bovine nares [20]. In addition, *B. trehalosi* has been shown to colonise ovine tonsils [33]. Frank showed *M. haemolytica* serotype A1 to colonise the tonsils of healthy calves for at least three weeks, suggesting that carriage could be prolonged in the tonsils [138]. Nasal secretions however, had low numbers of *M. haemolytica* with an A1 isolate, implying the tonsil may not continually shed bacteria, or they could be rapidly cleared [138]. Bovine respiratory bacteria and viruses are transmitted in nasal secretions to susceptible individuals in the herd [140] [35] [113]. Discrepancies regarding bacterial colonisation of the bovine tonsil or nasal passage could impact on understanding bacterial transmission, and sampling methods used to ascertain presence and density of colonisation accurately.

Swabs collected from the sinuses of healthy slaughtered cattle and those submitted for post mortem examination were cultured: bacteria were undetected from 94 of the 99 healthy animals (94.9%) and 17 of the 30 diseased animals (56.7%). Of the diseased animals, only nine were diagnosed with BRD, but *H. somni* (n = 5), *M. haemolytica* (n = 1), *E. coli* (n = 2) and *Clostridium spp*. (n = 1) were isolated from 8 of these 9 animals. This study provides weak evidence that the sinuses may act as reservoirs for bacteria commonly associated with BRD [141].

1.20 Colonisation dynamics

Rapid proliferation of bacterial pathogens in the nasopharynx can cause carrier cattle to become a source of infection for healthy non-infected cattle [65]. Transmission dynamics of opportunistic *Pasteurellaceae* are still not clear and it is debatable whether associated BRD episodes are due to predisposing factors allowing resident commensal flora to overcome the hosts immune system and cause disease or, whether a contagious virulent clone is spread between penmates [142]. Restriction endonuclease analysis, ribotyping, plasmid content analysis and antimicrobial resistance profiles have been used to distinguish different isolates of *M. haemolytica* and gain insight into its epidemiology [143]. Pulsed-field gel electrophoresis has also been applied to monitor transmission dynamics within BRD cases; significant within-pen diversity of *M. haemolytica* has led to the conclusion that disease did not occur as a result of spread of a single virulent clone [142]. Likewise in commercial feedlots, PCR-fingerprinting revealed significant diversity between *P. multocida* isolates from fatal BRD calf cases [144], indicating that complex bacterial communities exist within an individual's nasopharynx, although it is unclear to what extent predisposing factors have a role in enabling resident flora to cause disease.

1.21 Carriage rates

Culture of nasal swabs, bronchoalveolar lavage and tracheal aspirate samples has frequently revealed *M. haemolytica* and *P. multocida* to have involvement in BRD; with *M. haemolytica* being the predominant pathogenic agent detected [24] [136]. High isolation rates seen in nasal and bronchoalveolar lavage samples from clinically healthy cattle suggest that *P. multocida* is a commensal organism [145] [146] [147], but also exists as an opportunistic pathogen, evident from Angen et al. reporting detection from 82% and 74% of diseased animals sampled by trans-tracheal aspiration, processed by culture and PCR respectively [148].

Several authors have attempted to understand the relationship between nasopharyngeal commensals and disease in the bovine URT through assessing microbial flora, largely through nasopharyngeal swab sampling and culture-based methods. Table 1.2 summarises the key findings from a selection of studies chosen based on their interest in understanding carriage rates for bacterial species reported to be associated with BRD. It

can be seen that *P. multocida* has been reported with the highest prevalence, followed by *M. haemolytica* and *H. somni.* Difficulties exist when comparing studies due to inconsistencies in sampling and processing methods, advances in these methodologies over time, as well as differences between cohorts of animals sampled, for example age, breed, health status and farming system. *H. somni* has been reported at the lowest prevalence, which may not be a true reflection of carriage density; colonies are very slow growing and small, therefore overgrowth is easy [149] [67]. Recent advances have led to the development of several PCR assays which can reliably detect and in some cases quantify bacterial pathogens, overcoming issues posed by traditional culture [150] [151] [152]. A limitation of PCR is the possibility of detecting bacterial DNA in the absence of viable bacterial cells. However, when supplementing PCR with culture this issue can be addressed.

Table 1.2: Reported carriage rates in cattle for *Mannheimia haemolytica* (Mh), *Pasteurella multocida* (Pm), *Histophilus somni* (Hs) and other bacterial species.

	Bacterial carriage rates (%)					
Author	**Mh**	**Pm**	**Hs**	**Other**	**Methodology**	**Population sampled/location**
Hotchkiss et al. 2010 [149].		17			Nasopharyngeal swab, culture and PCR	Dairy and beef calves, mean prevalence, Scotland
Noyes et al. 2015 [153]	13.1				Nasopharyngeal swab sample, culture and PCR	Feedlot entry, age varied, unspecified (225kg – 400kg weight), Canada
Magwood et al. 1969 [145]	23	61.3		*Neisseria catarrhalis, Micrococcus spp.* and β-haemolytic *Streptococcus spp.*	Nasopharyngeal swab sample, culture	Healthy calves, Canada
Allen et al. 1991 [146]	31.7	46	6.7	*Mycoplasma bovis* (43%), *Mycoplasma bovirhinism* (35%), *Neisseria* (21.7%), *Streptomyces* spp. (3.3%).	Nasopharyngeal swab sample, culture	Healthy calves, Canada
Catry et al. 2006 [147]	9.8	57.4			Nasopharyngeal swab sample, culture and PCR	Apparently healthy calves (1 -4 months of age), Belgium

1.22 Predominant serotypes

A focus of previous work has been to determine the main serotypes of bacterial pathogens involved with BRD and their colonisation patterns. Frank et al. demonstrated *M. haemolytica* serotype A1 to be the most common isolate from nasal swab samples of stressed feeder calves [20], a finding concordant with work by DeRosa et al. [135]. *M. haemolytica* A1 and A2 are both able to colonise the upper respiratory tract of cattle and sheep. Capsular serotypes A1 and A6 are commonly associated with BRD [154] and more recently serotype A6 has shown to be increasingly prevalent in the UK and USA

[155]. These findings are supported by Katsuda et al. where investigation over a 20 year period showed serotypes A1, A2 and A6 to be most prevalent in calves affected with pneumonic pasteurellosis, with a similar recent increase in A6 [156]. In a further study, 92% of isolates from cattle with BRD were either A1 or A6 while recovery of A2 was substantially more prevalent from healthy cattle compared to those with disease [154], suggesting A2 to have a commensal role, opposed to the opportunistic nature of A1 and A6. Similarly, different serotypes of *P. multocida* are involved with pasteurellosis in different animal host species [157]. BRD is predominantly associated with serotype A isolates [65]. Serotyping however, is no longer considered to be sufficiently reliable for identifying *P. multocida* or *M. haemolytica* and laborious methodology based on culture and antigenic methods for detection and identification is being overtaken and replaced by PCR [66].

1.23 Respiratory microbiome

Using culture, Frank noted that the normal bacterial respiratory flora appeared to remain stable throughout exposure to *M. haemolytica* and respiratory viruses (BHV-1 or BPIV-3) but no attempts were made to provide further information on characterising bacterial nasal flora [158]. In addition, use of culture-based methods has resulted in research to date reporting association of culturable bacterial species with BRD, rather than those that are deemed unculturable but may have a role in modulating colonisation patterns with organisms associated with BRD. The potential value of attempting to characterise the URT microbiota further was demonstrated by Corbeil et al. who showed in most cases aerobic bacterial isolates from healthy bovine nasal flora to enhance the growth of *M. haemolytica*, *P. multocida*, and *H. somni in vitro*, and to a lesser extent inhibit them [159]. Their work provides evidence for the capacity of bacterial communities to regulate microbial populations, adding to understanding of how microbial communities in the bovine URT exist. Nevertheless, given the *in vitro* nature of the study, results may not accurately reflect dynamics in the host.

In children, it has been shown that stability of the respiratory microbiome changes with age and can be influenced by the presence or absence of certain bacterial species. Furthermore, patterns of change have been associated with parent-reported respiratory infection [160]. Therefore, enhancement of proliferation of certain species due to

respiratory virus infection could disrupt microbiome ecology and thus lead to changes in colonisation by occasionally pathogenic nasopharyngeal bacterial residents. The application of transcriptomic approaches may offer insight into conditions that promote up-regulation of opportunistic pathogens to elicit disease.

1.24 Viral-bacterial synergy

Viral-bacterial synergy refers to the phenomenon of increased risk of bacterial respiratory infection following a primary viral infection. It was first identified following human influenza epidemics when several secondary bacterial respiratory infections were associated with increased mortality, and has been observed for a variety of bacterial species [31]. Enhanced understanding of viral-bacterial synergism could aid future prevention, control and treatment strategies. Interactions between influenza and pneumococcal infections have been extensively researched [161]. In an early study, secondary bacterial pneumonia was experimentally induced in mice through intranasal co-infection with influenza virus A and either *Haemophilus influenzae, Streptococcus pneumoniae* or *Staphylococcus aureus* [162]. Given the multifactorial aetiology of BRD there is scope for greater understanding of viral-bacterial synergy elicited in the bovine URT as well as factors influencing transmission of potentially pathogenic bacteria.

1.25 Bacterial adherence following respiratory viral infection

It is thought that after infection with respiratory viruses in cattle, nasal mucosal commensals may proliferate, often replicating in tonsillar crypts and nasal mucin [30]. Disease can subsequently result from inhalation deeper into the respiratory tract [19] but it is uncertain as to whether high density bacterial colonisation is sufficient to cause pneumonia.

Respiratory viruses of cattle are transmitted in nasal secretions either by direct contact (nose-to-nose), indirectly through people and fomites or are aerosolised over short distances [163]. Viral infection in the upper respiratory tract can damage host epithelium rendering cells more susceptible to colonisation with bacteria. Loss of cells or damage can impair normal non-specific defense mechanisms e.g. reduced mucociliary function, or altered mucous composition and viscosity. Furthermore, bacterial elimination may be

reduced if virally infected cells do not express antimicrobial peptides sufficiently. Moreover, bacterial colonisation may be upregulated indirectly; viral infection upregulates various receptors (adhesion proteins) on a range of host cells (e.g. epithelial cells) to allow immune cells to bind to virally infected cells. Subsequently, bacterial adherence is promoted as bacteria can bind to the same adhesion proteins as immune cells [91].

1.26 Investigating viral-bacterial interactions in cattle

The distribution of these opportunist pathogens (*H. somni*, *M. haemolytica* and *P. multocida*), their density and co-occurrence with other bacterial and viral agents is variable within the bovine respiratory tract, thus influencing their pathogenicity and efficiency of transmission [24]. One hypothesis is that vaccination, particularly with live virus may enhance bacterial proliferation in the bovine URT through mimicking a natural viral infection [137]. Therefore, the use of live vaccines offers a practical and ethical model of viral infection, where this model can be applied to explore the effects of respiratory viral infection on the URT microbiome. Interestingly, calves suffering with BHV-1 induced respiratory disease are susceptible to active colonisation of the nasopharynx by *M. haemolytica* as a result of tonsillar colonisation [138]. This phenomenon has been shown by others, and subsequently bacterial shedding in nasal mucus for seven days or more has been demonstrated [158] [139]. Thus, findings are consistent with the argument that respiratory virus infection does indeed promote bacterial proliferation and hence shedding in nasal secretions.

1.27 Concluding remarks

Despite availability of antimicrobial drugs and vaccines, pneumonia still remains a major cause of morbidity, mortality and economic loss to beef and dairy industries. Understanding the disease syndrome can enhance treatment and prevention plans but this is complicated by the disease's multifactorial nature. At present, much of the research concerning bacterial species and their involvement with BRD has been conducted using culture. Molecular based methods such as PCR and sequencing can be employed to detect and quantify bacterial species rapidly, often with enhanced sensitivity and specificity. This review has provided strong evidence that *Pasteurellaceae* are common residents of the bovine nasal passages, but on occasion they are pathogens. However, the commensal

role members of *Pasteurellaceae* have within the bovine respiratory niche is not well defined and neither are the factors that drive the switch from commensal to pathogen status. Understanding the biology of carriage with respiratory bacteria in healthy animals is essential to inform future strategies to control disease. Furthermore, knowledge and understanding of BRD in suckler beef herds is limited; previous research has focused mainly on feedlot cattle and dairy calves, where substantial economic loss and welfare burden occurs. However, pneumonia is a disease that threatens all cattle, particularly calves. Moreover, health status and production efficiencies in all systems need to be carefully considered within a one-health framework to ensure both health and food security.

1.28 Hypothesis and aims

Histophilus somni, *Mannheimia haemolytica* and *Pasteurella multocida* are frequently implicated alongside respiratory viruses in cases of bovine respiratory disease worldwide. Given the recent evidence in humans and mice that following attenuated influenza infection nasal bacterial carriage rates, carriage duration, and density of carriage with important pathobionts increases, it was hypothesised that following respiratory viral infection, using a live-attenuated respiratory viral vaccine in cattle, rates and density of carriage with common bovine pathobionts may increase.

The aims of the work presented in this thesis were:-

i) To characterise the carriage rate and density of *Histophilus somni*, *Mannheimia haemolytica* and *Pasteurella multocida* in the nasal passages of healthy beef calves

ii) To investigate the effect of respiratory viral infection on nasal bacterial carriage rates and densities

Chapter 2 General Materials and Methods

2.1 The North Wyke Farm Platform

All cattle studies were performed at the North Wyke Farm Platform (NWFP), Devon, UK (Rothamsted Research). The research facility is a 'national capability' funded by the Biotechnology and Biological Sciences Research Council (BBSRC) and aims to improve sustainability of grazing livestock production through multi-disciplinary research, focusing on, but not exclusively: animal health, welfare and productivity, soil health, water quality and climate-related metrics.

The NWFP comprises three hydrologically-isolated farming systems called 'farmlets'. Each farmlet consists of five component fields of just over 20 ha in total per farmlet (Figure 2.1). Each farmlet is managed differently and the impact of these different management regimens (coded Green, Blue and Red) on beef and sheep production, water, air and soil are continually evaluated. Water leaving individual fields is restricted in vertical movement by a natural impervious layer of stagnogley and is channelled laterally through a network of French drains and perforated plastic pipes to individual, fully-instrumented flumes (n = 15), enabling measurement of flow rate and automated water collection for subsequent analysis for nutrient loss and water quality parameters. In addition, each farmlet field is equipped with a meteorological station, monitoring rainfall and soil water content.

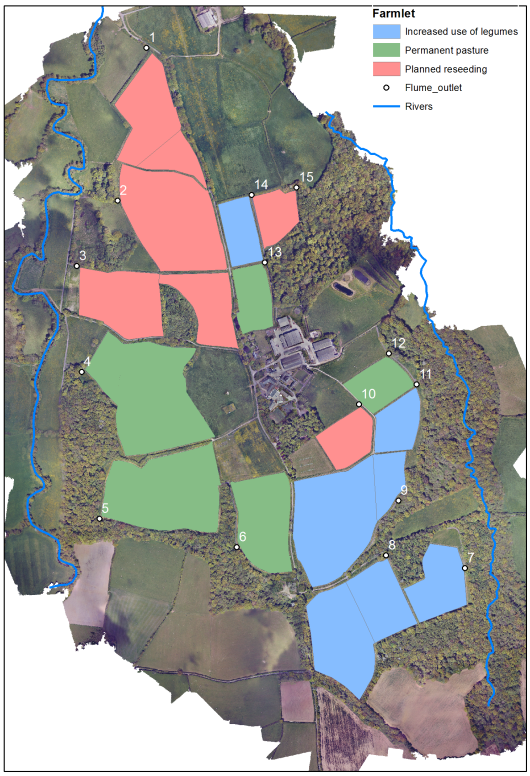

Figure 2.1: North Wyke Farm Platform field plan highlighting isolated Blue, Green and Red farmlets with respective component fields.

2.2 Management of farmlets

Prior to implementation of farmlet treatments baseline data collection was conducted over a two-year period between April 2011 and March 2013. Following baseline collection, each of the three farmlets progressively moved onto different pasture management systems, with swards of: 1) permanent pasture (Green Farmlet); 2) white clover/high sugar perennial ryegrass mix (Blue Farmlet); and 3) high sugar perennial ryegrass monoculture (Red Farmlet) [164]. Further details on sward management specifics are given in Appendix A.

2.3 Forage sampling of farmlets

For each barn/farmlet, pasture and silage samples were collected for forage quality analysis as part of the standard management practices on the NWFP. Pasture samples were collected for both 2015 and 2016 grazing years. Pasture samples were collected between April and October 2015 and between May and October 2016 from fields in which cattle grazed. For silage, samples were collected between October 2015 and March 2016 and between September 2016 and April 2017 from silage fed to animals during the respective housing period. Samples were

processed following standard protocols given below for estimation of metabolisable energy (ME), indicating digestibility, and crude protein (CP).

2.4 Forage processing protocol

For both pasture and silage samples the modified acid detergent fibre (MADF) composition was quantified using a FOSS Fibertec 8000 Auto Fiber Analysis System following the method of Clancy and Wilson (1966) [165]. The derived MADF fractions were converted to corresponding ME values using equations independently calibrated for UK pastures and silages [166]. These values were further converted to digestible organic matter content (DOMD; reported as digestible energy) using a separate equation [166] [167].

2.5 Forage quality statistical analysis

To investigate differences in ME and CP in each farmlet on the NWFP a linear mixed effect model was fitted with a fixed effect of farmlet and random effect of time to account for variation introduced by repeated measures. Where technical replicates were present (ME only) an additional random effect of replicate was included nested within time. The impact of the fixed effect (farmlet) versus the null model (no fixed effect) was assessed by comparing the change in residual deviance from a nested, simpler model with the upper-tailed critical value ($p < 0.05$) of the appropriate chi-squared distribution (as identified by the change in the residual degrees of freedom between the models). For significant effects, a Tukey test was used to determine which farmlets were different. Mixed effect models were conducted using the R package lme4 (version 1.1.17) and Tukey post-hoc tests conducted using the R package lsmeans (version 2.30.0). For silage fed to the 2016 born cohort there was considerable variation between silage samples collected from bales or the silage clamp. As animals were fed silage from both locations samples were stratified on location for statistical analysis. For CP of silage, one-way analysis of variance (ANOVA) was performed, including a fixed effect of farmlet (because the mixed model failed to converge). For significant effects, a Tukey test was used to determine which farmlets were different.

2.6 Livestock operations

A herd of 100 Suffolk ewes and 90 Hereford-Friesian x Charolais calves are bred each year. Livestock are born in the early Spring (March onwards) and stay with their respective ewe/dam housed until Summer turnout, usually around May to June. When calves and lambs are at

pasture with their mothers they are off the NWFP and graze a permanent pasture. During the winter housing period animals are fed a diet of conserved forage produced from the farmlet they are allocated to. The following Spring calves and lambs are turned out once more, but this time to graze their allocated farmlet pasture. One of the key metrics for production of both sheep and beef enterprises is growth rate. Animals with increased growth rates take less time to finish compared to less efficient animals, therefore all livestock are weighed on and off the grazing to determine live-weight gain. During winter, livestock are weighed approximately every two weeks.

Heifers are serviced by bulls naturally on the FP (further details are given in Appendix A). The calving period takes between March to May each Spring. In-calf heifers are housed on deep-litter straw bedding in a barn located on a site separate to the cattle winter housing facilities located at Rowden. Calves are ear tagged shortly after birth and ear notch tested for BVDV. From the maternity unit they are moved to a separate barn close by (~250 m). Here, calves are penned in groups of five per pen with their respective dams. At an age of approximately two months, and when the weather permits, they are turned out to pasture separate to the NWFP.

2.7 Cattle facilities

The cattle facility, newly built in winter 2013/2014 comprises of three identical purpose-built barns, silage clamps, farmyard manure middens and ancillary buildings, as seen in Figure 2.2. A distance of approximately 6 meters separates the three barns. Silage is stored in clamps or in bales, maintaining segregation respective to farmlet. Resulting farmyard manure collected during housing from each of the three barns/farmlets is returned to the corresponding farmlet pasture.

Figure 2.2: Aerial view of cattle housing and handling facilities at Rowden site, North Wyke Farm Platform (Rothamsted Research, Devon). Image source: Google maps.

Each barn has solid concrete sidewalls to animal height (~1.5 m) and is ventilated naturally above animal height with space boarding, there is a midden at the rear and feeding area in front of the scrape (Figure 2.3, panel a and b). Barns are orientated to face south west onto handling facilities (Figure 2.3, panel c) such that the prevailing winds [168] [169] assist with their ventilation through end apertures (solid gates approximately 2 m high with openings above and a space-boarded gable end). During harsh weather windbreaks are used to provide protection. The handling facilities are within a yard which includes several holding pens and a race leading up to a crush. Calves are housed loose-grouped unless otherwise stated.

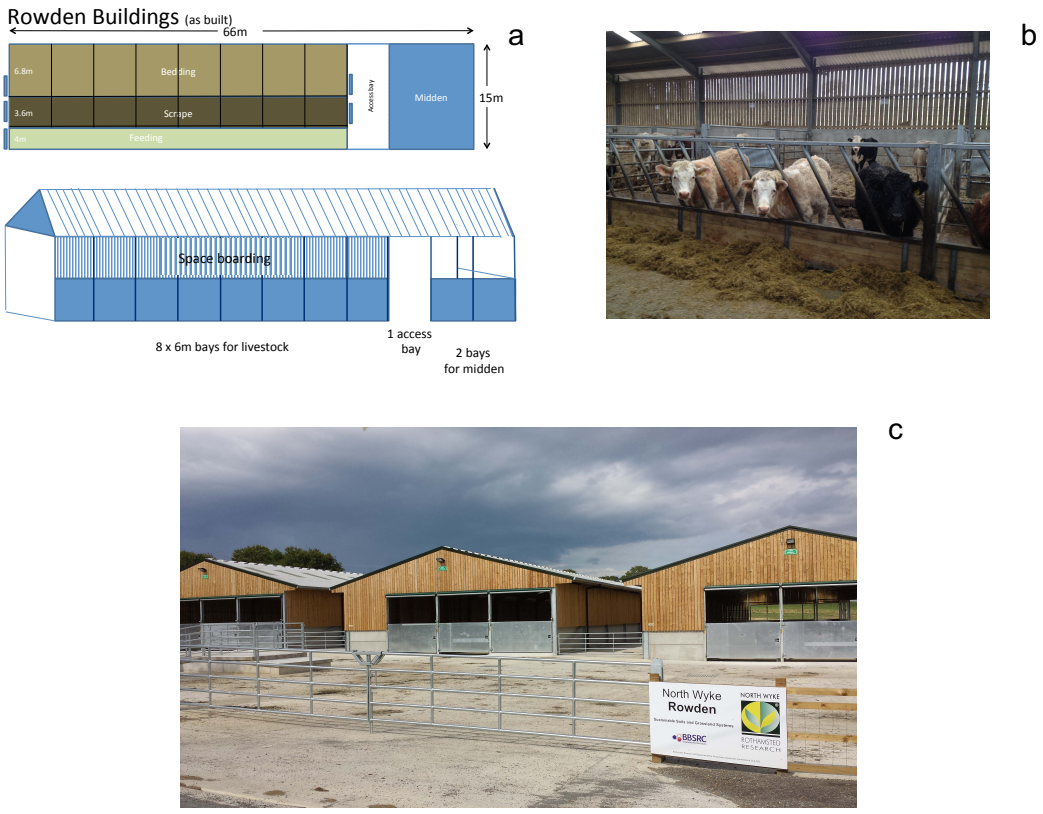

Figure 2.3: Exterior and interior barn environment: a) Floor plan of purpose-built cattle housing, b) calves feeding inside one of the three barns, and c) exterior of the three identical purpose-built cattle housing facilities, located at Rowden, 2.5 km from the main farm buildings where breeding heifers are housed.

2.8 Allocation of animals to farmlets

At the end of the summer grazing season on fields separate from the NWFP, 90 calves are weaned and housed in one of the three farmlet barns at approximately 7 months of age (n = 30 per barn). Calves are housed over the winter, together with approximately 15–20 finishing cattle from the previous year.

Two calf cohorts born in Spring 2015 and 2016 were studied. Allocation of calves to farmlet was conducted immediately prior to winter housing for both cohorts. In 2015, calves were allocated based on body weight. In 2016, allocation was performed following a modified method of covariate-constrained randomisation, the following covariates were considered: age, breed, body weight, growth rate, sex and sire [170]. Further details on the methods for each year are given in Chapters 4 and 6 respectively.

2.9 Sample Collection

2.9.1 Ethical Approval

All animal studies were approved by the Rothamsted Research Ethical Review Board and animal care and use protocol protocols adhered to the Animals (Scientific Procedures) Act 1986 as revised 1 January 2013 to comply with European Directive 2010/63/EU, permit number (3003338).

2.9.2 Animal handling

On the day of sampling, animals were herded from their barn to a handling area consisting of consecutive pens leading to a race and cattle crush. All procedures were performed on animals restrained within the crush. Animals were restrained using a halter for collection of nasal swabs, jugular blood samples and administration of intra-nasal vaccine/diluent. In some instances, smaller individuals were physically restrained by placing an arm over the animals' head and holding it close to the handlers' body. When collecting jugular blood, a tail bar was employed to prevent backwards movement of the animal in the crush.

2.9.3 Sample collection workflow

Procedures were performed in the following order: i) nasal swab, ii) rectal temperature, iii) intra-nasal vaccination/saline, and iv) jugular blood collection. The same individual (Amy Thomas; AT) collected nasal swabs, administered vaccine and performed clinical observations.

2.9.4 Sample labelling

Swabs and blood samples were marked with pre-printed labels, each consisting of a unique laboratory reference number, visit and study number, shortened management tag identification number and details of sample type. Laboratory reference numbers ranged between 1 to 90 for animals born in 2015, and between 91 to 179 for animals born in 2016. Each reference number was randomly affiliated to an animal's management tag number, this was performed by generating random values using the RAND() function in Microsoft Excel® (version 16.16.1 [180814]) for each animals management tag, then sorting the random number list in ascending order; the smallest random value corresponded to the start of the laboratory reference number list (ordered smallest to largest). Only laboratory reference numbers were used in the laboratory to identify samples during processing.

2.9.5 Nasal swabs: collection, processing and storage

2.9.5.1 Short nasal swabs

Nasal swabs with breakable cotton tips (Medical Wire & Equipment, Corsham, UK) were collected from each calf as follows: any excessive debris on nares was cleaned with a disposable tissue/paper towel. The 15 cm long swab was inserted to approximately 10cm depth and rotated 360° against the mucous membranes, then withdrawn carefully, avoiding contact with other areas of the nasal cavity. The cotton tip was aseptically broken off into 1.5 ml skim milk, tryptone, glucose, glycerol (STGG) broth (Media services, School of Cellular and Molecular Medicine, University of Bristol, UK) for culture and qPCR.

Dual-tipped cotton swabs (Dual HydraFlock, Standard Tip, Flexible Shaft, 30 mm Moulded Breakpoint, Medical Wire & Equipment, Corsham, UK) were collected according to single tipped swabs, however one tip was transferred to STGG and the other to RNA*later* stabilisation solution (ThermoFisher Scientific, UK). Swab samples were marked with a random number using pre-printed labels, maintained at 4°C for no more than 3 hours and then vortexed to release bacteria into the STGG and frozen at -70°C until further analysis [171] [172]. Gloves were changed between handling each animal.

2.9.5.2 Deep guarded nasal swabs

Deep guarded nasopharyngeal swabs with cotton tips (Duggan Veterinary Supplies Ltd., Ireland) were collected from a subset of calves following collection of short nasal swabs, providing a set of paired samples. The same nostril was sampled using both short and deep nasal swabs. Deep nasal swabs (Figure 2.4) were collected as follows: the distance from the nostril to the medial canthus of the eye was measured and the guarded swab inserted into the ventral meatus of the nose, then advanced as far as the pre-measured distance (from nostril to eye). The outer sheath was retracted 1–2 inches and the swab pushed through the protective capped-end and rotated against the pharyngeal mucosa. Finally, the swab was retracted back into the protective outer sheath (minimum retraction of 3 cm) and carefully withdrawn. Using a sterile pair of scissors (Rocket Suture Scissors 11cm, Rocket Medical) the swabs' shaft was cut approximately 1–2 cm below the cotton tip, and aseptically transferred into STGG medium for bacteriology and qPCR. Gloves were changed between animals. One pair of scissors was used per swab. Samples were labelled as described in 2.9.4.

Figure 2.4: Photograph of the tip of a deep guarded nasopharyngeal swab, pictured with i) the cap in place and ii) with the cap removed and inner swab extended.

2.9.5.3 Transport and storage of nasal swabs

Nasal swabs stored in STGG transport medium and RNA*later* stabilisation solution (ThermoFisher Scientific, UK) were maintained at 4°C during sample collection and transport to the laboratory for further processing and storage. Swabs stored in STGG were maintained for no more than 3 hours, then kept on ice, vortexed for 30 s and transferred to -70°C until analysis [171] [172]. Swabs stored in RNA*later* were processed identically following overnight storage at 4°C.

2.9.6 Jugular blood samples: collection, processing and storage

Paired jugular blood samples were collected to detect evidence of natural viral infection on the NWFP by common bovine viruses and *Mycoplasma bovis.*

A jugular venous blood sample was collected into a plain Vacutainer (Becton Dickinson, Plymouth UK). Blood samples were allowed to clot at room temperature for a minimum of 30–60 minutes and were either processed immediately or stored overnight at 4°C. Samples were centrifuged at room temperature for 15 minutes, 1000-1200 g and serum aspirated into cryovials (approximately 1.5ml aliquots). Sera were stored at -70°C until processed.

Sera were analysed for the presence of antibodies against BHV-1, BVDV, BRSV, BPIV-3 and *Mycoplasma bovis* using a semi-quantitative indirect ELISA (Bio K 284, Multiscreen Ab ELISA Bovine Respiratory, BioX Belgium). Following the manufacturer's protocol, test samples were tested in duplicate.

2.10 Calf health observations and rectal temperatures

Animals were observed daily by animal technicians for signs of abnormal behaviour or reduced feed intake. Any cattle showing abnormal behaviour that might have indicated poor health were observed in more detail by AT for signs of respiratory disease and observations were recorded using a standardised scoring system that included cough, nasal and ocular discharge, abnormal ear/head tilt and rectal temperature (as shown previously in Chapter 1, Figure 1.2) [36] [37]. Rectal temperatures were recorded using a livestock rapid read digital thermometer (Nettex, UK).

2.11 Vaccination

Calves were vaccinated with modified live BRSV and BPIV-3 (Rispoval RS+PI3 IntraNasal, Zoetis Animal Health). The vaccine contained BPIV-3 thermosensitive strain RLB103, between $10^{5.0}$ and $10^{8.6}$ cell culture 50% infective doses ($CCID_{50}$) and BRSV, strain 375, between $10^{5.0}$ and $10^{7.2}$ $CCID_{50}$, supplied with sterile diluent (water for injection and sodium chloride, 18 mg per 2 ml) for reconstitution. Vaccine was administered bilaterally as a single 2 ml dose with an intranasal applicator supplied by the vaccine manufacturer. Gloves and applicators were changed between animals. Control calves in the stepped-wedge trial received 2 ml of saline (0.9% w/v sodium chloride, Zoetis Animal Health) by an identical route.

2.12 Preparation and completion of ELISAs

2.12.1 BioX ELISA principle

The commercial BioX indirect ELISA employs a 96 well microtitration plate sensitized by monoclonal antibodies to BHV-1, BVDV, BRSV and BPIV-3. Recombinant protein from *Mycoplasma bovis* expressed in *E. coli* is also used (Figure 2.5). If specific immunoglobulins are present in the test sera the conjugate remains bound to the corresponding microwell and the enzyme catalyses the colour change to blue, the intensity of the blue colour is proportionate to the titre of specific antibody in the sample.

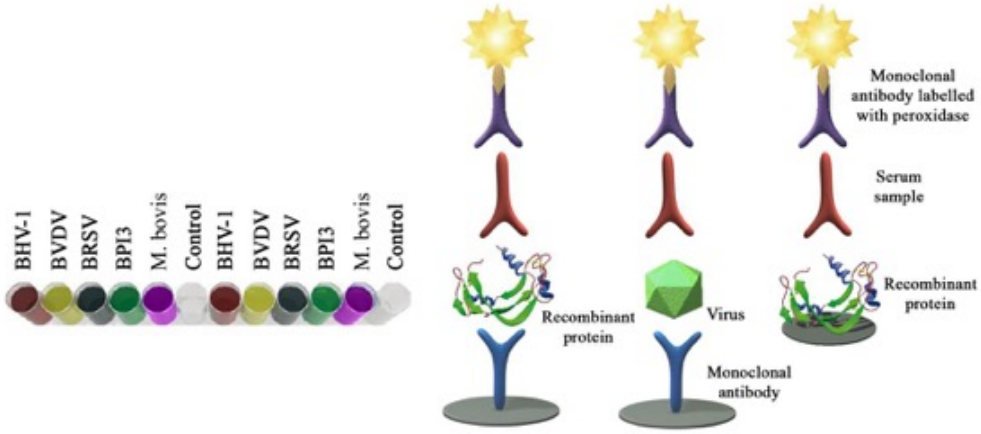

Figure 2.5: Principle of BioX multiplex ELISA detecting and semi-quantifying antibodies to: bovine herpes virus 1 (BHV-1), bovine viral diarrhoeal virus (BVDV), bovine respiratory syncytial virus (BRSV), bovine parainfluenza virus (BPIV-3) and *Mycoplasma bovis*.

2.12.2 BioX ELISA conduct

Each 96 well plate was loaded with 12 samples in total, tested in duplicate, an example of the plate layout is given Figure 2.6.

Diluted test sera (1:100) and positive and negative controls were incubated on a 96 well plate for one hour 21°C +/- 3°C. After washing, a peroxidase-labelled anti-bovine IgG1 monoclonal antibody (conjugate) was added to the wells and incubated to detect bound antibody. The plate was washed for a second time and a positive result was visualised following addition of chromogen (tetramethylbenzidine) - positivity was signified by the colourless chromagen transforming into a pigmented compound. Signals from negative control wells were subtracted from the corresponding positive microwells. Reactivity of test serum was quantified into six categories (0 to 5) of increasing antibody (negative = 0).

	1	2	3	4	5	6	7	8	9	10	11	12
A	SAMPLE 1	SAMPLE 1	SAMPLE 1	SAMPLE 1	SAMPLE 1	SAMPLE 1	SAMPLE 7	SAMPLE 7	SAMPLE 7	SAMPLE 7	SAMPLE 7	SAMPLE 7
B	SAMPLE 2	SAMPLE 2	SAMPLE 2	SAMPLE 2	SAMPLE 2	SAMPLE 2	SAMPLE 8	SAMPLE 8	SAMPLE 8	SAMPLE 8	SAMPLE 8	SAMPLE 8
C	SAMPLE 3	SAMPLE 3	SAMPLE 3	SAMPLE 3	SAMPLE 3	SAMPLE 3	SAMPLE 9	SAMPLE 9	SAMPLE 9	SAMPLE 9	SAMPLE 9	SAMPLE 9
D	SAMPLE 4	SAMPLE 4	SAMPLE 4	SAMPLE 4	SAMPLE 4	SAMPLE 4	SAMPLE 10	SAMPLE 10	SAMPLE 10	SAMPLE 10	SAMPLE 10	SAMPLE 10
E	SAMPLE 5	SAMPLE 5	SAMPLE 5	SAMPLE 5	SAMPLE 5	SAMPLE 5	SAMPLE 11	SAMPLE 11	SAMPLE 11	SAMPLE 11	SAMPLE 11	SAMPLE 11
F	SAMPLE 6	SAMPLE 6	SAMPLE 6	SAMPLE 6	SAMPLE 6	SAMPLE 6	SAMPLE 12	SAMPLE 12	SAMPLE 12	SAMPLE 12	SAMPLE 12	SAMPLE 12
G												
H												

Col: 6 & 12	One monoclonal antibody
	Positive serum H1 - H12
	Negative serum G1 - G12

Figure 2.6: BioX ELISA sample plate layout template.

The optical density (OD) of the blank wells (e.g. column 6) was subtracted from the OD of corresponding wells containing sample (e.g. columns 1 to 5). This was repeated for positive and negative control wells (e.g. G1 to G6; H1 to H6). The test was validated only if the positive serum yielded a difference in optical density at 10 minutes greater for each valence than:
BHV-1 > 1.000; BVDV > 1.100; BRSV > 1.100; BPIV-3 > 1.000; *M. bovis* > 1.100,
and the negative serum yielded a difference in optical density that was lower than 0.300.
The signal read for each sample was divided by the corresponding positive control serum signal and multiplied by 100 to express it as a percentage.
Value = (Delta OD Sample * 100) / (Delta OD positive)
The guide table provided in the kit instructions was used to determine the sample serum's degree of positivity (Table 2.1). A frank seroconversion was considered to have occurred if the signal increased by two orders of magnitude/two categories of seropositivity (for example, 2 to 4 or 1 to 3). A sample was considered positive if its category was determined at 1 or more (denoted by + in Table 2.1).

Table 2.1: Values to determine serum degree of positivity

	0		+		++		+++		++++		+++++
BoHV-1	Val <=	30 %	< Val <=	67 %	< Val <=	104 %	< Val <=	141 %	< Val <=	178 %	< Val
BVDV	Val <=	20 %	< Val <=	40 %	< Val <=	60 %	< Val <=	80 %	< Val <=	100 %	< Val
BRSV	Val <=	23 %	< Val <=	46 %	< Val <=	68 %	< Val <=	91 %	< Val <=	114 %	< Val
BPI3	Val <=	26 %	< Val <=	52 %	< Val <=	78 %	< Val <=	104 %	< Val <=	130 %	< Val
M.bovis	Val <=	29 %	< Val <=	47 %	< Val <=	64 %	< Val <=	82 %	< Val <=	100 %	< Val

2.13 Preparation and completion of bacterial nucleic acid extraction

2.13.1 Preparation of bacterial stocks

For bacterial stocks of reference strains stored in glycerol broth, a 50 µl aliquot of sample was diluted 1:10 with 450 µl of L6 lysis buffer (Public Health England, Bristol, UK). Dilutions were prepared in 2 ml screw cap extraction tube and extracted no later than 2 h post preparation.

2.13.2 Preparation of nasal swabs

Frozen nasal swab samples were thawed on ice and then vortexed for 30 s. Sample (300 µl) was aliquoted into a 2 ml screw cap extraction tube and extracted no later than 2 h post preparation.

2.13.3 Extraction of nucleic acid

Extractions of nucleic acid from bacterial stocks and nasal swabs were carried out using a proprietary kit (QIAsymphony DSP virus/pathogen Mini Kit, Qiagen, CA, USA) in an automated instrument (QIAsymphony SP, Qiagen, CA, USA). An elution volume of 140 µl was produced from 200 µl of the 300 µl sample aliquot. To determine successful DNA extraction and absence of PCR inhibition the enterobacteriophage T4 was used as an internal amplification control [171]. Prior to nucleic acid extraction, bacterial stocks either inactivated with heat or L6 buffer were plated onto solid agar and incubated overnight, no growth was observed for either methods confirming successful inactivation.

2.14 Conduct of real-time PCR assays for detection of *Pasteurellaceae*

PCR runs were carried out using MicroAmp optical 384-well reaction plates (Life Technologies, USA), performed on a ViiA7 real-time PCR instrument (ThermoFisher Scientific) or a QS7 real-time PCR instrument (ThermoFisher Scientific) where specified. The PCR was performed in a 20 µl reaction mix containing 10 µl TaqMan® (Applied Biosystems), 5 µl Primer/Probe Mix (Sigma Life Science) and 5 µl nucleic acid template. Working concentrations of primers and probes were 300 nM and 100 nM respectively.

Primer and probe details used to detect and quantify *H. somni, M. haemolytica* and *P. multocida* are given in Table 2.2 and those to detect T4 are given in Table 2.3. Cycling conditions for *H. somni, P. multocida* and T4 assays were performed using standard TaqMan cycling conditions: 95°C for 20 s hold stage, followed by 50 cycles of 95°C for 3 s and 60°C for 60 s. The T4 PCR assay detected presence of the enterobacteriophage T4 in all samples extracted by automated methods described in 2.13.3. Presence of T4 indicated successful DNA extraction and no evidence of PCR inhibition. Cross-reactivity was observed for *M. haemolytica* using standard TaqMan conditions (further details are given in Chapter 3). Optimised conditions were employed: 95°C for 20 s hold stage, followed by 50 cycles of 95°C for 3 s and 60°C for 60 s.

Table 2.2: Primer and probe sequences used to detect and quantify *Histophilus somni*, *Mannheimia haemolytica* and *Pasteurella multocida* from bovine nasal swabs using qPCR

Target Species	Gene Target	PP* Name	PP Sequence (5'-3')	Length	Melting Point (°C)	Reference
H. somni	16S rRNA	Hsomni-TMF	AGGAAGGCGATTAGTTTAAGAGATTAATT	29	58.8	Mahony and Horwood 2007
H. somni	16S rRNA	Hsomni-TMR	TCACACCTCACTTAAGTCACCACCT	25	60.0	Mahony and Horwood 2007
H. somni	16S rRNA	Hsomni-TMP	ATTGACGATAATCACAGAAGAAGCACCGGC	30	69.7	Mahony and Horwood 2007
M. haemolytica	*sodA*	Mhae-SGF	AGCAGCGACTACTCGTGTTGGTTCAG	26	65.6	Guenther et al. 2008
M. haemolytica	*sodA*	Mhae-SGR	AAGACTAAAATCGGATAGCCTGAAACGCC	29	68.7	Guenther et al. 2008
M. haemolytica	*sodA*	Mhae-TCR	TTGTAAACTGGGACGAAGCC	20	56.7	This study
M. haemolytica	*sodA*	Mhae-BV1P FAM	TTCAACCGCTAACCAGGACAACCCAC	26	59.7	This study
P. multocida	16S rRNA	Pmulti-TMF	CGCAGGCAATGAATTCTCTTC	21	56.2	Mahony and Horwood 2007
P. multocida	16S rRNA	Pmulti-TMR	GGCGCTCTTCAGCTGTTTTT	20	57.1	Mahony and Horwood 2007
P. multocida	16S rRNA	Pmulti-TMP	ACTGCACCAACAAATGCTTGCTGAGTTAGC	30	58.4	Mahony and Horwood 2007

* PP: Primer and probe

Table 2.3: Primer and probe sequences used to detect enterobacteriophage T4 for assurance of successful DNA extraction and amplification

Target	Gene Target	PP* Name	PP Sequence (5'-3')	Length	Melting Point (°C)	Reference
Enterobacterio phage T4	gp18 tail sheath gene	T4-BV1F	GTTGAAAACGAATATCGGACGTAGT	25	58.6	Unpublished B. Vipond
Enterobacterio phage T4	gp18 tail sheath gene	T4-BV1FR	CCTTGTAAGTACTGGGCAGTTTCTG	25	59.3	Unpublished B. Vipond
Enterobacterio phage T4	gp18 tail sheath gene	T4-BV1P	CAACGCGTTTACTCGTTCATCATTCC	27	68.5	Unpublished B. Vipond

* PP: Primer and probe

2.15 Analysis of PCR assays: thresholds and baseline settings

Table 2.4 illustrates threshold values set for *H. somni, M. haemolytica*, *P. multocida* and T4 PCR assays during method development and analysis of nasal swabs. Thresholds were manually set above any background amplification visualised on amplification plots, and in the exponential phase of amplification. Baseline settings were not changed from the software auto-baseline function. Cycle quantification (C_q) values were obtained when amplification curves intersected the defined threshold.

Table 2.4: Analysis settings used to define qPCR thresholds

Species/Target	Assay development threshold (fluorescence units)		Nasal swab threshold (fluorescence units)	
	Viia*	QS7*	Viia*	QS7*
H. somni	0.005	0.005	0.005	0.005
M. haemolytica	0.005	0.015	NA	0.015
P. multocida	0.005	0.005	0.005	0.005
T4	NA	NA	0.01	0.01

* PCR instrument

2.16 Sequencing

2.16.1 DNA preparation for sequencing

Bacterial isolates were sequenced following amplification of variable regions of the 16S rRNA genome. DNA was extracted from bacterial isolates as previously described (see 2.13.3). PCR runs were carried out using 96 well FrameStar® Break-A-way plates and sealed with FrameStrips™ (Brooks Life Sciences, 4titude, UK) performed on a Mx3005P qPCR instrument (Agilent Technologies, Santa Clara, USA). The PCR was performed in a 25 µl reaction mix containing: 9 µl Nuclease-Free Water (Promega, UK), 12.5 µl Go Taq Hot Start (Promega, Madison, USA), 0.5 µl SYBR™ Green I Nucleic Acid Gel Stain (1:1000 dilution in Nuclease-free water; Life Technologies, Carlsbad, USA), 1 µl forward primer, 1 µl reverse primer and 1 µl nucleic acid template. Working concentrations of primers were 100 nM (diluted in AE buffer; Qiagen, Hilden, Germany) and purchased from Eurofins Genomics (Ebersberg, Germany).

DNA extracts were amplified using two sets of primers (PP1: 337F & 518R; PP2: 928F & 1100R) described in (

Table 2.5) under the following cycling conditions: 95°C for 10 minutes (1 cycle, hot start stage), followed by 40 cycles of 95°C for 30 s and 60°C for 60 s, finally a dissociation

curve was run for 1 cycle of 95°C for 60 s, 55°C for 30 s and 95°C for 30 s. PCR products were visualised on a 1% agarose gel; 10 µl product with 2 µl orange loading dye (Sigma Aldrich). Gels were prepared according to the recipe given in Appendix A. Gels were run at 100 V for ~70 min and included 3 µl of a 50 bp and 100 bp ladder (Bioline, UK). Gels were visualised using a UV transilluminator instrument (Ultra-Violet Products Ltd, Cambridge, UK). PCR product sizes for PP1 and PP2 were expected at 181 bp and 172 bp respectively.

Table 2.5: Primer sequences used for sequencing bacteria isolated from bovine nasal swabs and purchased strains

Primer Name	Primer Sequence (5'-3')	Target	Reference and notes[1]
337F	GACTCCTACGGGAGGCWGCAG	16S	Modified Wang and Qian (2009) [173]
518R	GTATTACCGCGGCTGCTGG	16S	Modified Lane (1991) [174]
928F	TAAAACTYAAAKGAATTGACG GG	16S	Modified Lane (1991) [174]
1100R	GGGTTGCGCTCGTTG	16S	Lane (1991) [174]
785F	GGATTAGATACCCTGGTA	16S	Modified Wang and Qian (2009) [173]
907R	CCGTCAATTCCTTTRAGTTT	16S	Lane (1991) [174]

[1] Universal primers designed in other studies to detect conserved constant regions of the 16S rRNA gene of all bacterial species. Modifications included reduction in length to produce primers within a pair of similar melting temperatures or modification in reverse compliment.

2.16.2 Preparation for sequencing of purchased bacterial strains

DNA extracts were amplified using two sets of primers (PP3: 337F & 907R; PP4: 785F & 1100R as described in

Table 2.5 under the following cycling conditions: 95°C for 10 minutes (1 cycle, hot start stage), followed by 40 cycles of 95°C for 60 s, 54°C for 60 s and 72°C for 120 s, followed by 1 cycle of 72°C for 10 minutes. Working concentrations of primers were 100 nM (diluted in AE buffer; Qiagen, Hilden, Germany) and purchased from Eurofins Genomics (Ebersberg, Germany). PCR runs were carried out using 96 well FrameStar® Break-A-way plates and sealed with FrameStrips™ (Brooks Life Sciences, 4titude, UK)

performed on a SureCycler 8800 instrument (Agilent Technologies, Santa Clara, USA). The PCR was performed in a 25 µl reaction mix containing: 9.5 µl Nuclease-Free Water (Promega, UK), 12.5 µl Go Taq Hot Start (Promega, Madison, USA), 1 µl Forward Primer, 1 µl Reverse Primer and 1 µl nucleic acid template.

PCR products were visualised on a 1% agarose gel; 10 µl product with 2 µl orange loading dye (Sigma Aldrich). Gels were run at 100 V for ~90 minutes and included 3 µl of a 50 bp and 100 bp ladder. PCR product sizes for PP3 and PP4 were expected at 141 bp and 328 bp respectively.

2.16.3 Preparation for sequencing *H. somni*, *M. haemolytica* and *P. multocida* PCR products

Representative PCR products generated from amplification of target species (*H. somni, M. haemolytica* and *P. multocida*) were sequenced to confirm their identity. DNA extracts from liquid broth culture for each species were used as template. PCR products with low C_q values (~12) were selected based on their presumptive high DNA template concentration.

2.16.4 PCR product purification, sequencing and sequence analysis

All PCR products intended for sequencing were purified using a QIAquick PCR purification kit (Qiagen, CA, USA) as per manufacturing protocols. A 15 µl aliquot of purified PCR product was mixed with 2 µl of forward primer and sent to Eurofins (Eurofins Genomics GmbH, Ebersbergm, Germany). Purified PCR products were independently mixed with 2 µl of forward and 2 µl of reverse primer. Files were supplied as .ab and used to visually inspect chromatograms using SnapGene® Viewer software (Version 1.4.5, GSL Biotech, available at snapgene.com). Sequences were cleaned accordingly, for example where peaks were not evenly spaced and overlapping these areas of sequences were clipped (occurring at the start of the sequence). Cleaned sequences were supplied as FAST-All (FASTA) format to Basic Local Alignment Search Tool (BLAST). Homology between unknown candidate sequences to known sequences within the National Center for Biotechnology Information (NCBI) database was assessed.

2.17 Analysis of binary response variables

Binary responses take only two values: 0 or 1. For example, bacterial carriage is either present (1) or absent (0). Binary response variables were analysed using either logit models or log-linear models where stated. When explanatory variables had no non-unique values log-linear models were used by aggregating data into counts so that each count took a unique set of explanatory variables [175].

2.18 Construction of log-linear models

Log-linear models are generalised linear models used to analyse Poisson distributed data. They are commonly used for modelling cell counts in contingency tables; models specify how the number of counts within a cell depend on the levels of categorical explanatory variables for that cell. They are particularly useful when at least two variables in a contingency table are response variables; when one variable is the binary response and others are explanatory variables, certain log-linear and logit models are equivalent [176]. For all analyses using log-linear models count data was constructed in the form of a contingency table. A baseline model was then built which defined the overall structure of the data i.e. margins of the contingency table. To this baseline model explanatory terms were added in a sequence of increasing complexity until the saturated model, including all terms and the interactions between them was reached. Model parameters were interpreted by referring to the highest-order terms, relating directly to odds ratios. Model fit was assessed by comparing observed to fitted counts [176].

Chapter 3 Real-time PCR for detection and quantification of *H. somni*, *M. haemolytica* and *P. multocida*

3.1 Introduction

Bacterial carriage in the bovine upper respiratory tract has been detected most frequently by culture [135, 145-147, 153]. Difficulties have been reported due to the fastidious nature of organisms and overgrowth by faster growing species [149]. Bacterial involvement in bovine respiratory disease (BRD) frequently involves members of the *Pasteurellaceae* family. *Pasteurellaceae* normally inhabit the mucous membranes of the alimentary, genital and respiratory tracts of vertebrates [67]. *Histophilus somni, Mannheimia haemolytica, Pasteurella multocida* and to a lesser extent, *Bibersteinia trehalosi* are implicated in cases of BRD. The studies presented in this thesis focus on *H. somni*, *M. haemolytica* and *P. multocida*. The taxonomy of this family has frequently been revised: however, as molecular techniques have advanced, the differentiation between species has improved [78], consequently allowing in-depth investigation of organisms that are currently difficult or impossible to culture, for example by PCR [152] and sequencing [177-179].

Nucleic-acid-based amplification relies on sequence-based hybridisation chemistry using DNA (deoxyribonucleic acid) probes. Probes are short, labelled, single-stranded DNA segments which are designed to hybridise to complementary sequences of DNA. In 1980, use of probes to rapidly detect microbial DNA was demonstrated using a filter hybridisation assay method to detect enterotoxigenic *Escherichia coli* in stool samples [180]. The method showed enhanced performance as compared to culture. However, it relied on hybridisation of DNA probes to fixed target DNA (stool samples spotted onto filters), which increased the test time as compared to having both the probe and target sequence free in solution – this was the next advancement [181]. In 1983, Kary Mullis and colleagues invented PCR: a rapid, sensitive and simple technique to directly amplify target DNA. The capacity of PCR to amplify complete genomic sequences from tiny amounts of target molecules has led to its use in many analytical techniques and technological advances. Its profound effect within a range of fields has been recognised, and ten years after its invention, Mullis and colleagues were awarded the *'Nobel Prize for Chemistry*'. Figure 3.1 shows the principles of the reaction. In brief, the DNA

sequence of the target is used to design complementary oligonucleotide primers which hybridise to specific regions of the target DNA. The reaction is enzymatic, driven by a thermostable DNA polymerase, which amplifies the target sequence flanked by two primers in the presence of nucleotides. Repeat cycles of heating and cooling in a thermocycler allow DNA denaturation, primer hybridisation (annealing), and primer extension, resulting in exponential amplification of the target: the number of target DNA molecules theoretically doubles after each cycle, providing the reaction efficiency is 100% [182].

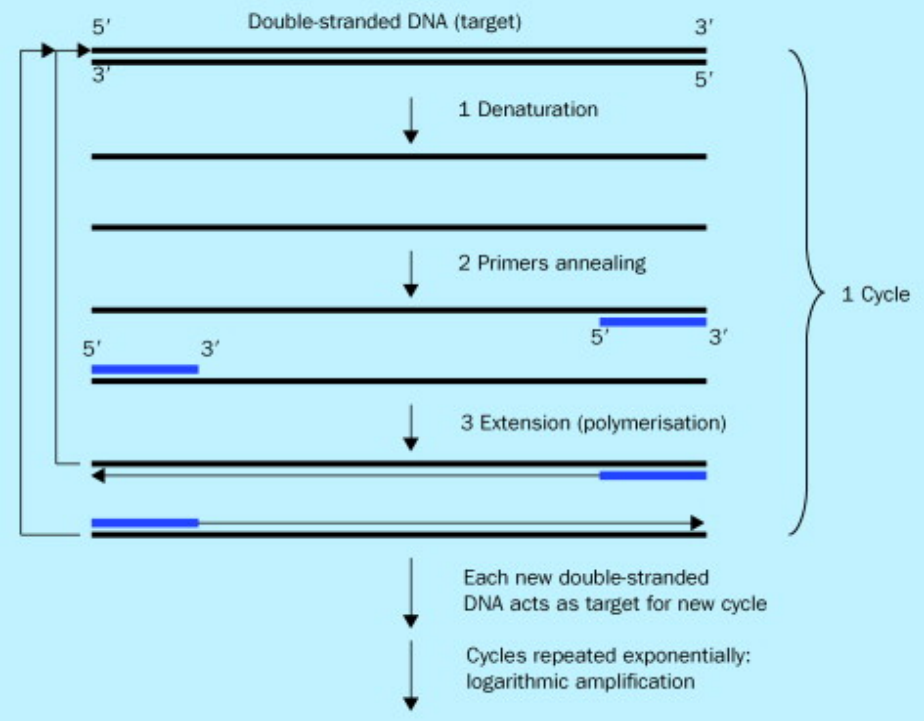

Figure 3.1: Schematic of the polymerase chain reaction: within a thermocycler DNA template is (1) denatured into single-stranded DNA; (2) primers anneal to complimentary sequence; (3) DNA polymerase extends primers to generate a new copy of the target DNA. The cycle is repeated, with newly synthesized strands of target DNA acting as further templates for subsequent cycles. Schematic unmodified from Yang et al. [182]

Following widespread use of conventional PCR, real-time PCR or quantitative (qPCR) was introduced as a further development of this method for detection and quantification of nucleic acids. The technique was pioneered by Russell Higuchi, who first described its use in 1993 [183]. Higuchi and colleagues utilised the fluorescence enhancement produced when DNA-binding dye ethidium bromide binds to dsDNA, allowing monitoring of fluorescence corresponding to increasing cycles of amplification. During the PCR reaction process, as dsDNA is produced, instead of measuring the amount of

PCR product produced at the end of thermocycling using gel electrophoresis (e.g. competitive PCR) [184] [185]. Higuchi *et al.* employed kinetic analysis of fluorescence in real-time (continual monitoring during the annealing/extension phase). This real-time monitoring allowed calculation, by backward extrapolation, of the starting number of DNA targets and was advantageous for DNA detection over a wide dynamic range, including investigation into the effect of different reaction conditions on PCR kinetics [183]. The ability of qPCR to detect target sequences reliably from a range of samples has led to its widespread use, for example, in agricultural, forensic, medical and historical settings [186].

DNA detection systems in qPCR have subsequently evolved to include probes: molecular beacons [187], hydrolysis and scorpion probes, although dsDNA intercalating dyes, for example cyanine dyes such as SYBR® Green are still used in some settings.
Probes are single-stranded nucleic acid molecules, with a sequence which is complementary to that of the target nucleic acid. A fluorescent moiety is attached to one end and a non-fluorescent quenching moiety to the other end. When the moieties are in close proximity to each other, the fluorescence of the fluorophore is quenched by fluorescence resonance energy transfer (FRET). When the fluorophore is not in close proximity to the quencher and is illuminated by ultraviolet light, it fluoresces [187].

In a TaqMan PCR assay a pair of primers and a non-extendable probe are used. The probe is a hydrolysis probe which binds to the target within the region delimited by the primers. As the probe is an oligonucleotide, its binding to its complimentary sequence can enhance an assay's specificity. Typically, the 5' terminus of the probe is labelled with a fluorophore (reporter) and the 3' terminus with a quencher. Dyes such as FAM™ or VIC™ are popular choices for the reporter, with TAMRA™ used for the quencher dye. As the reaction proceeds, the TaqMan probe hybridises to the target sequence downstream of one of the primers (Figure 3.2). The upstream primer begins to be extended and the *Taq* polymerase-mediated 5' to 3' hydrolysis of the probe begins. This exonuclease activity of *Taq* polymerase results in removal of any sequences in the enzyme's path. As a result, the probe is dissociated, and the fluorophore and quencher are no longer in close proximity to each other, disrupting the FRET and resulting in dye release. Upon subsequent illumination, fluorescence is detectable with a dye-specific wavelength and this fluorescence signal is proportional to the amount of accumulated

PCR product [188]. Quantification of DNA target may be achieved either through absolute or comparative quantification. Absolute quantification describes estimation of target copy numbers by reference to a standard curve constructed using a defined concentration of standards. Comparative (relative) quantification estimates the relative change in target copy numbers in relation to a reference (e.g. GAPDH); however, it relies on the assumption that the amplification efficiencies of the target and reference are very similar [189]. The fluorescence generated is reliant on complementarity between the TaqMan probe and the DNA template sequence, if there are mismatches between the sequences, failure appropriately to detect the DNA template may occur [190].

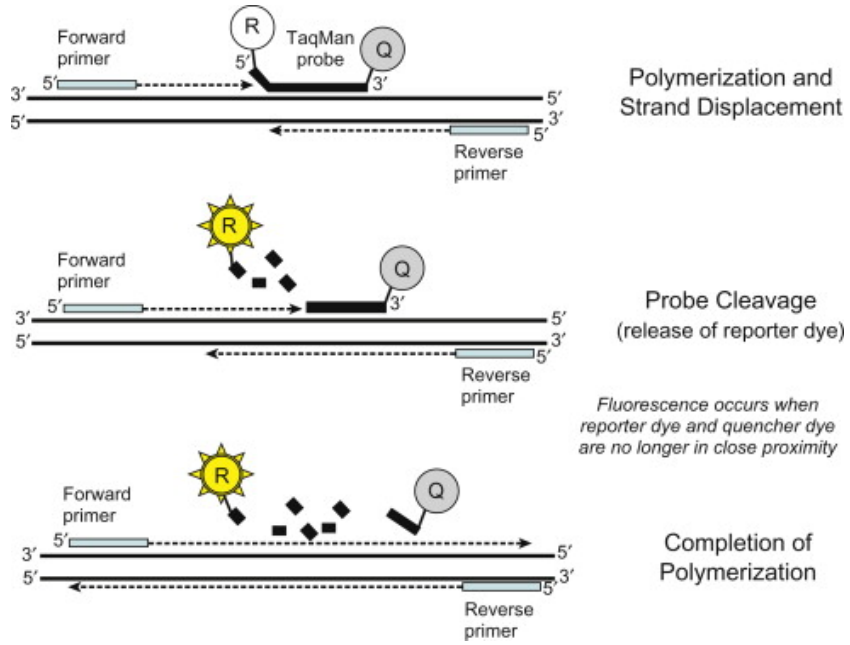

Figure 3.2: TaqMan 5’ nuclease activity [190]

The typical workflow for PCR primer design consists firstly of defining the target and designing primers, then testing specificity *in silico* with primer BLAST and finally screening for dimers. Next, primers may be characterised to determine optimum annealing temperatures and concentrations by performing a gradient PCR and generating a concentration matrix, respectively. If there are several primer candidates, then the optimal primer combination is determined. Next, specificity for target is determined by testing a panel of related and common heterologous DNA extracts – known as a specificity panel. In the case of a PCR to detect a particular species of bacteria, this panel would typically consist of DNA extracts from cultures of genetically-related but distinct species and of species typically found in the same milieu or habitat as the target organism.

Finally, serial dilutions of template are used to generate a standard curve for evaluating assay operating parameters such as: amplification efficiency, limits of detection and quantification, linearity and dynamic range [191] [192]. PCR amplification efficiency is given by the slope of the standard curve from linear regression of cycle quantification (C_q) value against log[quantity DNA], or log[quantity DNA] vs C_q value, depending on the error term of interest. With a ten-fold dilution series of DNA, if perfect doubling occurs with each amplification cycle, then the efficiency will be 100%, given by a C_q value increase of 3.3 for every ten-fold dilution, or 0.3 when log[quantity DNA] is given as the response variable. Deviations from this workflow may occur depending on the purpose of the assay. For example, typically research assays do not require as stringent assessment of operating parameters as diagnostic assays.

Historically, surveillance of *Pasteurellaceae* either from healthy animals or those suffering with BRD has largely relied on culture. PCR assays designed to detect *H. somni*, *M. haemolytica* and *P. multocida* and published prior to starting the studies presented in this thesis are shown in Table 3.1. Of these assays, only one was demonstrated to detect target species directly from clinical samples (trans-tracheal fluid) [148], whilst one other had the capability of quantification [151]. For the majority of assays described in Table 3.1, amplicon sizes were large and therefore primers were only suitable for use with conventional PCR. Generally, PCR assays have been developed to aid rapid detection of species from clinical cases, most commonly by culture-amplified PCR, which still requires initial culture of the clinical specimen and may employ transport media not suitable for PCR. Skim milk, tryptone, glucose, glycerol (STGG) broth is recommended by the World Health Organisation for studies investigating nasal carriage of *Streptococcus pneumoniae* [193] and is commonly used in human respiratory studies as a transport and storage medium suitable for bacterial culture and PCR [171] [83] [194] but, it has not been evaluated for use with *Pasteurellaceae* in veterinary settings. Cross-reactivity with closely-related species for *M. haemolytica* and *P. multocida* was reported for the assays presented in Table 3.1. However, published gene targets and primers showed potential for further development.

3.1.1 Objectives

The objectives of the work presented in this chapter were to evaluate, optimise and validate three real-time PCR assays for detection and quantification of *H. somni*, *M. haemolytica* and *P. multocida* from pure cultures and directly from bovine nasal swabs.

Table 3.1: Published PCR assays for *H. somni*, *M. haemolytica* and *P. multocida*

Species	**Gene Target**	**Amplicon size (bp)**	**Comments**	**Reference**
H. somni	16S rRNA	400		Angen et al. [152]
H. somni	16S rRNA	160		Mahony and Horwood [195]
M. haemolytica	*lkt*	170 and 206	Multiplex PCR for: *M. haemolytica, M. ruminalis*, and *M. glucosida.* Two regions of the leukotoxin D gene were targeted. Unable to distinguish *M. haemolytica* from haemolytic *M. ruminalis* strains encoding segments of the *leukotoxin* operon	Alexander et al. [48]
M. haemolytica	*sodA*	143	Multiplex SYBR-green PCR for: *M. haemolytica, M. ruminalis*, *M. glucosida, M. varigena* and *M. granulomatis.* Cross-reactivity between *M. haemolytica* and *M. glucosida* – resolvable by melt-curve analysis.	Guenther *et al.* [151]
M. haemolytica	*lktC-artJ*	385	Based on gene sequence upstream of the lineage-specific leucotoxin operon (lktCABD). Assay also recognised *M. glucosida*	Angen et al [148]

Table 3.1 continued

Species	Gene Target	Amplicon size (bp)	Comments	Reference
P. multocida	*kmt1*	460	Targets outer membrane protein of all serogroups. Cross-reactivity with *P. canis* biotype 2 was observed.	Townsend et al. [150]
P. multocida	*pm0762; pm1231*	567 and 601	Putative transcriptional regulator genes	Liu et al. [157]
P. multocida	23S rRNA	1432	Performed on colonies on primary isolation plates. Cross-reactivity with *P. canis* biovar 2 and *P. avium* biovar 2	Miflin et al. [196]
P. multocida	*toxA*	846	Differentiation between toxigenic and non-toxigenic isolates	Lichtensteiger [197]
P. multocida	(A) *hyaD-hyaC*; (B) *bcb*; (D) *dcbF*; (E) *ecbJ*; (F) *fcbD*	511 - 1,044	Serogroup-specific multiplex-PCR for serogroups: A, B, D, E, F	Townsend et al. [198]
P. multocida	16S rRNA	74		Mahony and Horwood [195]

3.2 Materials and Methods

3.2.1 Bacterial culture

H. somni American Type Culture Collection (ATCC) 43625*, M. haemolytica* ATCC 33396 and *P. multocida* ATCC 43137 were used as positive control strains for culture and PCR assay development. All reference strains used in the study (Table 3.2) for PCR assay optimisation and specificity testing were cultured on Columbia blood agar supplemented with 5% sheep blood (CBA; Thermo Fisher Scientific, Basingstoke, UK) overnight at 37°C with 5% CO_2, except for *H. somni* and *Haemophilus influenzae*, which were cultured on Chocolate agar (E&O laboratories, UK) at 37°C, for 24 – 48 hours with 5% CO_2. All cultures were sub-cultured and Gram-stained to ensure purity. For long term storage, bacterial cells were harvested into Brain Heart Infusion broth or *Haemophilus* Test Medium (*H. somni* only) supplemented with 20% glycerol (Media Services, School of Cellular and Molecular Medicine, University of Bristol, UK) and stored at -70ºC.

Table 3.2: Bacterial strains used in this study

Species	Strain/reference designation	Source
Actinobacillus equuli	NCTC[†] 8529	Equine, blood
Actinobacillus ligieresii	NCTC 4189	Bovine, sub-maxillary gland
Actinobacillus pleuropneumoniae	NCTC 11383	Ovine, arthritis
Actinobacillus suis	APHA[‡] IS14-13758	Species unknown, liver
Bibersteinia trehalosi	APHA IS21-03264	Bovine, swab (location unknown)
Enterococcus faecalis	JH2-2	Unknown
Escherichia coli	ATCC®[§] 25922	Species unknown, clinical isolate
Fusobacterium necrophorum subsp. necrophorum	APHA C977	Species unknown, foot
Haemophilus parainfluenzae	UoB[¶], other carriage studies	Unknown
Histophilus somni	ATCC® 43625, type strain	Bovine, brain
Mannheimia glucosida	APHA IS14-07997[*]	Bovine, lung
(n = 5)	CCUG[¥] 38459	Ovine, lung
	CCUG 38460	Ovine, lung
	CCUG 38467	Ovine, lung
	CCUG 38457, type strain	Ovine, lung
Mannheimia granulomatis	APHA IS14-13861[*]	Bovine, lung
(n = 2)	CCUG 45422, type strain	Bovine, subcutaneous granuloma
Mannheimia haemolytica	ATCC® 33396, type strain	Ovine, location unknown
(n = 4)	V1-53-2	Bovine, nasal swab
	V1-71-1-(19)	Bovine, nasal swab
	V1-37-1	Bovine, nasal swab
Mannheimia ruminalis	CCUG 38470, type strain	Ovine, rumen
(n = 2)	APHA IS23-01503[*]	Bovine, pericardium

Table 3.2 continued

Species	Strain/reference designation	Source
Mannheimia varigena	APHA IS12-04533	Bovine, lung
Moraxella bovis	NCTC 11013	Bovine, eye
Moraxella bovoculi	UoB, V1-26-1	Bovine, nasal swab
Moraxella catarrhalis	ATCC® 25240	Unknown
Mycobacterium bovis	BCG, Glaxo	Unknown
Mycoplasma bovis	ATCC® 25523, type strain	Bovine, mastitis
Pasteurella canis biotype 2	NCTC 11621, type strain	Canine, throat
Pasteurella multocida	ATCC® 43137, type strain	Porcine, location unknown
(n = 4)	UoB, V1-38-5	Bovine, nasal swab
	UoB, V1-52-2	Bovine, nasal swab
	UoB, V1-41-1	Bovine, nasal swab
Pseudomonas aeruginosa	UoB, other carriage studies	Unknown
Rhodococcus equi	NCTC 10673	Unknown
Salmonella dublin	APHA R07571	Bovine, lung
Salmonella typhimurium	DT104 strain 30	Bovine, faeces
Staphylococcus aureus	ATCC® 25923	Clinical isolate
Streptococcus agalactiae	ATCC® 12403, type strain	Fatal septicaemia
Streptococcus pluranimalium	APHA C06551	Bovine, nasopharyngeal swab
Streptococcus suis	APHA 25	Bovine, lung
Truepella pyogenes	NCTC 5224	Porcine

* Strains not included in final specificity panel testing

† NCTC: National Collection of Type Cultures; ‡ APHA: Animal and Plant Health Agency;

§ ATCC®: American Type Culture Collection; ¶ UoB: University of Bristol;

¥ CCUG: Culture Collection University of Gothenburg

3.2.2 Preparation of reference strains for DNA extraction

To generate dilutions of reference strains used in specificity testing and as positive controls in PCR runs, frozen bacterial stocks (described above) were thawed, then ten-fold serially diluted by taking 100 µl of starting suspension into 900 µl STGG broth.

For *H. somni* (ATCC 43625)*, M. haemolytica* (ATCC 33396) and *P. multocida* (ATCC 43137), prior to DNA extraction a 300 µl aliquot of dilutions 10^{-1} to 10^{-10} were heat inactivated at 100°C for 10 minutes using a digital heat block (Grant Boekel, BBD, Grant Instruments, Cambridge, UK). Dilutions 10^{-3}, 10^{-4} and 10^{-5} from the

Mannheimia haemolytica and *Pasteurella multocida* dilution series, and 10^{-2}, 10^{-3} and 10^{-4} from *Histophilus somni* were included in specificity panel testing and as positive controls in all PCR runs. All dilutions (10^{-1} to 10^{-10}) were used in evaluating and informing selection of the optimum primer and probe combinations for *H. somni*, *M. haemolytica* and *P. multocida* assays described below in 3.2.5.

Frozen stocks of reference strains used in specificity panel testing were ten-fold serially diluted in L6 lysis buffer (Public Health England, Bristol, UK). DNA extraction proceeded no later than 2 hours post preparation (see Chapter 2, section 2.13). Each bacterial species in the specificity panel was included at dilutions 10^{-3}, 10^{-4} and 10^{-5}.

3.2.3 Validation of STGG broth as storage and transport media for *Pasteurellaceae*

For comparison of *Pasteurellaceae* growth pre- and post-freezing in STGG broth bacterial reference strains representing *H. somni, M. haemolytica* and *P. multocida* were cultured according to conditions described above and Gram-stained to ensure purity. Approximately 8 well-isolated colonies of *M. haemolytica* and *P. multocida* were transferred to 1.5 ml STGG broth. A 50 µl aliquot of this neat inoculum was ten-fold serially diluted with STGG. Dilutions 10^{-1} to 10^{-10} were plated in triplicate by transferring 50 µl of each dilution to the surface of an agar plate (CBA; Thermo Fisher Scientific, Basingstoke, UK) and spread evenly over the entire agar plate surface with a sterile plastic loop. Plates were incubated overnight at 37°C 5% CO_2.

For *H. somni* 8 well isolated colonies were transferred to Veterinary Fastidious Medium (VFM) (Oxoid, Basingstoke, UK) broth and incubated to log-phase of growth, described later in section 3.2.12. A 100 µl aliquot of this log-phase suspension was ten-fold serially diluted into STGG broth. Dilutions 10^{-4} to 10^{-7} were plated (100 µl) onto Chocolate agar (E&O laboratories, UK) and incubated overnight at 37°C 5% CO_2. Immediately after plating, dilutions were transferred to -70°C. Dilutions were frozen for a minimum of 24 hours, thawed on ice, and re-cultured under the same conditions as had been used for unfrozen aliquots. Colony counts were recorded after overnight incubation for all species.

3.2.4 Selection and design of primers and probes

Primer and probe (PP) selection was informed by previously published targets. PPs used and designed in the development of each PCR assay are given in Table 3.3. PPs were designed to detect *M. haemolytica* by targeting the *sodA* gene encoding manganese-dependent superoxide dismutase (Mn-SOD), as described previously by Guenther et al. [151]. Assays targeting *sodA* have shown improved ability to discriminate between species within the *Mannheimia* genus compared to corresponding 16S rRNA genes [151]. A novel probe (Mhae BVIP) was designed to work with published primers (Mhae-SGF & Mhae-SGR) and a novel set of primers, again targeting *sodA* (Mhae-BV1F & Mhae-BV1R). For the development of the *P. multocida* assay, *kmt1* encoding the outer membrane protein, described by Townsend et al. [150], was used as a target for which novel primers and probe sequences were designed. One forward primer (Pmulti-BV1F) and two reverse primers (Pmulti-BV1R & Pmulti-BV2R) were designed to work with a Taqman probe (Pmulti-BV1P) targeting *kmt1*. Published PP sequences targeting the 16S rRNA region of the *P. multocida* (Pmulti-TMF & Pmulti-TMR + Pmulti-TMP) and *H. somni* (Hsomni- TMF & Hsomni- TMR + Hsomni- TMP) bacterial genome were evaluated unmodified for both assays. No suitable published gene targets were found for *H. somni* at the time of development other than 16S rRNA. Both novel and unmodified published PP sequences (shown in Table 3.3) were evaluated and optimized *in silico* using Primer Express Software 3.0 (Life Technologies). For each bacterial target, primers were aligned to all available complete genomes on Genbank. Specificity of PPs was assessed *in silico* by BLAST searches and using the National Center for Biotechnology Information database (NCBI). Following *in silico* analyses, the PPs shown in Table 3.3 were synthesized by Sigma-Aldrich for wet lab analyses.

Table 3.3: Primer and probe sequences used for qPCR assay development

Target Species*	Primer/Probe	Primer / Probe Sequence (5'-3')	Length (bp)	Gene	Melting Point (°C)	Reference	Primer Combination	Amplicon size (bp)
Hs	Hsomni- TMF	AGGAAGGCGATTAGTTTAAGAGATTAATT	29	16S rRNA	58.8	Mahony and Horwood 2007	1	160
Hs	Hsomni- TMR	TCACACCTCACTTAAGTCACCACCT	25	16S rRNA	60.0	Mahony and Horwood 2007		
Hs	Hsomni- TMP	ATTGACGATAATCACAGAAGAAGCACCGGC	30	16S rRNA	69.7	Mahony and Horwood 2007		
Mh	Mhae-BV1F	GCGTGGTTAGTATTAGAAGAGGGTAAATTA	30	*sodA*	59.7	This Study	2	144
Mh	Mhae-BV1R	GAAACGCCTGCCACTTCTTT	20	*sodA*	58.1	This study		
Mh	Mhae-SGF	AGCAGCGACTACTCGTGTTGGTTCAG	26	*sodA*	65.6	Guenther et al. 2008	3	92
Mh	Mhae-SGR	AAGACTAAAATCGGATAGCCTGAAACGCC	29	*sodA*	68.7	Guenther et al. 2008		144
Mh	Mhae-BV1P FAM	AAGACTAAAATCGGATAGCCTGAAACGCCTG	26	*sodA*	68.4	This study		

Table 3.3 continued

Target Species*	Primer/Probe	Primer / Probe Sequence (5'-3')	Length (bp)	Gene	Melting Point (°C)	Reference	Primer Combination	Amplicon size (bp)
						Mahony and	4	74
Pm	Pmulti-TMF	CGCAGGCAATGAATTCTCTTC	21	16S rRNA	58.5	Horwood 2007		
						Mahony and		
Pm	Pmulti-TMR	GGCGCTCTTCAGCTGTTTTT	20	16S rRNA	58.3	Horwood 2007		
Pm	Pmulti-BV1F	CCGGCAAATAACAATAAGCTG	21	*kmt1*	56.2	This study	5	87
					51.5 –			74
Pm	Pmulti-BV1R	TGTTGAGCCAATCYGCTTCC	21	*kmt1*	56.6†	This study		84‡
					57.5 –		6	
Pm	Pmulti-BV2R	TGTTGAGCCAATCYGCTTCC	20	*kmt1*	62.0†	This study		
Pm	Pmulti-BV1P	ATAAATAACGTCCAATCAGTTGCGCCGT	28	*kmt1*	67.4	This study		
						Mahony and		
	Pmulti-TMP	ACTGCACCAACAAATGCTTGCTGAGTTAGC	30	16S rRNA	69.2	Horwood 2007		

* Hs: *Histophilus somni*; Mh: *Mannheimia haemolytica*; Pm: *Pasteurella multocida*

† Wobble base in primer gives two T_m values; Y = T or C; ‡ BVIF and BVI2R additional primer pair evaluated

3.2.5 Viability of primer and probe combinations

Following *in silico* primer design and evaluation, wet lab primer characterisation was undertaken. The *M. haemolytica* and *P. multocida* assays had more than one forward and reverse primer candidate, generating the PP combinations given in Table 3.3. There was one forward and reverse primer candidate as per Mahony and Horwood 2007 for *H. somni.* For each PP combination, assays were first run with molecular grade water (Sigma Aldrich) as template to ensure purity of PP stocks. PCR reactions were conducted as detailed in Chapter 2, section 2.14, with the exception of the *M. haemolytica* assay which was performed under standard Taqman cycling conditions: 95°C for 20 s hold stage, followed by 50 cycles of 95°C for 3 s and 60°C for 60 s.

Next, for each bacterial target species, nucleic acid was extracted from dilutions 10^{-1} to 10^{-10} of a ten-fold dilution series as detailed above in section 3.2.2. Nucleic acid was included in triplicate as template for evaluating the optimum PP combination for each PCR assay. The optimum PP combination for each target species was evaluated by assessing reproducibility between replicates, linearity of dilution series and dynamic range.

3.2.6 Specificity panel

To determine the specificity of the three assays, a panel of 40 bacterial strains (Table 3.2) were selected based either on genetic relatedness to target organisms, known involvement with respiratory disease in ruminants, or being common bacteria of different genera. Specificity panel bacteria were cultured overnight as described above and diluted 10^{-3}, 10^{-4}, 10^{-5} in L6 lysis buffer (Public Health England, Bristol, UK), followed by automated DNA extraction using a QIAsymphony SP instrument (as described previously in Chapter 2, section 2.13.3).

3.2.7 Sequencing *Mannheimia* spp. *sodA* gene

Under standard TaqMan cycling conditions as described above, cross-reactivity was observed between *Mannheimia haemolytica* ATCC 33396 and *Mannheimia glucosida* CCUG 38457 T in specificity testing. The forward primer Mhae-SGF is located in a constant region of the *sodA* gene, therefore the specificity for this PP combination is generated by the reverse primer. It was hypothesized that inadequate divergence in the reverse primer region of *sodA* between *M. haemolytica* and *M. glucosida* was responsible

for the observed cross-reactivity. To test this hypothesis, a new reverse primer, Mhae-TCR (detailed in Chapter 2, Table 2.2), was designed to anneal upstream of Mhae-SGR and work with Mhae-SGF, amplifying the corresponding partial *sodA* sequences of *M. haemolytica* and *M. glucosida* (Figure 3.3).

ATGGCATATACATTACCAGAATTAGGCTACGCTTATGAT
GCGTTAGAGCCACATTTCGATGCTAAAACAATGGAAAT
CCACCATTCTAAACATCACCAAGCTTACATCAACAATG
CAAATGCAGCATTAGAAGCTCACCCTGAATTATTAGAA
AAATGTCCGGGTGCATTAATCAAAGATTTGAGCCAAGT
GCCTGCAGAAAAACGTATTGCAGTGCGTAACAACGTA
GGTGGTCATGTAAACCACACTTTATTCTGGAAAGGTTT
AAAAACAGGCACTACCTTACAAGGTGCATTAAAAGAA
GCGATTGAGCGTGATTTCGGTTCAGTTGAAGCTTTCC
AATCAGAATTTGAAAAAGCAGCGACTACTCGTGTTGG
TTCAGGCTGGGCGTGGTTAGTATTAGAAGAGGGTAAA
TTAGCCGTTGTTTCAACCGCTAACCAGGACAACCCAC
TAATGGGTAAAGAAGTGGCAGGCGTTTCAGGCTATCC
GATTTTAGTCTTAGACGTTTGGGAACACGCTTACTACT
TAAACTACCAAAACCGCCGTCCGGATTTCATTAAAGCA
TTCTGGAACGTTGTAAACTGGGACGAAGCCGCTCGC
GTTTTGAAGAAAAAGTAGCAACCTGCGGTTGTGCGAA
ATAA

Figure 3.3: Partial *Mannheimia haemolytica sodA* gene with primer positioning. Bases in red indicate where the partial sequences start and end. Yellow highlights the Mhae-SGF and Mhae-SGR primer positions. Green shows bases within primers at which *M. haemolytica* differs from *M. glucosida*. Blue highlights the position of primer Mhae-TCR, upstream of Mhae-SGR.

3.2.8 Investigating divergence in partial *sodA* sequences of *Mannheimia* spp.

Divergence in partial *Mannheimia sodA* sequences between all species of the genus was investigated using eleven representative strains of *Mannheimia* shown in Table 3.4 (additional strain info given above in Table 3.2). Strains included *Mannheimia* spp. isolated from nasal swabs collected from healthy cattle housed on the North Wyke Farm Platform and confirmed through 16S rRNA sequencing (further details given later in section 3.2.15).

Table 3.4: *Mannheimia* strains used to investigate divergence in the *sodA* gene

Species	**Strain**
M. haemolytica	ATCC 33396
M. varigena	APHA IS12-04533
M. glucosida	CCUG 38457 T
M. granulomatis	CCUG 45422 T
M. ruminalis	CCUG 38470 T
M. glucosida	CCUG 38459
M. glucosida	CCUG 38460
M. glucosida	CCUG 38467
M. haemolytica	UoB, V1-53-2
M. haemolytica	UoB, V1-71-1
M. haemolytica	UoB, V1-37-1

The *Mannheimia* species listed in Table 3.4 were PCR-amplified using the primer pair Mhae-SGF & Mhae-TCR (primer details given in Chapter 2, Table 2.2). PCR runs were carried out using 96 well Framestar® Break-A-way plates sealed with FrameStrips™ (Brooks Life Sciences, 4titude, UK), performed on a Mx3005P qPCR instrument (Agilent Technologies, Santa Clara, USA). The PCR was performed in a 2 µl reaction mix containing: 9.5 µl Nuclease-Free Water (Promega, UK), 12.5 µl Go Taq Hot Start (Promega, Madison, USA), 1 µl forward primer (Sigma Life Science), 1 µl reverse primer (Eurofins, Ebersberg, Germany) and 1 µl nucleic acid template. Working concentrations of primers were 100 nM (diluted in AE buffer; Qiagen, Hilden, Germany). Brain heart infusion (BHI) broth and L6 buffer were included as negative controls.

Cycling conditions were performed using: 95°C for 10 minutes (1 cycle, hot start stage), followed by 40 cycles of 95°C for 1 minute 54°C for 1 minute, 72°C for 2 minutes and a final elongation step of 72°C for 10 minutes. PCR products were visualised on a 1% agarose gel; 10 µl product with 2 µl orange loading dye (Sigma Aldrich). Gels were prepared according to the recipe given in Appendix A. Gels were run at 100 V for ~70 min and included 3µl of a 50 bp and 100 bp ladder (Bioline, London, UK). Gels were visualised using a UV transilluminator instrument (Ultra-Violet Products Ltd, Cambridge, UK). A PCR product of 212 bp was expected. PCR products were purified using a QIAquick PCR purification kit (Qiagen) as per manufacturing protocols. Purified

products were sent to Eurofins Genomics (UK) for 16S rRNA sequencing. Chromatograms of respective returned sequences were inspected using SnapGene® Viewer software (Version 1.4.5, GSL Biotech, available at snapgene.com) and cleaned accordingly.

3.2.9 Multiple alignment of *Mannheimia* spp. partial *sodA* gene sequences

The neighbour-joining method from a multiple alignment analysis was performed in Clustal Omega software (Online version, accessed on 10/04/2017) [199]. A phylogenetic tree showing the relationship between *Mannheimia* partial *sodA* sequences was drawn. The *sodA* sequence of *E. coli* strain K-12 was used as an outgroup to root the tree [200]. Bootstrap values were estimated and shown on each branch.

3.2.10 Thermal gradient PCR

A thermal gradient PCR allows a range of annealing temperatures to be tested during the same PCR run. The lower and upper limits are specified by the user and the thermocycler software defines temperatures in-between these bounds. Thermal gradients can be used to ascertain optimum annealing temperatures.

A thermal gradient PCR was performed to ascertain the optimum annealing temperature for *M. haemolytica* without observing cross-reactivity with *M. glucosida*. The aim was to identify a temperature at which *M. haemolytica* was successfully amplified but *M. glucosida* was not. Representative strains of *Mannheimia* spp. (as detailed in Table 3.4) were used as nucleic acid templates in the PCR reaction. BHI broth and L6 buffer were included as "no template" negative controls. PCR runs were carried out as detailed above in section 3.2.8 with an alteration to cycling conditions, testing a range of annealing temperatures; between 54.4°C to 73.4°C (as shown in Figure 3.4). Cycling conditions were as follows: 95°C for 10 min (1 cycle, hot start stage), followed by 35 cycles of 95°C for 30 s, 54.4°C to 73.9°C for 30 s, and a final elongation step of 72°C for 1 min (1 cycle). Amplicons produced from the thermal gradient PCR were visualised on a 1% agarose gel as described in 3.2.8.

	1	2	3	4	5	6	7	8	9	10	11	12
A	54.4	54.9	56.6	59.1	61.0	62.9	65.0	66.7	68.8	71.1	73.4	73.9
B	54.4	54.9	56.6	59.1	61.0	62.9	65.0	66.7	68.8	71.1	73.4	73.9
C	54.4	54.9	56.6	59.1	61.0	62.9	65.0	66.7	68.8	71.1	73.4	73.9
D	54.4	54.9	56.6	59.1	61.0	62.9	65.0	66.7	68.8	71.1	73.4	73.9
E	54.4	54.9	56.6	59.1	61.0	62.9	65.0	66.7	68.8	71.1	73.4	73.9
F	54.4	54.9	56.6	59.1	61.0	62.9	65.0	66.7	68.8	71.1	73.4	73.9
G	54.4	54.9	56.6	59.1	61.0	62.9	65.0	66.7	68.8	71.1	73.4	73.9
H	54.4	54.9	56.6	59.1	61.0	62.9	65.0	66.7	68.8	71.1	73.4	73.9

Figure 3.4: Thermal gradient PCR temperature layout in a 96 well plate format with rows labelled A to H and columns 1 to 12

3.2.11 Sequencing *H. somni*, *M. haemolytica* and *P. multocida* PCR products

PCR products generated from amplification of positive control reference strains for each assay were purified using a QIAquick PCR purification kit (Qiagen, CA, USA) according to the manufacturer's instructions and sequenced (Eurofins Genomics, Ebersberg, Germany) with identification based on BLAST analysis of the target 16S rRNA gene.

3.2.12 Growth curves in liquid broth culture

Logarithmic-phase (log-phase) liquid cultures of *H. somni*, *M. haemolytica* and *P. multocida* were used to construct a 10-fold dilution series for each organism, quantified at each dilution by culture and colony counting. Log-phase cultures were used to construct standard curves as most bacterial cells are viable during the log-phase of growth: the number of target gene copies detected in a given broth sample are likely to equate reasonably accurately to the number of viable bacteria. Growth curves were repeated on three separate days for *M. haemolytica* and *P. multocida* and twice for *H. somni* (biological replicates). *M. haemolytica* and *P. multocida* reference strains were grown in liquid medium as described in [201] & [202]. In brief, 4–6 colonies from pure plate cultures were used to inoculate 20 ml Brain Heart Infusion (BHI) broth (Media Services, School of Cellular and Molecular Medicine, University of Bristol) and incubated overnight at 37°C with shaking at 200 rpm. An aliquot of overnight inoculum was transferred to fresh BHI broth the next morning to achieve a starting optical density (OD) measured at 600 nm (Thermo Spectronic Genesys 6, Thermo Electron Scientific Instruments LLC, WI, USA) of 0.05 (approximately 10^7 CFU/mL). After 1 hour, and at subsequent regular intervals, 1 ml aliquots were taken for further OD measurements until

stationary phase was reached. A final reading was taken at 24 hours. For *H. somni,* Veterinary Fastidious Medium (VFM) (Oxoid, Basingstoke, UK) was directly inoculated with 4–6 colonies from pure plate culture (starting OD of 0.05 at 600 nm, approximately 10^7 CFU/ml) and incubated at 37°C, with shaking at 200 rpm and 5% CO_2 [203]. For all 3 bacterial species, at late log-phase, a 100 µl aliquot of liquid culture was taken and 10-fold serial dilutions prepared in 900 µl STGG. For *M. haemolytica* and *P. multocida,* 50 µl aliquots of dilutions 10^{-3} to 10^{-8} of the series were plated out in triplicate onto BHI agar. For *H. somni*, 100 µl aliquots from dilutions 10^{-3} to 10^{-8} were plated onto Chocolate agar in triplicate. All plates were incubated for 12–24 hours at 37°C, in 5% CO_2 for colony counts. Counts over 750 were considered too numerous to count and where necessary were extrapolated from higher dilutions yielding lower counts. Bacterial counts were performed in triplicate and the mean expressed as $\log_{10}$ colony count/ml. After plating, the dilution series was immediately cooled and held frozen at -70°C.

3.2.13 Real-time PCR standard curves

Liquid broth cultures of each bacterial species were used to generate qPCR standard curves [171] which were used to evaluate assay performance and to quantify template from bovine nasal swabs. Dilutions of liquid cultures for each organism (described above) were thawed on ice and a 300 µl aliquot of each dilution (10^{-1} to 10^{-10}) was inactivated at 100°C for 10 minutes using a digital heat block (Grant Boekel, BBD, Grant Instruments, Cambridge, UK) [171]. Successful inactivation was confirmed through appropriate plate cultures for each species. Nucleic acid was extracted from all dilutions and PCR runs were conducted for each bacterial species as described above.

Standard curves were generated by linear regression of cycle quantification (C_q) values versus $\log_{10}$ CFU/ml values for corresponding 10-fold serial dilutions of broth cultures. Five technical replicates of C_q values were performed at each dilution. The linear operating range, C_q cut-off value and amplification efficiency were determined for each assay. The amplification efficiency (*E*) was calculated based on the slope of the standard curve as follows: $E\ (\%) = (10^{-slope} - 1) \times 100$. The endpoint dilution of the standard curve at which tested samples were positive was used to determine C_q cut-off values.

3.2.14 Bacterial culture of bovine nasal swabs

For validation of PCR assays, a subset (n = 60) of bovine nasal swabs (collected as part of the study detailed in Chapter 4) were cultured and assayed using the PCR assays developed in this chapter to detect *H. somni*, *M. haemolytica* and *P. multocida*. Both culture and sequencing were used to re-confirm PCR results.

Nasal swabs were thawed on ice, vortexed and a 50 µl broth aliquot was spread over the entire agar surface for isolation of *Pasteurellaceae* [204] and were cultured onto CBA, *Pasteurella* selective agar and MacConkey agar with salt (Thermo Fisher Scientific, Basingstoke, UK) for detection of *M. haemolytica* and *P. multocida. Haemophilus* selective agar (Thermo Fisher Scientific, Basingstoke, UK) and Chocolate agar plates (E&O laboratories, UK) were used for the enumeration of *H. somni.* Plates were cultured in an atmosphere containing 5% CO_2 at 37°C for 16 – 72 hours and were examined after 16 hours. Colonies phenotypically resembling *M. haemolytica* or *P. multocida* were subcultured onto CBA and presumptive *H. somni* colonies were subcultured onto Chocolate agar. Prior to further testing, colonies were Gram-stained to ensure purity. Bacterial identification was done according to standard microbiological techniques for *H. somni* [205], *M. haemolytica* [206] and *P. multocida* [207]. Briefly, isolates' species were confirmed based on characteristic colony morphology, Gram stain, oxidase, catalase, indole and growth on MacConkey agar. Further identification was performed using biochemical strips, either API 20NE (*M. haemolytica* and *P. multocida*) or API NH (*H. somni*) as per the manufacturer's protocol (bioMérieux, Basingstoke, UK). The bacteriology workflow followed is summarised in Figure 3.5. For long term storage, bacterial cells were harvested into Brain Heart Infusion broth or *Haemophilus* Test Medium (*H. somni* only) supplemented with 20% glycerol (Media Services, School of Cellular and Molecular Medicine, University of Bristol, UK) and stored at -70ºC.

For isolates giving doubtful biochemical results, phenol red carbohydrate fermentation tests were carried out to aid identification. Sucrose, trehalose, mannitol or lactose (0.5 ml) were aseptically added to 4.5 ml peptone broth containing a Durham tube. The broth was inoculated with ~12 well-isolated colonies and incubated overnight aerobically at 37°C. Broths were observed for a yellow colour change, indicating carbohydrate fermentation/acid production and production of gas (further details given in Appendix B, Table B.1).

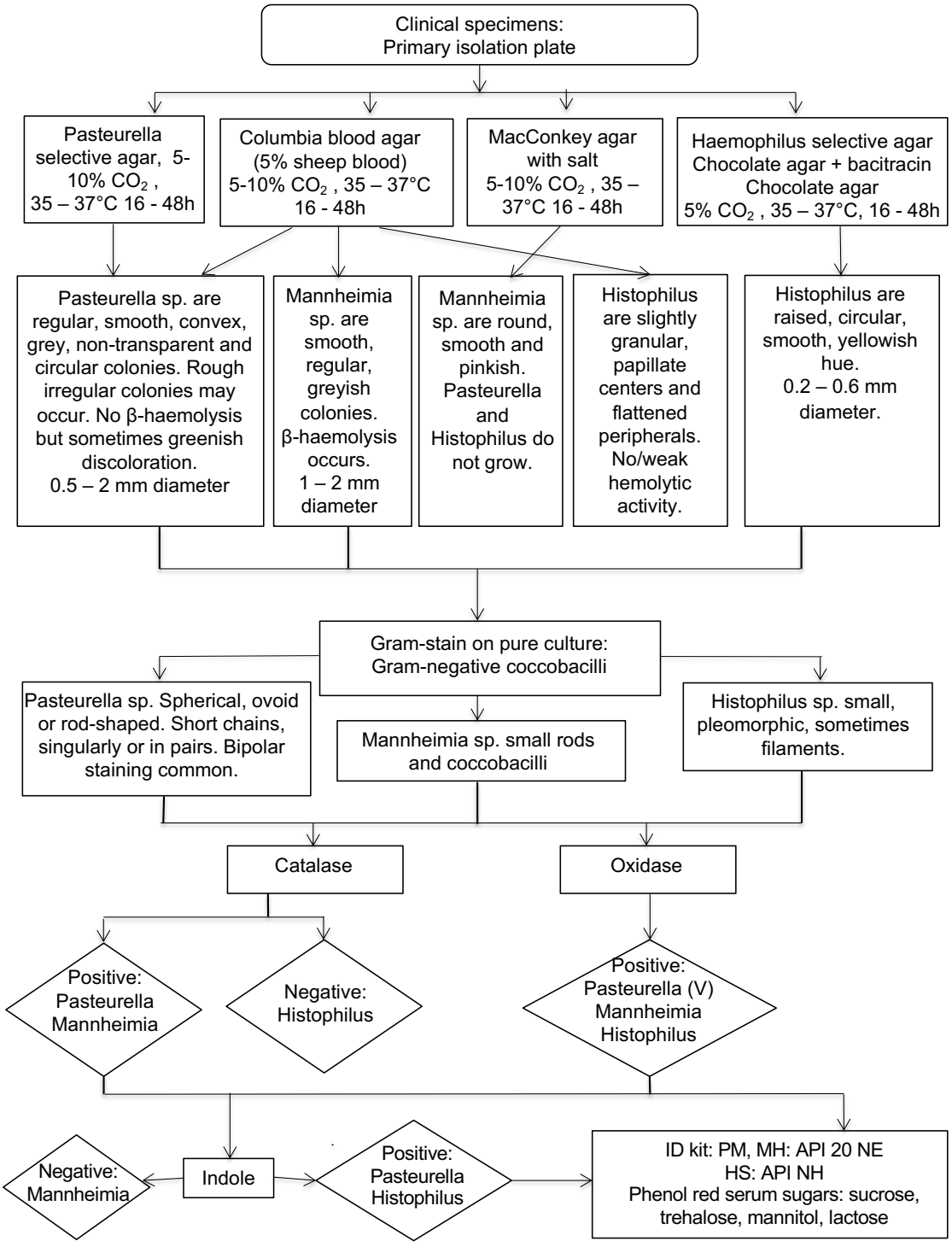

Figure 3.5: Flow chart illustrating identification of *Pasteurellaceae* species using culture.

3.2.15 Sequencing bacterial isolates

Bacterial isolates cultured from nasal swabs and either classified as *H. somni, M. haemolytica* or *P. multocida,* or with presumptive but unconfirmed bacteriology were amplified using an in-house real-time SYBR green PCR assay, developed at University of Bristol (Bristol Veterinary School, Infection and Immunity Department). Two sets of universal primers (primer pair 1 and 2) designed to target two variable regions of 16S rRNA were used. Full details are given previously in Chapter 2, section 2.16. PCR products were purified using a QIAquick PCR purification kit (Qiagen, CA, USA) according to the manufacturer's instructions and sequenced (Eurofins Genomics, Ebersberg, Germany) with identification based on BLAST analysis of the target 16S rRNA gene.

3.2.16 Data analysis

3.2.16.1 Variability in colony-forming units after freezing

The coefficient of variation (expressed as a percentage; %CV) was calculated to estimate the variability observed in replicate colony-forming units obtained from triplicate plating of each ten-fold serial dilution series of reference strain in STGG broth. The difference between mean counts produced at each dilution of the series pre-and post-freeze was calculated as a percentage change. The %CV was calculated as follows: -

$$Coefficient\ of\ variation\ (\%) = \frac{standard\ deviation}{mean} \times 100$$

3.2.16.2 Generation time of reference strains

The generation time (doubling time) of each bacterial reference strain cultured in liquid medium was estimated during the exponential phase of growth. First, a logistic model was fitted to each bacterial growth curve (given by temporal reads of optical turbidity, OD_{600}) using the R package 'Growthcurver' [208]. Growthcurver fits a basic form of the logistic equation commonly used to evaluate bacterial population dynamics. The logistic equation below gives the number of cells N_t at time t. Growthcurver finds the best values of: K, the maximum possible population size or carrying capacity; r, the population growth rate; and N_0, the population size at the beginning of the growth curve: -

$$N_t = \frac{K}{1 + \left(\frac{K - N_0}{N_0}\right) e^{-rt}}$$

The generation time was estimated according to: -

$$Generation\ Time\ (\tau_g) = \frac{\ln(2)}{r}$$

3.2.16.3 PCR variability

Variability between cycle quantification (C_q) values was assessed by calculating the %CV. For the different primer and probe combinations evaluated, the variability between C_q values at each dilution between technical replicates was assessed. The inter- and intra-assay variability between C_q values for both technical replicates and biological replicates of qPCR standard curves was also calculated.

3.2.16.4 PCR standard curves

At each dilution of the standard curve, bacterial counts were performed in triplicate and the mean expressed as $\log_{10}$ colony count/ml. A linear regression model was fitted to colony counts and C_q values obtained from liquid culture as described above. The $\log_{10}$ mean colony count/ml was considered as the response variable. Mean C_q value (n = 5) was an explanatory variable. The degree of linear correlation between the response and the explanatory variable was estimated for each standard curve by calculating the coefficient of determination (r^2). A parallel lines model was fitted to allow for differences in the intercept between biological replicates of the growth curves, obtaining the best estimate of the slope by assuming an additive effect of each biological replicate. After fitting a parallel lines model, a predictive model was produced for each species using the mean intercept across the biological replicates. All analyses were performed in R version 3.5.0, using base functions. C_q values obtained from collected nasal swabs were converted to genome copies/ml by interpolation using the predictive models. *In vivo*, clinical samples are likely to contain both viable and non-viable bacterial cells. Accordingly, colony forming units/ml (CFU/ml) and genome copies/ml cannot be used interchangeably for these assays, and genome copies/ml are presented.

3.3 Results

3.3.1 Bacterial culture

Plate cultures for *H. somni*, *M. haemolytica* and *P. multocida* reference strains conformed to described and accepted macroscopic, microscopic and biochemical characteristics (characteristics used to differentiate isolates are given in Appendix B, Table B.1).

3.3.2 Validation of STGG broth as storage and transport media for *Pasteurellaceae*

Cells of *H. somni*, *M. haemolytica* and *P. multocida* were ten-fold serially diluted in STGG broth, quantified and frozen at -70°C. Post freezing, bacterial cells were thawed and quantified. Viability of bacterial cells after freezing was assessed by comparing plate counts of the ten-fold dilution series obtained before and after. All reference species were viable following freezing, evident through overnight growth on solid agar (Table 3.5). For all species, as the starting inoculum became more dilute the colony counts decreased (count data not shown), and the variability between replicate colony-forming units increased (evident though increasing %CV values). Colony-forming unit counts were similar for *H. somni* and *M. haemolytica* pre- and post-freeze, although a slight decrease was observed (Table 3.5). *P. multocida* was recovered from all dilutions which had viable colonies present pre-freezing; however, cell counts were reduced to a greater extent compared to *H. somni* and *M. haemolytica* (1 order of magnitude less post-freeze). In addition, variability in colony-forming unit counts between pre- and post-freezing was generally greatest for *P. multocida* (Table 3.5).

Table 3.5: Recovery of *H. somni, M. haemolytica* and *P. multocida* from skim milk, tryptone, glucose, glycerol broth: mean colony-forming unit (CFU) counts pre and post-freezing of bacterial cells stored in STGG broth

Species	**Dilution**	**Pre-freeze Mean CFU***	**%CV‡**	**Post-freeze Mean CFU***	**%CV‡**	**Percent change§**
H. somni	10^{-4}	4.85×10^{6}	9.1	4.16×10^{6}	NA	-14.2
	10^{-5}	5.87×10^{5}	7.1	6.00×10^{5}	NA	2.20
	10^{-6}	3.67×10^{5}	56.8	5.00×10^{4}	NA	-86.4
	10^{-7}	3.33×10^{3}	173.2	0	NA	100
M. haemolytica†	10^{-6}	1.50×10^{8}	4.7	1.27×10^{8}	7.3	-15.3
	10^{-7}	1.43×10^{8}	10.7	1.50×10^{8}	20	4.90
	10^{-8}	2.33×10^{8}	24.7	2.33×10^{8}	24.7	0
	10^{-9}	1.33×10^{9}	43.3	6.67×10^{8}	173	-49.8
	10^{-10}	0	NA	0	NA	NA

Table 3.5 continued

Species	Dilution	Pre-freeze Mean CFU*	%CV‡	Post-freeze Mean CFU*	%CV‡	Percent change§
P. multocida†	10^{-5}	3.73×10^{7}	11.7	1.27×10^{7}	5.6	-70.0
	10^{-6}	5.33×10^{7}	13.2	9.67×10^{6}	41.8	-81.9
	10^{-7}	3.33×10^{7}	45.8	6.67×10^{6}	86.6	-80.0
	10^{-8}	1.00×10^{8}	100	3.33×10^{7}	173.2	-66.7
	10^{-9}	3.33×10^{8}	173.2	3.33×10^{8}	173.2	0
	10^{-10}	0	0	NA	NA	NA

***** Mean colony-forming unit (CFU); dilution series plated out in triplicate and colony counts performed. The *H. somni* dilution series post-freeze was plated out once without replication.

† Colonies too numerous to count (>750 counts per plate) for dilutions 10^{-1} to 10^{-5} for *M. haemolytica* and for dilutions 10^{-1} to 10^{-4} for *P. multocida*.

‡ Coefficient of variation (%): variability in CFUs obtained from colony counts performed in triplicate.

§ Percent change: difference in mean CFUs pre- and post-freezing (%).

3.3.3 In-silico analysis of primer and probe combinations

Primers and probes (PPs) for each bacterial assay were aligned to all available complete genomes on Genbank. All PPs were demonstrated as viable; amplicon sizes were well conserved, but primer positions were dependent on the particular strain used in the alignment (see Appendix B). No non-specific amplification of non-target strains *in silico* was detected by BLAST searches.

3.3.4 Wet-lab analysis of optimum primer and probe combinations

Primer and probe combinations for each qPCR assay were evaluated using a ten-fold dilution series of reference strains: *H. somni* ATCC 43625; *M. haemolytica* ATCC 33396; *P. multocida* ATCC 43137. Prior to extraction, ten-fold dilutions of reference strains were heat-inactivated. Successful inactivation was confirmed after observing no overnight bacterial growth on solid agar. To ensure purity of PP stocks, molecular grade water was used as template and amplified under standard TaqMan cycling conditions for each assay. For each PP combination, no amplification signal was produced.

One PP combination was evaluated for *H. somni* using type strain ATCC 43625. This PP showed high repeatability across C_q values obtained from assaying the dilution series in triplicate on the same run (%CV <3, shown in Table 3.6). Variation in C_q value was slightly increased at higher dilutions with less template. The dynamic range spanned across 6 dilutions.

Table 3.6: Inter-assay variability of *Histophilus somni* (ATCC 43625) amplification using primer and probe (PP) pair 1: TMF & TMR + TMP

PP Combination	Dilution	Replicate 1	Replicate 2	Replicate 3	%CV*
PP1: TMF & TMR + TMP	10^{-1}	15.667	15.909	15.679	0.866
	10^{-2}	18.805	19.120	19.071	0.892
	10^{-3}	21.952	22.574	22.241	1.39
	10^{-4}	25.574	26.037	25.789	0.898
	10^{-5}	28.950	29.764	29.198	1.42
	10^{-6}	34.136	33.585	32.199	3.00
	10^{-7}	UN†	UN	UN	NA‡
	10^{-8}	UN	UN	UN	NA
	10^{-9}	UN	UN	UN	NA
	10^{-10}	UN	UN	UN	NA

* %CV: coefficient of variation

† UN: undetermined. No template detected

‡ NA: not applicable, no target nucleic acid detected for calculation of coefficient of variation

To determine C_q values, a threshold value of 0.01 was set.

Figure 3.6 shows the amplification plot for *Histophilus somni* PP1 combination. The threshold for detection was set at 0.01, illustrated above the background and in the exponential section of the amplification curve. As expected, C_q values increased as template became more dilute. Template was not detected in dilutions 10^{-7} to 10^{-10}. Observed background was minimal. At lower starting template concentrations (C_q values of around 32), amplification curves at plateau phase were detected with lower absorbances compared to samples with higher quantities of template.

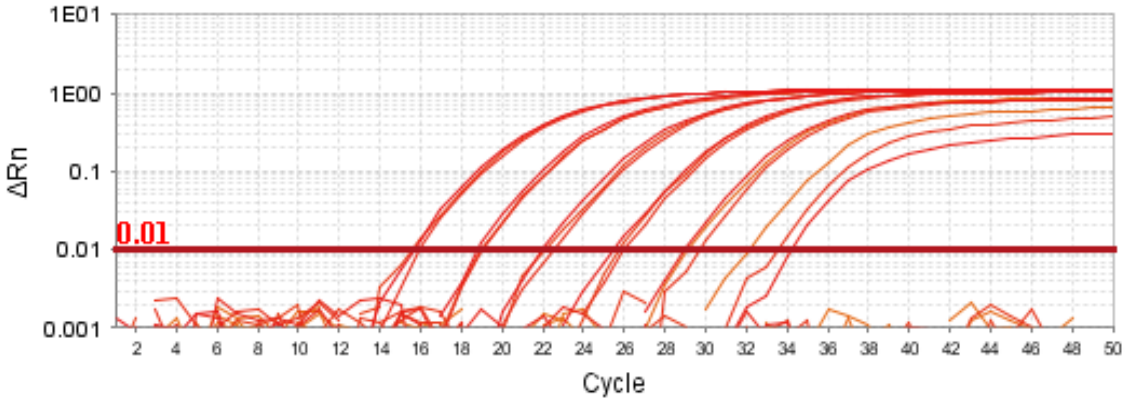

Figure 3.6: Amplification plot for *Histophilus somni* strain (ATCC 43625) over ten dilutions amplified using primer pair Hsomni-TMF & Hsomni-TMR and probe Hsomni-TMP. Delta Rn represents adjusted absorbance; cycle number is shown on the y-axis. Setting of the threshold is shown by a horizontal line at 0.01.

Of the two PP combinations tested for *Mannheimia haemolytica*, both were shown to be viable candidates, with PP3 (Mhae-SGF & Mhae-SGR + Mhae-BV1P-FAM) demonstrated to be optimum (Table 3.7). Amplification with PP2 extended across 7 dilutions, however amplification was not consistent between replicates of these dilutions, and inter-assay variability was higher (%CV < 22.3) compared to PP2 (%CV <1.82).

Table 3.7: Inter-assay variability of *Mannheimia haemolytica* (ATCC 33396) amplification using two primer and probe (PP) pairs: BVIF & BVIR + BVIP FAM and SGF & SGR + BVIP FAM

PP Combination	Dilution	Replicate 1	Replicate 2	Replicate 3	%CV*
PP2: BVIF & BVIR + BVIP	10^{-1}	14.859	14.728	14.845	0.486
	10^{-2}	17.763	17.926	22.086	12.7
	10^{-3}	21.152	21.216	30.583	22.3
	10^{-4}	24.777	24.512	UN	0.760
	10^{-5}	27.855	27.979	28.582	1.38
	10^{-6}	31.264	32.549	UN	2.84
	10^{-7}	UN	33.251	UN	NA‡
	10^{-8}	UN	UN	UN	NA
	10^{-9}	UN	UN	UN	NA
	10^{-10}	UN	UN	UN	NA
PP3: SGF & SGR + BVIP	10^{-1}	17.032	16.653	17.267	1.82
	10^{-2}	20.268	19.972	20.478	1.26
	10^{-3}	24.921	25.034	24.922	0.260
	10^{-4}	28.277	28.345	27.713	1.23
	10^{-5}	31.206	31.305	31.164	0.232
	10^{-6}	31.590	UN†	UN	NA
	10^{-7}	UN	UN	UN	NA
	10^{-8}	UN	UN	UN	NA
	10^{-9}	UN	UN	UN	NA
	10^{-10}	UN	UN	UN	NA

* %CV: coefficient of variation.

† UN: undetermined; no template detected.

‡ NA: not applicable, no target nucleic acid detected for calculation of coefficient of variation.

To determine Cq values a threshold value of 0.01 was set.

Figure 3.7 illustrates the amplification plot for *Mannheimia haemolytica* PP combination SGF & SGR + BVIP FAM. C_q values increased as starting template concentration decreased. Pronounced drop-off in absorbance at plateau phase for increasingly dilute samples was observed. Selection of the threshold at 0.01 is shown, the threshold was set above the background amplification and within the exponential phase.

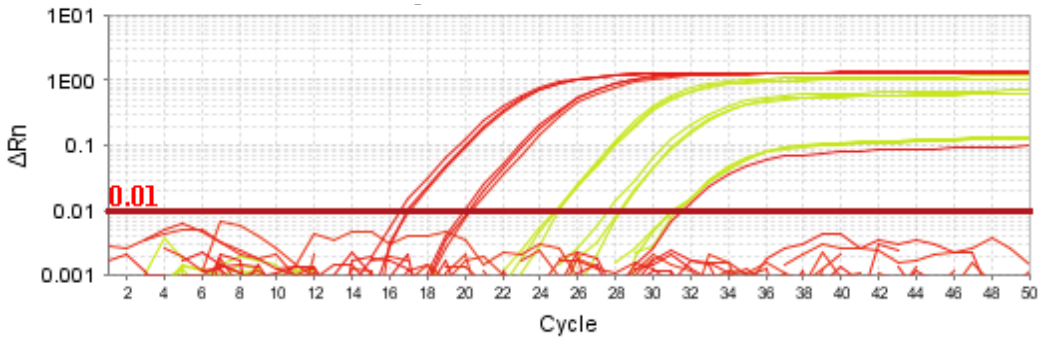

Figure 3.7: Amplification plot for *Mannheimia haemolytica* (ATCC 33396) using primer pair Mhae-SGF & Mhae-SGR + Mhae-BVIP. A ten-fold dilution series was run in triplicate, successful amplification was observed at dilutions 10^{-1} to 10^{-6}. The threshold was set at 0.01 shown by a horizontal line. Delta Rn represents adjusted absorbance; cycle number is shown on the y-axis.

Three different PP combinations were run against a ten-fold dilution of *P. multocida* type strain ATCC 43137. Of the three combinations tested all were shown to be viable (Table 3.8). PP combination 4 (TMF & TMR + TMP) showed the best repeatability, demonstrated by lowest observed variability (%CV < 2.72). Template was detected across 8 dilutions for this PP, however in dilution 8 only one of the three replicates was positive. Given its low inter-assay variability PP4 was selected as the optimum PP combination for further validation.

Table 3.8: Inter-assay variability of *Pasteurella multocida* (ATCC 43137) amplification using three primer and probe (PP) pairs: TMF & TMR + TMP; BV1F & BV1R + BVIP; BV1F & BV2R + BVIP

PP Combination	Dilution	Replicate 1	Replicate 2	Replicate 3	%CV*
PP4: TMF & TMR + TMP	10^{-1}	14.603	14.729	14.377	1.22
	10^{-2}	17.176	17.041	17.392	1.03
	10^{-3}	20.697	19.520	20.194	2.93
	10^{-4}	23.989	23.710	23.915	0.605
	10^{-5}	27.345	27.416	27.768	0.823
	10^{-6}	30.309	31.482	30.823	1.90
	10^{-7}	33.161	34.868	34.657	2.72
	10^{-8}	UN	UN	34.876	NA‡
	10^{-9}	UN	UN	UN	NA
	10^{-10}	UN	UN	UN	NA
PP5: BV1F & BV1R + BV1P	10^{-1}	12.978	12.484	12.559	2.10
	10^{-2}	15.855	15.313	15.385	1.90
	10^{-3}	18.868	18.272	18.427	1.67
	10^{-4}	22.253	21.902	21.869	0.967
	10^{-5}	24.787	25.643	25.345	1.72
	10^{-6}	28.776	28.617	28.536	0.426
	10^{-7}	31.711	33.759	31.466	3.90
	10^{-8}	UN	UN	33.571	NA
	10^{-9}	UN	UN	33.896	NA
	10^{-10}	UN	UN	UN	NA

Table 3.8 continued

PP Combination	Dilution	Replicate 1	Replicate 2	Replicate 3	%CV*
PP6: BV1F &					
BV2R + BV1P	10^{-1}	13.007	12.522	12.817	1.91
	10^{-2}	15.270	15.141	14.955	1.05
	10^{-3}	18.935	18.595	18.097	2.27
	10^{-4}	21.857	21.697	21.622	0.553
	10^{-5}	24.994	25.018	25.766	1.74
	10^{-6}	29.319	28.832	28.829	0.973
	10^{-7}	31.958	UN†	34.640	5.70
	10^{-8}	UN	UN	UN	NA
	10^{-9}	UN	UN	34.218	NA
	10^{-10}	UN	UN	UN	NA

* %CV: coefficient of variation.

† UN: undetermined; no template detected.

‡ NA: not applicable, no target nucleic acid detected for calculation of coefficient of variation.

To determine C_q values a threshold value of 0.01 was set.

Figure 3.8 shows the amplification plot for PP combination Pmulti-TMF & Pmulti-TMR + Pmulti-TMP. Template was not detected at dilutions 10^{-9} and 10^{-10}. Minimal background was observed for this assay. Selection of the threshold at 0.007 is shown, the threshold was set above background amplification and within the exponential phase.

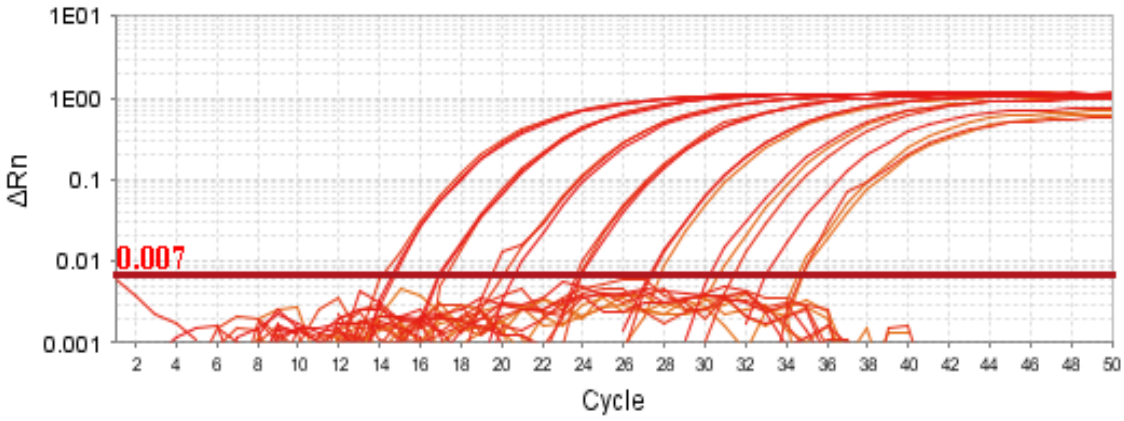

Figure 3.8: Amplification plot for *Pasteurella multocida* (ATCC 43137) amplified over ten dilutions using primer pair TMF & TMR and probe TMP. The threshold was set at 0.007 shown by a horizontal line. Delta Rn represents adjusted absorbance; cycle number is shown on the y-axis.

For all dilutions of each reference strain, the T4 internal amplification control assay C_q values were as expected, indicating successful DNA extraction with no evidence of PCR inhibition. Three dilutions from each reference strain's dilution series were selected to act as positive controls when assaying bovine nasal swabs. Dilutions 10^{-3} to 10^{-5} were selected for *M. haemolytica and P. multocida,* dilutions 10^{-2} to 10^{-3} were selected for *H. somni*. These dilutions had high reproducibility between replicates and were positioned within the dilution series such that C_q values obtained would be likely to be similar to those obtained for nasal swabs.

3.3.5 Specificity panel

To determine the specificity of the three assays, a panel of bacterial strains (Table 3.2) was tested for each assay using the optimum PP combinations determined above. For *H. somni* and *P. multocida* assays, all 3 dilutions of the heterologous bacterial strains comprising the specificity panel yielded negative results. For all species, no amplification was observed using no-template controls. Cross-reactivity was observed for *M. haemolytica* with *Mannheimia glucosida* APHA IS14-07997, *Mannheimia granulomatis* APHA IS14-13861 and *Mannheimia ruminalis* APHA IS23-01503. Sequencing of two variable regions of the 16S rRNA gene from strains revealed that the original identification of the isolates supplied was incorrect. The sequences were homologous to *Mannheimia haemolytica* when analysed using BLAST. Sequences for all ten strains supplied by APHA and amplified using primer pair 337F & 907R and 785F & 1100R are shown in Tables B.3 and B.4 of Appendix B, together with BLAST outputs. The specificity panel was repeated following replacement of these mis-identified type strains with *Mannheimia spp.* sourced from CCUG. However, cross-reactivity was again observed, this time with *Mannheimia glucosida* CCUG 38457 under standard TaqMan cycling conditions. Following optimization of annealing temperature (described later in section 3.3.7) no cross-reactivity with any heterologous species was observed. Successful inactivation using L6 lysis buffer prior to nucleic acid extraction of the reference strains used in the specificity testing was confirmed after observing no overnight bacterial growth on solid agar.

3.3.6 Sequencing *Mannheimia* spp. *sodA* gene

To investigate divergence within the *Mannheimia sodA* gene, a phylogenetic tree was constructed from a multiple alignment analysis of the *sodA* partial sequences obtained for the PCR products generated using primer pair Mhae-SGF & Mhae-TCR. The phylogenetic tree showed clustering of *sodA* partial sequences into four clades (Figure 3.9). Sequences relating to *M. haemolytica* appeared in their own clade and inspection of the reverse primer binding region revealed complete nucleotide homology among the four strains (Appendix B, Table B.5). Sequences relating to two strains of *M. glucosida* (38457T and 38459) occurred together and were a sister group to strains of *M. haemolytica*. *M. glucosida* 38460, *M. ruminalis* 38467 and *M. glucosida* 38460 appeared in a separate clade, but confidence for *M. glucosida* 38460 within this clade was low (34). Finally, *M. granulomatis* 45422T and *M. varigena* APHA appeared in one clade: a sister group to all other clades.

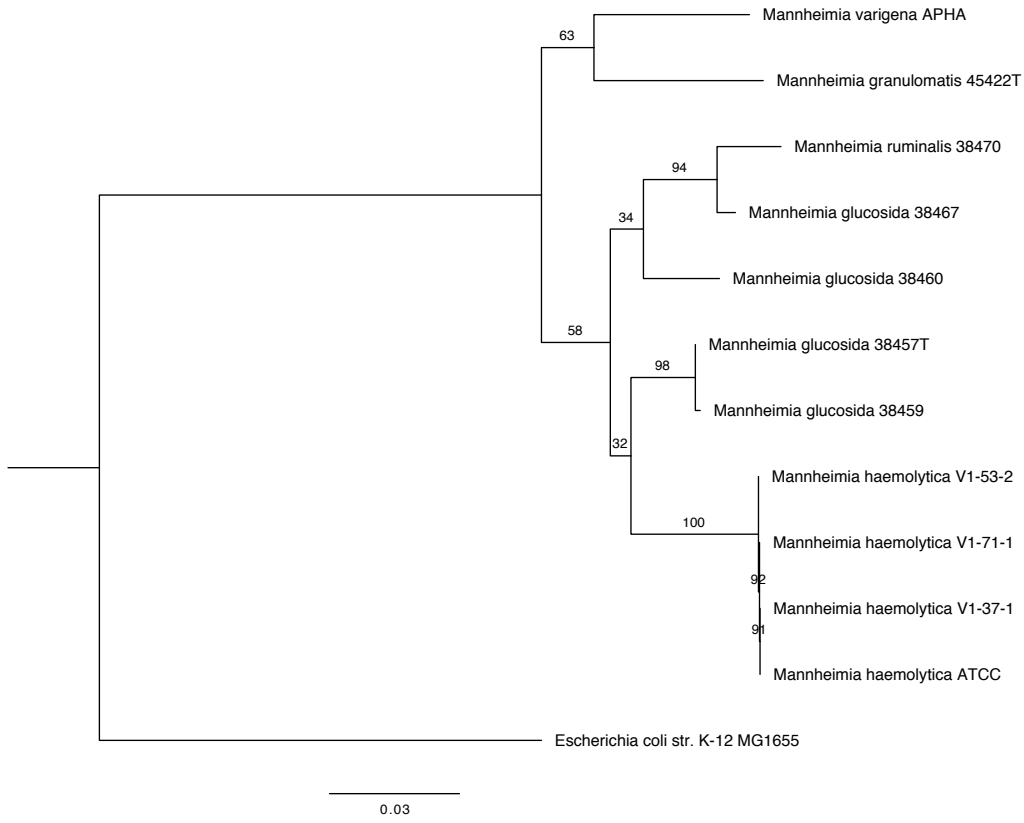

Figure 3.9: Phylogenetic tree showing the relationship among *sodA* gene sequences of *Mannheimia* species. The tree was constructed using the neighbour-joining method from a multiple alignment analysis of the *sodA* partial sequences obtained from amplification using primer pair SGF and TCR. The *sodA* sequence of *Escherichia coli* strain K-12 was used as an outgroup to root the tree. The value on each branch is the bootstrap value; the estimated confidence limit for the position of the branch.

3.3.7 Thermal gradient PCR: investigating *Mannheimia* spp. cross-reactivity

Divergence between partial *sodA* gene sequences of *Mannheimia* spp. (Figure 3.9) prompted further investigation into assay optimisation for the PP combination SGF & SGR + BVIP, with the aim of eliminating previously observed cross-reactivity between members of the *Mannheimia* genus.

A thermal gradient PCR was conducted, amplifying *Mannheimia* spp. over a range of temperatures. Gel electrophoresis of PCR products revealed a temperature range towards the upper end of the tested gradient (68.8 – 73.9 ºC) where PCR products were produced for *M. haemolytica* but not *M. glucosida* (Figure 3.10). Variability between *M. haemolytica* strains was observed (Figure 3.10, panels A - D), evident by PCR products produced at different temperatures for type strain *M. haemolytica* ATCC 33396 and nasal swab isolates of *M. haemolytica* (V1-71-1, V1-37-1, V1-53-2) collected from cattle on the North Wyke Farm Platform as described in Chapter 4. No amplicons were produced from *M. ruminalis* or no-template negative controls (BHI broth and L6 buffer), consistent with qPCR specificity results. Based on these findings a new annealing temperature of 69°C was selected to discriminate between *M. haemolytica* and *M. glucosida*. Previously tested cycling parameter conditions remained the same. No cross-reactivity to non-target species following repeat specificity panel testing was observed at 69°C annealing.

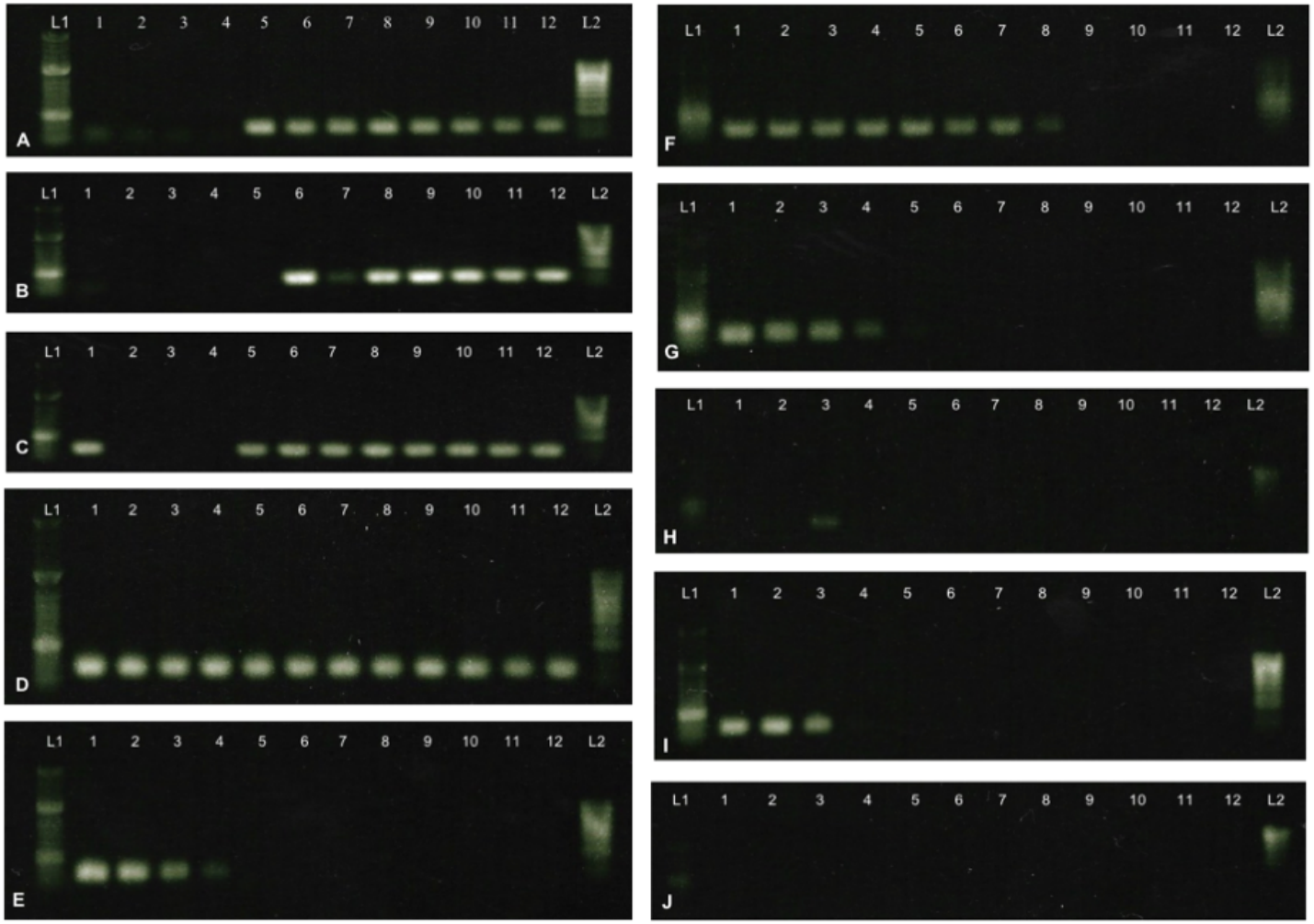

Figure 3.10: Agarose gel electrophoresis images representing *Mannheimia* spp.: (A) *M. haemolytica* ATCC 33396; (B) *M. haemolytica* V1-53-2; (C) *M. haemolytica* V1-71-1; (D) *M. haemolytica* V1-37-1; (E) *M. glucosida* 38457T; (F) *M. glucosida* 38467; (G) *M. glucosida* 38460; (H) *M. glucosida* 38459; (I) *M. granulomatis* 38470 T;(J) *M. varigena* APHA. PCR products amplified over a range of temperatures are shown in lanes 1–12 as follows: lane 1 = 54.4°C, lane 2 =54.9°C, lane 3 = 56.6°C, lane 4 = 59.9°C, lane 5 = 61.0°C, lane 6 = 62.9°C, lane 7 = 65.0°C, lane 8 = 66.7°C, lane 9 = 68.8°C, lane 10 = 71.1°C, lane 11 = 73.4°C and lane 12 = 73.9°C. L1 = 50bp molecular weight ladder and L2 = 100bp molecular weight ladder.

3.3.8 Growth curves in liquid culture

Pure cultures were maintained throughout growth curve studies for each bacterial species (*H. somni*, *M. haemolytica* and *P. multocida*), as confirmed by well-isolated colonies and pure Gram-stains of overnight plate cultures. Ten-fold serial dilutions yielded appropriate colony counts for all three bacterial species. Growth rates of *M. haemolytica* and *P. multocida* determined by optical density measurements were similar for the first 6 hours in liquid media. Thereafter the rise in optical density of *M. haemolytica* halted and then slowly declined, whilst *P. multocida* optical density continued to increase for a further 5 hours until stationary phase. Growth of *H. somni* reached the highest final optical density of the 3 (Figure 3.11). Using fitted logistic curves the estimated bacterial doubling times varied between species: *M. haemolytica* (27.9 minutes), *H. somni* (60.0 minutes) and *P. multocida* (80.4 minutes), see Appendix B, Figure B.1.

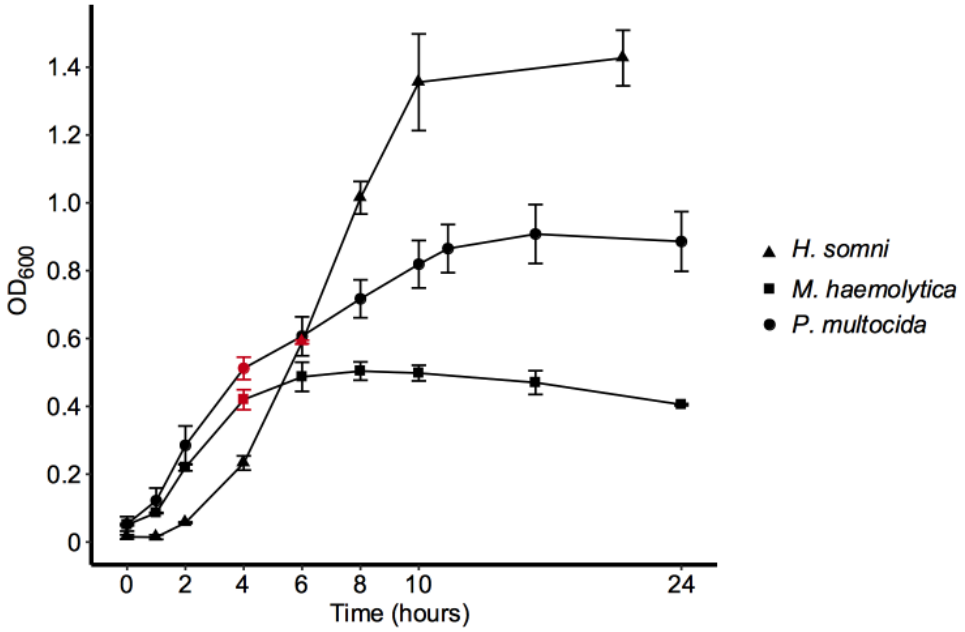

Figure 3.11: Liquid broth cultures of *Histophilus somni*, *Mannheimia haemolytica* and *Pasteurella multocida*. Optical density at 600nm of the cultures of the three species was measured approximately every 2 hours up to 24 hours. Timings of harvest of cells for generation of qPCR standard curves is shown in red at late log phase. The results are the mean optical density from two independent experiments (*H. somni*) and three independent experiments (*M. haemolytica* and *P. multocida*). Error bars represent the standard error of the mean.

3.3.9 Real-time PCR standard curves and assay performance

Cultures of *H. somni*, *M. haemolytica* and *P. multocida* in liquid medium were used to construct standard curves for each organism (Figure 3.12 and values given in Table 3.9) using the same PCR conditions used to amplify DNA targets in nasal swabs stored in STGG broth. Linear regression of C_q value versus observed and extrapolated $\log_{10}$ mean colony count/ml for corresponding 10-fold serial dilutions of bacterial broth cultures provided equations for conversion of C_q values to CFU/ml [171]. These equations were later applied to C_q values obtained from nasal swabs to obtain genome copies/ml. For all standard curve dilutions, bacteriophage T4 internal amplification controls gave C_q values as expected, indicating successful DNA extraction and providing no evidence of PCR inhibition.

All the assays were highly reproducible and repeatable for all bacterial species, producing consistent C_q values at each dilution of the standard curve for biological replicates tested on separate days (coefficient of variation, %CV <6), and for technical replicates performed on the same day of testing (%CV <4) (see Appendix B). For all standard curves, coefficient of determination values were high (r^2 >0.99). Amplification efficiency was >95% for both *M. haemolytica* and *H. somni* and lower for *P. multocida* at 84% (Table 3.9). For all three assays, DNA extracts from three dilutions of all the heterologous bacterial strains comprising the specificity panel (Table 3.2) yielded negative results following optimisation as described above (section 3.3.6 and 3.3.7).

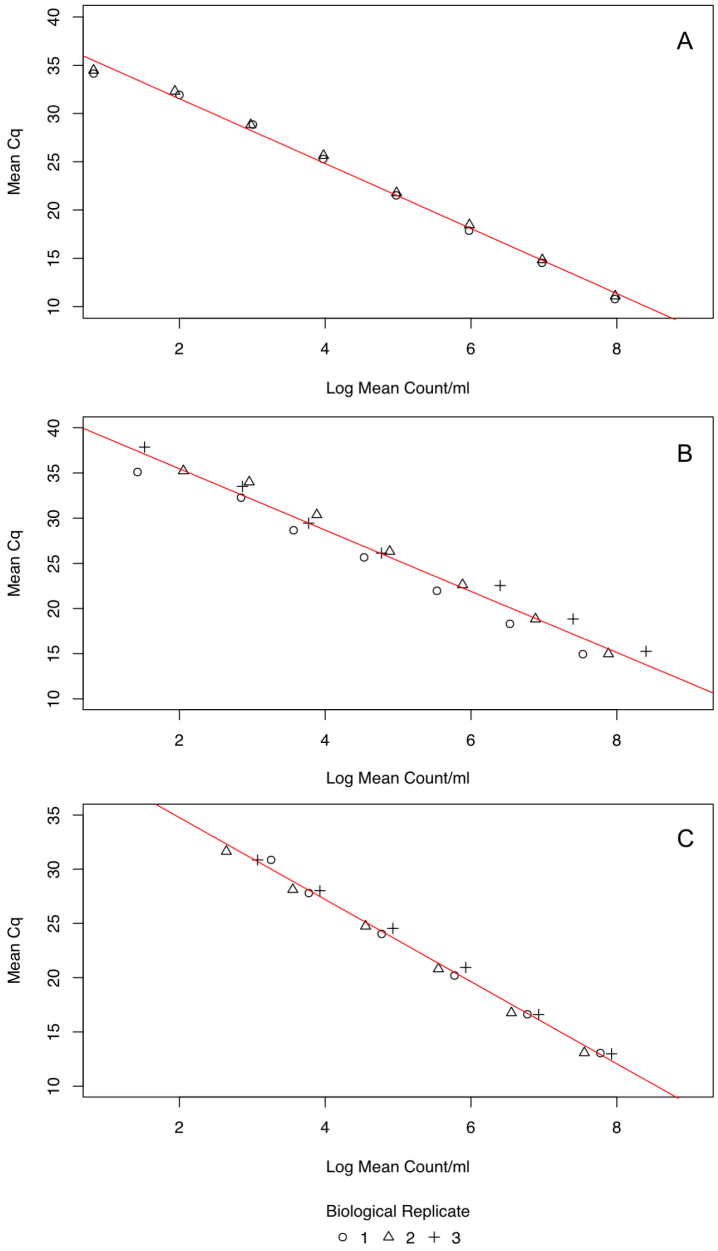

Figure 3.12: Standard curves for conversion of C_q values into genome copies/ml. *Histophilus somni* (panel A) liquid culture performed on two different days. *Mannheimia haemolytica* (panel B) and *Pasteurella multocida* (panel C) liquid culture performed on three different days. Mean C_q values were calculated from 5 technical PCR replicates at each dilution, for each biological replicate. Each biological replicate is represented by a symbol: circle, triangle or cross. Colony counts were performed in triplicate and expressed as the mean.

Table 3.9: Evaluation of *Histophilus somni*, *Mannheimia haemolytica* and *Pasteurella multocida* qPCR assays on pure log-phase broth cultures of reference strains

Assay characteristic		***Histophilus somni***	***Mannheimia haemolytica***	***Pasteurella multocida***
Standard Equation*				
	Slope (standard error)	-0.295 (0.00610)	-0.292 (0.00688)	-0.264 (0.00332)
	Intercept	11.3	12.4	11.2
	r^2	0.995	0.991	0.998
	Biological replicates	2	3	3
	Degrees of freedom (total)	13	17	14
Efficiency (%)†		97.5	96.0	83.5
Linear dynamic range (log_{10})		8	7	6
C_q cut-off value‡		35 cycles	34 cycles	35 cycles

* Linear regression of log_{10} colony count/ml against cycle quantification (C_q) value to generate standard equation for conversion of swab C_q value to genome copies/ml.

† PCR Amplification Efficiency (%) = $[(10^{-slope}) -1] \times 100$

‡ The C_q value corresponding to the endpoint dilution of the standard curve at which samples tested positive.

3.3.10 Sequencing of reference strain PCR products

PCR products of reference strains for each assay were sequenced and analysed using BLAST. All products had correct homology to target species (Appendix B, Table B.7).

3.3.11 Comparison of PCR with culture of bovine nasal swabs

Sixty nasal swabs collected from cattle (full details in Chapter 4) were cultured for the presence of *H. somni, M. haemolytica* and *P. multocida* and assayed by PCR. Culture results and their concordance to PCR are presented in Table 3.10. As only one swab was determined positive for *H. somni* by culture, PCR products from *H. somni* PCR-positive nasal swabs (n = 5) were sequenced to confirm identity. In all five, the sequences were representative of *H. somni* (Appendix B, Table B.7) as evident following Basic Local Alignment Search Tool (BLAST) searches: 100% homology to *H. somni* was seen for 3 of 5 queried sequences, 99% to the fourth and 98% to the fifth. For all 5 queried swab sequences there was homology between 96–100% for sequences deposited as 'uncultured bacterium clone', probably representing *H. somni*. One swab had 93% homology to one sequence deposited as *Actinobacillus capsulatus*. The majority of these swabs (43/60) were determined positive for *P. multocida* both by culture and PCR, with a smaller number PCR-positive and culture-negative (14/60). Fewer swabs were determined positive for *M. haemolytica* (4/60) both by culture and PCR. Similarly, a number (5/60) were PCR-positive and culture-negative. No swabs for any species were determined culture-positive and PCR-negative.

Table 3.10: Presence of *Histophilus somni*, *Mannheimia haemolytica* and *Pasteurella multocida* determined by culture and qPCR of bovine nasal swabs (n = 60)

Species	PCR	Culture	Total
H. somni	+	+	**1**
H. somni	-	+	**0**
H. somni	+	-	**28**
H. somni	-	-	**31**
M. haemolytica	+	+	**4**
M. haemolytica	-	+	**0**
M. haemolytica	+	-	**5**
M. haemolytica	-	-	**51**
P. multocida	+	+	**43**
P. multocida	-	+	**0**
P. multocida	+	-	**14**
P. multocida	-	-	**3**

Isolates obtained from culture of nasal swabs identified as *M. haemolytica* and *P. multocida*, or those with doubtful biochemistry were sequenced. Sequencing confirmed the identity of those identified as *M. haemolytica* and *P. multocida* by culture and consequently these isolates were included in the specificity panel. Biochemical testing of one isolate using API test strips suggested identification as *Moraxella*, sequencing confirmed this isolate to be *M. bovoculi* (Appendix B, Table B. B.2).

3.4 Discussion

Three real-time quantitative PCR (qPCR) assays were developed, optimised and validated for the detection and quantification of *Histophilus somni*, *Mannheimia haemolytica* and *Pasteurella multocida* from bovine nasal swab specimens and bacterial cultures. Real-time quantitative PCR offers a rapid platform to detect and quantify closely-related bacterial species from a range of clinical samples reliably. TaqMan real-time PCR assays use a probe alongside oligonucleotide primers to enhance an assay's specificity [208]. To my knowledge this is the first demonstration of qPCR assays capable of detecting and quantifying bacterial species directly from bovine nasal swabs.

Pre-existing published PCR assays may report potentially suitable primer targets and designed primer sets but their effective implementation across laboratories is not always reproducible. Between laboratories, extraction and purification methods, reagents and thermocyclers may differ. Consequently, if an assay has been published it may not work optimally in a different laboratory under different conditions [191] and optimisation is necessary. The *sodA* gene of *M. haemolytica* and 16S rRNA gene sequences of *H. somni* and *P. multocida* proved to be qPCR primer targets capable of separating these pathobionts from closely-related and common non-pathogenic bacterial species (Table 3.2). Evaluating specificity ensures species-specific amplification signals and no cross-reactivity to non-target bacterial species. Hitherto, discrimination between *M. haemolytica* and *M. glucosida* by PCR has generally relied either on analysis of melting curves following SYBR® green qPCR, or on the assumption that PCR positive samples are *M. haemolytica* because *M. glucosida* has not been implicated in clinical cases of bovine respiratory disease [148] [151]. The *M. haemolytica* qPCR assay presented here was able to discriminate successfully between all members of the *Mannheimia* genus using a TaqMan probe following optimisation of cycling parameters, in particular increased annealing temperature. Cross-reactivity with three isolates (*Mannheimia* spp.) provided by a UK reference laboratory was observed when first optimising the *M. haemolytica* assay: isolates were from clinical cases submitted to the reference laboratory and were identified as *M. haemolytica* using in-house culture techniques. Interestingly, following sequencing of these isolates their identification was not confirmed as *M. haemolytica* (Appendix B, Table B.3 and Table B.4). This further highlights the difficulty in accurately identifying this genus and adds value to using molecular techniques in addition to culture. Interestingly, microbiome publications

reporting the use of 16S rRNA and metagenomics-based approaches between 1995–2017 have been consistently increasing, whilst publications using culture were at their peak in 1995 and have steadily decreased since. Despite these trends, citations made in 2018 to microbiome publications published prior to 2000, and hence those largely employing culture are not declining, suggesting that the conclusions from culture are still valued [209].

For *P. multocida*, primers targeting the 16S rRNA gene sequence were shown to be superior over *kmt1*, targeting the outer membrane protein (Table 3.8). This was also true for *H. somni*, where the 16S rRNA gene sequence as described by Mahony and Horwood was suitable for detection and quantification in pure culture [195]. In accordance with these findings, 16S rRNA-dependent strain identification is regarded by most as the gold standard for molecular identification of bacterial species [210] [151] [211]. PCR amplification efficiencies estimated from standard curves were within the recommended ranges of 90–110% [212] for *H. somni* (97.5%) and *M. haemolytica* (96%). Lower efficiency for *P. multocida* (83.5%) was observed. This may reflect presence of primer dimers or pipetting error, although the latter is unlikely given the low inter- and intra-assay variation (%CV <4). Optimising primer concentration and/or annealing temperature could also increase the amplification efficiency of the *P. multocida* assay, given that the maximum amount of primer bound to its target is defined by its annealing temperature [191]. However, given these assays were developed for research purposes, rather than diagnostic purposes, the lower efficiency for *P. multocida* is not a cause for concern with its application in this thesis.

In human respiratory studies STGG broth has been widely used as a storage and transport medium for bacteria and viruses [193] but its use with members of the *Pasteurellaceae* has not been reported previously. For all 3 species (*H. somni*, *M. haemolytica* and *P. multocida*) minimal loss of viable bacterial cells stored in STGG was observed following one freeze-thaw cycle, suggesting its probable suitability as a transport medium capable of storing and recovering cells held at -70ºC for longer periods. As expected, colony counts decreased as inoculum became more dilute, and at higher dilutions (with fewer bacterial cells) the variability in the numbers of colony-forming units observed increased. Recovery of bacterial cells was possible for all species tested over a range of dilutions, validating usability of STGG broth for storage use following

collection of bovine nasal swabs. Nevertheless, recovery of *P. multocida* cells after freezing was less efficient than recovery of *H. somni* and *M. haemolytica*. This evidence for suitability of STGG broth is supported by subsequent findings following collection of bovine nasal swabs which were held at -70ºC for several months and successful detection of bacterial species using culture, PCR and 16S rRNA sequencing (Table 3.10 and Appendix B Table B.2, and in forthcoming chapters).

A well-known limitation of PCR is that it does not distinguish viable from non-viable organisms. Cells were harvested from liquid cultures in the exponential phase of growth to maximise the probability that the bacterial cell populations used for production of calibration curves were likely to be viable [171]. While standard curves were calibrated using defined numbers of viable organisms, cycle quantification (C_q) values for unknown samples were expressed as genome copies/ml and not CFU/ml as, in biological mucosal samples it was uncertain what proportion of DNA detected by PCR came from viable organisms. A well-designed PCR assay will yield linearity of a ten-fold dilution series of target DNA, ideally over 5 dilutions [191]. For the species evaluated using standard curves, as the template concentration decreased, the variability among replicates increased, although linearity over at least 6 dilutions was observed for all species. In addition, coefficient of determination values were high (>0.99), suggesting that linear regression models fitted the data well.

A high degree of genetic relatedness within *P. multocida* and between *P. multocida*-like organisms has been demonstrated using DNA-DNA hybridisation and 16S rRNA sequencing [73] [213]. Townsend et al. reported cross-reactivity between *P. canis* biotype 2 and *P. multocida* when targeting the *kmt1* gene [150] and Miflin et al. observed cross-reactivity with biovar 2 strains of *P. avium* and *P. canis* biotype 2 when detecting a DNA fragment of unknown identity [196]. In addition, Scherrer et al. observed cross-reactivity with a *P. canis* strain isolated from a cat wound with their qPCR detecting toxigenic *P. multocida* (*toxA* gene) [214]. Reclassification of biovar 2 strains of *P. avium* and *P. canis* to *P. multocida* has been proposed [213]. Interestingly, no cross-reactivity was observed with the PCR assay presented in this chapter between *P. canis* biotype 2 and *P. multocida*.

The limit of detection (LOD), defined as the lowest amount of analyte detected at or above reasonable certainty (most commonly 95% confidence) [212] can be used to inform selection of an assays C_q cut-off value. The C_q cut-off represents the number of cycles at or below which C_q values from amplification of test samples are considered; values above the C_q cut-off are not deemed to reliably represent amplified target [215]. For the assays presented in this study, the lowest positive dilution of the standard curve was used to inform selection of the C_q cut-off value and provide insight into assay sensitivity. However, the limit of quantification (lowest amount of quantifiable analyte [212]) or LOD at a stated confidence was not determined for any of the three assays. As an approximation for the LOD, C_q values obtained from the lowest detectable dilution of each standard curve could be converted to genome copies/ml using the predictive regression models presented. However, this estimate relies on the accuracy of the original estimate quantifying standardised material used in the standard curve (i.e. colony counts). An alternative, and somewhat sophisticated approach could be to create a standard curve with known quantities of bacterial DNA, for example using a plasmid to standardise the approach [216]. In addition to these limitations, assay sensitivity using mixed cultures was not determined; in order to do this, cultures of target species could be spiked with non-target species at known dilutions [151].

The optimum annealing temperature for primer combination SGF-SGR detecting *M. haemolytica* was determined empirically using a thermal gradient PCR. No amplification of non-target species was observed at 69°C. Incidentally, Guenther et al. noted cross-reactivity between *M. haemolytica* and *M. glucosida* using the primer combination SGF & SGR at 64°C annealing, subsequently differentiating between the two species using melt curve analysis after PCR amplification [151]. It is accepted that increased specificity will negatively impact on assay sensitivity and to some extent this was observed through the C_q cut-off value determined at 34 cycles for *M. haemolytica* compared to 35 cycles for both *H. somni* and *P. multocida*. Despite the reduced sensitivity at 69°C for this primer pair (SGF & SGR) a good dynamic range (7 orders of magnitude) and efficiency (96%) was observed.

Partial sequences of the *Mannheimia sodA* gene revealed no nucleotide differences in the reverse primer (Mhae-SGR) binding region among the four *M. haemolytica* strains

assessed (Appendix B, Table B.5). These similarities were evident in phylogenetic analysis (Figure 3.9) where all *M. haemolytica* sequences were placed in the same clade with a high bootstrap value of 100 (estimated confidence). Of note, the clades identified were in concordance to those described for *Mannheimia* based on *rpoB* sequences, in particular, sequence similarities were observed for *M. haemolytica*, *M. glucosida* and *M. ruminalis*, whilst *M. varigena* and *M. granulomatis* were more similar to each other than the other *Mannheimia* species [200]. Differences of 19 to 21 nucleotides in the reverse primer binding region were seen between *M. haemolytica* and all other species in the genus (Appendix B, Table B.5). These mismatches were sufficient for divergence between *Mannheimia* spp. but their presence at lower annealing temperatures contributed difficulty in adequately distinguishing between *M. haemolytica* and *M. glucosida*. As no full genome sequence exists for *M. glucosida,* PCR assay development and troubleshooting was difficult. Such a sequence would facilitate novel and potentially improved PCR target and primer design. Diversity among the *M. haemolytica* bovine nasal isolates included in the phylogenetic analysis was evident following amplification using the thermal gradient PCR; gel electrophoresis revealed different amplification fingerprints for each strain (Figure 3.10). This raises questions about the genetic diversity of *Mannheimia* carried in a healthy population of animals. Future work could employ approaches such as pulse-field gel electrophoresis, multilocus sequence typing [217] and whole genome sequencing [218] to elucidate trends in diversity and transmission events.

To validate detection of target bacteria using the qPCR assays presented in this study, a subset of nasal swabs collected from heathy cattle on the North Wyke Farm Platform (full experimental details given in Chapter 4) were cultured. In all cases, swabs negative by PCR were also negative by culture and detection of all species was enhanced using PCR, probably reflecting swabs with target DNA but too few viable organisms for successful culture. In contrast, a high proportion of oropharyngeal swabs collected from healthy school and university students were determined culture-positive but PCR-negative for meningococcus. Greatest discordance between the two methods was observed at the lower limits of detection for both techniques. Although, at these lower limits a marginally greater number of samples were positive by qPCR, suggesting increased sensitivity than culture. It is likely that the culture-positive/PCR-negative samples reflect the poor sensitivity of PCR to detect very low numbers of organisms from mixed samples, whereas culture may detect single organisms [83]. Similar discordances

between culture and PCR were seen for nasal swabs collected from healthy children for a number of bacterial species (*Streptococcus pneumoniae*, *Moraxella catarrhalis*, *Haemophilus influenzae*, *Staphylococcus aureus* and group A *Streptococcus*; GAS). Again, lowest concordance was seen at lower bacterial densities, where the number of samples positive by both culture and PCR was lower than the number of swabs positive by either method alone [171].

During culture of nasal swabs 6 isolates were identified as either *Moraxella* or *Pasteurella* and a further 13 isolates could not be reliably identified based on biochemistry using API test strips. This reflects the difficulty in reliably identifying isolates based on phenotypic characteristics, especially when bacterial species are closely related. These results prompted the decision to perform 16S rRNA gene sequencing for reliable identification of isolates. To date, much of the focus surrounding BRD bacterial agents is directed at *H. somni*, *M. haemolytica* and *P. multocida*, but 16S rRNA gene sequencing also allows investigation of other bacterial species colonising the healthy bovine nasopharynx, these otherwise may be undetected when using targeted approaches. Sequencing successfully confirmed the identification of isolates cultured as *M. haemolytica* and *P. multocida* and these were then incorporated into the specificity panel. Of particular interest was one nasal isolate confirmed as *Moraxella bovoculi* which is the causative agent of infectious bovine keratoconjunctivitis along with *M. bovis,* although its precise role in pathogenesis is unclear [219]. Therefore, it would be interesting to know whether this isolate was an inhabitant of the nasal mucosa or conjunctiva and has migrated to/from the nasopharynx. In addition, this finding raises the question as to whether there are other *Moraxella* species carried in the bovine URT, given their role in respiratory disease in humans [220] [221].

In conclusion, qPCR is a rapid and reliable tool for studying the epidemiology of bovine respiratory disease and *Pasteurellaceae* colonisation dynamics in a range of settings. Colonisation with members of the *Pasteurellaceae* is not exclusive to respiratory biome of cattle. *Pasteurellaceae* have been found to colonise the mucous membranes of wild and domestic animals, for example, small ruminants, pigs, dogs, cats, and more recently were implicated in haemorrhagic septicaemia of Saiga antelopes [222] [223] [224]. The sample collection methods and qPCR assays described here could be applied to range of species to investigate the biology of *Pasteurellaceae* carriage.

Chapter 4 *Pasteurellaceae* carriage dynamics in the nasal passages of healthy beef calves

4.1 Introduction

Respiratory microbiota are diverse communities in humans and livestock [225]. In humans, *Staphylococcus aureus* and *Streptococcus pneumoniae* are frequently carried in the nasal passages as commensals but are also significant pathogens on occasion [226]. Bacteria with this dual commensal-pathogen behaviour have been dubbed pathobionts, although key drivers between commensal and pathogenic states remain to be identified. Similarly, healthy cattle carry pathobionts in their nasal passages, most commonly members of the *Pasteurellaceae* family: *Histophilus somni*, *Mannheimia haemolytica* and *Pasteurella multocida* [179].

Bacterial colonisation over a period of time is often referred to as carriage. Sometimes carriage may be persistent for long periods of time, thus uninterrupted, or it may be rare, or with low bacterial numbers, so that individuals studied may be misidentified as non-carriers. Alternatively, carriage may be intermittent, and an individual may acquire, clear, and re-acquire the organism [227]. It is likely that persistent carrier types are responsible for maintaining carriage in a population [81], however it is not clear which carrier types are at increased risk of invasive disease [228]. However, it has been suggested that carriage is a prerequisite for invasive disease, and if organisms are carried at a high density there is increased risk of disease, for example by inhalation to the lower respiratory tract [229].

Clearance of a bacterial organism can occur through immune mediated mechanisms, such as antibody opsonization and phagocytosis [130], or by displacement due to competition [230]. If adequate immune responses are triggered against an organism it is possible future colonisation may be prevented. In a healthy individual, most of the time, the respiratory microbiome is in homeostasis but following certain triggers dysbiosis may occur and alter the microbial niche such that certain members flourish and colonisation with others can no longer be sustained. This may lead to exclusion and potentially replacement by existing or new species [231].

Bacterial carriage in the bovine upper respiratory tract has generally been detected by culture of swabs [135, 145-147, 153], but this can be problematic due to the fastidious and often slow growth of *Pasteurellaceae*, which can be associated with over-growth by faster-growing species such as *Proteus* [149]. Advances in molecular techniques have allowed in-depth investigation of organisms that are currently difficult or impossible to culture, for example by PCR [152] and sequencing [177-179]. Real-time PCR (qPCR) can be used to detect and quantify bacterial species, as described in the previous chapter (Chapter 3). Density of carriage of bovine respiratory pathobionts has not previously been investigated and may be an important predictor or determinant of disease.

Entrance to the nasal passages is through the nostrils but the exact sites of colonisation with *Pasteurellaceae* in the respiratory tract have been poorly described. Given the differences in temperature, cell type, gas exchange and pH, it is reasonable to assume colonisation may be different along the length of the respiratory tract. Historically, it has been noted by culture that *M. haemolytica* preferentially colonises deeper in the nasopharynx, at the palatine tonsil, as seen in Figure 4.1 [138] [139]. However, despite advances in molecular approaches, such as PCR, colonisation sites in the bovine upper respiratory tract have not been investigated. Characterisation of colonisation locations may reveal specific sites as reservoirs of infection, and these sites could be targeted to reduce shedding and transmission of clinically important species. In addition, determining colonisation locations may facilitate detection of organisms, which may have a greater role to play in disease than currently appreciated.

Figure 4.1: Mid-sagitally sectioned adult bovine head with approximate locations of 1) palatine tonsil; 2) choana; and 3) external nasal meatus, as indicated by the arrows. Photo: Amy Thomas

Bacterial carriage is often assessed over time by repeated sampling and assaying for the presence or absence of target organisms. This longitudinal approach provides rich data by following the same participant over time. By comparison, cross-sectional study designs sample participants at one point in time – there is no follow up and therefore no investigation into the influence of time on variables of interest. Cross-sectional studies can be repeated but the participants may be entirely or largely different on each occasion [232]. Compared to cross-sectional studies, longitudinal studies using sequential sampling are expensive and time-consuming, and inherently give rise to interval-censored data; when an event of interest is known to occur within an interval [233]. In humans, upper respiratory tract pneumococcal carriage has been modelled using exponential interval-censored survival models to determine the rate of clearance and duration of carriage [234], but these approaches have rarely been used in veterinary research [233]. In survival analysis, the relationship between explanatory variables and the time-to-event is investigated. It can be performed using non-parametric, semi-parametric or parametric methods. In medical settings, survival analysis is common, as the time to an event is often of interest. It's also common that the data are censored – some of the participants may experience the event, other's might not, and subsequently their survival times will be unknown. *Right censoring* occurs when an event has not occurred during the study, but it is assumed to occur beyond the follow-up period. If the event of interest has occurred before the study period begins, then that participant is said

to have *left censoring*. Finally, *interval-censoring* occurs when the time-to-event is not observed directly but is known to occur within a particular interval. This commonly occurs in monitoring for infectious diseases when discrete time points are chosen to monitor carriage/infection status [233].

The survival function/survival probability is defined as the probability of the outcome 'event' *not* occurring up to a specific point in time, including the time point of observation (t), and is denoted by *S(t)*. When t = 0, the probability = 1; 100% survival at the onset. The median survival time is the point in time with 50% survival probability. An event refers to one of two responses of the binary categorical outcome variable. In the context of bacterial carriage, the event may be 'acquisition' or 'loss of carriage', and events may occur more than once e.g. recurrence of infection. In some instances, only the first event will be modelled but this ignores information. One approach is to model all recurrent events, preserving information, but account for clustering between events within the same individual (a cluster effect), using cluster robust standard errors. [235] [236] The hazard rate, denoted by *h(t)* is the probability that an individual at risk of having an event, will experience an event at time *t*. Survival and hazard are directly related. Examples of interval-censored analysis in veterinary medicine include: investigating bacterial dynamics in udder infections of dairy cows, using a gamma frailty model [237]; estimating the age at onset of *Mycobacterium avium* subsp. *paratuberculosis* faecal shedding in cattle, using Weibull proportional hazards [238]; and *Campylobacter* infection dynamics in broiler flocks, using a proportional hazards model [239]. More recently, advances in regression analysis of interval-censored data have led to computationally efficient and easy-to-implement statistical methods. The package icenReg in R statistical software offers a flexible and easy-to-use environment for non-parametric, semi-parametric and parametric interval-censored regression analysis [240]. Given that interval-censored data is frequent in veterinary medicine, using these advances in statistical methods there is an opportunity for veterinary research to employ interval-censored survival analysis. Understanding bacterial colonisation dynamics in healthy individuals will improve our understanding of the fundamental biology of carriage, including transmission dynamics, in turn helping inform prevention and control strategies.

4.1.1 Objectives

The objectives of the work presented in this chapter were to investigate rates and densities of nasal carriage with *Histophilus somni*, *Mannheimia haemolytica* and *Pasteurella multocida* in heathy beef calves using the three real-time PCR assays described in Chapter 3. A secondary objective was to investigate differences in nasopharyngeal colonisation locations (posterior and anterior) using real-time PCR for these three bacterial species through collection of short and long nasal swabs.

4.2 Materials and Methods

4.2.1 Longitudinal carriage study

An observational cohort study was conducted to determine bacterial colonisation dynamics in the upper respiratory tract of healthy beef cattle bred and housed on the Biotechnology and Biological Sciences Research Council (BBSRC) North Wyke Farm Platform (NWFP) National Capability, Devon, UK [164]. Some information on the respiratory health status of these cattle was available from veterinary practice records.

4.2.2 Cattle and husbandry

Beef calves, either Charolais, Hereford or Limousin crosses, were bred at Rothamsted Research, North Wyke Farm, Devon, UK. In November 2015 at weaning, 60 calves aged 5 to 7 months were transferred to the NWFP National Capability [167] and allocated to one of two identical, physically adjacent purpose-built cattle housing facilities, designated the 'Green Barn' and the 'Red Barn'. Animals housed in the Blue barn were involved in a separate study not reported.

Animals were allocated to housing, ensuring bodyweight, sire breed and sex were balanced between the two barns. In January 2016, within each barn, calves were separated into six pens each of five animals. Calves were housed on deep litter straw bedding with access to water and silage *ad libitum*. Animals were observed daily throughout all studies by animal technicians and any cattle showing abnormal behaviour that might have indicated poor health were examined in more detail by one of us (AT) using the Wisconsin scoring system for signs of respiratory disease (cough, nasal and ocular discharge, abnormal ear/head tilt and rectal temperature) [241].

4.2.3 Sample collection

4.2.3.1 Nasal swabs

Nasal swabs were collected from each calf housed in the Green and Red barns (n = 60) on five separate visits between January 2016 to April 2016, on days: 0, 33, 47, 62 and 75. Swabs 15 cm in length were collected as described in Chapter 2, 2.9.5. On Day 62, deep guarded nasopharyngeal swabs were collected from a subset of animals predominately housed in the red barn (Red, n = 25; Green, n = 5) as described previously

in Chapter 2, section 2.9.5. Deep swabs were collected immediately after collection of short swabs to ascertain differences in detection rates by different swab lengths.

4.2.3.2 Parasitological and serological sampling

Shortly after housing, composite samples of 10 freshly deposited faecal pats collected from the floor of each barn were tested for the presence of respiratory nematode larvae (*Dictyocaulus viviparus*) using the Baermann technique. Following parasitological testing, all calves were treated once routinely with 200 mg ivermectin (Noromectin®, Norbrook) pour-on (40 ml of product) to control respiratory and gastrointestinal nematodes and external parasites. Paired blood samples were collected from all housed animals to detect evidence of infection by BRSV, BPIV-3, BHV-1, BVDV and *Mycoplasma bovis.* Jugular venous blood samples were collected into plain Vacutainers as described in Chapter 2, section 2.9.6 on Days 33 (Green, n = 30; Red, n = 30) and 47 (Green, n = 29; Red, n = 29).

4.2.4 ELISAs to detect serological responses to bovine respiratory pathogens

Serum samples were tested to detect the presence of antibodies against BHV-1, BVDV, BRSV, BPIV-3 and *Mycoplasma bovis* using a multiplex indirect ELISA (BIOX K 284 ELISA®, BioX, Belgium) according to the manufacturer's instructions (see Chapter 2, section 2.12). Briefly, duplicate optical density (OD) results for test and control samples were imported into Microsoft® Excel for calculation of degree of positivity. According to the formulae specified in the kit instructions, each test sample OD was adjusted for control sample OD and categorised as either 0 (seronegative, having the lowest OD) or 1, 2, 3, 4, or 5 (all seropositive, category 5 having the highest OD). Seroconversion was indicated to have occurred by an increase of at least two categories between paired (acute and convalescent) samples for all agents, as per kit instructions. Further details on the principle of the test and determination of degree of positivity are given in the Chapter 2, section 2.12.

4.2.5 Real-time PCR for bacteria

Real-time Taqman PCR (qPCR) assays targeting *sodA* and the 16S rRNA regions of the bacterial genome were performed for *M. haemolytica, H. somni* and *P. multocida* respectively, using methods as described in Chapter 2, section 2.14.

4.2.6 Data analysis

4.2.6.1 Real-time PCR

Cycle quantification (C_q) values obtained from qPCR analysis of nasal swabs were converted to genome copies/ml by interpolation using the predictive models described in Chapter 3.

In vivo, clinical samples are likely to contain both viable and non-viable bacterial cells. Accordingly, colony forming units/ml (CFU/ml) and genome copies/ml cannot be used interchangeably for these assays, and genome copies/ml are presented.

4.2.6.2 Carriage and co-carriage

Rates of carriage of *H. somni*, *M. haemolytica* and *P. multocida* were calculated as the numbers of animals positive by qPCR for each agent divided by the numbers of animals sampled on each occasion, unless stated otherwise. Carriage estimates for each bacterial species were calculated for each barn (Green and Red) and as an overall average. Co-carriage rate, defined as carriage of either two or three of the bacterial species on the same occasion, was calculated as an overall average for the two barns. Confidence intervals for proportions and differences between proportions were calculated using the Wilson score [242] and Newcombe-Wilson hybrid score [243] methods respectively [244]. Levels of co-carriage of *H. somni*, *M. haemolytica* and *P. multocida* were assessed at each visit using Fisher's exact test (because of expected values lower than 5) to assess for the independence of the carriage of pairs of different bacterial species, based on the counts of calves with different combinations of positive/negative qPCR results. Levels of *P. multocida* carriage were assessed for short and long swabs using Fisher's exact test to assess for the independence of carriage between swab types.

4.2.6.3 Interval-censored survival analysis

Interval-censored survival analysis was used to estimate the rate ('hazard') of clearance of bacterial carriage. A parametric proportional hazards regression model for interval-censored data with an exponential distribution was fitted to carriage episodes from all animals. Animals were combined into one cohort (n = 60) following insufficient evidence to suggest a difference in carriage between pens and barns (Appendix C, Effect of pen and barn on bacterial carriage rates). An episode was defined as a period of uninterrupted

H. somni or *P. multocida* carriage. Further details on rules defining carriage episodes and on dataset construction are provided in Appendix C, Interval-censored survival analysis). The number of carriage episodes for each bacterium contributing to the survival analysis was not equal to the number of animals observed; some animals experienced multiple carriage episodes whilst others were carriage-free. Adjustment for correlation between recurrent episodes of carriage within the same animal was made by including animal identity as a clustering variable and calculating cluster robust standard errors [235]. The effects of sex and density of carriage when first positive were considered as covariates in univariable analyses. To assess the relationship between log hazard ratio and density ($\log_{10}$ genome copies/ml) the observations were grouped into categories based on the density quartiles. Parameter estimates for each density category were plotted to assess the fit. The hazard for each sex and density category was estimated and expressed as a hazard ratio relative to the baseline category. Median carriage duration was calculated as $-\log_e(0.5)$ divided by the estimated hazard value. Improvement in model fit between the unconditional model (no covariates specified) and the model with the covariate of interest was assessed by calculating the log-likelihood test ratio statistic. The strength of the relationship between categorical covariates (sex/carriage density) and hazard of clearance was assessed using the hazard ratio p-value. All analyses were performed in R version 3.5.0, using base functions and the following supplementary packages: ggplot2 (version 2.2.1), longCatEDA (version 0.31 [245]), icenReg (version 2.0.7 [240]).

4.2.6.4 Seroprevalence

For each of the five respiratory disease agents tested, seroprevalences on Days 33 and 47 were calculated as the number of animals seropositive by ELISA (i.e. results in categories 1 to 5) divided by the total number of animals sampled.

4.3 Results

4.3.1 Characteristics of the study animals and signs of respiratory disease

A total of sixty mixed breed animals were included in the study. The nutritional plane of animals housed in each barn was similar (see Appendix C, Table C.1 for details on forage analysis) strengthening the consideration of housing arrangements as replicates. Animal characteristics (sex, sire breed, age and weight) are shown in Table 4.1. Animals were separated into groups of five per pen in both barns. Animals were monitored for signs of respiratory disease using the Wisconsin calf respiratory scoring system. Nasal discharges were observed on three occasions (scored between 1–3), two of which were in the same animal. Coughing was observed in one animal on one occasion. No *Dictyocaulus viviparous* larvae were detected in faeces of any animal.

Table 4.1: Sex, sire breed, age and weight of calves in the observational study (n = 60)

	Green Barn (n = 30)	**Red Barn (n = 30)**	**Total**
Sex			
Heifer	15/30	14/30	29/60
Steer	15/30	16/30	31/60
Sire Breed			
Charolais	20/30	21/30	41/60
Hereford	4/30	3/30	7/60
Limousin	6/30	6/30	12/60
Median Age (Day 0)			
Days (range)	305 (276–319)	307 (258–324)	305 (258–324)
Median Weight*			
Kilograms (range)	364 (266–441)	354 (277–455)	359 (266–455)

* Weight 16 days before Day 0

4.3.2 Carriage rates

A total of 299 nasal swabs obtained during winter housing of calves were analysed by qPCR to determine carriage rates and densities of *H. somni, M. haemolytica* and *P. multocida*; 238 swabs were positive for at least one of these three target bacterial genes. *P. multocida* was most frequently detected (227/299; 75.9%), followed by *H. somni* (80/299; 26.8%) and *M. haemolytica* (17/299; 5.7%). The overall proportions

of swabs positive in each barn were similar for *P. multocida* (Green Barn: 118/150; 78.7%, Red Barn: 109/149; 73.2%; p = 0.327) and *M. haemolytica* (Green Barn: 7/150; 4.7%, Red Barn: 10/149; 6.7%; p = 0.608). The proportion of swabs positive for *H. somni* was lower in the Green (20/150; 13.3%) than in the Red Barn (60/149; 40.3%; p < 0.001). In all cases, the T4 internal amplification control assay C_q values were as expected, indicating successful DNA extraction with no evidence of PCR inhibition.

Target bacterial nucleic acid was detected in swabs from each of the sixty animals on at least one sampling occasion. Carriage rates were highest on the first occasion of sampling (Day 0), and declined for all bacterial species thereafter, with similar trends observed in both barns. *P. multocida* was carried at a higher rate than *H. somni* and *M. haemolytica* on all sampling occasions in the Green Barn, and on Days 0 and 47 in the Red Barn. Clearance of *H. somni* and *M. haemolytica* was observed in the Green barn from Days 62 and 47, respectively (Figure 4.2 and Appendix C, Table C.2). Log-linear models provided insufficient evidence to suggest any difference in carriage rates between barns and pens (see Appendix C, Effect of pen and barn on bacterial carriage rates).

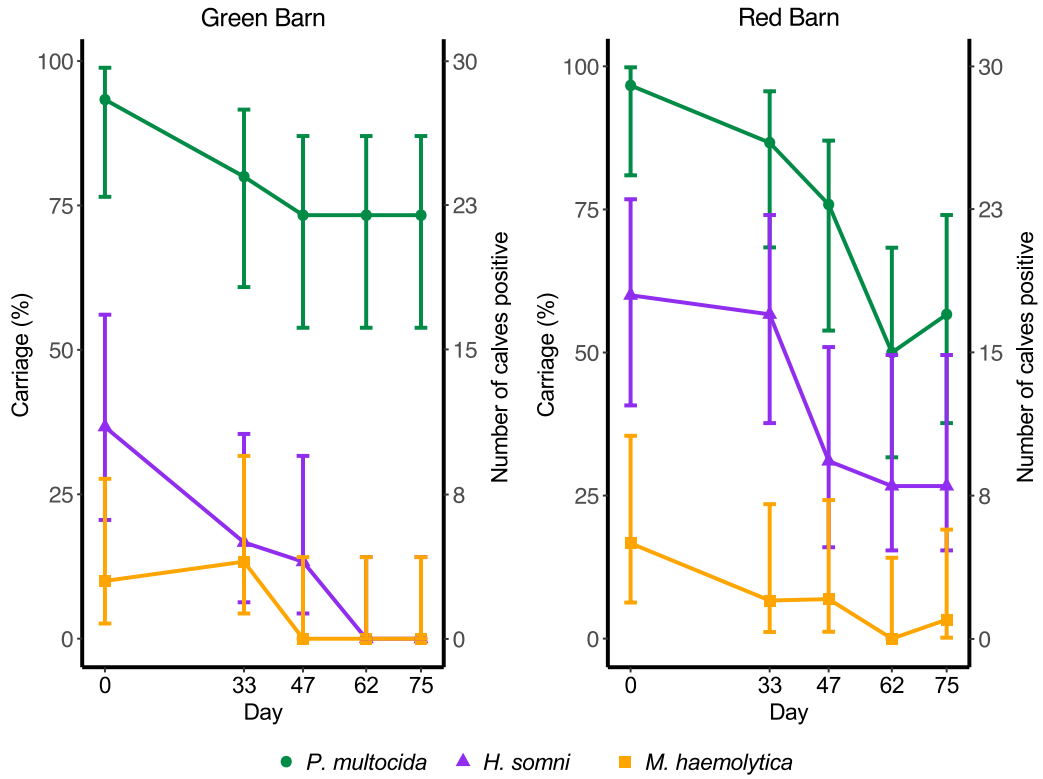

Figure 4.2: Carriage of *Pasteurellaceae* during the observational study. Carriage of *Pasteurella multocida* (green circles), *Histophilus somni* (purple triangles) and *Mannheimia haemolytica* (orange squares) determined by qPCR on nasal swabs collected on five occasions from sixty calves housed in two identical barns (n = 30 Green Barn, n = 30 Red Barn). Error bars represent Newcombe 95% confidence intervals for the single proportion.

4.3.3 Colonisation at different locations within the bovine nasopharynx

Paired short and long swabs were collected from a subset of calves (n = 29) on one occasion (Day 62) to investigate carriage of *H. somni*, *M. haemolytica* and *P. multocida* at different nasopharyngeal locations. *H. somni* was detected from 6/29 short and 2/29 long swabs. No animal was positive for *H. somni* by both swab types. Conversely, *P. multocida* was detected using both swab types in six of 29 animals, with a greater proportion of animals found positive by sampling with short (17/29) than with long swabs (7/29). Carriage was not significantly associated with either swab type for *P. multocida* ($p = 0.187$; *H. somni* rates too low for statistical analysis). *M. haemolytica* was not detected in any sample on this occasion (Table 4.2).

Table 4.2: Comparison of short and long swabs for detection of *H. somni*, *M. haemolytica* and *P. multocida* by qPCR

	Short swab	Long swab	N
H. somni	+	+	0
	+	-	6
	-	+	2
	-	-	21
M. haemolytica	+	+	0
	+	-	0
	-	+	0
	-	-	29
P. multocida	+	+	6
	+	-	11
	-	+	1
	-	-	11

Density of *H. somni* and *P. multocida* carriage determined using short and long swabs is given Table 4.3. *P. multocida* was detected at a higher median density by short compared to long swabs. Only two animals were positive for *H. somni* by long swab, with carriage at a lower density compared to short swabs.

Table 4.3: Density of *Histophilus somni* and *Pasteurella multocida* carriage determined by qPCR on short and long swabs

	Short swab		Long swab	
Species	**Median density (genome copies/ml)**	**N**	**Median density (genome copies/ml)**	**N**
H. somni	52.8	6	20.3	2
P. multocida	3590	17	445	7

4.3.4 Carriage patterns

A carriage episode was defined as a period of carriage detected in consecutive samples without interruption. Forty-five (75%) of the 60 calves were positive for *H. somni* on at least one occasion: 36 of these calves had a single carriage episode and 9 had two episodes. *H. somni* was detected at the first visit in 29 calves, of which two remained positive at all subsequent study visits. Details of individual carriage trajectories are shown in Figure 4.3.

Carriage of *P. multocida* was detected in 57 (95%) of the 60 calves at Day 0: 38 of these calves had a single carriage episode and 19 had two episodes. Carriage was detected in 26 calves on all study visits. Of three calves negative for *P. multocida* on Day 0, carriage was detected in two at the subsequent visit, while the third remained negative throughout the study. Carriage of *M. haemolytica* was detected in 8 (13%) of the 60 animals at the first visit, of which 7 had one carriage episode and one had three. In three further calves, *M. haemolytica* was detected at the second visit, while this species of pathobiont was not detected in the remaining 49 animals at any visit.

Co-carriage was defined as detection of more than one bacterial species in the same sample and co-carriage of two and three species was found in 47 and three animals respectively.

Co-carriage with *H. somni* and *P. multocida* occurred most frequently and *M. haemolytica* was co-carried with *P. multocida* more commonly than with *H. somni* (see Appendix C, Table C.3 for co-carriage rates). No evidence of associations between pairs of species were apparent using Fisher's exact test ($p > 0.221$).

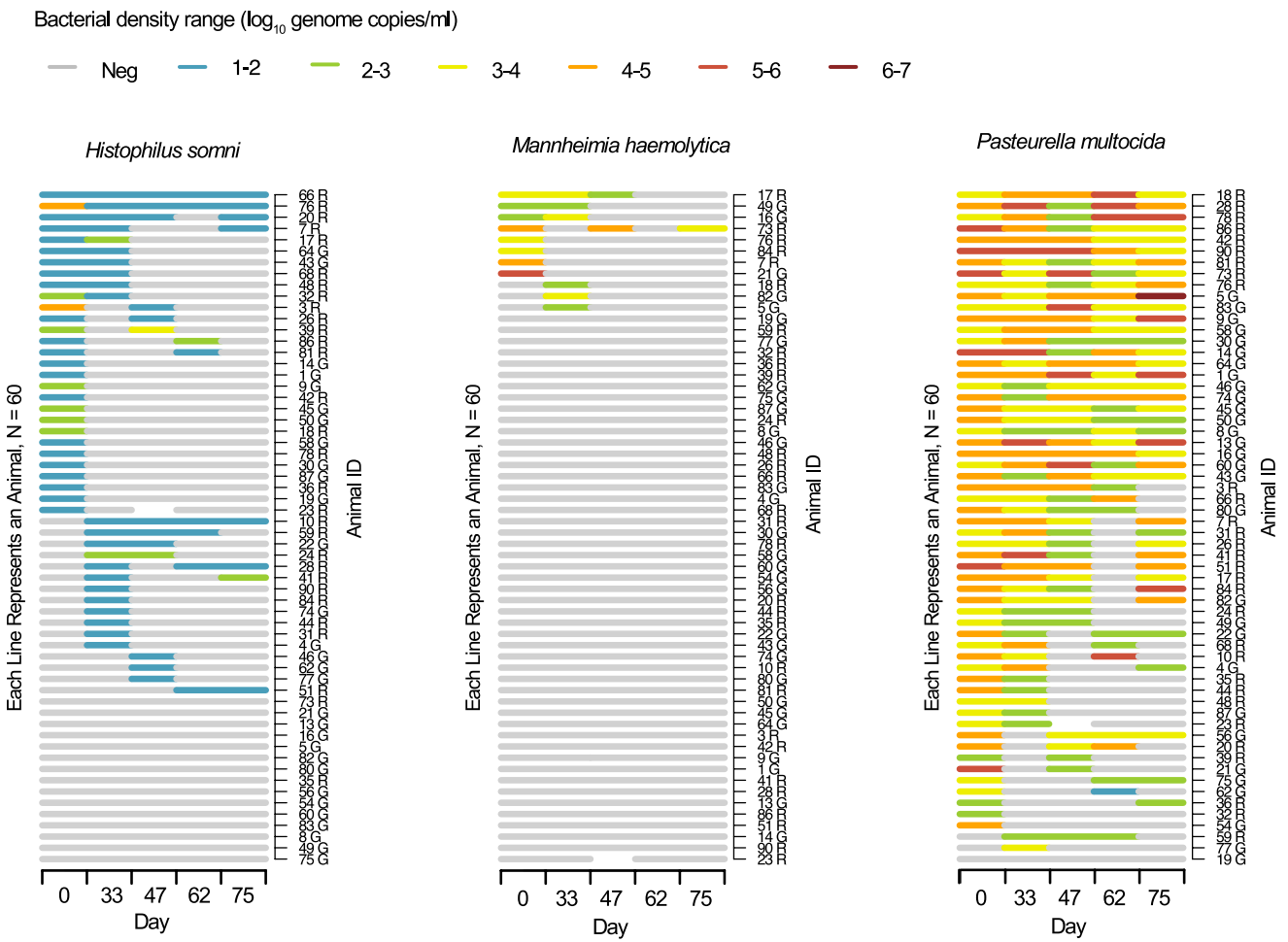

Figure 4.3: Carriage patterns and density of *Histophilus somni*, *Mannheimia haemolytica* and *Pasteurella* determined by qPCR on nasal swabs collected on five sampling days (0, 33, 47, 62 and 75) from sixty calves. Animals housed in Green and Red barns are identified by G and R following ID numbers respectively. Density is represented as $\log_{10}$ genome copies/ml. One animal (ID 23 R) had a missing sample at Day 47.

4.3.5 Carriage density

For each bacterium, density values for all positive samples were plotted as histograms revealing distinct density profiles Figure 4.4. The modal value for *H. somni* carriage density accounting for the vast majority (82.5%) of swabs was 1–2 $\log_{10}$ genome copies/ml with fewer samples (13.8%) between 2–3 logs. Only two samples in two calves were in the 4–5 log range and one sample in the 3–4 log range. Although carriage rates were low for *M. haemolytica*, carriage density ranged between 2 and 6 logs when it occurred. *Pasteurella multocida* was also carried over a wide range of densities, most commonly between 3 and 5 $\log_{10}$ genome copies/ml, extending up to 6.08 (ID: 5G) logs in one sample. Although density of *P. multocida* carriage was also dynamic within and between calves, some animals maintained carriage at high densities in the 4–6 log range over several sampling visits, and only one sample in one calf (ID: 62G) was in the 1–2 log range (Figure 4.3).

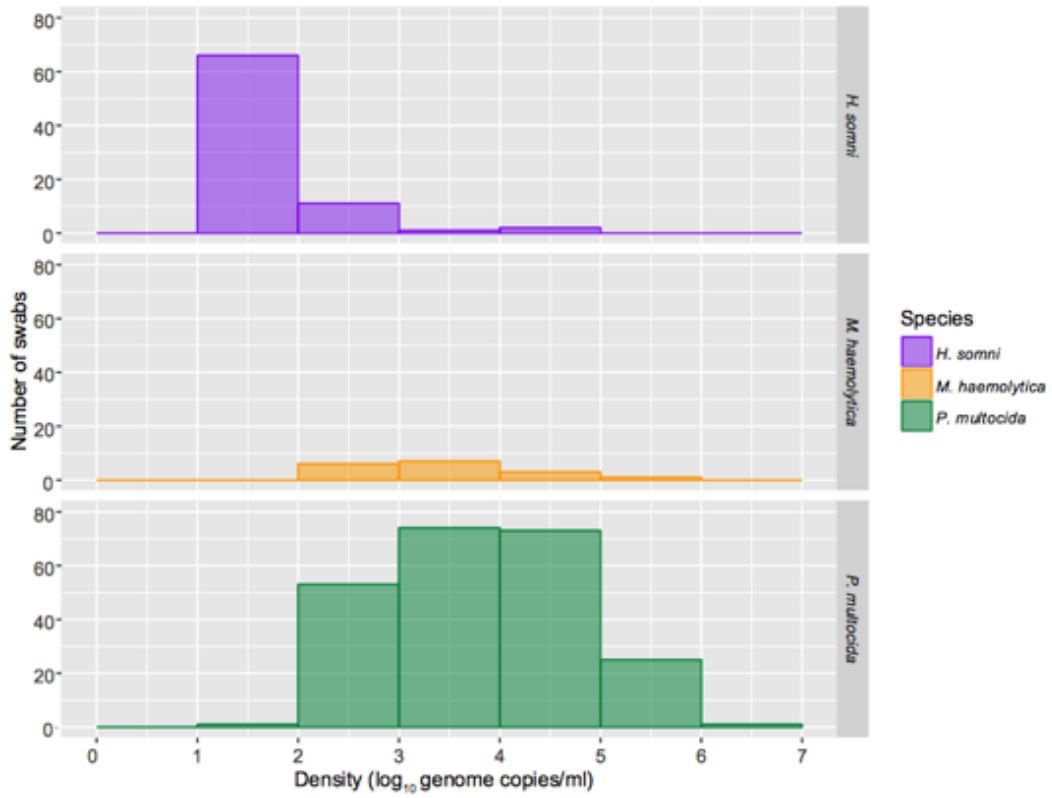

Figure 4.4: Histograms for all positive swabs summarising density distribution profiles of *Histophilus somni* (n = 80), *Mannheimia haemolytica* (n = 17) and *Pasteurella multocida* (n = 227).

4.3.6 Duration of carriage and hazard of clearance

Interval-censored exponential survival models for carriage (without inclusion of carriage density or host animal sex as covariates) estimated the median duration of *H. somni* carriage to be 14.8 days ($CI_{95\%}$: 10.6–20.9) and the hazard of clearance to be 0.0467 per day ($CI_{95\%}$: 0.0326–0.0634). For *P. multocida*, the median carriage duration was estimated to be 55.5 days ($CI_{95\%}$: 43.3–71.3) and hazard of clearance to be 0.0125 per day ($CI_{95\%}$: 0.00969–0.0159) (Figure 4.5). Carriage rates of *M. haemolytica* were too low for meaningful survival modelling.

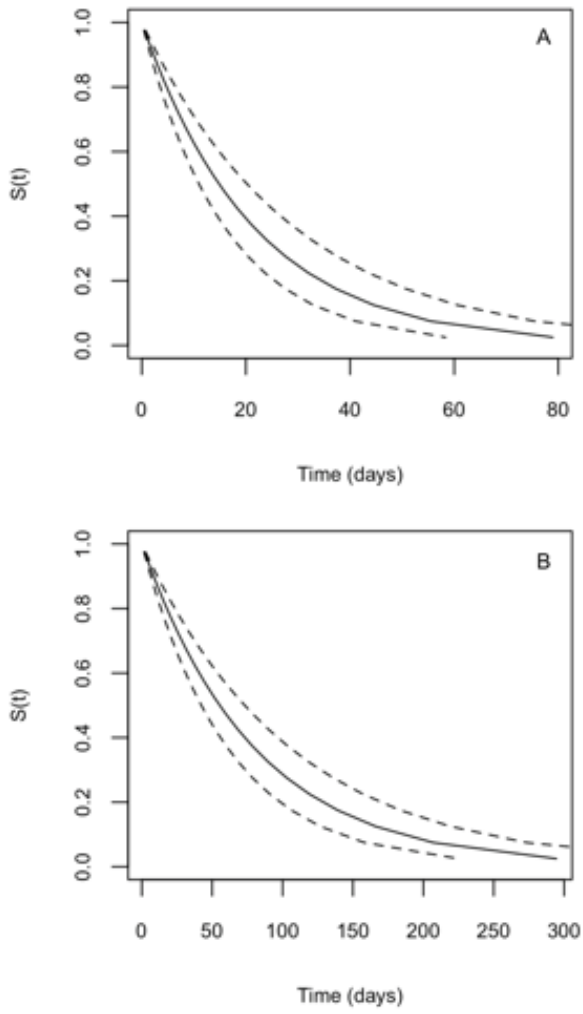

Figure 4.5: Fitted survival curves: proportion of carriage episodes still ongoing by time for *Histophilus somni* (panel A; 14.8 days median carriage duration) and *Pasteurella multocida* (panel B; 55.5 days median carriage duration). Dotted lines represent 95% confidence interval.

The effects of carriage density and host animal sex on carriage duration was modelled in univariable analyses. Log hazard ratio and density data were suggestive of a non-linear

trend for both *H. somni* and *P. multocida*, therefore the effect of density was modelled using categories based on density quartiles rather than continuously. For *P. multocida,* density of carriage significantly influenced subsequent carriage duration ($p = 0.036$, Table 4.5). Categories 2–4 of *P. multocida* density were significantly associated with increased carriage duration compared to the reference category (1) (Table 4.4). Density was not seen to influence *H. somni* carriage duration (Table 4.4) nor did the animals' sex significantly influence carriage duration for either bacterium.

Table 4.4: Interval-censored exponential survival models: *H. somni*

Species	Model	Covariate	Hazard ratio [exp(b_i)]	$CI_{95\%}$ of hazard ratio	Hazard ratio p-value	Log-likelihood
H. somni						
(n = 54)	M0: Unconditional		0.0467*	0.0333 – 0.0655		-55.8
	M1: Density†	Category 1 (n = 14)	0.0556*	0.0261 – 0.112		-55.0
		Category 2 (n = 13)	0.967	0.383 – 2.44	0.943	
		Category 3 (n = 13)	0.610	0.219 – 1.69	0.342	
		Category 4 (n = 14)	0.850	0.266 – 2.72	0.784	
	M2: Sex	Heifer	0.0411*	0.0260 – 0.0617		-55.5
		Steer	1.29	0.635 – 2.61	0.484	

H. somni log-likelihood ratio test statistic: (M0 vs. M1), χ^2 (3 df) = 1.62, p = 0.655; (Model 0 vs. Model 2), χ^2 (1 df) = 0.668, p = 0.414

* Hazard for unconditional model and baseline category

† *H. somni* density categories based on quartiles (log_{10} genome copies/ml): <1.26; ≥1.26 to 1.45; ≥1.45 to 1.96; ≥1.96

Table 4.5: Interval-censored exponential survival models: *P. multocida*

Species	Model	Covariate	Hazard ratio [exp(b_i)]	$CI_{95\%}$ of hazard ratio	Hazard ratio p-value	Log-likelihood
P. multocida						
(n = 78)	M0: Unconditional		0.0125*	0.00950 – 0.0164		-109
	M1: Density†	Category 1 (n = 20)	0.0280*	0.0145 – 0.0524		-104
		Category 2 (n = 19)	0.393	0.189 – 0.814	**0.0119**	
		Category 3 (n = 19)	0.321	0.153 – 0.674	**0.00267**	
		Category 4 (n = 20)	0.414	0.197 – 0.868	**0.0196**	
	M2: Sex	Heifer	0.0108*	0.00791 – 0.0146		-108
		Steer	1.33	0.464 – 1.23	0.255	

P. multocida log-likelihood ratio test statistic: (M0 vs. M1), χ^2 (3 df) = 8.52, p = 0.036; (Model 0 vs. Model 2), χ^2 (1 df) = 1.028, p = 0.311

* Hazard for unconditional model and baseline category

† *P. multocida* density categories based on quartiles (log_{10} genome copies/ml): <3.40; ≥3.40 to 3.99; ≥3.99 to 4.77; ≥4.77

4.3.7 Serological responses to bovine respiratory viruses and *Mycoplasma bovis*

Among the bovine respiratory pathogens tested (BHV-1, BPIV-3, BRSV, BVDV and *M. bovis*), antibodies to BPIV-3 were detected most frequently (20/29 up to 30/30 animals positive) with three animals also showing evidence of seroconversion. Exposure to BRSV was detected in slightly fewer animals (17/29 up to 24/30), and *M. bovis* in fewer still (7/29 up to 11/30). One calf had antibodies to BHV-1 at Day 33 and no animals had antibodies to BVDV (Table 4.6).

Results for each agent were assigned either to a negative category or to one of 5 categories of increasing seropositivity. The number of animals within each category for each agent is shown in Table 4.7. The number of calves with antibodies detected at varying degrees of seropositivity was similar between sampling days for all agents tested. The majority of calves positive for *M. bovis* had detectable antibodies between categories 1–2. Antibodies were detected across a wider range of categories for BRSV (categories 1–4) and BPIV-3 (categories 1–5); however, the majority of calves with detectable antibodies were within the lower category range (1–2).

Table 4.6: Serological status of calves in the study (n = 60)

Barn	Agent	Day 33			Day 47			Seroconversion‡	
		Number of animals positive (n/N) †	%	$CI_{95\%}$*	Number of animals positive (n/N) †	%	$CI_{95\%}$*	Number of animals positive (n/N) †	%
BVDV	Green	0/30	0.0	0 – 14.1	0/29	0.0	0 – 14.1	0/29	0.0
	Red	0/30	0.0	0 – 14.1	0/29	0.0	0 - 14.1	0/29	0.0
BHV-1	Green	1/30	3.3	0.174 – 19.1	0/29	0.0	0 – 14.6	0/29	0.0
	Red	0/30	0.0	0 – 14.1	0/29	0.0	0 – 14.6	0/29	0.0
M. bovis	Green	11/30	36.7	20.5 – 56.1	9/29	31.0	16.0 – 51.0	0/29	0.0
	Red	9/30	30.0	15.4 – 49.6	7/29	24.1	11.0 – 43.9	0/29	0.0
BRSV	Green	24/30	80.0	60.9 – 91.6	24/29	82.8	63.5 – 93.5	0/29	0.0
	Red	19/30	63.3	43.9 – 79.5	17/29	58.6	39.1 – 75.9	0/29	0.0
BPIV-3	Green	30/30	100	85.9 – 100	29/29	100	85.4 – 100	0/29	0.0
	Red	22/30	73.3	53.8 – 87	20/29	70.0	49.4 – 83.8	3/29	10.3

* Confidence intervals for single proportions were calculated using the Wilson score

† Samples were considered seropositive in that calculated optical densities corresponded to categories 1 to 5 of the ELISA kit instructions (see Chapter 2 for further details).

‡ Seroconversion was considered to have occurred if there was an increase of at least two categories of seropositivity between paired samples.

Table 4.7: Number of calves seronegative and seropositive for BHV-1, BVDV, BRSV, BPIV-3 and *Mycoplasma bovis*, with 5 categories of increasing seropositivity. Serological status was determined by ELISA using a commercially available kit. Acute and convalescent blood samples were collected 14 days apart at Day 33 (visit 2) and Day 47 (visit 3) respectively.

		Green Barn		**Red Barn**	
		Day	**Day**	**Day**	**Day**
	Seropositivity category	**33**	**47**	**33**	**47**
BVDV	Negative	30	29	30	29
	+	0	0	0	0
	++	0	0	0	0
	+++	0	0	0	0
	++++	0	0	0	0
	+++++	0	0	0	0
BHV-1	Negative	29	29	30	29
	+	1	0	0	0
	++	0	0	0	0
	+++	0	0	0	0
	++++	0	0	0	0
	+++++	0	0	0	0
M. bovis	Negative	19	20	21	22
	+	8	7	7	6
	++	2	1	2	1
	+++	1	1	0	0
	++++	0	0	0	0
	+++++	0	0	0	0
BRSV	Negative	6	5	11	12
	+	13	15	12	8
	++	8	7	6	7
	+++	2	1	0	1
	++++	1	1	1	1
	+++++	0	0	0	0
BPIV-3	Negative	0	0	8	9
	+	1	4	7	8
	++	14	13	12	7
	+++	9	8	2	2
	++++	6	4	1	2
	+++++	0	0	0	1

4.4 Discussion

This is the first longitudinal investigation into nasal carriage patterns and densities of common bovine respiratory pathobionts in healthy animals using qPCR. The detailed quantitative profiles obtained over a typical housing period demonstrate marked differences between the bacteria studied in terms of frequency, duration of carriage and microbial density. These results provide methodological and biological information that could be useful for future study of bacterial carriage and transmission in housed animals, and of the impact of vaccines and viral infections upon respiratory disease.

Cattle remained generally healthy throughout the study; on only a few occasions were mild signs of respiratory disease observed (nasal discharge and cough). No bovine lung worm (*Dictyocaulus viviparous*) larvae were detected. Surveillance data on diagnostic submissions to Veterinary Investigation Centres confirm that the bacterial species studied here are important in bovine pneumonia in the UK; most frequently *Mannheimia* spp. closely followed by *P. multocida* [246]. Although the prevalence of *P. multocida* as a commensal in the healthy bovine respiratory tract is unknown, the high carriage rates by PCR (61.7–95.0%; Figure 4.2, Table C.2) reported in this study in healthy animals suggest it may function as part of the core nasal microbiota. Using culture, nasal carriage of *H. somni* has been reported in healthy calves (6.6%) and those with respiratory disease (11.9%) [146]; however, rates reported by PCR in this study were higher (13.3% to 48.3%). This may reflect the increased sensitivity of detection by qPCR compared to culture, suggesting that *H. somni* may have been underreported previously. By contrast, *M. haemolytica* was rarely detected (carriage rates of up to 13.3%), although when carriage did occur it was over a wide range of densities (2–6 logs; Figure 4.4). It has been suggested that *M. haemolytica* is carried preferentially deeper in the nasopharynx at the palatine tonsil [139] [158]. To explore differences in colonisation locations, paired short and long swabs were collected. Unfortunately, *M. haemolytica* was not detected in any swab on the occasion that these paired samples were collected. Therefore, this warrants further investigation either through sampling a larger number of animals, or sampling animals where carriage rates of *M. haemolytica* are known to be higher in order to reduce the number of animals sampled using a more invasive method. Nevertheless, *M. haemolytica* was detected from short swabs on other sampling occasions. For both *H. somni* and *P. multocida* a greater proportion of short swabs were positive, however no pairs of short and long swabs from the same animal were both positive for *H. somni*. In addition, density of carriage tended to be higher

in short swabs, although sample sizes were too small for meaningful statistical analysis. Only one animal had a negative short but positive long swab for *P. multocida* (6 animals with pairs of swabs both positive); this observation reflects a very small proportion of animals (1/29) likely to have carriage undetected if sampled solely with short swabs. Of note, short swabs were collected prior to long swabs in the same nostril, avoiding contamination of short swabs by material originally deeper in the nasopharynx pulled anterior by a longer swab.

Seropositivity to BRSV and BPIV-3 was high for both viruses. This is unsurprising given other studies reporting their widespread occurrence [247] [248] [249], and reflects the likelihood of repeated exposure and viral infection in the absence of vaccination. Three animals showed evidence of seroconversion to BPIV-3; however, for all other agents seropositivity either declined or remained the same between paired samples (Day 33 and 47).

Patterns of carriage for all three pathobiont species were similar between barns but not identical (clearance of *H. somni* was observed in the Green barn only). This suggests epidemiology may vary somewhat in different but overtly similar groups of animals. Furthermore, carriage rates for all species declined over the study period in both barns. This observation may reflect immunological maturation as animals become older or development of specific immune responses following exposure or both enabling them to clear bacteria more efficiently than younger animals.

An episode of carriage was defined as a period when an animal was positive for any one bacterial species in consecutive samples without interruption. One animal experienced three such episodes of carriage with *M. haemolytica* and carriage was often transient for all three species. While such apparent transient carriage episodes may reflect genuine clearance and re-acquisition, negative results could also be due to sampling error or intermediate and other sample(s) below the limit of detection of the assay, in the context of apparent large fluctuations in density over time (Figure 4.3).

It is not known to what extent the bacteria are evenly distributed within the upper respiratory tract of colonised animals. Conversely, apparent continuous episodes of carriage in our study could also represent repeated acquisition and successive carriage episodes with the same or different strains of *H. somni, M. haemolytica* or *P. multocida*. This is a limitation of repeated sampling studies which can be partially addressed by taking more frequent samples or undertaking more detailed characterisation of the bacteria detected. Approaches such as pulsed-field gel electrophoresis, multilocus sequence typing [217] and whole genome sequencing can

be used to study transmission events, however their success is dependent on isolation by culture and adequate genetic diversity [218].

Serotype displacement and replacement is known to occur following dysbiosis of the respiratory niche. For example reduction in carriage of pneumococcal vaccine serotypes following universal vaccination in childhood, suggesting that non-vaccine serotypes are outcompeted in the absence of vaccination [82]. In cattle, although differences in serotype prevalence have been suggested between healthy animals and those suffering with respiratory disease, this area of microbiology is relatively unexplored [154] [156].

Interval-censoring occurs when the time-to-event is not observed precisely but is known to have occurred within a particular interval. This commonly occurs in monitoring for infectious diseases when discrete time points are chosen to monitor carriage/infection status [233]. Biased estimation can result if this imprecision is ignored and the midpoint or right end point of the observed interval is taken as the exact event/failure time [250]. Using interval-censored exponential survival analysis the median duration of *H. somni* carriage was estimated at 14.8 days (hazard; 0.0467 per day) and at 55.5 days for *P. multocida* (hazard; 0.0125 per day), concordant with the increased prevalence observed for *P. multocida*. However, prevalence depends on acquisition and clearance rates also. Increasing *P. multocida* carriage density was significantly associated with increased carriage duration. One explanation for reduced carriage duration at lower densities could be the requirement of a certain number of bacteria for colonisation [251]; however, at higher densities (over a threshold) the opportunity for naïve individuals to become exposed increases. Incidentally, *H. somni* was predominately carried at lower densities (1–2 logs) and was not significantly associated with carriage duration (Figure 4.4). *M. haemolytica* carriage episodes were too few (prevalence 1.7–13.3%) to model using survival analysis but carriage density did extend transiently up to 6 $\log_{10}$ genome copies/ml. Given the infrequency of observed second episodes for both bacterial species, it was not possible to generate precise estimates for the median duration of carriage per episode type. Only two animals had sustained carriage of *H. somni* for the entire study, but twenty-six had sustained carriage of *P. multocida*. It would be of interest to define factors which predict and determine persistence of carriage with these pathobionts.

A greater incidence of respiratory disease has been reported in male calves than in female calves [28], suggesting sex may influence respiratory pathobiont colonisation dynamics. Sex was included as a covariate in exponential survival models but was not found to be significantly

associated with carriage duration for either *H. somni* or *P. multocida*. Furthermore, when carriage rates and densities observed at each occasion were stratified by sex there was no difference between the two proportions carrying on any occasion (data not presented). This may indicate that reported differences in disease rates may not be due to marked differences in carriage biology but instead to other factors [82].

Between the three bacterial species studied, unexpected marked differences in prevalence, carriage duration and density were observed. These observed differences provide evidence for genuine differences in the carriage biology of these organisms and do not reflect sampling artefact. Quantitative molecular techniques have identified increased nasal bacterial carriage and density following respiratory viral infection in the upper respiratory tract of healthy mice and children [252, 253]. One hypothesis is that density may be important for transmission of bovine pathobionts between herd members and may affect the likelihood of invasive disease. Moreover, respiratory viral infection may influence bacterial colonisation dynamics. The methodological approaches and carriage patterns presented in this chapter lay the foundation for exploring transmission models of bovine respiratory disease and intervention studies exploring the effects of respiratory viral infection on bacterial colonisation dynamics.

Chapter 5 *Pasteurellaceae* colonisation in early-life of cattle

5.1 Introduction

Work investigating the role of microbiota in health of humans and rodents, and more recently of livestock has exploded since the advent of culture-independent and novel technologies [254] [177]. Microbiota have been demonstrated to play an important role in immune maturation, metabolism, mucosal barrier functions and colonisation resistance for pathogens [254] [255] [256]. At birth, calves are exposed to microbiota from the dam directly and from the maternal environment [257]. Traditionally it has been considered that initial colonisation by the microbiome occurs during birth and that subsequent colonisation proceeds through a dynamic succession of stages. This process leads to a complex host microbiome that continues to change during life [160] [257]. Recent evidence in humans suggests that colonisation can occur *in utero* [258] but the evidence is controversial [259].

Biesbroek et al. reported that the respiratory microbiomes of children aged between 6 weeks and 2 years fell into distinct clusters. Children with microbiomes characterised either by *Moraxella* or by *Corynebacterium* combined with *Dolosigranulum* at 6 weeks old tended to be more stable up to 2 years old, in that these individuals tended to maintain microbiomes dominated by these organisms, whereas children with microbiomes dominated by, for example, *Staphylococcus* tended to be more variable over time. Notably, children with microbiomes dominated by *Corynebacterium* in combination with *Dolosigranulum* went on to develop fewer upper respiratory tract infections [160]. Studies in humans, therefore, seem to suggest that the composition of the respiratory microbiota in early life may be important for determining subsequent respiratory health.

There has been considerable interest in characterising colonisation patterns in the neonatal calf rumen, with a view to manipulating microbiomes for enhanced health and productivity [260] [261]. In addition, mucosal immune responses in the gastrointestinal tract of neonatal pigs have been shown to be influenced by changes in rearing environment [262]. However, despite respiratory disease frequently occurring in calves <6 months of age, there is little known about the patterns of bacterial colonisation of the respiratory tract of bovine neonates. One study used culture to report the nasal and tracheal microbiota of calves from the first day of life up to 3.5 months. Calves were housed in controlled environments experiencing different climatic conditions (varying temperature and relative humidity). The authors reported colonisation

within the first days of life with *M. haemolytica* regardless of climatic differences [137]. Only one study [149] has surveyed carriage of *P. multocida* in a UK farm setting and reported prevalence of *P. multocida* in the nasal passages of 637 Scottish calves based on culture-amplified PCR. The median age of calves sampled was 22 days, and carriage was detected in 17% of calves: however, carriage rates stratified by age were not reported [149]. From the literature, then, it is not clear when healthy beef suckler calves become colonised with common respiratory pathobionts. Such information on bacterial colonisation is essential for detailed understanding of the biology of carriage and will be of value for informing effective vaccination strategies.

5.1.1 Objectives

The objective of the work presented in this chapter was to characterise colonisation with *H. somni*, *M. haemolytica* and *P. multocida* from shortly after birth and up to weaning by collection of short nasal swabs and analysis using real-time PCR.

5.2 Materials and methods

5.2.1 Calves and husbandry

Healthy beef suckler calves born from dams resident at the North Wyke Farm Platform during spring 2016 were included in the study. Calves (n = 28) were purebred Stabiliser or were crossbred from Hereford-Friesian dams by either Charolais or Limousin sires. Soon after calving, dams and their respective calves were housed in penned groups: 5 dams with their respective calf. Pen 1 contained six calves as one cow had twins, but neither of these calves were sampled. One other set of twins which were sampled were located in Pen 10 (Figure 5.3). Bull calves were castrated at 1–2 days of age by elastration. Disbudding was performed between 4–8 weeks of age. Calves remained with dams up to, and during spring/summer turnout. Weaning occurred at the time of housing in November 2016. All calves remained apparently healthy throughout the course of the study. None were either diagnosed with or treated for respiratory infections.

5.2.2 Sample collection

Nasal swabs were collected from calves on four occasions: within their first week of life; at approximately 2 months; approximately 3 months; and approximately 7 months of age. The swabs collected at 2 and 3 months of age were taken when calves were brought in temporarily from pasture for management purposes. At 7 months of age swabs were collected shortly after weaning and housing (16 days). Swabs 15 cm in length were collected as previously described in Chapter 2, section 2.9.5 into skim milk, tryptone, glucose, glycerol (STGG) broth and kept at -70ºC until further processing. Sampling points for detecting *Pasteurellaceae* during early life are illustrated in Figure 5.1.

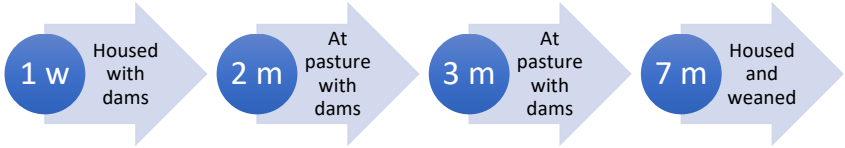

Figure 5.1: Collection of nasal swabs from calves aged approximately 1 week to 7 months for detection *Pasteurellaceae*.

5.2.3 Real-time PCR for bacteria

Real-time PCR (qPCR) assays targeting *sodA* and the 16S rRNA regions of the bacterial genome were performed for *M. haemolytica, H. somni* and *P. multocida* respectively, using

methods as described in Chapter 2, section 2.14. In all cases, the T4 internal amplification control assay C_q values were as expected, indicating successful DNA extraction with no evidence of PCR inhibition.

5.2.4 Data analysis

5.2.4.1 Real-time PCR

Cycle quantification (C_q) values obtained from collected nasal swabs were converted to genome copies/ml by interpolation using the predictive models described in Chapter 3, Figure 3.12 and Table 3.9.

5.2.4.2 Carriage

Rates of carriage of *H. somni*, *M. haemolytica* and *P. multocida* were calculated as the numbers of animals positive by qPCR for each bacterium divided by the total number of animals sampled on each occasion, unless stated otherwise.

Confidence intervals for proportions and differences between proportions were calculated using the Wilson score [242] and Newcombe-Wilson hybrid score [243] methods, respectively [244]. Association of *H. somni* and *P. multocida* carriage at 7 months of age was compared to carriage previously using Fisher's exact test (because expected values were fewer than 5) to assess for the independence of carriage, based on the number of calves with different combinations of positive/negative qPCR results. Association between carriage (*H. somni, M. haemolytica* and *P. multocida*) and sex was assessed using Fisher's exact test. All statistical analyses were performed in R version 3.5.0 using base functions. Figures were generated using the supplementary package ggplot2 (version 2.2.1).

5.3 Results

5.3.1 Study animal characteristics

Characteristics of the animals sampled in this study are shown in Table 5.1. The majority of calves were Charolais-cross (18/28). There were equal numbers of heifers and steers.

Table 5.1: Sex, sire breed and age of calves sampled shortly after birth to 7 months of age on four occasions to determine patterns of bacterial colonisation.

	Breed*			
	CHX	**LIMX**	**ST**	**Total**
Sex				
Heifer	10	4	0	14
Steer†	8	3	3	14
Median Age				
Visit	**Days (range)**		**Months (range)**	
1	4 (1–9)		0.1 (0.03–0.3)	
2	68 (54–81)		2.3 (1.8–2.7)	
3	103 (89–116)		3.4 (3.0–3.7)	
4	218 (204–231)		7.2 (6.8–7.7)	

* CHX: Charolais cross; LIMX: Limousin cross; ST: Stabiliser

† Calves castrated at 1–2 days of age by elastration

5.3.2 Carriage rates and patterns

Carriage rates for *H. somni*, *M. haemolytica* and *P. multocida* were determined by qPCR for the calves at all time points sampled. Carriage with *H. somni* was observed from 1 week of age and carriage rates at the group level remained similar up to 3 months of age (Figure 5.2). The proportion of calves positive for *H. somni* was not dissimilar between 1 week [8/28, (29%); $CI_{95\%}$: 13.9–48.9], 2 months [5/28 (18%); $CI_{95\%}$: 6.8–37.6] and 3 months [9/28 (32%); $CI_{95\%}$: 16.6–52.4]. However, at the individual level, carriage was transient, and no calves positive at 1 week of age maintained carriage to 2 months although two calves, positive at 1 week, had detectable levels again at 3 months. At 7 months of age, carriage rates were increased [12/28 (43%); $CI_{95\%}$: 25.0–62.6; Figure 5.2], although there was no association between the carriage of *H. somni* at 7 months and carriage at any age sampled previously ($p \geq 0.687$).

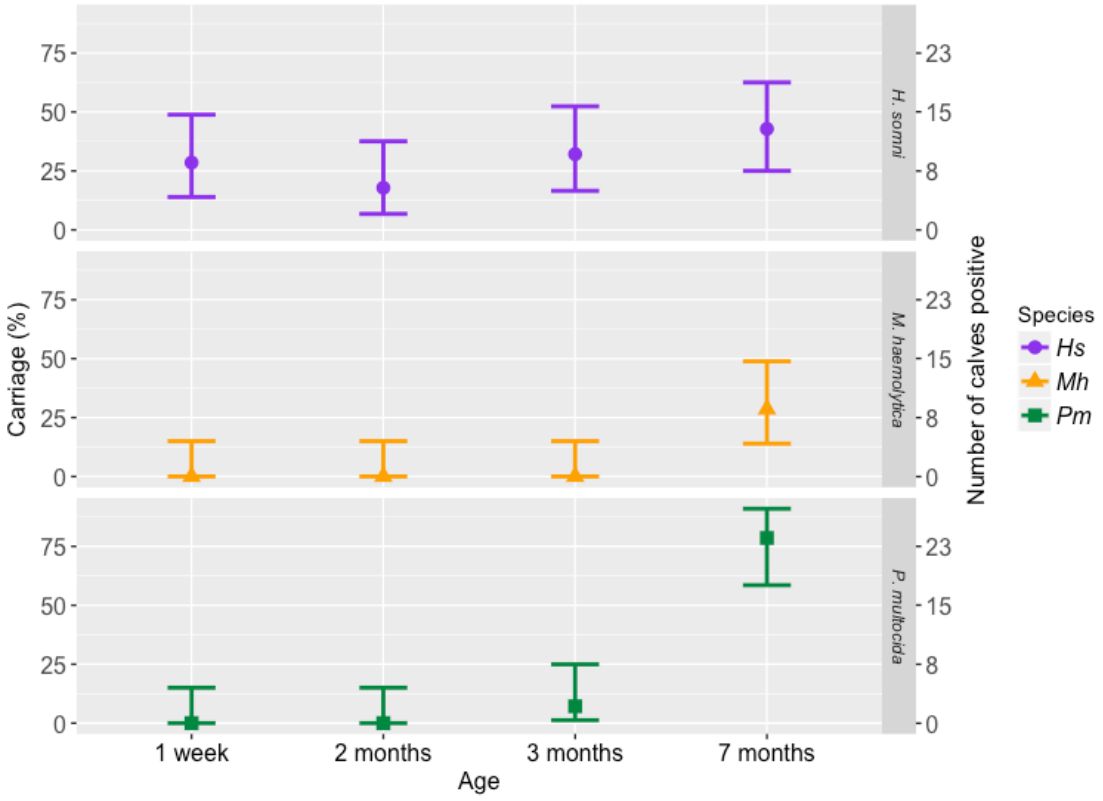

Figure 5.2: Patterns of nasal bacterial carriage for healthy calves at 1 week, 2 months, 3 months and 7 months of age.Carriage of *Histophilus somni* (top panel; purple), *Mannheimia haemolytica* (middle panel; orange) and *Pasteurella multocida* (bottom panel; green) determined by qPCR. Error bars represent 95% confidence intervals calculated using the Wilson score.

In contrast to *H. somni*, carriage of *M. haemolytica* was not detected in any animals until the age of 7 months [8/28 (29%); $CI_{95\%}$: 14.0–48.8; Figure 5.2]. Similarly, carriage of *P. multocida* was not detected until the age of 3 months, at which point only two calves were colonised [2/28

(7%); $CI_{95\%}$: 1.2–25.0], both of them also carrying *H. somni*. At 3 months, carriage of *H. somni* was significantly higher than both *P. multocida* (p = 0.044) and *M. haemolytica* (p = 0.00361). At 7 months, *P. multocida* carriage was the highest of all bacterial species at any age [22/28 (79%); $CI_{95\%}$: 58.5–91.0%; Figure 5.2]. However, as for *H. somni*, carriage at 7 months was not significantly associated with carriage previously (p = 1). The two animals colonised with *P. multocida* at 3 months of age had detectable carriage again at 7 months but no co-carriage of *H. somni* or *M. haemolytica*.

5.3.3 Spatial distribution of positive calves

Calves at 1 week of age were co-housed in pens of 5 with their respective dams. The spatial distribution of calves colonised with *H. somni* at 1 week of age is given in Figure 5.3. There was no obvious clustering of calves positive for *H. somni* in the same pen. Of those positive, 2/8 and 3/8 were housed in pens 1 and 9 respectively. The remaining 3/8 positive calves were housed in adjacent pens.

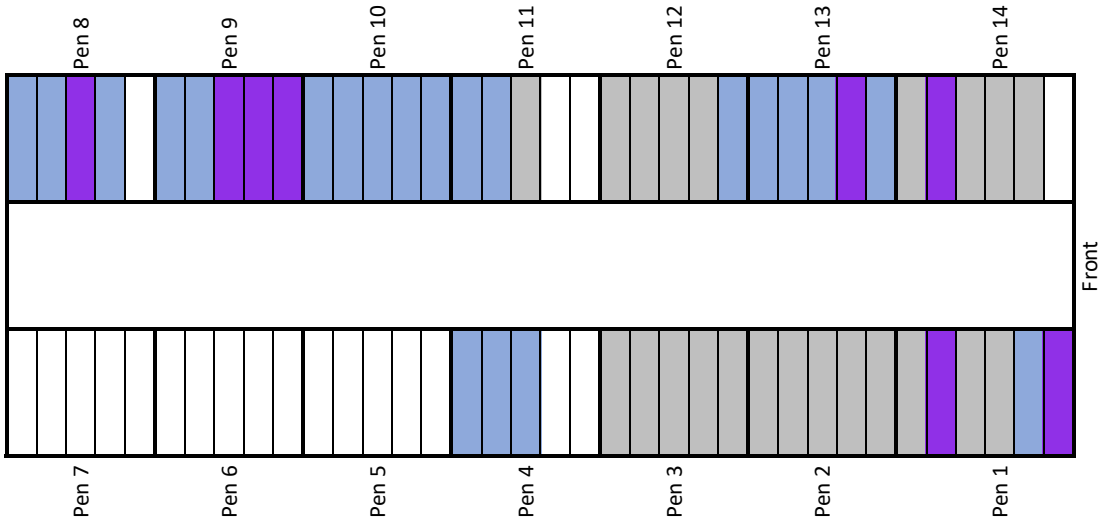

Figure 5.3: Spatial distribution of housed calves positive for *Histophilus somni* at approximately 1 week of age. Each pen contains 5 calves (pen 1 with 6 calves). Cells shaded purple represent calves positive for *H. somni*; blue shaded cells represent calves negative for *H. somni*; grey shaded cells represent calves in pens that were not sampled but co-housed with sampled calves; white shaded cells show no calf present. Each row of seven pens is separated by the midden.

5.3.4 Association of early life colonisation patterns with sex

Carriage for all three bacterial species stratified by sex is given in Table 5.2. On four of the seven occasions when carriage was observed, carriage rates were marginally higher in steers compared with heifers. However, for *H. somni*, colonisation was not significantly associated with sex at any age ($p \geq 0.209$). This was also true at 7 months of age for *M. haemolytica* ($p = 0.678$) and *P. multocida* ($p = 0.648$), and for *P. multocida* at 3 months ($p = 0.482$).

Table 5.2: Early life carriage with *Histophilus somni*, *Mannheimia haemolytica* and *Pasteurella multocida* stratified by sex

Species	**Age**	**Carriage rate**				
		Heifer	**(%)**	**Steer**	**(%)**	**P-value**[‡]
H. somni	1 week	2/14	(14.3)	6/14	(42.9)	0.209
H. somni	2 months	4/14	(28.6)	1/14	(7.14)	0.326
H. somni	3 months	3/14	(21.4)	6/14	(42.9)	0.420
H. somni	7 months	6/14	(42.9)	6/14	(42.9)	1
M. haemolytica[*]	7 months	3/14	(21.4)	5/14	(35.7)	0.678
P. multocida[†]	3 months	0/14	(0.0)	2/14	(14.3)	0.482
P. multocida[†]	7 months	10/14	(71.4)	12/14	(85.7)	0.648

[*] Carriage of *M. haemolytica* was undetected prior to 7 months of age

[†] Carriage of *P. multocida* was undetected prior to 3 months of age

[‡] P-values shown are for the null hypothesis of no association between carriage and sex as assessed by Fisher's exact test

5.3.5 Density of colonisation

Density values for all positive swabs for each bacterium were plotted as histograms and showed distinct density profiles for each species (Figure 5.4 and Figure 5.5). The distribution of density of *H. somni* carriage remained similar as calves aged (Figure 5.4). *H. somni* carriage density was observed most frequently between 1–2 $\log_{10}$ genome copies/ml. At 7 months of age, one animal had higher carriage density between 4–5 $\log_{10}$ genome copies/ml.

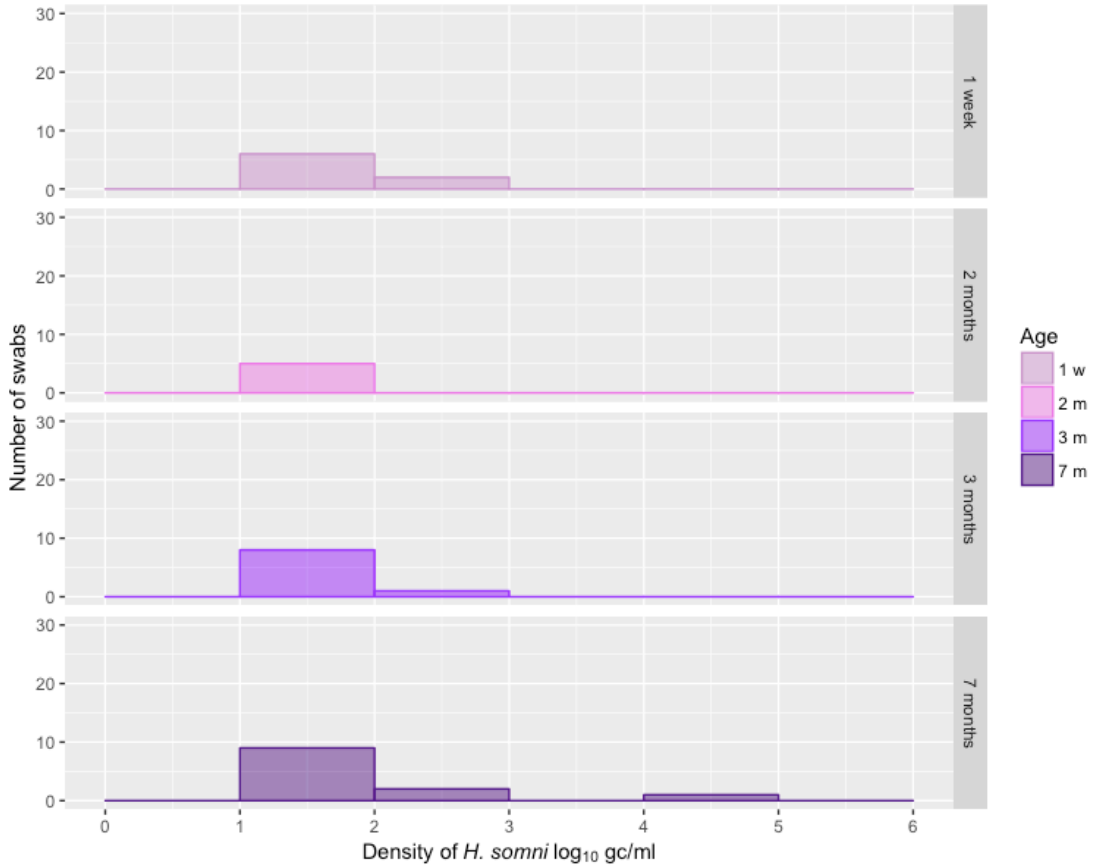

Figure 5.4: Density distribution profiles of *Histophilus somni.* Histograms for all positive swabs collected in early life summarising density of *H. somni* determined by qPCR at ages 1 week (n = 8), 2 months (n = 5), 3 months (n = 9) and 7 months (n = 12). Density given as $\log_{10}$ genome copies/ml.

Carriage density for *M. haemolytica* at 7 months of age ranged between 2 and 6 $\log_{10}$ genome copies/ml. *P. multocida* was also carried over a wide range of densities at 7 months of age (1–6 $\log_{10}$ genome copies/ml), most commonly between 3–4 $\log_{10}$ genome copies/ml (Figure 5.5). At 3 months of age two calves carried *P. multocida* at 4.5 and 4.8 $\log_{10}$ genome copies/ml.

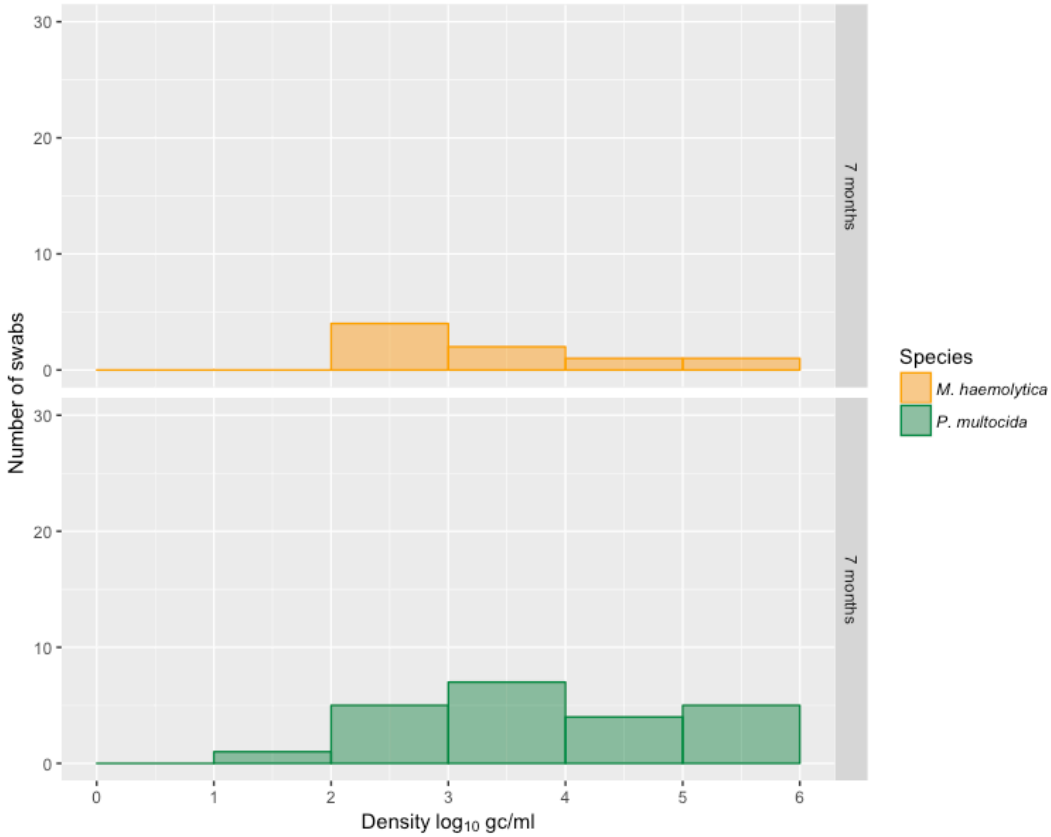

Figure 5.5: Density distribution profiles of *Mannheimia haemolytica* and *Pasteurella multocida*.Histograms for all positive swabs summarising density of *M. haemolytica* (top panel; orange; n = 8) and *P. multocida* (bottom panel; green; n = 22) determined by qPCR at 7 months of age. Density given as log10 genome copies/ml.

5.4 Discussion

Using targeted molecular approaches, this work has provided novel insights into the colonisation patterns of important bovine respiratory pathobionts in early life in apparently healthy calves. Marked differences between bacterial species in the frequency of colonisation were observed as calves aged. *Histophilus somni* was detected in the first week of life and at subsequent sampling points (2 m, 3 m and 7 m), with carriage consistently at low densities (1–2 $\log_{10}$ genome copies/ml). This suggests *H. somni* may function as part of the core respiratory microbiota, in which case it may be that it was also present in animals determined to be carriage-negative, but below the limit of detection for this assay. Conversely, *P. multocida* was not detected until 3 months of age and, even then, in only two calves also carrying *H. somni*. Dowling et al. detected high antibody titres to *P. multocida* and respiratory viruses in calves sampled under 56 days of age [263]. However, Dowling et al. did not culture *P. multocida* from any nasal swab sample from the same animals. Unfortunately, no details of colostrum intake were given but these reportedly high titres, although possibly antibody produced by the calf, probably reflect maternal antibody and as such provide only weak evidence for colonisation within the first week of life. This study has echoes of the observation that *P. multocida* is not an early coloniser of the bovine URT niche, possibly as a result of protective maternally-derived antibody.

In the studies reported here, *M. haemolytica* was not detected until 7 months of age. This finding differs from that of Woldehiwet et al. who isolated *M. haemolytica* from both nasal and tracheal swabs collected from 1-day-old Friesian male calves, purchased directly from nearby farms [137]. These differences could be due to breed (dairy versus beef) or to increased transmission from the maternal environment at birth. Interestingly, Woldehiwet et al. reported that *M. haemolytica* constitutes a very small proportion of the total flora cultured (0.5–8.5%) at one day of age. However, as calves aged, *M. haemolytica* was isolated with increased abundance relative to the total flora.

As discussed, predominance of certain bacterial species in human infants in early life has been suggested to have a protective role in later respiratory health [160]. Evidence is more limited for domesticated animals, but next-generation sequencing of 16S rRNA performed on nasal swabs collected from Holstein calves revealed the total bacterial load of 3-day-old calves to be higher in animals that developed pneumonia than in healthy animals. Differences in the relative abundance of genera were noted between healthy calves and those diagnosed with pneumonia:

abundance of *Mannheimia* and *Moraxella* was significantly higher in sick calves at 14 days old compared to healthy calves. Similarly *Mannheimia* and *Mycoplasma* were higher in sick calves at 28 days old than healthy calves [264].

When carriage of *M. haemolytica* and *P. multocida* at 7 months occurred, it was over a wide range of densities (up to 6 $\log_{10}$ genome copies/ml) although the majority of calves carrying *M. haemolytica* were colonised at lower densities (2–3 $\log_{10}$ genome copies/ml). In the studies reported in Chapter 4 a longer duration of *P. multocida* carriage in individuals was significantly associated with higher density carriage. Higher rates of *P. multocida* carriage (22/28; 79%) in older calves aged 7 months may be a consequence of increased potential for onward transmission as a result of higher carriage density: animals carrying for longer periods have potentially increased opportunity to transmit and acquire bacteria. It may also be that both the higher rates of carriage in the population and the higher density reflect a change with age in the upper respiratory environment, creating an increasingly favourable niche for *P. multocida.*

Carriage rates for all three bacterial species were highest after weaning and housing at 7 months of age. This may be a simple consequence of age (increased probability of acquisition over time, or changes in the function of the respiratory mucosa with age) or of weaning, transportation and housing, all of which are thought to enhance bacterial proliferation in the nasal passages [19] [23]. Since animals were sampled 16 days after weaning, the increased carriage rates observed at this age could be a consequence of several factors: stress of weaning and/or housing i.e. change in diet and social re-organisation; the increased stocking-density in a housed environment in turn increasing the likelihood for transmission; or change in climate from warmer spring/summer weather at pasture to a cooler less ventilated housed environment in winter. Similar carriage rates were also seen in the previous year's cohort of animals while housed at 10 months of age (see Chapter 4). Calves carrying *H. somni* in the first week of life were clustered either in the same or adjacent pens, possibly reflecting transmission between in-contact animals. However, carriage rates were low (18%) and a relatively small number of animals were studied, and thus meaningful inference is difficult; highlighting a limitation to this study. Although it is possible that carriage rates could be higher in housed environments compared to that at pasture as a result of increased transmission.

Aside from changes in environment, differences in colonisation among individuals during early life may be the result of differences in maturation rates of the immune system, particularly the

mucosal immune system in the respiratory tract. As discussed in Chapter 1, colostrum is essential for transfer of maternal antibodies in ruminants due to lack of transfer of immunoglobulins from cow to calf *in utero*, with IgG1 the predominant immunoglobulin of colostrum [29]. In beef calves, it has been shown that maternally acquired antibodies against *P. multocida* and *M. haemolytica* wane to baseline values at 60–120 days of age. Calves appear to start producing their own antibodies against these bacterial species at 60–90 days of age, with IgG1 demonstrated as the predominant antibody isotype against both of these bacterial species [106]. However, IgG2a is thought to protect against *H. somni*: cattle with low titres of IgG2a against *H. somni* have shown increased susceptibility to disease associated with *H. somni* infection and animals with infection have higher titres of IgG2a specific to *H. somni* compared to other immunoglobulin isotypes [265]. Furthermore, protective IgG2 responses have been found to develop at different ages, with IgG2a expressed early (<60 days) and IgG2b expressed later (3–4 months) [266]. It may be that colonisation during different stages of life differs as a result of waning maternally-derived antibody and differences in the timing of production of antibody by the calf.

The respiratory microbiota of calves is likely to reflect that of the dam and maternal environment. Yeoman et al. described the influence of maternal sources (udder skin, colostrum, and vaginal microbiomes) on the early succession of the calf gastrointestinal tract. Overall they found 46% of luminal and 41% of mucosal operational taxonomic units seen throughout the calf gastrointestinal tract were present in at least one of the maternal sources investigated [267]. However, similar detailed studies of the source of the respiratory microbiota has not been carried out in calves, and the role of *H. somni*, *M. haemolytica* and *P. multocida* as commensals within the respiratory microbiome remains to be elucidated. Recent indirect evidence suggests that colonisation with *Mannheimia* in early life may be protective against subsequent respiratory disease. Lima et al. reported calves born from dams with a high abundance of *Mannheimia* in their vaginal microbiome are less likely to experience URT disease [268]. Interestingly, differences in gut microbiota have been reported between vaginally and Caesarean-delivered infants. Infants delivered vaginally acquire gut bacterial communities similar to the mother's vaginal microbiota whereas those delivered via Caesarean acquire communities more similar to those found on the skin, in addition to demonstrating delayed colonisation [269]. Furthermore, children up to 36 months of age delivered by Caesarean have been found to have a higher incidence of wheezing, asthma and recurrent lower respiratory tract infection compared to vaginally delivered children [270]. It is not clear from human studies

whether the effects observed on respiratory 'health' are a direct consequence of the respiratory microbiome or an indirect consequence of the gut microbiome on, for example, the common mucosal immune system. However, it seems that the maternal vaginal microbiota may be important for determining bovine neonatal respiratory health, whether directly or indirectly. Future studies could be designed to sample the calf, dam and maternal environment. Such samples could potentially provide sequential information to determine the patterns of bacterial transmission to neonatal calves.

Together, these results suggest that bacterial colonisation in the upper respiratory tract is dynamic, with different organisms predominating as cattle age. While it is not yet clear how these colonisation dynamics affect or are affected by host mucosal immune responses, early life colonisation could be an important factor in determining later respiratory health. Logical next steps would be to conduct longitudinal studies employing high-throughput sequencing approaches to determine bovine neonatal respiratory profiles, to identify how those profiles may differ as a consequence of environment and management practices, and how they may affect long-term health of the animals.

Chapter 6 A double-blind, randomised controlled trial of the effect of respiratory viral infection on bacterial carriage in the bovine nasopharynx

6.1 Introduction

The effect of viral infection on upper respiratory tract carriage of bacteria remains poorly understood in both humans and livestock. However, recent evidence in humans suggests that viral infection can affect bacteria carried in the URT [256] [271] [272]. Infections with respiratory viruses in cattle, most commonly bovine respiratory syncytial virus (BRSV), bovine parainfluenza virus-3 (BPIV-3) and bovine herpesvirus-1 (BHV-1) are usually transient and in temperate climates, outbreaks of infection typically occur during autumn and winter months [273] [274] [275]. Viral infection may alter the environment for bacteria colonising the respiratory tract. As discussed previously in Chapter 1, viruses can modify innate and adaptive immune responses, in turn promoting secondary bacterial infection [22] [19]. Viral infection may also cause physiological disruption to the respiratory mucosa, for example compromising mucociliary apparatus to favour migration of bacteria to the lower respiratory tract (4) (6). In addition, viral infection can cause nasal discharge promoting opportunity for transmission of viruses and bacteria to susceptible individuals within a herd. Consequently, understanding viral involvement may be pivotal in improving understanding of bacterial transmission dynamics and successful implementation of bovine respiratory disease (BRD) prevention and control strategies [21] [19].

Both BRSV and BPIV-3 are in the family *Paramyxoviridae*, BRSV belonging to the genus *Pneumovirus* within the subfamily *Pneumovirinae* and BPIV-3 belonging to the genus *Respirovirus*; both are single-stranded, negative sense RNA-viruses [276] [274]. These viruses are widespread and have been detected in cattle herds worldwide [276] [277]. Reinfection with BRSV in calves is common and viruses from recurrent infections have been reported to vary up to 11% in nucleic acid sequence analysis of the genes coding for the glycoprotein and the small hydrophobic protein in closed herds [273]. Clinical signs of BRSV include serous to mucopurulent nasal discharge, slightly to moderately increased respiration rate, tachypnoea and coughing in moderate infections, and severe dyspnea with subpleural and interstitial emphysema and emphysematous bullae in severely affected calves [278]. Interlobular emphysema and bullae are differentiating features of BRSV infection and have not been reported with BPIV-3 [274]. While both BRSV and BPIV-3 may act in synergy with other

agents to cause disease, infection with BRSV alone can induce severe respiratory disease and be fatal [115] [279]. In comparison, infection with BPIV-3 alone is either subclinical or usually associated with mild clinical illness [274]. Transmission of both viruses can occur via aerosolised droplets, direct animal-to-animal contact or indirectly via fomites [140].

Work presented in previous chapters has demonstrated the utility of real-time PCR (qPCR) for detection and quantification of bacteria from bovine nasal swabs. In healthy cattle of various ages, bovine respiratory pathobionts were detected over a wide range of densities and at different rates depending on the bacterial species. However, it is not known whether or how patterns of carriage and/or density are influenced by respiratory viral infection in cattle. It can be hypothesised that animals suffering respiratory viral infection carry bacterial pathobionts at higher densities. Mina et al. recently showed that vaccination with an intranasally administered live attenuated influenza vaccine (LAIV) to significantly increases bacterial carriage densities of clinically important bacterial pathogens within the upper respiratory tract of mice (*Streptococcus pneumoniae* and *Staphylococcus aureus*) [252]. Thors et al. later demonstrated that administering LAIV increases bacterial carriage densities of *S. pneumoniae* and *Haemophilus influenzae* in healthy pre-school children [253]. These findings raise the possibility that the short-term effects of viral vaccination could modulate onward transmission of a range of non-target bacterial opportunistic pathogens, while inducing beneficial acquired immune response to vaccination resulting in protection against the target pathogen. Similarly, it can be hypothesised that wild-type viral infection may have similar and possibly more marked effects [280]. Together, these findings suggest it may be rewarding to study bacterial colonisation dynamics of nasal bacteria using vaccination as a model viral infection system.

Live attenuated vaccines contain a version of the pathogen that has been changed such that it does not elicit serious disease but is processed by the immune system nevertheless. This occurs because vaccine pathogens can replicate in the host, mimicking a natural infection, and as such do not require an adjuvant [281]. However, it should be noted that live attenuated vaccines may have the potential to revert back to virulence and cause disease [281]. Vaccines for protection against respiratory infections should ideally induce both local and systemic immunity; however, the effectiveness of immune responses hinges partly on the immunisation route [282]. Beef calves have been estimated to possess maternal antibody against BRSV and BPIV-3 for approximately 6 months [49]. During this period when maternal antibody wanes and antibody is starting to be produced by the calf, rates of BRD are high, with outbreaks typically occurring

in calves under 6 months of age. It is therefore desirable to vaccinate calves early to protect against disease later on, but this can be challenging in the presence of maternally derived antibody which can interfere with vaccination strategies. In youngstock, intranasal delivery of a bivalent live attenuated respiratory vaccine (Rispoval® RS + PI3 Intranasal, Zoetis UK Ltd) has been demonstrated to replicate in the presence of maternally derived antibody[278] [283].

In cattle, several live attenuated intranasal respiratory viral vaccines are available in the UK, including bivalent BRSV and BPIV-3 (Bovalto Respi Intranasal, Boehringer Ingelheim Animal Health UK Ltd; and Rispoval® RS + PI3 Intranasal; Zoetis UK Ltd), bivalent BPIV-3 and IBR (Imuresp RP; Zoetis UK Ltd), and monovalent BRSV (Rispoval® RS; Zoetis UK Ltd). Rispoval® RS + PI3 Intranasal is administered as a single dose to calves from 9 days of age with onset of immunity from 5 days for BRSV and 10 days for BPIV-3 – immunity lasting for 12-weeks. However, immunity against BPIV-3 may be reduced in calves with maternally derived antibody before 3 weeks of age [284]. Vangeel et al. demonstrated vaccine efficacy through reduced BRSV and BPIV-3 nasal shedding after viral challenge, following intranasal vaccination with Rispoval in calves with and without maternal antibody. It is uncertain how viral replication may be inhibited following vaccination, although several mechanisms have been proposed: virus specific antibody produced in the respiratory tract (predominately IgA), cell-mediated immune responses, viral-specific IFN-γ and enhanced production of neutrophil chemotactic factors from alveolar macrophages resulting in enhanced clearance through neutrophils [278] [283].

Randomised controlled trials (RCTs) are robust research designs used to establish a cause-effect relationship between an intervention and outcome [285]. In cluster randomised trials (CRTs) clusters are randomised to receive the intervention, rather than randomisation at the individual level as in RCTs. CRTs are often more feasible than conventional RCTs when evaluation of an intervention needs to be pragmatic [285]. In settings where interventions are delivered at the group level, for example in health care settings such as a hospital, hospital ward, or general practice, randomisation at the individual level often is not feasible, so these scenarios lend themselves well to CRTs. When the intervention under investigation is an infectious agent or live-attenuated vaccine, then rolling out an intervention to clusters can be favourable to reduce the threat of cross-contamination between intervention and control arms of the study.

A stepped wedge trial is an extension of a CRT. In stepped wedge trials, the intervention is rolled out to different clusters successively. Each cluster acts as a control providing observations before and after implementation of the intervention, and data are collected from all clusters throughout the study. Clusters are randomised so as to first receive the intervention at different staggered timepoints (crossover points) - eventually all clusters will have switched from the control to receiving the intervention phase. The timing of these different crossover points gives rise to the name stepped wedge; the 'shape' of the intervention rollout is apparent in illustrations as seen in Figure 6.1 [286]. The number of clusters per group, the number of groups, and the time between crossover points are key aspects of the allocation strategy [287].

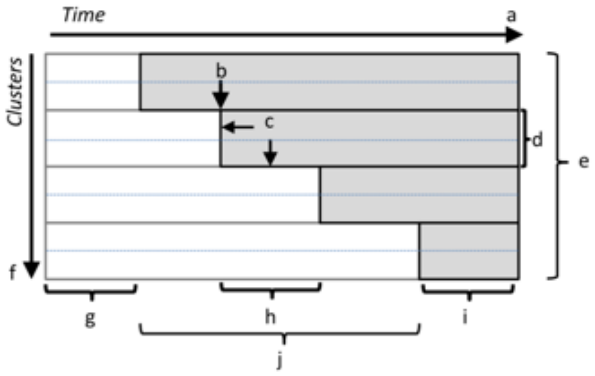

a. Duration of trial
b. Crossover point
c. (2nd) step
d. Number of clusters in (2nd) group
e. Number of groups
f. Total number of clusters
g. Pre-rollout period
h. Time between (2nd and 3rd) crossover points
i. Post-rollout period
j. Rollout period

Figure 6.1: Diagrammatic illustration showing characteristics and terminology of stepped wedge cluster randomised controlled trials. Clusters are shown in grey once exposed to the intervention. Illustration as in Copas et al. [288]

Copas *et al.* classified stepped wedge trials into three types of design: i) continuous recruitment with short exposure, where participants are recruited as the trial begins, with others participating once eligible overtime; ii) closed cohort with participants recruited at the start and remain until the study end and iii) open cohort with participants recruited from the start but some may leave during the study, whilst others become eligible [287]. The proportion of clusters exposed to the intervention gradually increases over time; consequently, control clusters will contribute observations earlier than intervention clusters and therefore time is a potential confounder

during longitudinal (horizontal) analysis of outcomes, particularly if secular trends in the measured outcome exist [289].

One of the earliest examples of a stepped wedge trial was the Gambia hepatitis study in 1980 [290]. However, its popularity has grown only in recent years, particularly within human health service evaluation [291] [292]. As such, there are challenges for sample size calculations, analysis and reporting, for which there are not yet agreed standard protocols [293] [287]. Nevertheless, this pragmatic design boasts several advantages over the conventional CRTs outlined above, particularly when study constraints may exist. For example, it may be ethically unacceptable to deliver the intervention to only one group of participants if there is existing evidence for its effectiveness. As most participants in stepped wedge studies experience both the control and intervention phase this constraint can be overcome [294]. Staggered implementation of the intervention might also be preferable due to logistical, practical and financial constraints [285].

In stepped wedge trials the treatment or intervention effect is estimated by comparing data from participants within the control (unexposed) to exposed (intervention) phase. This can be achieved through within-cluster comparisons and between-cluster comparisons, referred to as 'horizontal' and 'vertical' analyses respectively. Unlike parallel CRTs, in stepped wedge trial designs, statistical power can be increased by estimating the intervention effect using both horizontal and vertical analysis approaches simultaneously [285]. Analysis of stepped-wedge trials has largely been conducted using mixed effect models following the seminal paper by Hussey and Hughes in 2007 [293]. Using a mixed modelling framework allows for a more nuanced error structure than is possible with a simple fixed effects model with a single error term, including, for example the possibility of specifying random effects for individuals nested within clusters or specific correlation structures [295].

6.1.1 Objectives

The objectives of the work presented in this chapter were to determine the effect of viral infection (live-attenuated viral vaccination) on nasal carriage and density of *H. somni*, *M. haemolytica* and *P. multocida* in healthy beef suckler calves.

6.2 Materials and Methods

6.2.1 Study design

Calves were vaccinated intranasally with bivalent BRSV and BPIV-3 (Rispoval® RS+PI3 Intranasal, Zoetis) as a model viral infection system using a double-blind cluster randomised controlled trial following a stepped wedge design. Outcomes 2 and 4 weeks after viral infection were of primary interest. Figure 6.2 shows the design pattern matrix [292] for the study design implemented. Each barn represents a cluster (n = 29 calves per cluster). All clusters entered the trial at the same point (November 2016, Week 0) and acted as a control until the intervention (vaccination) was introduced by random allocation to one cluster at a time, at regular intervals. All clusters eventually received the intervention.

	Time (Week)						
	0	**2**	**4**	**6**	**8**	**10**	**12**
1 (Red)	1	0	2	0	2	0	0
2 (Blue)	2	0	1	0	2	0	0
3 (Green)	2	0	2	0	1	0	0

Figure 6.2: Study design pattern matrix showing collection of nasal swabs (0), collection of nasal swab and administration of vaccine (1), and collection of nasal swab and administration of diluent (2). Clusters in the intervention phase are shown in darker shading.

6.2.2 Power calculation

Sample size calculations for stepped-wedge trials have been a rapidly expanding area of research during the course of designing and implementing this study. Suitable methods were not available at the outset for this particular study design (closed cohort).

Given the population size (n = 90) and considering a study design of 540 observations, with an average cluster size of ten animals and an intracluster correlation coefficient (ICC) of 0.01 [296] the study had 80% statistical power to detect an effect size of 16% (i.e. an increase in colonisation from 30 to 46%) at $p < 0.05$ significance level. Power was calculated using Stata Statistical Software, using the Stata command 'stepped-wedge' [297]. This analytical method did not allow for repeated measures on the same animals and therefore is approximate in this case [298]. Methods have since been proposed to calculate sample sizes for stepped-wedge

trials under closed cohort designs and as such this study has for the same population (n = 90), assuming an ICC of 0.01, a minimum detectable effect size of 10% (increase in colonisation from 30 to 40%) at 80% power, $p < 0.05$ significance level [299].

6.2.3 Cattle and husbandry

Beef calves, either Charolais or Limousin crosses, or pure bred Stabiliser, were bred at Rothamsted Research, North Wyke Farm, Devon, UK. In November 2016, at weaning, 87 calves aged 5 to 9 months were transferred to the Biotechnology and Biological Sciences Research Council (BBSRC) North Wyke Farm Platform National Capability [167] and randomly allocated to one of three identical, physically adjacent, purpose-built cattle housing facilities, designated the 'Blue Barn', 'Green Barn' and the 'Red Barn' (barns are respective to the three farmlet treatments as described previously Chapter 2, section 2.2). Calves were loose-group housed (n = 29 per barn) on deep litter straw bedding with access to water and silage *ad libitum*. The nutritional plane of animals housed in each barn was similar (see appendix D for details on forage analysis). Calves were acclimatised to their surroundings for 16 days prior to starting the study i.e. the period between the first day of housing (and weaning) and Week 0.

Animals were observed daily throughout the study by animal technicians and any cattle showing abnormal behaviour that might have indicated poor health were observed in more detail for signs of respiratory disease and health scored using a standardised scoring system that included cough, nasal and ocular discharge, abnormal ear/head tilt, rectal temperature and faecal consistency [37] [36] [241]. During the weeks of sample collection, calf respiratory health was scored on the day immediately prior to sampling, on the day of sampling and one day later.

6.2.4 Allocation of animals to clusters

Animals were allocated to clusters (i.e. barns) following a modified covariate-based randomisation [170] to maximise balance in three categorical variables (breed, sex and sire) and three continuous covariates (age, weaning weight, average daily growth rate) across the three treatment groups. Covariate-based randomisation in medical studies conventionally uses cluster- or group-based covariates to determine a balanced allocation of clusters or groups of patients to treatments – in this study, it is the individual animals that are being allocated to the treatment groups, and so animal-level covariates are considered. Units are allocated to treatment by randomly selecting one potential allocation from several which meet a specified level of

balance on relevant covariates [170] [300]. The study statistician (Andrew Mead; AM) determined the random allocation of the 87 calves to three clusters. First, constraints on breed/sex/sire combinations were selected to give as balanced allocation across the three treatment groups as achievable. The majority of calves (69/87) were cross-bred Charolais, the remaining animals were cross-bred Limousin (12/87) and Stabiliser (6/87). Given this demographic, 7 groups of breed/sex/sire combinations were identified (see Appendix D) with a total of 2.3 $x10^{33}$ permutations possible for the allocation to three treatment groups based on these breed/sex/sire combinations. In a conventional covariate-based randomization all possible permutations would be considered. However, the size of the problem made this unfeasible. Therefore, an arbitrary and manageable 50,000 random permutations were constructed based on separate permutations of each of the 7 breed/sire/sex groups to allocate 29 animals to each of the 3 clusters. Summary statistics were calculated for each possible permutation assessing the mean and standard deviation of the three continuous covariates for the 3 clusters. Of these 50,000 permutations, only 423 satisfied the following criteria: daily growth rate (range of mean and standard deviation less than 0.05 kg between clusters), most recent weight (range of mean and standard deviation less than 5 kg between clusters) and age (range of mean and standard deviation less than 10 days between clusters). Finally, one permutation of the 423 was selected at random as the final allocation of animals to clusters. The principles describing this randomization approach were presented as a poster at the 29th International Biometric Conference in Barcelona, 2018 [300].

6.2.5 Study blinding

The rollout order of vaccination was determined prior to starting the stepped wedge study, by a 'blinding team' who were privy to this information, unlike those involved in running the cattle experiment, recording data and collecting and testing samples. The Blinding Team comprised: -

1.) Andrew Mead (AM) – Statistician, RR
2.) Hannah Fleming (HF) - Farm Animal Technician, RR
3.) Mark Eisler (ME) - Project Licence Holder, UoB
4.) Robert Orr (RO) – NWFP manager, RR
5.) Melanie Mils (MM) – Named Information Officer (NIO), RR

Clusters (barns) were assigned numbers 1 to 3 randomly, determining their order of vaccination by AM in October 2016. AM was neither involved in sample collection nor processing, did not

have access to subsequent results before the trial was unblinded and shared the blinding key (intervention rollout order) directly with other members of the Blinding Team.

HF was responsible for reconstitution of the vaccine and preparation of syringes with nasal applicators for administration (see 2.9) and for ensuring all doses were adequately administered by AT. AT collected nasal swabs from cattle, rectal temperatures, jugular bloods, performed respiratory calf health scoring, and monitored the temperature and humidity of the barns. Cattle were assigned a randomly-generated identification number separate to their management tag. Samples were labelled with new identification numbers for laboratory analysis by AT. AT remained blinded until all data had been collected and analysed.

ME and RO were given the blinding key in case of any unforeseen need relating to animal health and welfare, although no such need arose. This rationale applied to MM, whose role as NIO at the NWFP also demanded records of procedures and administered medicines for each calf kept on regulated procedures. No farm animal staff involved in handling animals and their day to day management had access to the blinding key.

Key details to the study design, study outcomes, methodology and raw data obtained were published as an unblinding protocol [301]. Following publication of the unblinding protocol the study was unblinded.

6.2.6 Concealing preparation of vaccine and diluent

Preparation of either vaccine or diluent was performed for each cluster on weeks 0, 4 and 8 by HF. Vaccine was reconstituted in a room out of sight from the cattle-handling facilities whilst calves were brought into the handling area. As saline was pre-prepared, no reconstitution was necessary: however, for continuity the same protocol was followed for saline, whereby HF remained in the same room out of sight for the same amount of time (15 minutes). Contents of syringes were concealed from all other personnel during administration and sample collection periods. Concealment was essential as the vaccine had a slight pink colour compared to diluent (colourless saline). Concealment was achieved by keeping vials containing prepared vaccine and saline in a covered box, all vials were covered in tape to conceal the contents, and prepared syringes were further concealed with a black sheath (Figure 6.3).

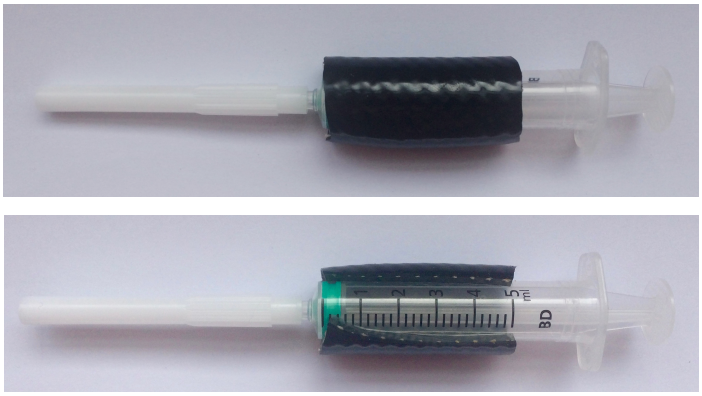

Figure 6.3: Intranasal applicator device for delivery of saline and vaccine, front and back of device pictured respectively

6.2.7 Administration of vaccine and diluent

Following an assessment to ensure calves were in good health, vaccine and diluent doses were administered intranasally. The vaccine (Rispoval RS+PI3 IntraNasal, Zoetis Animal Health) contained bovine parainfluenza type 3 (BPIV-3) thermosensitive strain RLB103, between $10^{5.0}$ and $10^{8.6}$ cell culture 50% infective doses ($CCID_{50}$) and modified live bovine respiratory syncytial virus (BRSV) strain 375, between $10^{5.0}$ and $10^{7.2}$ $CCID_{50}$, as supplied by the manufacturer with sterile diluent (water for injection and sodium chloride, 18 mg per 2 ml) for reconstitution.

Vaccine and diluent were stored in a temperature-monitored box during administration. Vaccine was administered to calves as a 2 ml dose with an intranasal applicator supplied by the vaccine manufacturer and modified to ensure blinding, see section 6.2.6. Diluent (saline; 0.9% w/v sodium chloride, Zoetis Animal Health) was administered as a 2 ml dose by an identical route as a placebo. Gloves and applicators were changed between animals.

6.2.8 Biosecurity measures to avoid cross-contamination between barns

Stockman coats and overalls worn by individuals directly handling animals or collecting samples were changed between barns to prevent transmission of infectious material. Personnel directly handling animals wore gloves and changed these between barn groups. In addition, gloves were changed between each animal by the individual collecting samples.

6.2.9 Nasal swabs and rectal temperatures

Nasal swabs (dual-tipped) were collected from each animal as described previously in Chapter 2, section 2.9.5. Rectal temperatures were recorded on the same day as nasal swab collection using a livestock rapid read digital thermometer (Nettex, UK).

6.2.10 Parasitological sampling

Shortly after housing of cattle, composite samples of 10 freshly deposited faecal pats collected from the floor of each barn were tested for the presence of respiratory nematode larvae (*Dictyocaulus viviparus*) using the Baermann technique. Following parasitological testing, all calves were treated once routinely with 200 mg ivermectin (Noromectin®, Norbrook) pour-on (40 ml of product) to control respiratory and gastrointestinal nematodes and external parasites.

6.2.11 Serological sampling

Paired blood samples were collected into plain Vacutainers as described in Chapter 2, section 2.9.6 on Week 0 (n = 78) and Week 12 (n = 86) for evidence of natural infection by common bovine respiratory viruses (BRSV, BPIV-3 and BHV-1), BVDV and *Mycoplasma bovis*.

6.2.12 Measurement of barn temperature and relative humidity

Temperature and relative humidity was monitored in each barn and recorded every 4 hours using a Perfect-Prime TH0165WH Micro USB High Accuracy Temperature Humidity Data Logger Meter (Perfect-Prime, London, UK).

6.2.13 Laboratory analyses

6.2.13.1 ELISAs to detect serological responses to bovine respiratory pathogens

Serum samples were tested in duplicate microplate wells using a multiplex indirect ELISA (BIOX K 284 ELISA®, BioX, Belgium) to detect presence of antibodies against BHV-1, BVDV, BRSV, BPIV-3 and *Mycoplasma bovis* as described previously in Chapter 2, 2.12.

6.2.13.2 Real-time PCR for bacteria

Real-time PCR (qPCR) assays targeting *sodA* and the 16S rRNA region of the bacterial genome were performed for *M. haemolytica, H. somni* and *P. multocida* respectively, using methods as described in Chapter 2, 2.14.

6.2.14 Data analysis

6.2.14.1 Barn temperature and relative humidity

Pearson correlation coefficients were computed for the relationships between the barns for i) relative humidity and ii) temperature. Correlograms (graphical representations of correlation matrices) for Pearson correlation coefficients were computed using the R function 'corrplot'.

6.2.14.2 Seroprevalence

For each of the five respiratory disease agents tested, seroprevalences on Week 0 and 12 were calculated as the number of animals seropositive by ELISA (i.e. results in categories 1 to 5, see Chapter 2, section 2.12) divided by the total number of animals sampled.

6.2.14.3 Real-time PCR

Cycle quantification (C_q) values obtained from qPCR reactions on nasal swab samples were converted to genome copies/ml using the equations derived from predictive models fitted to standard curves for each assay as described in Chapter 3.

6.2.14.4 Carriage and co-carriage

Rates of carriage of *H. somni*, *M. haemolytica* and *P. multocida* were calculated as the numbers of animals positive by qPCR for each agent divided by the numbers of animals sampled on each occasion, unless stated otherwise. Carriage estimates for each bacterial species were calculated for each cluster/barn and as an overall average. Co-carriage rate, defined as carriage of either two or three of the bacterial species on the same occasion, was calculated as an overall average for each of the three barns. Confidence intervals for proportions and differences between proportions were calculated using the Wilson score [242] and Newcombe-Wilson hybrid score [243] methods respectively [244].

6.2.14.5 Differences between clusters in carriage rates at Week 0

Pearson's χ^2 test was used to assess for differences in carriage at Week 0. Counts of the number of calves in each cluster positive and negative by qPCR for each bacterial species were compared.

6.2.14.6 Effect of viral infection on bacterial carriage rate

6.2.14.6.1 Bacterial carriage combining 1st and 2nd crossover points

A preliminary analysis was conducted to compare bacterial carriage rates in animals in the control phase with those in the intervention phase. Each cluster (barn) received the vaccine at one of three different time points, subsequently referred to as crossover points. This analysis did not consider differences in the timing of vaccination or clustering of animals within barn, it simply treated the first two crossover points as replicates by combining comparisons as follows: Red Barn vs Blue and Green barns (replicate 1); Blue Barn vs Green Barn (replicate 2), as shown in Figure 6.4. The Red Barn was excluded from replicate 2 as animals had already been exposed to the intervention for 4 weeks; if included in analyses then the two replicates would not be comparable in terms of exposure time since vaccination. Generalised linear logistic models of the rates of carriage of *M. haemolytica* and *P. multocida* were used to estimate the odds ratios for the effect of vaccination 2 and 4-weeks after it was administered. Models included vaccination as a predictor and replicate (1 and 2 as above) as a covariate. *H. somni* was not detected from animals housed in the Green Barn from Week 2 (based on PCR), therefore the first vaccine crossover period excluding observations from the Green barn was considered (i.e. Red vs Blue).

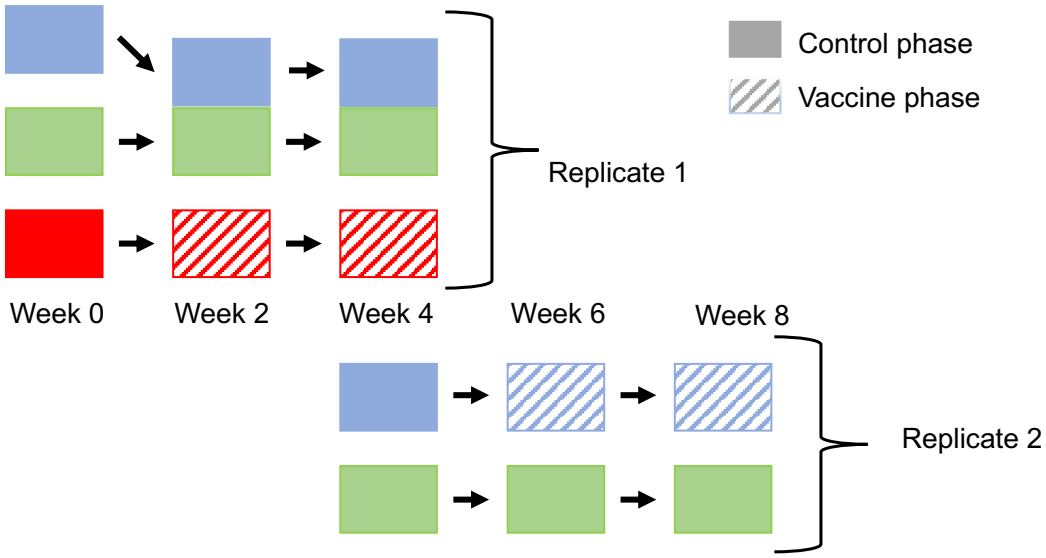

Figure 6.4: Illustration showing analysis of bacterial carriage rates combining the 1st and 2nd crossover points. Clusters in the control phase (solid shading) and clusters in the intervention phase (diagonal shading) are illustrated. Replicate 1: At Week 0 all clusters are in the control phase and Red receive the vaccine, at Week 2 the Blue and Green clusters remain in the control phase with Red in the intervention phase. Replicate 2: At Week 4, the Blue cluster is vaccinated and subsequently at Week 6 and Week 8 is in the intervention phase – the Green cluster remains in the control phase.

6.2.14.6.2 Vertical analysis of bacterial carriage following each crossover point

For each bacterial species, at each crossover point, the odds ratio of carriage was estimated for animals in the intervention phase 2 and 4-weeks post vaccination compared to those remaining in the control phase. Analysis at each of the crossover points was conducted as follows:

1.) 1st crossover: carriage at Week 2 & Week 4; Red (n = 29) vs Blue and Green (n = 58)

2.) 2nd crossover: carriage at Week 6 & Week 8; Red and Blue (n = 58) vs Green (n = 28)

3.) 3rd crossover: carriage at Week 10 & Week 12; Green (n = 28) vs Red and Blue (n = 58)

At the 3rd crossover all animals had received the vaccine, therefore this analysis assessed whether the carriage rate in the most recently vaccinated (Green) cluster differed from that in the other two clusters (Red and Blue) vaccinated two or four weeks previously. A sequence of nested general linear models with a Poisson error distribution and log-link function were fitted to constructed count data using the base 'glm' function of R version 3.5.0 (see Chapter 2, section 2.18 for an introduction to these models). Datasets were constructed by counting the number of calves positive and negative for carriage at Week 2 to Week 12 (response), for each level of the explanatory variables: treatment (vaccine/control), prior carriage of the response bacterium at day of vaccination (positive/negative) and cluster (blue/green/red). The nested term of cluster within treatment assessed for differences in carriage between two clusters in the same intervention phase. Nested models of increasing complexity were built from the simplest, baseline model to investigate the effect of explanatory variables on carriage post vaccination (see Appendix D, Table D.1 for sequence of models). The impact of additional terms included in a more complex model was assessed by comparing the change in residual deviance from a nested, simpler model with the upper-tailed critical value ($p < 0.05$) of the appropriate chi-squared distribution (as identified by the change in the residual degrees of freedom between the models). The odds ratios for the main effect terms of vaccination and prior carriage on subsequent carriage (2 and 4 weeks post vaccination) were estimated by exponentiating the coefficient for interaction terms between carriage and the term of interest for the parsimonious model (see Appendix D for details on model selection and evaluation of fit). Profile confidence intervals for odds ratios were estimated using the 'confint' function in R (version 3.5.0) [302].

6.2.14.6.3 Longitudinal assessment of bacterial carriage: mixed effect models

Generalized linear mixed effect models were used to estimate the odds ratio of carriage for animals in the intervention phase compared with the control phase. For each bacterial species, presence or absence of carriage was considered as the response variable. Two cross-classified multilevel models [303] were fitted to assess either the overall effect of viral infection on

bacterial carriage (Model 1) or a transient effect of viral infection on carriage (Model 2). In Model 1, vaccination was included as a fixed effect with two levels: unvaccinated (control) or vaccinated. In Model 2, vaccination was included as a fixed effect ('vaccination status') with four levels: unvaccinated (control), vaccinated 2 weeks previously, vaccinated 4 weeks previously, or vaccinated 6 or more weeks previously. Model 2 was simplified to Model 3 where appropriate to include fewer categories of vaccination status: unvaccinated (control), vaccinated 2 weeks previously or vaccinated 4 or more weeks previously. In all models, once animals received the vaccine, they remained in the intervention phase. As proposed by Hooper et al. for the analysis of closed cohort stepped wedge trials [303] a nested random effect of calf within cluster (barn), and a crossed random effect of time within cluster was included. Random effects accounted for correlation between observations assessed in the same calf within a given cluster at different time points and differences in conditions experienced by a given cluster i.e. experiencing the control or intervention condition at different time points [303]. The nested effect of calf within cluster and crossed-random effect of time within cluster can be seen in Figure 6.5. The significance of viral infection on bacterial carriage was assessed by comparing the simpler unconditional model (no fixed effect of viral infection) with the model including a fixed effect of viral infection (vaccination/vaccination status). Models were compared by calculating the likelihood ratio test (LRT) statistic by comparing the change in residual deviance between models with the upper-tailed critical value ($p < 0.05$) of the appropriate chi-squared distribution (with degrees of freedom equal to the change in the residual degrees of freedom between the models). Similarly, the fit of both random effects was assessed by sequentially removing each effect from the model containing no fixed effects and calculating the LRT statistic between competing models. The Akaike Information Criterion (AIC) was also used to compare model fit, with a lower AIC value indicating a better fit.

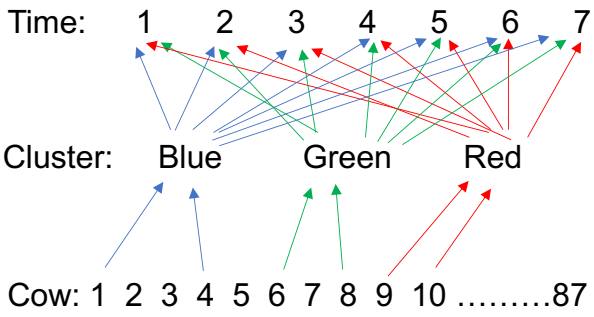

Figure 6.5: Nested random effects structure of calves within clusters (random variation among spatial blocks) and cross-classified random effects structure of clusters with time (each cluster is observed at each time; random variation among temporal blocks).

6.2.14.7 Effect of viral infection on bacterial carriage density

6.2.14.7.1 Bacterial density combining 1st and 2nd crossover points

Vertical analysis of density was performed in a manner analogous to the logistic regression models of bacterial carriage (see above, section 6.2.14.6) comparing unvaccinated cluster(s) with vaccinated cluster(s) pre- and post-vaccination. In brief, replicate 1 for this analysis compared unvaccinated animals in the Blue and Green Barns with vaccinated animals in the Red Barn and for replicate 2 compared vaccinated animals in the Blue Barn to unvaccinated animals in the Green Barn. A gamma general linear model was fitted to estimate the difference in mean density of *P. multocida* carriage (genome copies/ml) between animals positive in the control and intervention condition. *P. multocida* carriage density (genome copies/ml) was the response variable, with vaccination as a predictor and replicate (1 and 2 as above) as a covariate. Density of carriage 2 and 4-weeks after vaccination was assessed. Gamma regression, using a log link was chosen because density was positively skewed.

6.2.14.7.2 Horizontal analysis of *P. multocida* density within barn

The density of *P. multocida* determined by PCR was natural log transformed for positive swabs collected in each barn on the day of vaccination, 2 weeks post vaccination and 4 weeks post vaccination. The difference in log density between paired swabs positive on two occasions was calculated for i) the day of vaccination and 2 weeks post vaccination and, ii) the day of vaccination and 4 weeks post vaccination. The mean of the differences in log *P. multocida* carriage was exponentiated to obtain a ratio of geometric means [304]. To assess whether the mean log *P. multocida* density before and after vaccination (2 and 4 weeks) was significantly different within each barn a paired t-test was performed on paired swabs positive on the occasions outlined above.

6.2.14.7.3 Vertical analysis of *P. multocida* density following each crossover point

The mean of the differences for swabs positive for *P. multocida* as described above (section 6.2.14.7.2) was calculated for each barn. To assess for differences in *P. multocida* density 2 and 4-weeks following vaccination between barns, a one-way ANOVA was fitted with a fixed effect of cluster (barn) and the natural log change in *P. multocida* density as the response variable. For significant effects, a Tukey test was used to determine which barns were different.

6.2.14.7.4 Horizontal and vertical analysis of *H. somni* and *M. haemolytica* density

Too few animals were positive for *H. somni* or *M. haemolytica* for meaningful statistical analysis.

6.3 Results

6.3.1 Monitoring barn climate

The internal climate (temperature and relative humidity) of each barn was monitored during the housing period. Both parameters fluctuated over the study period (Week 0 to 12) with similar trends observed across barns (Figure 6.6). Temperatures ranged from -2.3ºC to 14.8ºC; relative humidity ranged from 53.4% to 100%. The lowest temperature recorded occurred in the Green barn at Week 7.6 with a corresponding humidity of 91.3%. The lowest humidity occurred at Week 10 in the Green barn, with a corresponding temperature of 6.8ºC. Peak temperature occurred in the Green barn at Week 4 with a corresponding humidity of 79%. Peak humidity occurred at Week 11.8 in the Blue barn (100%) with a corresponding temperature of 7.3ºC. Barn temperature and humidity were similar between the three barns at the 1st and 2nd crossover points (Week 0, Blue: 10.2ºC; Green: 10.2ºC; Red: 9.9ºC and Week 4, Blue: 12.8 ºC; Green: 12.6ºC; Red: 12.7ºC). However, at the 3rd crossover point (Week 8) the temperature was lower (~6ºC) for all barns (Blue: 5.2ºC; Green: 5.1ºC; Red: 5.3ºC) than at prior crossover points (Week 0 and 4).

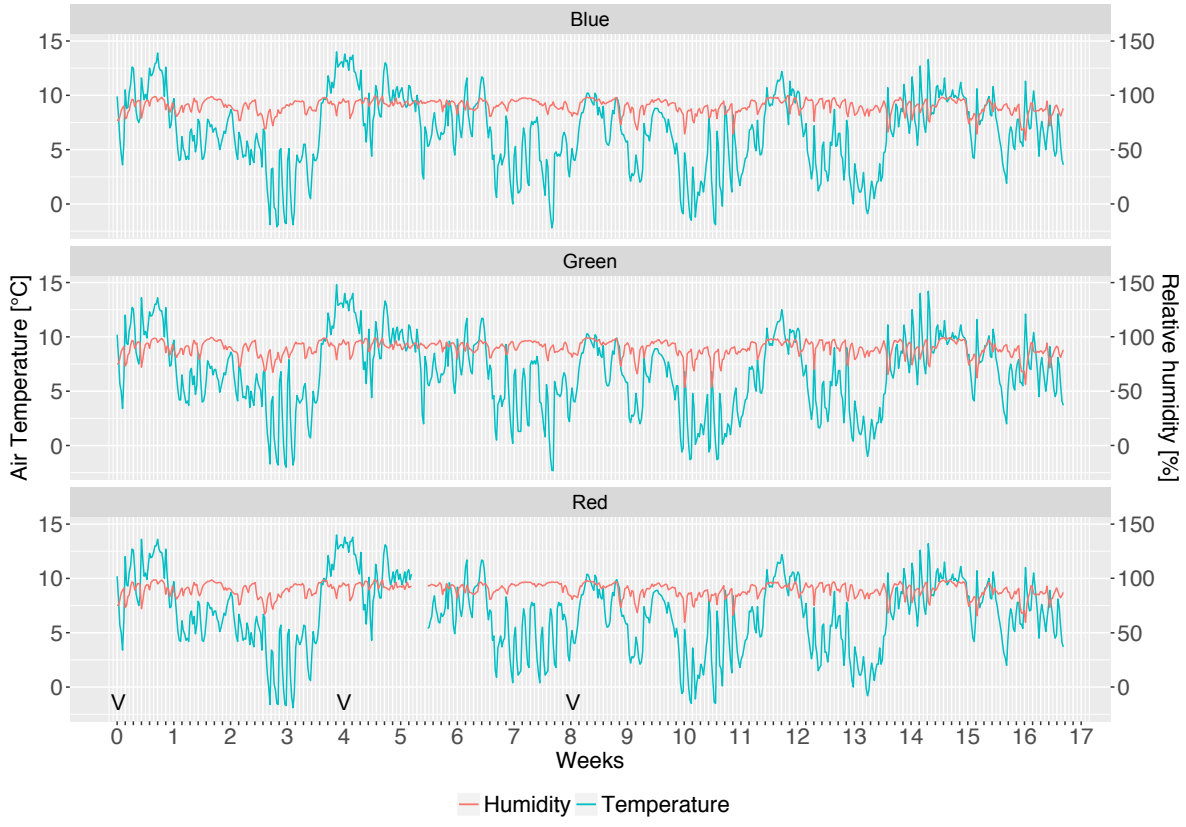

Figure 6.6: Air temperature and relative humidity of the three barns during the stepped wedge study

Temperature and relative humidity were positively correlated among barns (Figure 6.7). Temperature was more similar between the Blue and Green (r = 0.965) barns than between the Red and Green (r = 0.102) or Red and Blue (r = 0.101) barns. Similarly, humidity was highly correlated between the Blue and Green barns (r = 0.920), but less so between Red and Green (r = 0.190), and Red and Blue (r = 0.223).

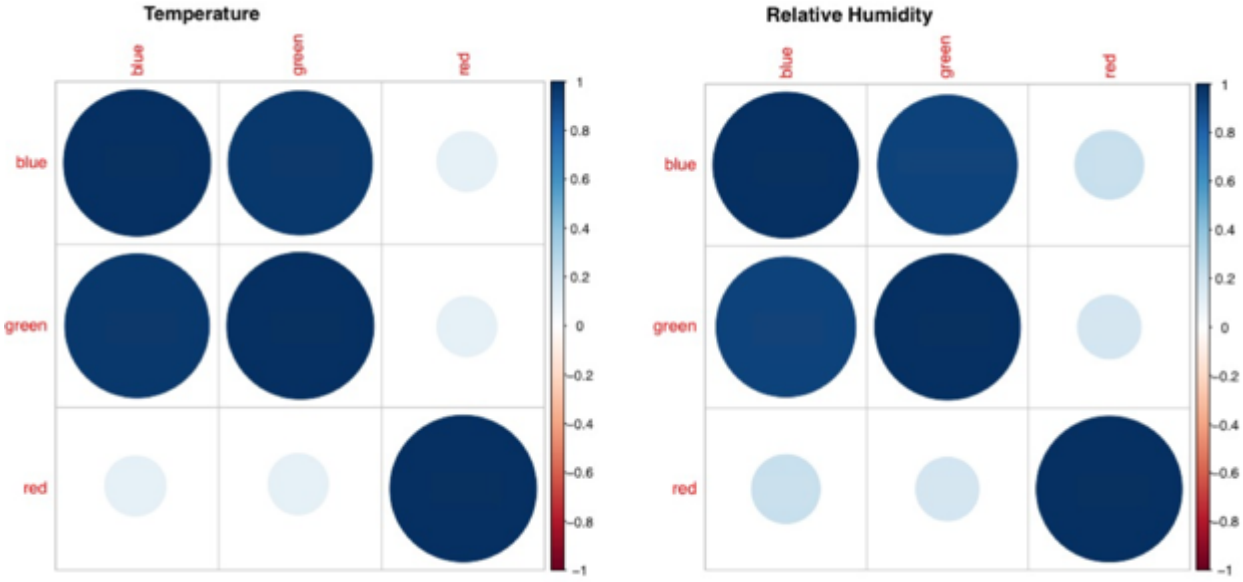

Figure 6.7: Correlograms depicting Pearson correlations between the barns for temperatures (left) and relative humidity levels (right) monitored in each barn. Positive correlations are displayed in blue. The colour intensity and the size of the circle are proportional to the correlation coefficients, which are shown in the legend on the right-hand side of the correlogram.

6.3.2 Characteristics of the study animals

Characteristics of the animals following covariate-based constrained randomisation at the start of the study are shown in Table 6.1.

Table 6.1: Sex, sire breed, age and weight of calves (n = 87) housed in the Blue, Green and Red barns during the stepped-wedge study

	Cluster			
	Blue Barn	**Green Barn**	**Red Barn**	
				Total
Sex				
Heifer	15	15	15	45
Steer	14	14	14	42
Sire Breed				
Charolais	23	23	23	69
Limousin	4	4	4	12
Stabiliser	2	2	2	6
				All clusters
Age at Week 0 (days)				
Median	228	231	224	228*
Min	154	147	164	147
Max	274	249	260	260
Weight at Week 0 (kg)				
Median	308	315	313	312*
Min	198	159	177	159
Max	417	435	418	435

* Median age and weight of all animals (n =87)

6.3.3 Signs of respiratory disease

Animals remained healthy over the course of the study apart from three individuals. One animal died during the second study week (ID: 160). The animal presented with colic/abdominal symptoms. At post-mortem a distinct length of small intestine was dark purple in colour and almost gangrenous, but adjacent intestine was normal and further abdominal findings were unremarkable, as were the lungs and heart. Although Clostridial disease or *Salmonella* was suspected on the basis of post-mortem examination, laboratory tests proved negative. Intestinal torsion was given as the likely cause of death. At Week 10, one animal (ID: 177) presented with increased respiration rate, elevated temperature and dry adventitious lung sounds detected on auscultation, clinical signs highly suggestive of pneumonia. No nasal discharge was observed. The animal was treated with tulathromycin (Draxxin, Zoetis UK Limited) and the non-steroidal anti-inflammatory drug meloxicam (Metacam, Boehringer Ingelheim Animal Health UK Ltd). Another animal (ID: 140) was diagnosed with infectious keratoconjunctivitis one week before starting the study and was treated with oxytetracycline hydrochloride (Engemycin 10% DD, MSD Animal Health). Transient bouts of coughing were observed in animals on a few occasions only. This largely occurred following bedding down with fresh straw.

6.3.4 Serological results for respiratory disease agents

Serological results for the five respiratory disease agents tested are shown in Table 6.2. For all 5 agents tested and in all three barns, some cattle were serologically positive on at least one occasion. No cattle were serologically positive for all five agents on the same day of testing. Antibodies to BRSV were detected in more than half the animals at Week 0 (57.5–75.0 %), and the rate of seropositivity increased still further by Week 12 (85.7–100.0 %). Only four animals had detectable antibodies to BPIV-3 at Week 0, with much higher levels of seropositivity at Week 12 (75–89.7%). Few animals (<4) had detectable antibodies to BVDV or BHV-1 at Week 0 and Week 12. Seropositivity to *Mycoplasma bovis* was similar among the three barns at Week 0 (21.4–37.5%); by Week 12, the proportion of animals with detectable antibodies to *M. bovis* in the Red Barn (72%) was significantly higher ($p = 0.0229$), although similar increases were not seen in the Blue (17.2%) or Green (25%) barns. Laboratory analysis of collected bloods from animal 177 which presented with signs of pneumonia provided evidence of a rising titre to BRSV.

Table 6.2: Serological results for BVDV, BHV-1, *M. bovis*, BRSV and BPIV-3 at Week 0 and Week 12 of the stepped wedge study

Barn	**Agent**	**Week 0**			**Week 12**			**Seroconversion‡**	
		Number of animals positive (n/N)†	**%**	**$CI_{95\%}$***	**Number of animals positive (n/N)†**	**%**	**$CI_{95\%}$***	**Number of animals positive (n/N)†**	**%**
BVDV	Blue	2/26	7.7	1.3 – 26.6	0/29	0.0	0.0 – 14.6	0/26	0.0
	Green	1/28	3.6	0.2 – 20.2	1/28	3.6	0.2 – 20.2	1/28	3.6
	Red	0/24	0.0	0.0 - 17.2	1/29	3.4	0.2 – 19.6	1/24	4.2
BHV-1	Blue	2/26	7.7	1.3 – 26.6	0/29	0.0	0.0 – 14.6	0/26	0.0
	Green	2/28	7.1	1.2 – 25.0	2/28	7.1	1.2 – 25.0	1/28	3.6
	Red	1/24	4.2	0.02 – 23.1	0/29	0.0	0.0 – 14.6	0/24	0.0
M. bovis	Blue	9/26	34.6	17.9 – 55.6	5/29	17.2	6.5 – 36.5	2/26	7.7
	Green	6/28	21.4	9.0 – 41.5	7/28	25.0	11.4 – 45.2	2/28	7.1
	Red	9/24	37.5	19.6 – 59.2	21/29	72.4	52.5 – 86.6	11/24	45.8

Table 6.2 continued

Barn	Agent	Week 0			Week 12			Seroconversion‡	
		Number of animals positive (n/N)†	%	$CI_{95\%}$*	Number of animals positive (n/N)†	%	$CI_{95\%}$*	Number of animals positive (n/N)†	%
BRSV	Blue	15/26	57.7	37.2 – 76.0	29/29	100.0	85.4 –100.0	15/26	57.7
	Green	21/28	75.0	54.8 – 88.6	24/28	85.7	66.4–95.3	5/28	17.9
	Red	19/24	71.2	57.3 – 92.1	29/29	100.0	85.4–100.0	12/24	50.0
BPIV-3	Blue	1/26	3.8	0.2 – 21.6	24/29	82.8	63.5–93.5	19/26	73.1
	Green	3/28	10.7	2.8 – 29.4	21/28	75.0	54.8–88.6	19/28	67.9
	Red	0/24	0.0	0.0– 17.2	26/29	89.7	71.5–97.3	20/24	83.3

* Confidence intervals for single proportions were calculated using the Wilson score

† Samples were considered seropositive in that calculated optical densities corresponded to categories 1 to 5 of the ELISA kit instructions (see Chapter 2 for further details).

‡ Seroconversion was considered to have occurred if there was an increase of at least two categories of seropositivity between paired samples.

6.3.5 Carriage of *Pasteurellaceae*

6.3.5.1 Carriage at Week 0

A total of 604 nasal swabs were analysed using qPCR for the presence of *H. somni, M. haemolytica* and *P. multocida*. Carriage rates for all three bacterial species at each week are shown in Table 6.3. All three species of *Pasteurellaceae* were detected in all three barns at Week 0. *P. multocida* was carried at high prevalences in the Green (93.1%), Red (86.2%) and Blue (69%) barns. Carriage rates of *H. somni* were very similar at Week 0 in all three barns: Blue (41.4%), Green (44.8%) and Red (37.9%). Similar rates of *M. haemolytica* carriage were observed in the Blue and Red barns at 48.3% and 44.8% respectively, with a lower rate in the Green barn (24.1%). There was very little evidence to suggest a difference between barns in *H. somni* ($p = 0.867$; χ^2) or *M. haemolytica* ($p = 0.125$; χ^2) carriage at Week 0. However, there was evidence to suggest a difference in *P. multocida* carriage between barns at baseline ($p = 0.0432$; χ^2).

6.3.5.2 Overall rates of bacterial carriage and co-carriage

Bacterial nucleic acid was detected in 472 of 604 samples. Nucleic acid of more than one bacterial species (i.e. co-carriage) was detected in 168 of these 472 samples. *P. multocida* was detected the most frequently (399/604; 66.1%;), followed by *M. haemolytica* (154/604; 25.5%) and *H. somni* (109/604; 18.0%). Of the 168 samples with co-carriage detected, *P. multocida* and *M. haemolytica* was the most frequent combination recorded (86/168; 51.2%), followed by *P. multocida* and *H. somni* (53/168; 31.5%). Co-carriage with *H. somni* and *M. haemolytica* was detected in seven samples (7/168; 4.2%) and co-carriage with all three species was detected in 22/168 samples (13.1%).

Table 6.3: Carriage rates of *Histophilus somni*, *Mannheimia haemolytica* and *Pasteurella multocida* in the Blue, Green and Red barns over the course of the study

		Number (%)*													
	Week	0		2		4		6		8		10		12	
H. somni	**Red**	11	(37.9)	2	(6.9)	4	(13.8)	3	(10.3)	6	(20.7)	3	(10.3)	1	(3.4)
	Blue	12	(41.4)	9	(31.0)	6	(20.7)	17	(58.6)	10	(34.5)	4	(13.8)	8	(27.6)
	Green	13	(44.8)	0	(0.0)	0	(0.0)	0	(0.0)	0	(0.0)	0	(0.0)	0	(0.0)
M. haemolytica	**Red**	13	(44.8)	6	(20.7)	6	(20.7)	7	(24.1)	12	(41.4)	5	(17.2)	5	(17.2)
	Blue	14	(48.3)	7	(24.1)	6	(20.7)	5	(17.2)	5	(17.2)	1	(3.4)	9	(31.0)
	Green	7	(24.1)	3	(10.3)	8	(28.6)	12	(42.9)	14	(50.0)	2	(7.1)	7	(25)
P. multocida	**Red**	25	(86.2)	13	(44.8)	19	(65.5)	16	(55.2)	28	(96.6)	22	(75.7)	13	(44.8)
	Blue	20	(69.0)	14	(48.3)	16	(55.2)	13	(44.8)	19	(65.5)	10	(34.5)	12	(41.4)
	Green	27	(93.1)	21	(72.4)	19	(67.9)	23	(82.1)	27	(96.4)	26	(92.9)	16	(57.1)

Shaded cells indicate the intervention phase of the stepped wedge study

*n = 29 for all barns at all sampling occasions apart from Weeks 4–12 in the Green Barn where n = 28 (one animal died)

6.3.5.3 Trends in bacterial carriage over the study period at the barn level

6.3.5.3.1 *H. somni*

Carriage rates of *H. somni* within clusters over the study period are shown for each barn in Figure 6.8. Prevalence of carriage at Week 0 was very similar in all three barns: between Week 0 and Week 2 carriage decreased for all barns, but thereafter there were barn differences. At Week 2 and at subsequent sampling points until the end of the study, *H. somni* was not detected from any animal in the Green Barn. Carriage peaked in the Blue Barn at Week 6, two weeks post vaccination (58.6%) and declined thereafter. Carriage was maintained at similarly low rates in the Red Barn between Week 2 to 12 following vaccination at Week 0.

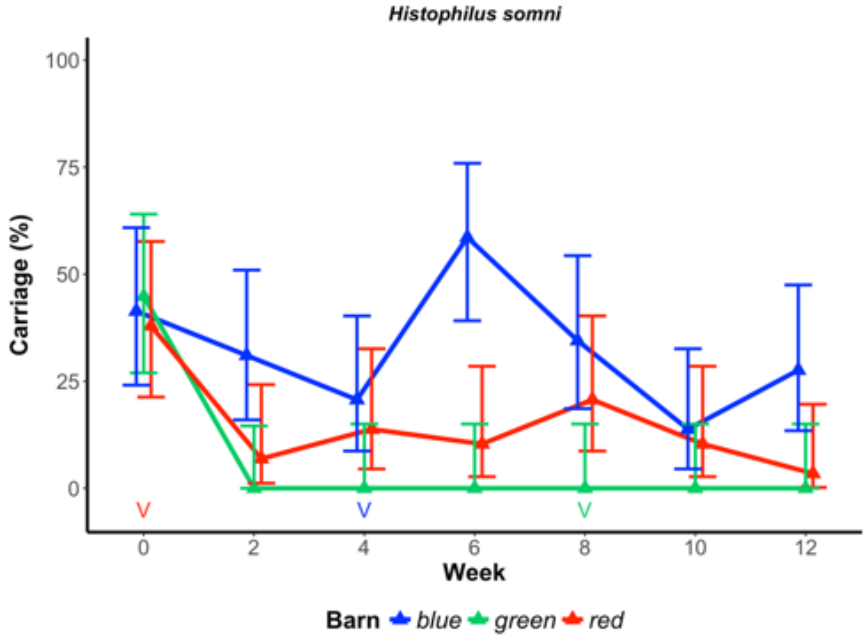

Figure 6.8: Carriage rates of *Histophilus somni* within clusters over the study period. Timing of vaccination for each barn marked with a 'V' in the corresponding colour.

6.3.5.3.2 *M. haemolytica*

Trends in *M. haemolytica* carriage for each barn are shown in Figure 6.9. Carriage rates were highest at Week 0 for both the Blue (48.3%) and Red (44.8%) barns. The highest carriage rate observed for any barn occurred at Week 8 in the Green barn (50.0%). Carriage rates for vaccinated animals fell following vaccination in each barn. Following vaccination in the Red barn at Week 0, carriage decreased and was maintained at a similar rate between Week 2 and 6. Carriage fell slightly 2 and 4-weeks post vaccination in the Blue Barn (only 1 animal lost carriage). Between Week 2 and 8, carriage in the Green Barn steadily increased, thereafter (2 and 4 weeks post vaccination) carriage rates were lower.

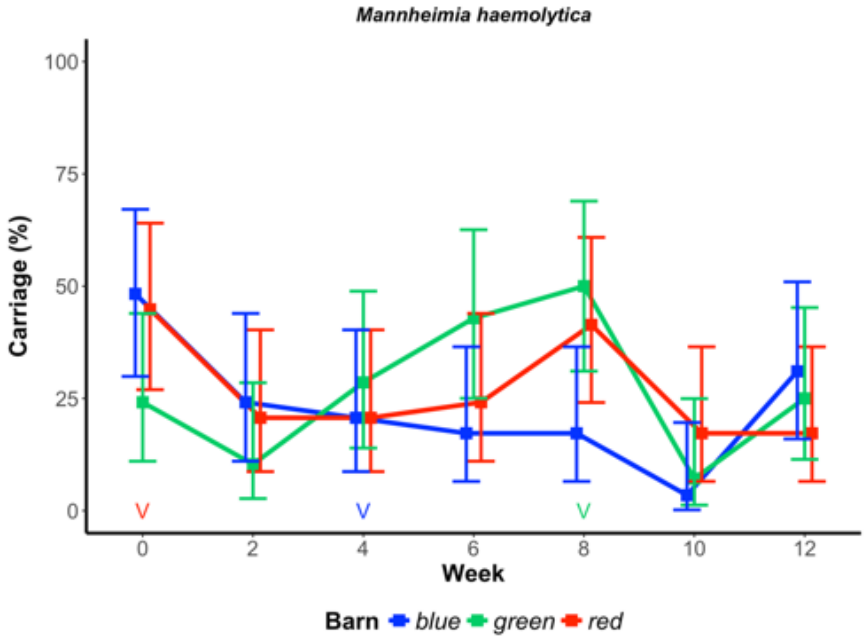

Figure 6.9: Carriage rates of *Mannheimia haemolytica* within clusters over the study period. Timing of vaccination for each barn marked with a 'V' in the corresponding colour.

6.3.5.3.3 *P. multocida*

Over the study period, similar fluctuations in carriage of *P. multocida* were observed between barns. In general, carriage was maintained at higher rates in the Green Barn and lower rates in the Blue Barn (Figure 6.10). The highest colonisation rates (~96%) were observed at Week 8 (Green and Red barns), with colonisation lowest in the Blue Barn at Week 10 (35%). For all barns, carriage decreased to some degree 2 weeks post vaccination.

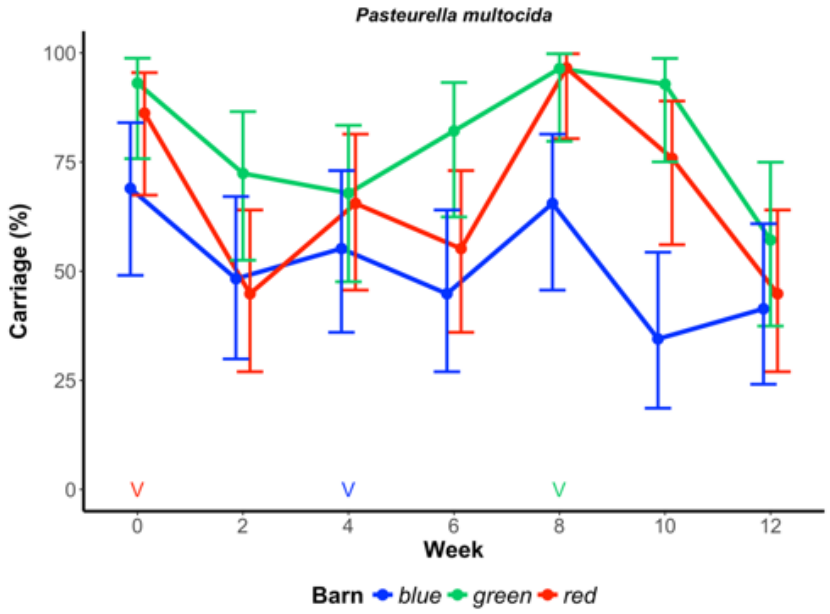

Figure 6.10: Carriage rates of *Pasteurella multocida* within clusters over the study period. Timing of vaccination for each barn marked with a 'V' in the corresponding colour.

6.3.5.3.4 Trends in bacterial carriage over the study period at the animal level

Detected carriage of *H. somni*, *M. haemolytica* and *P. multocida* was transient across the study period with the majority of animals experiencing both apparent acquisition and loss of carriage (Figure 6.11). Neither carriage with *H. somni* nor *M. haemolytica* was sustained throughout the whole study duration by any animal. Conversely, twelve animals sustained carriage across all visits with *P. multocida*, the majority (nine) being housed in the Green Barn. Only one animal did not experience colonisation with *P. multocida* at any observation (ID: 139; Blue Barn). In the Green Barn, around half of the animals (13/29) were colonised with *H. somni* at Week 0, but these infections were cleared from Week 2 onwards and no others were detected (Figure 6.11c). Totals of 30 and 16 animals were never colonised at any visit with *H. somni* nor *M. haemolytica*, respectively.

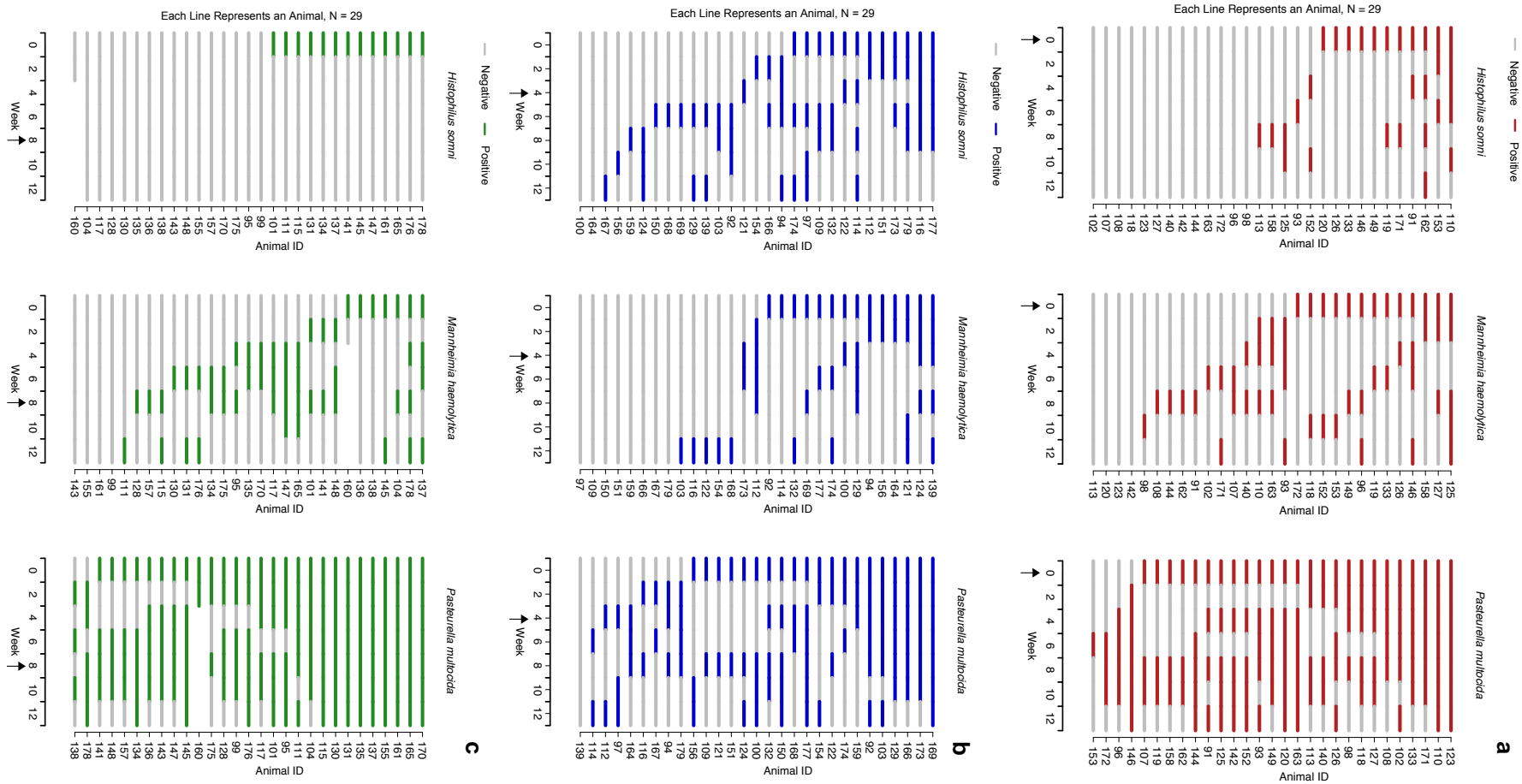

Figure 6.11: Carriage patterns of *Histophilus somni*, *Mannheimia haemolytica* and *Pasteurella multocida* over the study period in the Red (panel a), Blue (panel b) and Green (panel c) barns determined by qPCR on nasal swabs. Time of vaccination indicated by an arrow. One animal (ID: 160) died, as shown by no coloured shading from Week 4 in the Green Barn. Animals ordered with respect to carriage patterns: those with persistent, uninterrupted carriage appear at the top of the figure; animals with increasingly transient to no carriage appear in descending order; animals with similar carriage patterns are grouped together.

6.3.6 Effect of viral infection on bacterial carriage rate

6.3.6.1 Bacterial carriage rates combining 1st and 2nd crossover points

Rates of carriage of *H. somni*, *M. haemolytica* and *P. multocida* for animals in the control and vaccine groups are shown in Figure 6.12. For the three bacterial species, carriage rates were lower in animals 2 and 4-weeks after vaccination than in unvaccinated controls.

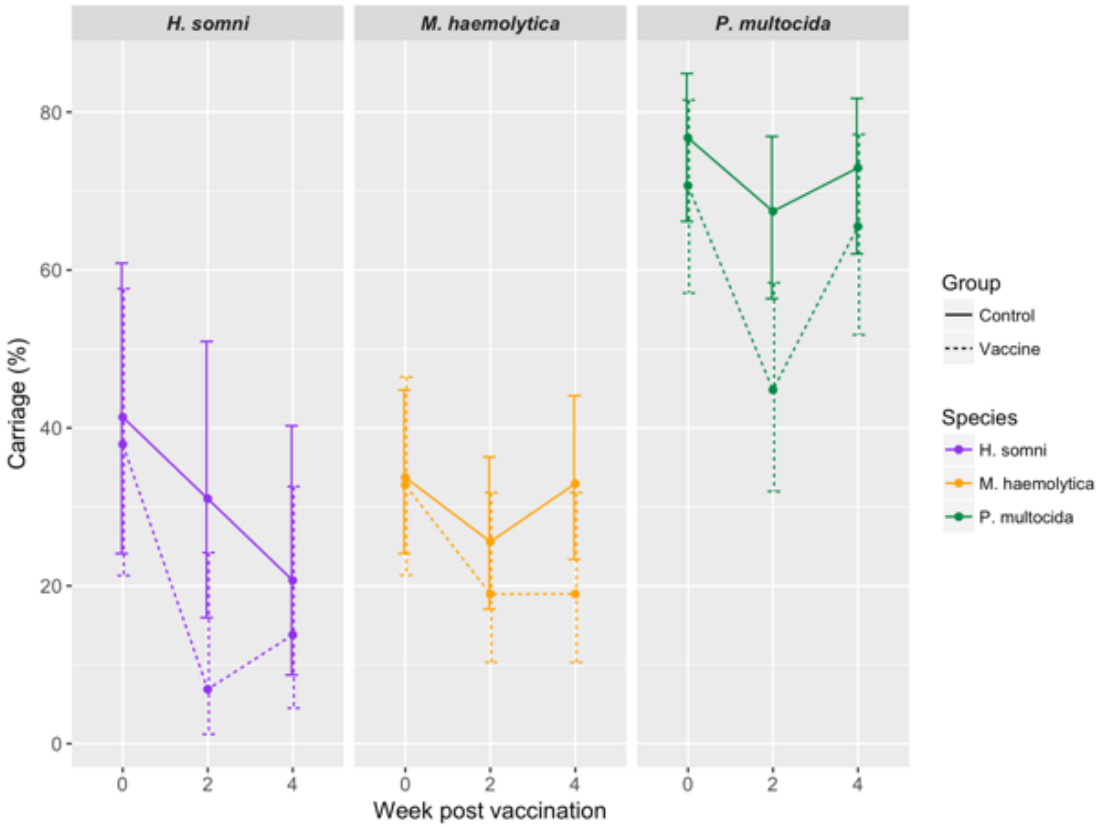

Figure 6.12: Between cluster analysis of *Pasteurellaceae* carriage rates combining data from the 1st and 2nd crossover points as if they were replicates. Carriage of *Pasteurellaceae* for animals in the control or vaccine group at 0, 2 and 4-weeks post vaccination. Confidence intervals for single proportions were calculated using the Wilson score.

Results from logistic regression are given in Table 6.4. There was evidence to suggest that the odds of bacterial carriage were significantly lower in vaccinated compared with control animals 2-weeks post vaccination for *P. multocida* (OR: 0.351, CI_{95}: 0.170–0.709) and *H. somni* (OR: 0.165; $CI_{95\%}$: 0.0234–0.725). At 4 weeks, similar trends were observed for both bacteria, albeit with little evidence to suggest a difference in carriage rates between vaccinated and unvaccinated animals (*P. multocida*: OR: 0.165; $CI_{95\%}$: 0.0234–0.725; *H. somni*: OR: 0.613; $CI_{95\%}$: 0.141–2.42). For *M. haemolytica*, again, the

odds of carriage were lower for animals in the vaccine group compared with those in the control group at 2-weeks post vaccination (OR: 0.591; $CI_{95\%}$: 0.247–1.35), and significantly so at 4-weeks post vaccination (OR: 0.417; $CI_{95\%}$: 0.177–0.929).

Table 6.4: *Pasteurellaceae* carriage rates combining data from the 1st and 2nd crossover points as if they were replicates

		Carriage rate						
Species	**Week***	**Controls**	**(%)**	**Vaccine**	**(%)**	**Odds Ratio**	**$CI_{95\%}$†**	**P-value**
H. somni	0	12/29	(41.4)	11/29	(37.9)	1.08	0.518–2.23	0.788
	2	9/29	(31.0)	2/29	(6.90)	0.165	0.0234–0.725	**0.0308**
	4	6/29	(20.7)	4/29	(13.8)	0.613	0.141–2.42	0.489
M. haemolytica	0	29/86	(33.7)	19/58	(32.8)	1.08	0.518–2.23	0.840
	2	22/86	(25.6)	11/58	(19.0)	0.591	0.247–1.35	0.221
	4	28/85	(32.9)	11/58	(19.0)	0.417	0.177–0.929	**0.038**
P. multocida	0	66/86	(76.7)	41/58	(70.7)	0.877	0.401–1.95	0.745
	2	58/86	(67.4)	26/58	(44.8)	0.351	0.170–0.709	**0.00398**
	4	62/85	(72.9)	38/58	(65.5)	0.585	0.272–1.25	0.165

* Week post vaccination

† Odds ratio of carriage and its 95% confidence interval ($CI_{95\%}$) of the odds for carriage in the vaccine group compared with the control group calculated at 0, 2 and 4-weeks post vaccination using logistic regression adjusting for number of replicate determinations.

6.3.6.2 Vertical analysis of carriage rates following the 1st crossover point

Following the 1st crossover point (of vaccination) the rates of carriage of *Pasteurellaceae* were generally less in the vaccinated animals (Red Barn) compared with controls (Green and Blue barns). There was no evidence for a difference between vaccinated and unvaccinated animals in terms of carriage rate for any of the three bacterial species at Week 2 or Week 4 (2 and 4-weeks post vaccination respectively) as shown in Table 6.5, Table 6.6 and Table 6.7. Prior carriage of *H. somni* was significantly associated with subsequent carriage, where the odds of carriage were 4.5 times greater ($CI_{95\%}$: 1.18–22.0) given prior carriage at Week 0. There was no significant interaction between vaccination and prior carriage for any bacterium at either Week 2 or Week 4.

Table 6.5: Vertical analysis of *Histophilus somni* carriage following the 1st crossover point

(a) Carriage at Week-2, following vaccination at Week-0

		Carriage						Total	Odds Ratio			
		No			Yes				Univariate	Model	$CI_{95\%}$	P-value
Phase	**Farmlet**	**Prior Carriage**		**Subtotal**	**Prior Carriage**		**Subtotal**					
		No	Yes		No	Yes						
Control§	**Blue**	14	6	20	3	6	9	**29**				
	Green	16	13	29	0	0	0	**29**				
	Subtotal	30	19	49	3	6	9	**58**				
Vaccinated	**Red**	18	9	27	0	2	2	**29**	0.403	0.417‡	0.059–1.84	0.233
Total		**48**	**28**	**76**	**3**	**8**	**11**	**87**	4.571	4.5†	1.18–22.0	**0.024**

(b) Carriage at Week-4, following vaccination at Week-0

		Carriage						Total	Odds Ratio			
		No			Yes				Univariate	Model	$CI_{95\%}$	P-value
Phase	**Farmlet**	**Prior Carriage**		**Subtotal**	**Prior Carriage**		**Subtotal**					
		No	Yes		No	Yes						
Control§	**Blue**	15	8	23	2	4	6	**29**				
	Green	15	13	28	0	0	0	**28**				
	Subtotal	30	21	51	2	4	6	**57**				
Vaccinated	**Red**	17	8	25	1	3	4	**29**	1.360	1.5‡	0.346–6.01	0.659
Total		**47**	**29**	**76**	**3**	**7**	**10**	**86**	3.782	3.89†	0.990–19.3	**0.056**

† Odds ratio for carriage in animals that had prior carriage compared to those that did not. ‡ Odds ratio for carriage in animals that received the vaccine compared to those that did not. § Likelihood ratio test statistic for evidence of differences in carriage rates between barns in the same phase: Week 2 (M5 vs. M2), χ^2 (1 df) = 14.1, $p < 0.001$ and Week 4 (M5 vs. M2), χ^2 (1 df) = 8.79, p = 0.00303; Likelihood ratio test statistic for evidence of interaction between vaccination and prior carriage: Week 2 (M4 vs. M3), χ^2 (1 df) = 1.62, p = 0.203 and Week 4 (M4 vs. M3), χ^2 (1 df) = 0.282, p = 0.596

Table 6.6: Vertical analysis of *Mannheimia haemolytica* carriage following the 1st crossover point

(a) Carriage at Week-2, following vaccination at Week-0

		Carriage						Total	Odds Ratio			
		No			Yes				Univariate	Model	CI95%	P-value
Phase	**Farmlet**	**Prior Carriage**		**Subtotal**	**Prior Carriage**		**Subtotal**					
		No	Yes		No	Yes						
Control§	**Blue**	14	8	22	1	6	7	**29**				
	Green	19	7	26	3	0	3	**29**				
	Subtotal	33	15	48	4	6	10	**58**				
Vaccinated	**Red**	13	10	23	3	3	6	**29**	1.252	1.25‡	0.386–3.81	0.698
Total		**46**	**25**	**71**	**7**	**9**	**16**	**87**	2.366	2.37†	0.790–7.36	0.124

(b) Carriage at Week-4, following vaccination at Week-0

		Carriage						Total	Odds Ratio			
		No			Yes				Univariate	Model	CI95%	P-value
Phase	**Farmlet**	**Prior Carriage**		**Subtotal**	**Prior Carriage**		**Subtotal**					
		No	Yes		No	Yes						
Control§	**Blue**	13	10	23	2	4	6	**29**				
	Green	16	4	20	6	2	8	**28**				
	Subtotal	29	14	43	8	6	14	**57**				
Vaccinated	**Red**	12	11	23	4	2	6	**29**	0.801	0.8‡	0.255–2.29	0.686
Total		**41**	**25**	**66**	**12**	**8**	**20**	**86**	1.093	1.09†	0.381–3.02	0.151

† Odds ratio for carriage in animals that had prior carriage compared to those that did not. ‡ Odds ratio for carriage in animals that received the vaccine compared to those that did not. § Likelihood ratio test statistic for evidence of differences in carriage rates between barns in the same phase: Week 2 (M5 vs. M2), χ^2 (1 df) = 1.98, p = 0.160 and Week 4 (M5 vs. M2), χ^2 (1 df) = 0.479, p = 0.489; Likelihood ratio test statistic for evidence of interaction between vaccination and prior carriage: Week 2 (M4 vs. M3), χ^2 (1 df) = 0.640, p = 0.424 and Week 4 (M4 vs. M3), χ^2 (1 df) = 0.851, p = 0.356

Table 6.7: Vertical analysis of *Pasteurella multocida* carriage following the 1st crossover point

(a) Carriage at Week-2, following vaccination at Week-0

		Carriage						Total	Odds Ratio			
		No			Yes				Univariate	Model	CI95%	P-value
Phase	**Farmlet**	**Prior Carriage**		**Subtotal**	**Prior Carriage**		**Subtotal**					
		No	Yes		No	Yes						
Control§	**Blue**	5	10	15	4	10	14	**29**				
	Green	0	8	8	2	19	21	**29**				
	Subtotal	5	18	23	6	29	35	**58**				
Vaccinated	**Red**	3	13	16	1	12	13	**29**	0.534	0.534‡	0.214–1.31	0.171
Total		**8**	**31**	**39**	**7**	**41**	**48**	**87**	1.512	1.51†	0.492–4.745	0.468

(b) Carriage at Week-4, following vaccination at Week-0

		Carriage						Total	Odds Ratio			
		No			Yes				Univariate	Model	CI95%	P-value
Phase	**Farmlet**	**Prior Carriage**		**Subtotal**	**Prior Carriage**		**Subtotal**					
		No	Yes		No	Yes						
Control§	**Blue**	4	9	13	5	11	16	**29**				
	Green	1	8	9	1	18	19	**28**				
	Subtotal	5	17	22	6	29	35	**57**				
Vaccinated	**Red**	2	8	10	2	17	19	**29**	1.194	1.19‡	0.475–3.11	0.709
Total		**7**	**25**	**32**	**8**	**46**	**54**	**86**	1.610	1.61†	0.510–5.01	0.044

† Odds ratio for carriage in animals that had prior carriage compared to those that did not. ‡ Odds ratio for carriage in animals that received the vaccine compared to those that did not. § Likelihood ratio test statistic for evidence of differences in carriage rates between barns in the same phase: Week 2 (M5 vs. M2), χ^2 (1 df) = 3.57, p = 0.0587 and Week 4 (M5 vs. M2), χ^2 (1 df) = 0.971, p = 0.324; Likelihood ratio test statistic for evidence of interaction between vaccination and prior carriage: Week 2 (M4 vs. M3), χ^2 (1 df) = 0.283, p = 0.595 and Week 4 (M4 vs. M3), χ^2 (1 df) = 0.0982, p = 0.754

6.3.6.3 Vertical analysis of carriage rates following the 2nd crossover point

Following the 2nd crossover point at Week 4, odds ratios were estimated comparing bacterial carriage rates in intervention phase animals housed in the Blue and Red barns to control phase animals housed in the Green Barn. There was moderate evidence to suggest the carriage rate of *M. haemolytica* was reduced in vaccinated animals compared to controls 2 weeks post vaccination (Week 6; OR: 0.355; $CI_{95\%}$: 0.122–1.00) and weak evidence to suggest carriage rates were reduced further still 4 weeks post vaccination (Week 8; OR: 0.432; $CI_{95\%}$: 0.162–1.14, Table 6.8). There was strong evidence to suggest a difference in *P. multocida* carriage rates between the vaccine and control group 2 weeks post vaccination (OR: 0.219; $CI_{95\%}$: 0.065–0.628, Table 6.9), with weaker evidence at 4 weeks post vaccination (OR: 0.164; $CI_{95\%}$: 0.00862–0.947). For both bacterial species, the odds of subsequent carriage were significantly higher given prior carriage either 2 or 4-weeks earlier. As carriage rates of *P. multocida* were very similar between the Red and Green barns at Week 8 these two barns were combined and considered as an alternative analysis (Table 6.9c). Again, there was evidence to suggest that carriage rates were significantly reduced in the Blue (vaccine group) compared to Red and Green (control group), and the odds of subsequent carriage were significantly higher given prior carriage 4-weeks earlier. There was no significant interaction between vaccination and prior carriage for either species at Week 6 or Week 8. Carriage of *H. somni* was not observed in the Green barn from Week 2 onwards, so vertical analysis could not be conducted for this bacterial species following the second or third crossover point.

Table 6.8: Vertical analysis of *Mannheimia haemolytica* carriage following the 2nd crossover point

(a) Carriage at Week-6, following vaccination at Week-4

		Carriage						Total	Odds Ratio			
		No			Yes				Univariate	Model	$CI_{95\%}$	P-value
Phase	**Farmlet**	**Prior Carriage**		**Subtotal**	**Prior Carriage**		**Subtotal**					
		No	Yes		No	Yes						
Control	**Green**	14	2	16	6	6	12	28				
Vaccinated§	**Blue**	**21**	**3**	**24**	**2**	**3**	**5**	**29**				
	Red	**18**	**4**	**22**	**5**	**2**	**7**	**29**				
	Subtotal	**39**	**7**	**46**	**7**	**5**	**12**	**58**	0.348	0.355‡	0.122–1.00	**0.0505**
Total		**53**	**9**	**62**	**13**	**11**	**24**	**86**	4.983	4.91†	1.65–15.3	**0.00423**

(b) Carriage at Week-8, following vaccination at Week-4

		Carriage						Total	Odds Ratio			
		No			Yes				Univariate	Model	$CI_{95\%}$	P-value
Phase	**Farmlet**	**Prior Carriage**		**Subtotal**	**Prior Carriage**		**Subtotal**					
		No	Yes		No	Yes						
Control	**Green**	11	3	14	9	5	14	**28**				
Vaccinated§	**Blue**	22	2	24	1	4	5	**29**				
	Red	14	3	17	9	3	12	**29**				
	Subtotal	36	5	41	10	7	17	**58**	0.415	0.432‡	0.162–1.14	0.0886
Total		**47**	**8**	**55**	**19**	**12**	**31**	**86**	3.711	3.59†	1.26–10.8	**0.0167**

† Odds ratio for carriage in animals that had prior carriage compared to those that did not. ‡ Odds ratio for carriage in animals that received the vaccine compared to those that did not. § Likelihood ratio test statistic for evidence of differences in carriage rates between barns in the same phase: Week 6 (M5 vs. M2), χ^2 (1 df) = 0.421, p = 0.516 and Week 8 (M5 vs. M2), χ^2 (1 df) = 4.17, p = 0.0411; Likelihood ratio test statistic for evidence of interaction between vaccination and prior carriage: Week 6 (M4 vs. M3), χ^2 (1 df) = 0.230, p = 0.632 and Week 8 (M4 vs. M3), χ^2 (1 df) = 0.671, p = 0.413.

Table 6.9: Vertical analysis of *Pasteurella multocida* carriage following the 2nd crossover point

(a) Carriage at Week-6, following vaccination at Week-4

		Carriage						Total	Odds Ratio			
		No			Yes				Univariate	Model	$CI_{95\%}$	P-value
Phase	**Farmlet**	**Prior Carriage**		**Subtotal**	**Prior Carriage**		**Subtotal**					
		No	Yes		No	Yes						
Control	**Green**	1	4	5	8	15	23	**28**				
Vaccinated§	**Blue**	6	10	16	3	10	13	**29**				
	Red	6	7	13	4	12	16	**29**				
	Subtotal	12	17	29	7	22	29	**58**	0.217	0.219‡	0.065–0.628	**0.00399**
Total		**13**	**21**	**34**	**15**	**37**	**52**	**86**	1.527	2.44†	0.953–6.45	**0.06287**

(b) Carriage at Week-8, following vaccination at Week-4

		Carriage						Total	Odds Ratio			
		No			Yes				Univariate	Model	$CI_{95\%}$	P-value
Phase	**Farmlet**	**Prior Carriage**		**Subtotal**	**Prior Carriage**		**Subtotal**					
		No	Yes		No	Yes						
Control	**Green**	11	3	14	9	5	14	**28**				
Vaccinated§	**Blue**	6	4	10	7	12	19	**29**				
	Red	1	0	1	9	19	28	**29**				
	Subtotal	7	4	11	16	31	47	**58**	0.158	0.164‡	0.00862–0.947	**0.0332**
Total		**8**	**4**	**12**	**24**	**50**	**74**	**86**	4.167	4.05†	1.12–16.8	**0.025**

† Odds ratio for carriage in animals that had prior carriage compared to those that did not. ‡ Odds ratio for carriage in animals that received the vaccine compared to those that did not. § Likelihood ratio test statistic for evidence of differences in carriage rates between barns in the same phase: Week 6 (M5 vs. M2), χ^2 (1 df) = 0.622, p = 0.430 and Week 8 (M5 vs. M2), χ^2 (1 df) = 10.3, p = 0.00134; Likelihood ratio test statistic for evidence of interaction between vaccination and prior carriage: Week 6 (M4 vs. M3), χ^2 (1 df) = 2.94, p = 0.0865 and Week 8 (M4 vs. M3), χ^2 (1 df) = 0.964, p = 0.326

Table 6-9: Vertical analysis of *Pasteurella multocida* carriage following the 2nd crossover point (continued)

(c) Carriage at Week-8, following vaccination at Week-4 – alternative analysis

		Carriage						Total	Odds Ratio			
		No			Yes				Univariable	Model	$CI_{95\%}$	P-value
Phase	**Farmlet**	**Prior Carriage**		**Subtotal**	**Prior Carriage**		**Subtotal**					
		No	Yes		No	Yes						
Control§	**Green**	1	0	1	8	19	27	**28**				
	Red	1	0	1	9	19	28	**29**				
	Subtotal	2	0	2	17	38	55	**57**				
Vaccinated	**Blue**	6	4	10	7	12	19	**29**	0.069	0.070‡	0.0099-0.307	**0.00021**
Total		**8**	**4**	**12**	**24**	**50**	**74**	**86**	4.167	4.05†	1.02-18.7	**0.047**

† Odds ratio for carriage in animals that had prior carriage compared to those that did not. ‡ Odds ratio for carriage in animals that received the vaccine compared to those that did not. § Likelihood ratio test statistic for evidence of differences in carriage rates between barns in the same phase: Week 8 (M5 vs. M2), χ^2 (1 df) = 0.000638, p = 0.980; Likelihood ratio test statistic for evidence of interaction between vaccination and prior carriage: Week 8 (M4 vs. M3), χ^2 (1 df) = 2.031, p = 0.154

6.3.6.4 Vertical analysis of carriage rates following the 3rd crossover point

After the 3rd crossover point all barns had received the vaccine, therefore, there was no comparison between vaccinated and unvaccinated animals. Instead, differences in bacterial carriage rates were assessed for animals in the most recently vaccinated (Green) cluster compared to the other two clusters (Red and Blue) vaccinated two or four weeks previously. The rate of carriage of *M. haemolytica* (Table 6.10) in the most recently vaccinated animals (Green Barn) was compared with that of animals vaccinated on earlier occasions (Red and Blue barns); two weeks after vaccination of the Green Barn animals, the carriage was lower in those animals than in the other two barns (Week 10; OR = 0.667; $CI_{95\%}$: 0.0933–3.13), but after 4 weeks the rates were similar (Week 12; OR: 1.05; $CI_{95\%}$: 0.352–2.92). There was no evidence to suggest carriage at Week 8 was significantly associated with subsequent *M. haemolytica* carriage either 2 or 4-weeks later (Table 6.10).

The carriage rate of *P. multocida* (Table 6.11) was greater 2 weeks post vaccination (approximately 8-fold higher) in the late vaccine cluster compared to the early vaccine cluster, but the confidence interval for this estimate was very large (OR: 8.68; $CI_{95\%}$: 2.21–58.7). The odds of subsequent carriage were significantly increased given prior carriage 2 weeks earlier, but again the confidence interval for this estimate was large (OR: 6.48; $CI_{95\%}$: 1.62–34.1). At Week 12, the odds of carriage were slightly higher for animals vaccinated at Week 8 and for animals with prior carriage at Week 8 (Table 6.11). There was no significant interaction between vaccination and prior carriage for any bacterium at either Week 10 or Week 12.

Table 6.10: Vertical analysis of *Mannheimia haemolytica* carriage following the 3rd crossover point

(a) Carriage at Week-10, following vaccination at Week-8

		Carriage						Total	Odds Ratio			
		No			Yes				Univariate	Model	$CI_{95\%}$	P-value
Phase	**Farmlet**	**Prior Carriage**		**Subtotal**	**Prior Carriage**		**Subtotal**					
		No	Yes		No	Yes						
Early vaccine§	**Blue**	23	5	28	1	0	1	**29**				
	Red	13	11	24	4	1	5	**29**				
	Subtotal	36	16	52	5	1	6	**58**				
Late vaccine	**Green**	14	12	26	0	2	2	**28**	0.667	0.667‡	0.0933–3.13	0.625
Total		**50**	**28**	**78**	**5**	**3**	**8**	**86**	1.071	1.07†	0.207–4.70	0.929

(b) Carriage at Week-12, following vaccination at Week-8

		Carriage						Total	Odds Ratio			
		No			Yes				Univariate	Model	$CI_{95\%}$	P-value
Phase	**Farmlet**	**Prior Carriage**		**Subtotal**	**Prior Carriage**		**Subtotal**					
		No	Yes		No	Yes						
Early vaccine§	**Blue**	16	4	20	8	1	9	**29**				
	Red	14	10	24	3	2	5	**29**				
	Subtotal	30	14	44	11	3	14	**58**				
Late vaccine	**Green**	9	12	21	5	2	7	**28**	1.048	1.05‡	0.352–2.92	0.931
Total		**39**	**26**	**65**	**16**	**5**	**21**	**86**	0.469	0.467†	0.140–1.36	0.169

† Odds ratio for carriage in animals that had prior carriage compared to those that did not. ‡ Odds ratio for carriage in animals that received the vaccine at Week-8 (late vaccine group) compared to those that received the vaccine 2 or 4 weeks earlier (early vaccine group) § Likelihood ratio test statistic for evidence of differences in carriage rates between barns in the same phase: Week 10 (M5 vs. M2), χ^2 (1 df) = 3.22, p = 0.0728 and Week 12 (M5 vs. M2), χ^2 (1 df) = 1.52, p = 0.217; Likelihood ratio test statistic for evidence of interaction between vaccination and prior carriage: Week 10 (M4 vs. M3), χ^2 (1 df) = 3.46, p = 0.0629 and Week 12 (M4 vs. M3), χ^2 (1 df) = 0.315, p = 0.575

Table 6.11: Vertical analysis of *Pasteurella multocida* carriage following the 3rd crossover point

(a) Carriage at Week-10, following vaccination at Week-8

		Carriage						Total	Odds Ratio			
		No			Yes				Univariate	Model	$CI_{95\%}$	P-value
Phase	**Farmlet**	**Prior Carriage**		**Subtotal**	**Prior Carriage**		**Subtotal**					
		No	Yes		No	Yes						
Early vaccine§	**Blue**	8	11	19	2	8	10	**29**				
	Red	1	6	7	0	22	22	**29**				
	Subtotal	9	17	26	2	30	32	**58**				
Late vaccine	**Green**	0	2	2	1	25	26	**28**	10.563	8.68‡	2.21–58.7	**0.00104**
Total		**9**	**19**	**28**	**3**	**55**	**58**	**86**	8.684	6.48†	1.62–34.1	**0.00748**

(b) Carriage at Week-12, following vaccination at Week-8

		Carriage						Total	Odds Ratio			
		No			Yes				Univariate	Model	$CI_{95\%}$	P-value
Phase	**Farmlet**	**Prior Carriage**		**Subtotal**	**Prior Carriage**		**Subtotal**					
		No	Yes		No	Yes						
Early vaccine§	**Blue**	5	12	17	5	7	12	**29**				
	Red	1	15	16	0	13	13	**29**				
	Subtotal	6	27	33	5	20	25	**58**				
Late vaccine	**Green**	1	11	12	0	16	16	**28**	1.760	1.76‡	0.712–4.45	0.222
Total		**7**	**38**	**45**	**5**	**36**	**41**	**86**	1.326	1.33†	0.389–4.84	0.654

† Odds ratio for carriage in animals that had prior carriage compared to those that did not. ‡ Odds ratio for carriage in animals that received the vaccine at Week-8 (late vaccine group) compared to those that received the vaccine 2 or 4 weeks earlier (early vaccine group) § Likelihood ratio test statistic for evidence of differences in carriage rates between barns in the same phase: Week 10 (M5 vs. M2), χ^2 (1 df) = 1.73, p = 0.188 and Week 12 (M5 vs. M2), χ^2 (1 df) = 10.4, p = 0.00128; Likelihood ratio test statistic for evidence of interaction between vaccination and prior carriage: Week 10 (M4 vs. M3), χ^2 (1 df) = 0.0703, p = 0.791 and Week 12 (M4 vs. M3), χ^2 (1 df) = 0.837, p = 0.360

6.3.6.5 Longitudinal assessment of bacterial carriage rates

Results from mixed effects models estimating the odds ratio of bacterial carriage for animals in the intervention phase compared with those in the control phase are shown in Table 6.12. Model 1 assessed for a lasting effect of vaccination on bacterial carriage rate. There was strong evidence that the odds of *M. haemolytica* carriage were reduced after vaccination [OR: 0.48, $CI_{95\%}$: 0.27–0.85; change in deviance on removing the term 'vaccination', χ^2 (1 df) = 5.49, p = 0.0191]. Model 2 assessed for a transient effect of vaccination on bacterial carriage rate, assessing differences in carriage between control and intervention phase animals either 2, 4 or ≥6 weeks post vaccination. There was weak evidence to suggest a transient effect of vaccination on rates of *M. haemolytica* carriage [change in deviance on removing the term 'vaccination status', χ^2 (3 df) = 6.53, p = 0.0887]. There was little evidence for a lasting (Model 1) or a transient (Model 2) effect of vaccination on carriage rates of *P. multocida* or *H. somni* although the odds of carriage were reduced following vaccination. Estimates for the odds of carriage 4 or ≥6 weeks post vaccination (Model 2) were similar for *M. haemolytica* and *P. multocida*, so Model 2 was simplified to Model 3 by combining 4 and ≥6 weeks into one category. For both bacterial species, the Akaike information criterion was slightly lower for the simpler model, suggesting an improved fit. In addition, there was no evidence that Model 2 was a better fit when models were compared by performing a likelihood ratio test (*M. haemolytica* p = 0.931 and *P. multocida* p = 0.412). When evaluating Model 3 there was evidence for a transient effect of vaccination on *M. haemolytica* carriage [change in deviance on removing the term 'vaccination status', χ^2 (2 df) = 6.51, p = 0.0384]. However, there was no evidence for a transient effect of vaccination on *P. multocida* carriage. Simplification of Model 2 for *H. somni* was not justified (M2 vs M3, χ^2 (2 df) = 6.99, p = 0.0303). Likelihood ratio test statistics showed that for all three bacterial species model fit was significantly improved by including the two random effects (calf within cluster and time within cluster). For *M. haemolytica*, nesting calf within cluster resulted in a singular fit, hence this random effect of was not nested.

Table 6.12: Results from mixed effect models assessing the overall and transient effect of viral infection on bacterial carriage rates

Species	Model	Covariate	Odds ratio	$CI_{95\%}$	P-value	AIC[§]
H. somni	M1: Lasting effect	Vaccination	0.48	0.12 – 2.00	0.317	493
	M2: Transient effect	2 wpv[*]	0.63	0.09 – 4.35	0.638	496
		4 wpv	0.52	0.08 – 3.60	0.509	
		≥6 wpv	0.39	0.07 – 2.12	0.276	
M. haemolytica	M1: Lasting effect	Vaccination	0.48	0.27 – 0.85	**0.012**	671
	M2: Transient effect	2 wpv	0.34	0.14 – 0.82	**0.016**	674
		4 wpv	0.52	0.23 – 1.21	0.130	
		≥6 wpv	0.54	0.28 – 1.07	0.077	
	M3: Transient effect (b)	2 wpv	0.34	0.14 – 0.82	**0.016**	672
		≥4 wpv	0.54	0.29 – 0.98	**0.041**	

Table 6.12 continued

Species	Model	Covariate	Odds ratio	$CI_{95\%}$	P-value	AIC[§]
P. multocida	M1: Lasting effect	Vaccination	0.49	0.21 – 1.16	0.103	716
	M2: Transient effect	2 wpv	0.51	0.15 – 1.73	0.283	720
		4 wpv	0.49	0.15 – 1.62	0.243	
		≥6 wpv	0.47	0.16 – 1.36	0.163	
	M3: Transient effect (b)	2 wpv	0.49	0.13 – 1.88	0.300	718
		≥4 wpv	0.44	0.17 – 1.14	0.090	

[*] wpv: weeks post vaccination; [§] Akaike information criterion

H. somni likelihood ratio test statistic: -

unconditional model (no covariate) vs. M1, χ^2 (1 df) = 0.916, p = 0.339; unconditional model vs M2, χ^2 (3 df) = 1.127, p = 0.771; M2 vs M3, χ^2 (2 df) = 6.99, p = 0.0303

M. haemolytica likelihood ratio test statistic: -

unconditional model (no covariate) vs. M1, χ^2 (1 df) = 5.49, p = **0.0191**; unconditional model vs M2, χ^2 (3 df) = 6.53, p = 0.0887; unconditional model vs M3, χ^2 (2 df) = 6.51, p = 0.0384; M2 vs M3, χ^2 (1 df) = 0.01, p = 0.931

P. multocida likelihood ratio test statistic: -

unconditional model (no covariate) vs. M1, χ^2 (1 df) = 2.47, p = 0.116; unconditional model vs M2, χ^2 (3 df) = 2.49, p = 0.476; unconditional model vs M3, χ^2 (2 df) = 0.713, p = 0.398; M2 vs M3, χ^2 (2 df) = 1.78, p = 0.412

6.3.7 Overall bacterial carriage density

For each bacterium, density values for all positive samples were plotted as histograms revealing distinct density profiles (Figure 6.13). The modal value for *H. somni* carriage density accounting for the vast majority (78.0%) of swabs was 1–2 $\log_{10}$ genome copies/ml with fewer samples (11.0%) between 2–3 $\log_{10}$ genome copies/ml and fewer still between 3–4 $\log_{10}$ genome copies/ml (5.5%). Only four samples were in the 4–5 log range and two samples in the 5–6 log range (highest value observed at 5.27 logs in one sample). Carriage density for *M. haemolytica* ranged between 2 and 6 $\log_{10}$ genome copies/ml when it occurred, with the majority of swabs occurring between 3–4 $\log_{10}$ genome copies/ml (40.9%), the highest density observed in one sample was 6.05 $\log_{10}$ genome copies/ml. *Pasteurella multocida* was also carried over a wide range of densities, most commonly between 2–3 $\log_{10}$ genome copies/ml (40.0%), with the proportion of swabs positive steadily decreasing as density increased; density extended up to 6.26 $\log_{10}$ genome copies/ml in one sample.

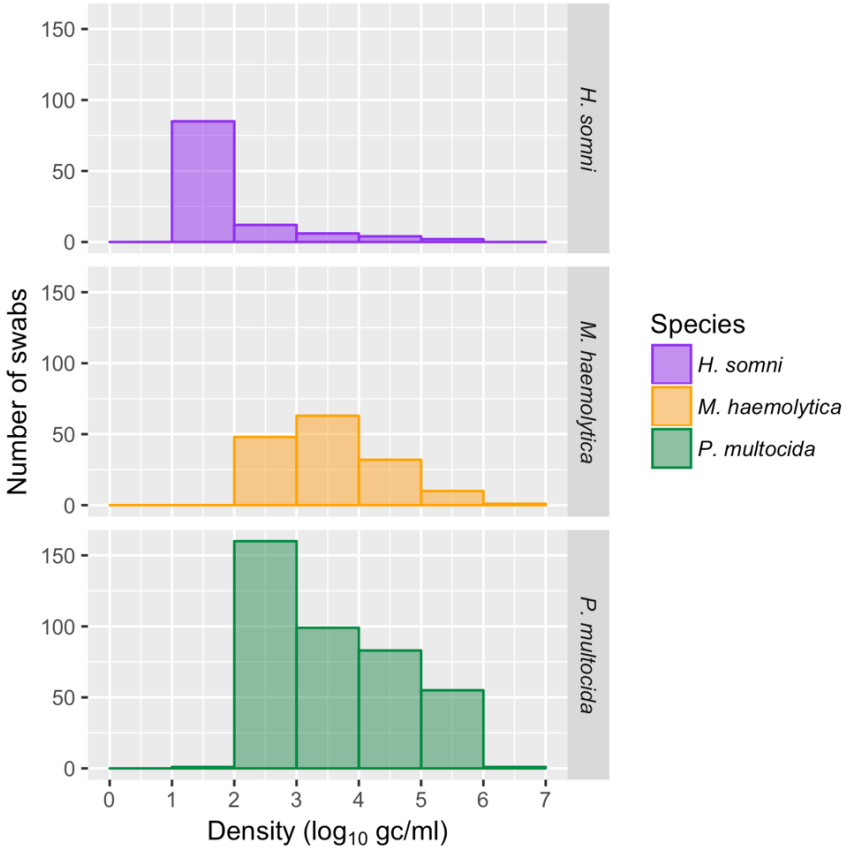

Figure 6.13: Histograms for all positive swabs summarising density distribution profiles of *Histophilus somni* (n = 109), *Mannheimia haemolytica* (n = 154) and *Pasteurella multocida* (n = 399).

6.3.8 Trends in bacterial carriage density at the barn level

Carriage densities for all swabs positive for each bacterium over the study period are shown in Figure 6.14. Carriage density for all three bacterial species varied among calves on the same day and between days. There was a transient increase in the mean carriage density of *H. somni* following vaccination in the Red Barn, but a decrease was observed following vaccination in the Blue Barn (no *H. somni* was detected in the Green Barn from Week 2 onwards). The mean carriage density of *M. haemolytica* was relatively constant for the first 6 weeks in the Red Barn following vaccination at Week 0. *M. haemolytica* carriage density in the Blue and Green barns fluctuated overtime, regardless of vaccination status. Similarly, density of *P. multocida* fluctuated over the study period in all barns with no apparent consistent trends in density following vaccination.

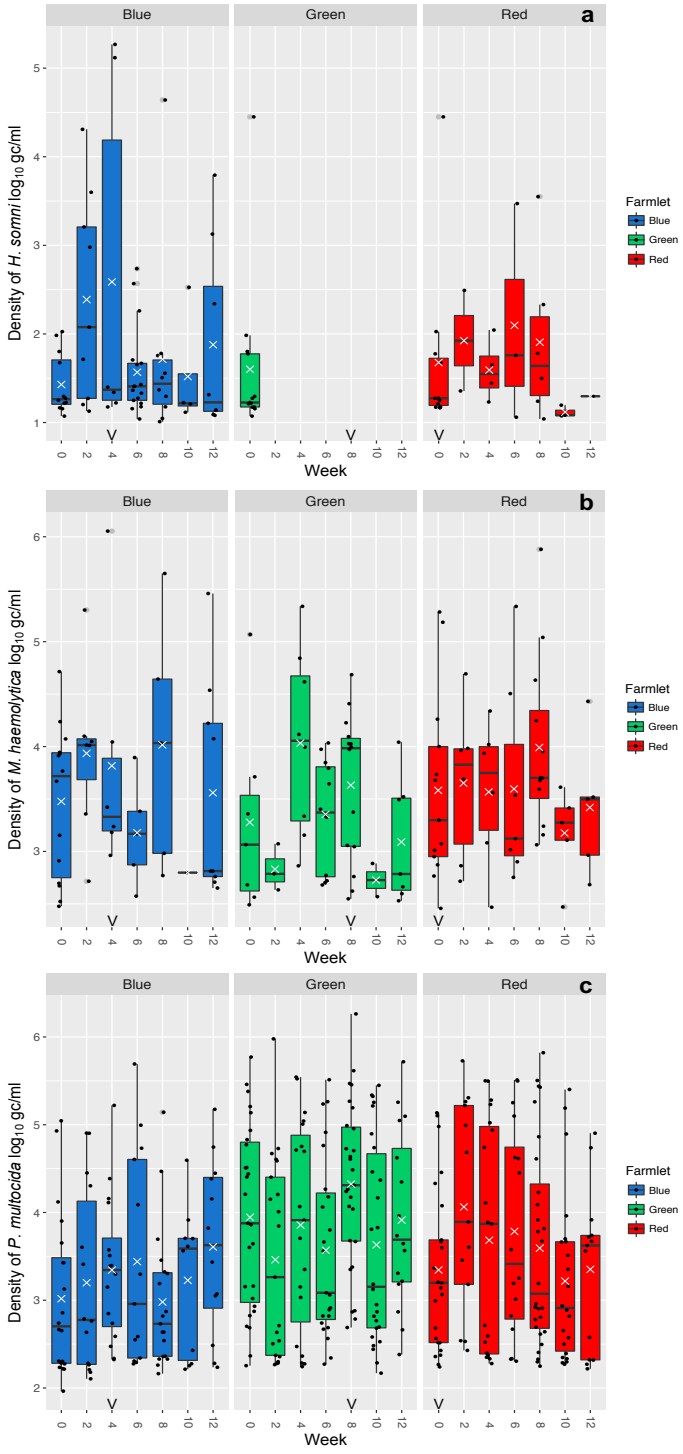

Figure 6.14: Boxplots and scatterplots showing density of *Pasteurellaceae* carriage. *H. somni* (panel a), *M. haemolytica* (panel b) and *P. multocida* (panel c) determined by qPCR on positive nasal swabs collected over the study period. Each black dot represents an animal. White crosses show the geometric mean density (log_{10} genome copies/ml). The middle line (hinge) corresponds to the median. The lower and upper hinges of the boxplots correspond to the first and third quartiles respectively. The upper and lower whiskers extend from the upper and lower hinges to the largest and smallest value (no further than 1.5 times the interquartile range) respectively. Outliers are shown in grey and are greater than 1.5 times the interquartile range.

6.3.9 Trends in bacterial carriage density at the animal level

6.3.9.1 Red Barn

Trends in bacterial carriage density for each animal following vaccination in the Red Barn are shown in Figure 6.15, panel a. Only two out of nine animals with *H. somni* carriage at Week 0 sustained carriage two weeks later, of which density was similar (ID: 153) or decreased (ID:110). Five calves not colonised with *H. somni* at Week 0 acquired carriage from Week 4, with density commonly between 1–2 $\log_{10}$ genome copies/ml. Similar trends were seen for *M. haemolytica*: 10 out of 13 calves that were colonised at Week 0 lost carriage 2 weeks later and only 3 sustained carriage over a range of densities until Week 2. A further 3 initially uncolonized animals acquired carriage 2 weeks later, with carriage maintained for a maximum of three consecutive visits in any one animal and in only two animals (IDs: 93 and 125). Colonisation with *H. somni* or *M. haemolytica* was not observed on any occasion in 13 and 4 animals respectively. All animals experienced carriage of *P. multocida* on at least one occasion and over a wide range of densities (2–6 $\log_{10}$ genome copies/ml). Carriage of *P. multocida* was not detected at Week 2 in 13 out of 25 calves that were colonised at Week 0, with re-acquisition of carriage in 8 of these 13 calves 2 weeks later (Week 4). In general, *P. multocida* carriage was maintained for longer uninterrupted periods than either *H. somni* or *M. haemolytica* carriage, with two animals (IDs: 110 and 123) sustaining *P. multocida* carriage for the whole study duration, one of which (ID: 123) at densities between 4–6 $\log_{10}$ genome copies/ml.

6.3.9.2 Blue Barn

Carriage rates of *H. somni* increased in the Blue Barn 2 and 4-weeks post vaccination, with this apparent increase due to colonisation in naïve animals (Figure 6.15, panel b). Two subpopulations of animals can be seen to become colonised with *H. somni*, the first with transient carriage from Week 0; the second with transient carriage 2 weeks following vaccination (from Week 6). Only two animals were not colonised at any visit (ID: 164 and 100). *H. somni* carriage density was similar pre- and post-vaccination. At Week 0 carriage with *M. haemolytica* occurred between 2 and 5 logs. Two and four-weeks post vaccination, rates of *M. haemolytica* carriage were unchanged and density was similar. *M. haemolytica* was undetected in 5 animals for 10 weeks, until acquisition on Week 12. A further 8 of the 29 animals were not colonised on any occasion. No

animals sustained carriage for the whole study period and of those colonised density ranged between 2 and 6 log_{10} genome copies/ml. Carriage of *P. multocida* was maintained for the study period in only one animal (ID:169), over a range of densities (2–5 logs). One animal was not colonised on any occasion (ID: 139). Otherwise, carriage was transient and over a range of densities 2–6 log_{10} genome copies/ml.

6.3.9.3 Green Barn

At Week 0 *H. somni* was detected in 13 animals. All but one of these 13 animals experienced carriage between 1–2 log_{10} genome copies/ml, the exception (ID 176) carrying at 4–5 logs (Figure 6.15, panel c). *H. somni* was undetected from Week 2. *M. haemolytica* carriage was not maintained by any animal for the entire study period and densities ranged between 2–6 logs. Following vaccination at Week 8, carriage rates of *M. haemolytica* decreased, and only one naïve animal experienced acquisition 4 weeks later. *M. haemolytica* was undetected from 4 animals. All animals experienced colonisation with *P. multocida* on any one occasion over a range of densities. No animal was found to be colonised on fewer than three occasions, other than ID 160 which died in Week 3 having been colonised the two previous weeks. *P. multocida* was detected at every occasion in 8 animals and, in general, carriage density was higher in these animals than in those experiencing transient carriage.

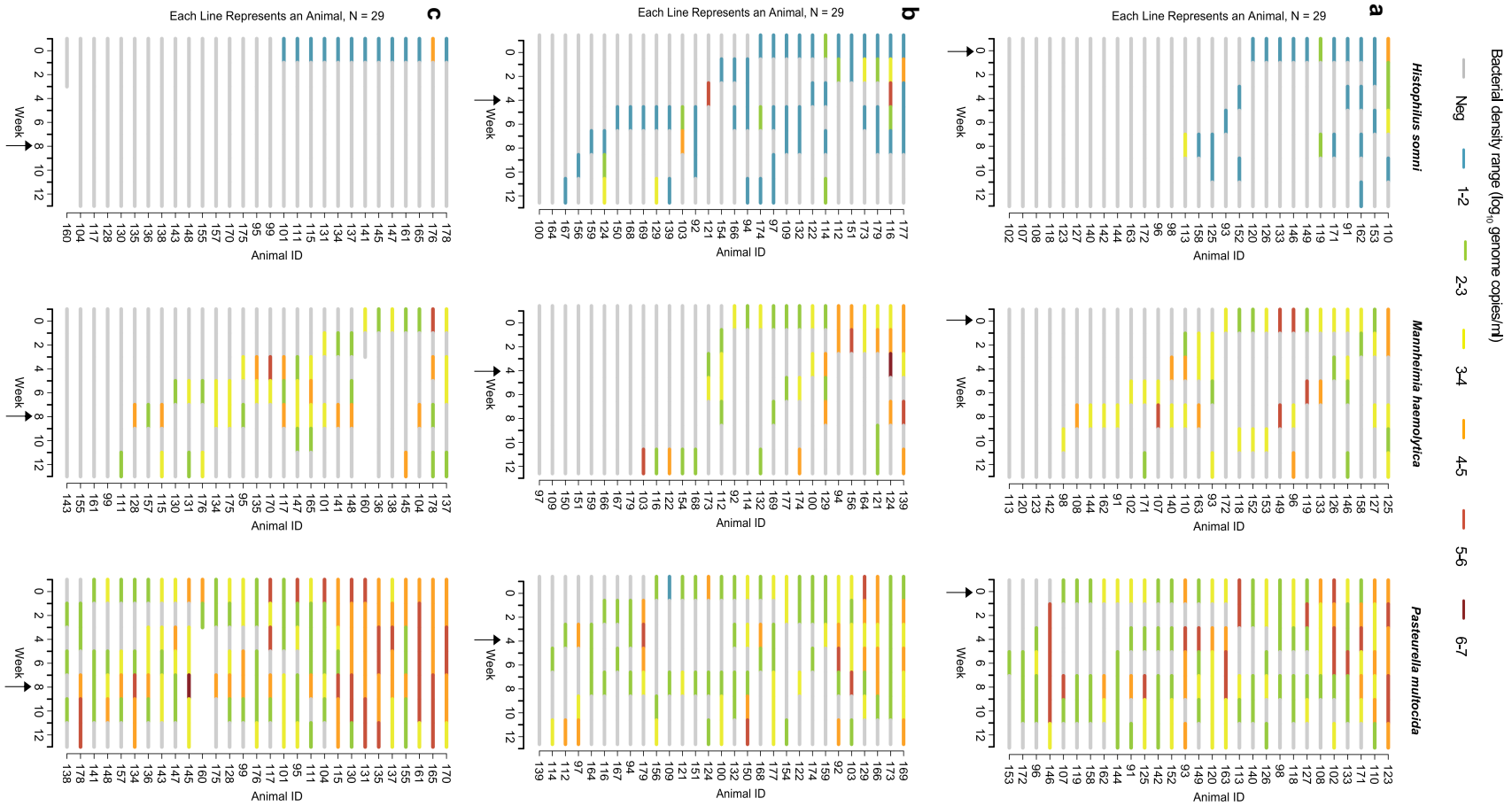

Figure 6.15: Density carriage patterns of *Histophilus somni*, *Mannheimia haemolytica* and *Pasteurella multocida*. Density determined by qPCR on nasal swabs collected on Weeks 0 to 12 from 29 calves housed in the Red Barn (panel a), Blue Barn (panel b) and Green Barn (panel c). Density of carriage is depicted as a colour series each representing a range of $\log_{10}$ genome copies/ml. Time of vaccination is indicated by an arrow. One animal (ID: 160) died, as shown by no coloured shading from Week 4 in the Green Barn. Animals are ordered based on their carriage patterns: animals sustaining carriage over consecutive visits appear first, animals with transient to no carriage detected appear in descending order.

6.3.10 Effect of viral infection on bacterial carriage density

6.3.10.1 Bacterial carriage density combining 1st and 2nd crossover points

Changes in the mean bacterial density between groups created from combining the 1st and 2nd crossover points are visualised in Figure 6.16. Density of *H. somni* was seen to decrease 2 and 4-weeks post vaccination, but very few animals had carriage in either control or vaccine groups (Table 6.13). At Week 0 mean carriage density of *M. haemolytica* was greater in vaccine group animals compared to controls but declined and increased to similar levels of control animals thereafter. Density of *P. multocida* carriage was lower in animals in the vaccine group compared with controls at Week 0. Two weeks after receiving vaccine there was an apparent increase in *P. multocida* carriage density in vaccinated animals not observed in unvaccinated controls, while at 4 weeks density appeared somewhat higher than at baseline in both groups.

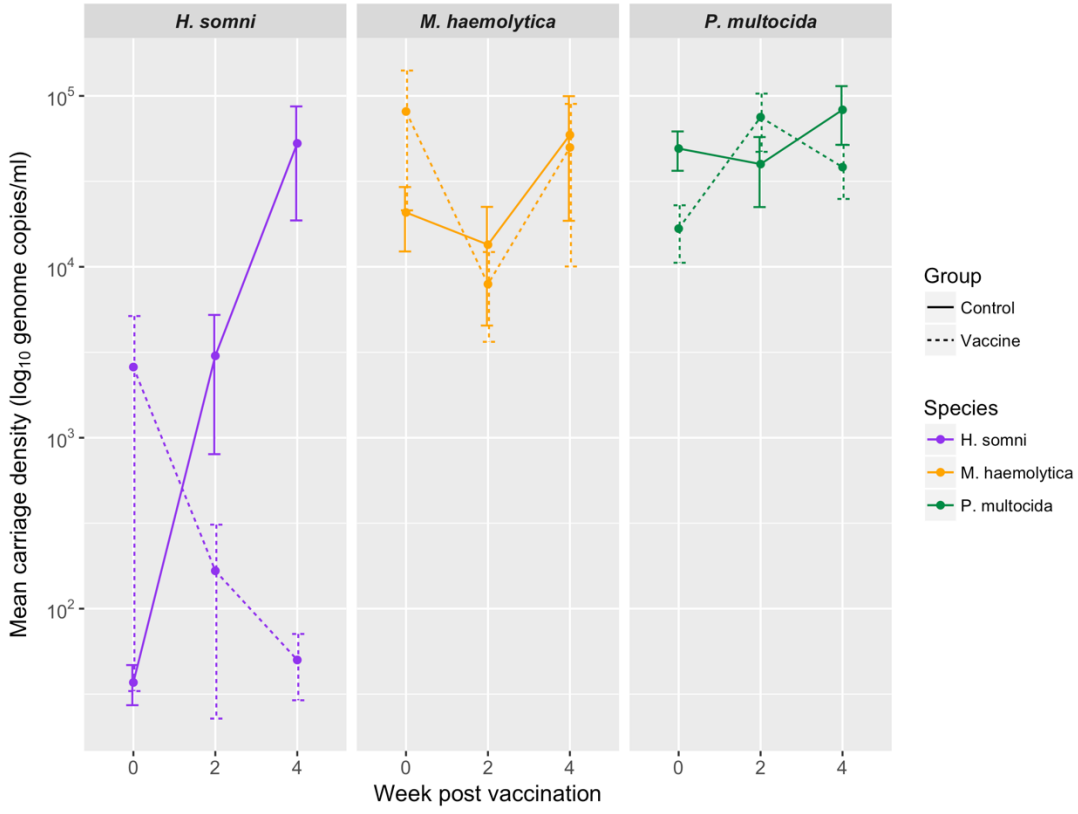

Figure 6.16: Between cluster analysis of *Pasteurellaceae* carriage considering the 1st and 2nd crossover points as replicates. Carriage densities of *Histophilus somni*, *Mannheimia haemolytica* and *Pasteurella multocida* in control and vaccine group animals are shown at 0, 2 and 4-weeks post vaccination. Error bars represent standard error of the mean.

The mean carriage densities of the three bacterial species for animals in the control and vaccine group at Week 0, 2 and 4 are shown in Table 6.13. There was no evidence to suggest a difference in mean *M. haemolytica* or *P. multocida* density between animals in either group 2 or 4-weeks after vaccination. Following vaccination, density of carriage of *H. somni* and *M. haemolytica* tended to decrease, whereas an approximate two-fold increase in density of *P. multocida* was observed 2-weeks post vaccination (Figure 6.16).

Table 6.13: Density of *Histophilus somni*, *Mannheimia haemolytica* and *Pasteurella multocida* carriage in control and vaccine groups: at 0, 2 and 4-weeks post vaccination considering 1st and 2nd vaccine crossover points as replicates

		Arithmetic mean carriage density* (genome copies/ml)						
Species	**Week**	**Control group**	**(N)**	**Vaccine group**	**(N)**	**Mean Ratio†**	**$CI_{95\%}$**	**P-value**
H. somni	0	37	(12)	2592	(11)	NA‡	NA‡	NA‡
	2	3016	(9)	166	(2)	NA‡	NA‡	NA‡
	4	52,744	(6)	50	(4)	NA‡	NA‡	NA‡
M. haemolytica	0	20793	(29)	81,064	(19)	2.99	0.841–12.0	0.0974
	2	13,477	(22)	7,922	(11)	0.571	1.75–2.21	0.380
	4	59,116	(28)	49,920	(11)	0.844	0.0928–19.2	0.889
P. multocida	0	49,207	(66)	16,735	(41)	0.341	0.148–0.851	**0.0177**
	2	39,906	(58)	75,094	(26)	1.87	0.528–8.39	0.361
	4	82,917	(62)	38,305	(38)	0.462	1.60–1.47	0.165

* Arithmetic mean carriage density in animals positive

† Ratio and its 95% confidence interval ($CI_{95\%}$) of the arithmetic mean for vaccinated animals to that of unvaccinated animals calculated at 0, 2 and 4-weeks post vaccination using gamma regression adjusting for number of replicate determinations.

‡ NA: not applicable; too few observations for meaningful analysis

6.3.10.2 Density of *P. multocida* following vaccination: within-barn comparisons

The geometric mean *P. multocida* density for paired positive swabs taken from the same animal on the day of vaccination and either 2 or 4-weeks post vaccination and found to be positive is shown for each barn in Table 6.14. At the 1st crossover point (Red Barn vaccinated) there was no evidence for an increase in density at 2 and 4-weeks post vaccination. Similarly, there was no evidence for an increase in density 2-weeks post vaccination at the 2nd crossover point in the Blue Barn; however, at 4 weeks density was slightly reduced and differences were not significant. There was evidence to suggest a significant decrease in carriage density 2-weeks post vaccination at the 3rd crossover point (Green Barn, p = 0.040). At 4 weeks, density was reduced further in the Green Barn (p = 0.0508). Confidence intervals for these estimates in the Green Barn were large. The change in geometric mean *P. multocida* density between paired swabs for each barn is given in Table 6.15.

Table 6.14: Within barn comparison of *Pasteurella multocida* nasal carriage density before and after respiratory viral vaccination

Vaccine crossover point	**Week***	**Geometric mean *P. multocida* density (genome copies/ml)**				**$CI_{95\%}$†**	**P-value‡**
		Before vaccination	**After vaccination**	**N**	**Ratio**		
1st (Red: Week 0)	2	4735	9270	12	1.96	0.0563–4.628	0.534
	4	3030	4292	17	1.55	0.107–3.89	0.622
2nd (Blue: Week 4)	2	3229	5689	10	1.76	0.056–5.74	0.611
	4	1785	1196	12	0.670	0.269–8.38	0.635
3rd (Green: Week 8)	2	20635	4845	25	0.235	**1.07-17.0**	**0.040**
	4	42607	8194	16	0.192	0.993-27.2	0.0508

* Week post vaccination; †Confidence interval for the change in mean density before and after vaccination (ratio of geometric means). ‡ Paired *t*-test to assess whether the mean natural log *P. multocida* density before and after vaccination were significantly different

6.3.10.3 Density of *P. multocida* following vaccination: between-barn comparisons

Comparisons among barns of the changes in *P. multocida* density post vaccination following each crossover point are shown in Table 6.15. For all analyses, residuals and variances were approximately normally distributed and homogenous respectively. There was weak evidence to suggest a difference between barns in density 2-weeks post vaccination at the 1st and 3rd crossover point - density of carriage was increased in vaccinated animals following the 1st crossover point but decreased following the 3rd crossover point. There was no evidence to suggest a significant difference in the change in density between barns on other occasions.

Table 6.15: Between-barn comparison of the fold-change in geometric mean *Pasteurella multocida* nasal carriage densities before and after respiratory viral vaccination in healthy beef cattle. The fold-change was calculated for paired positive swabs on the day of vaccination and either 2 or 4-weeks post vaccination.

Vaccine crossover point	**Week**	**Fold-change in geometric mean *P. multocida* density**						**F-statistic**	**df(w)***	**df(b)***	**P-value**
		Red	(N)	Blue	(N)	Green	(N)				
1st (Red: Week 0)	2w/0w	1.96	(12)	1.01	(10)	0.224	(19)	2.77	38	2	0.0753
	4w/0w	1.55	(17)	1.19	(11)	0.378	(18)	1.19	43	2	0.313
2nd (Blue: Week 4)	2w/0w	0.708	(12)	1.76	(10)	0.744	(15)	0.442	34	2	0.646
	4w/0w	1.04	(19)	0.670	(12)	3.99	(19)	1.87	47	2	0.166
3rd (Green: Week 8)	2w/0w	0.394	(22)	2.20	(8)	0.235	(25)	2.55	52	2	0.088
	4w/0w	0.211	(13)	1.84	(7)	0.192	(16)	1.50	33	2	0.238

Shaded cells represent barns in the intervention phase

The ratio of geometric mean density was compared between barns using ANOVA

* within (w) and between (b) degrees of freedom

6.4 Discussion

A double blind randomised controlled trial using a stepped wedge design was conducted to investigate the effect of respiratory viral infection on upper respiratory pathobiont colonisation dynamics in healthy cattle, using a live attenuated intranasal viral vaccine as a model infection system.

Studies in humans and mice have demonstrated nasal bacterial carriage rates, carriage duration, and density of carriage with important pathobionts to increase following intranasal vaccination with LAIV [253] [252]. In mice, these increases in pathobiont carriage duration and density were similar to those observed following wild-type influenza virus infection, raising the possibility that wild-type virus infection in cattle may cause a similar phenomenon. Consistent with these observations, respiratory viruses infecting cattle are considered as primary pathogens which lead to secondary bacterial pneumonia [19]. Therefore, in this study it was hypothesised that following deliberate respiratory viral infection in cattle, nasal carriage and density of carriage with important respiratory pathobionts may increase.

For the three bacterial species studied, the odds of carriage were lower following viral infection (Table 6.12). There was evidence of a significant, lasting effect of viral infection on carriage of *M. haemolytica* (OR: 0.48, $CI_{95\%}$: 0.27–0.85). Viral infection may only have a transient effect on bacterial carriage; this was investigated in mixed effect models by including time since vaccination as a predictor specified as three categories: vaccinated 2, 4 or ≥6 weeks (Model 2). There was weak evidence to suggest a transient effect of vaccination for *M. haemolytica* ($p = 0.0887$) but no such evidence for *H. somni* or *P. multocida.* The odds of carriage were similar among the 4 week and ≥6 week categories for *M. haemolytica* and *P. multocida*, so this model was simplified to include two categories: 2 or ≥4 weeks (Model 3). Model simplification resulted in a better fit for both bacteria and provided evidence to suggest a transient effect of vaccination on *M. haemolytica* carriage ($p = 0.0384$).

Pathobiont carriage was assessed 2 and 4-weeks after each vaccination ‘crossover point’, in ‘vertical’ (between cluster) analyses using log-linear models. As did the mixed models, these analyses suggested bacterial carriage rates tended to decrease following vaccination

(Tables 6.5 to 6.11). The advantage of this vertical analysis approach is that it makes use of the study design staggering the rollout of intervention, thus allowing for investigation into the impact of vaccinating animals at different times (i.e. preserves the randomisation order) and indeed, whether animals housed in separate barns respond comparably. Similar trends in carriage of *M. haemolytica* were seen regardless of the timing of vaccination (i.e. following the three crossover points): carriage rates either decreased following vaccination or remained similar to their pre-vaccination level (Table 6.6, Table 6.8 and Table 6.10). The odds of *P. multocida* carriage were lower in vaccinated animals 2 weeks following the 1st and 2nd vaccination crossover points (OR: 0.534, $CI_{95\%}$: 0.214–1.31; OR: 0.219, $CI_{95\%}$: 0.065–0.628), and at 4 weeks, the carriage rate in vaccinated animals was either lower than (OR: 0.164, $CI_{95\%}$: 0.00862–0.947) or similar to (OR: 1.19, $CI_{95\%}$: 0.475–3.11) controls. These results suggest that despite differences in the timing of vaccination, the effect of vaccination on bacterial carriage rate was broadly similar among the barns. One exception of note was that following the 3rd crossover point, the odds of *P. multocida* carriage in the most recently vaccinated cluster (Green Barn) were higher (OR: 8.68, $CI_{95\%}$: 2.21–58.7; OR: 1.76, $CI_{95\%}$: 0.712–4.45) compared to the earlier vaccinated clusters (Blue and Red Barns).

Log-linear models were also used to assess the effect of prior bacterial carriage on subsequent bacterial carriage. The odds of subsequent carriage given prior carriage were similar or increased for the three bacterial species at each crossover point, bar one occasion (3rd crossover) where the odds of subsequent *M. haemolytica* carriage were lower (OR: 0.467, $CI_{95\%}$: 0.140–1.36). On a few occasions, large confidence intervals for estimated odds ratios were wide (Table 6.5, Table 6.8, Table 6.9, and Table 6.11), indicating uncertainty around these estimates. This was probably due to low variation in counts of animals across covariates There might be an effect of vaccination on bacteria already colonising the upper airways different to that for the likelihood of colonisation of uncolonised upper airways. Therefore, to investigate whether the relationship between vaccination and bacterial carriage also depended on prior carriage, the interaction between prior carriage and vaccination was assessed. There was no evidence of an interaction between prior carriage and vaccination in any of the analyses, but the study was probably insufficiently powered to detect such an interaction.

The observation of reduced bacterial carriage rates following vaccination was also seen in the analysis combining the 1st and 2nd crossover points as experimental replicates. Although quite crude in its approach, this analysis did again identify that the odds of carriage for all three bacterial species studied was lower 2 and 4-weeks post vaccination (Table 6.4), consistent with results from log-linear and mixed effect models.

One possible explanation for the reduction in bacterial carriage observed in this study following vaccination could be as a consequence of vaccine-induced immune responses triggered by administration of the vaccine. This could occur through several possible mechanisms arising from the ability of both BRSV and BPIV-3 to infect bovine epithelial cells, albeit replicating poorly [14] [5], and that intranasal delivery of both viruses triggers local mucosal immune responses [18].

Firstly, as live vaccine viruses replicate in host cells, at least some level of innate immune responses will be subsequently activated [305]. The consequent immune responses are likely to create an unfavourable mucosal environment which may inhibit not only viral replication but also bacterial replication and promote pathogen clearance. As an example, human RSV triggers toll-like receptor 4 signalling (usually associated with Gram-negative bacteria), with the potential for downstream nuclear factor NF-κß mediated production of antimicrobial peptides. Similarly, inflammation leads to quantitative changes in mucin production for several weeks following respiratory viral infection [306]. In cattle, several MUC genes have been identified [307], and MUC gene expression is potentially altered following attenuated viral infection leading to increased mucin secretion and/or differences in the type of mucins produced at the respiratory mucosa, in turn affecting microbial adhesion [308].

Secondly, as part of this process of infection and subsequent immune response, virus is likely to cause at least some damage to the epithelium, creating the potential for translocation of bacteria to the lamina propria. Mucosal adaptive immune responses to translocated bacteria may then trigger production of local, bacteria-specific IgA in addition to virus-specific antibody induced by vaccine. Secretion of IgA back across the epithelial surface, could then lead to inhibition of bacterial proliferation through classical adaptive mechanisms such as agglutination and blockade of functional surface molecules [309]. It is unknown how much ‘damage’ an attenuated virus may cause and indeed whether this mechanism is likely to occur, but this would be possible to test experimentally.

Thirdly, changes in local host innate and/or adaptive immune responses may be sensed not only by resident pathobionts, but also by other components of the microbiota (16). However, since the respiratory microbiome, like other microbiomes, is an ecosystem in which species interact continuously with each other, alterations in the level of any of the other commensal organisms are likely to impact on the levels of the pathobionts tested. If certain organisms proliferate or die back then this changes the niche (e.g. changes in nutrient or binding site availability). Contrary to the study hypothesis, this study suggests that, in some cases, nasal pathobiont carriage rates in healthy cattle decrease following attenuated respiratory viral infection, although no discernible effects on density of carriage were observed. This observation was unexpected as rates of bacterial carriage, carriage density and carriage duration has been seen to increase in other studies using LAIV [252] [253]. There are important differences to this study and those using LAIV which may have contributed to the differences in biological outcomes, including the host species, host respiratory microbiome and the vaccines used.

Aside from vaccine-induced immune responses, the observed reduction in bacterial carriage rates following vaccination may be a result of differences in the natural history of carriage among the three bacterial species. Of the three bacteria, overall carriage rates were lowest for *H. somni* (109/604; 18.0%) and carriage was transient, with apparent clearance also observed. Conversely, *P. multocida* was detected most frequently (399/604; 66.1%) with carriage commonly sustained for long durations or even the whole study period. Carriage with *M. haemolytica* was transient but carried at a lower rate than *P. multocida* (154/604; 25.5%). It could be possible that vaccination non-specifically inhibits acquisition of bacterial carriage, an effect more profoundly observed for *M. haemolytica* as a consequence of both being commonly carried and transient.

Density profiles for each bacterium (Figure 6.13) were similar to those obtained for animals sampled the previous year (Chapter 4, Figure 4.4): *H. somni* was carried at low densities (1–2 $\log_{10}$ genome copies/ml), whereas *M. haemolytica* and *P. multocida* carriage extended over a wide range (2–6 $\log_{10}$ genome copies/ml). When carriage was maintained over several consecutive weeks it tended to occur at higher densities (Figure 6.15), corroborating results reported in Chapter 4. This suggests that the density profiles

obtained for each bacterium are reflective of their natural history and not due to sampling error. This study did not detect any discernible effects of viral infection on bacterial density, but the study was not powered to do so, it was powered primarily to detect changes in carriage rates. Variation in the density of carriage among animals in the same barn on the same day was high (Figure 6.14) and often carriage rates were low. When the difference in *P. multocida* density within clusters before and after vaccination was considered (Table 6.15), the direction and magnitude of effects varied between barns. It is likely that density of *Pasteurellaceae* carriage is influenced more by other factors than by vaccine viral infection, such as recency of acquisition, environment or even host genetics and hence studies of carriage density undertaken in more controlled settings might be more informative [137]. On the other hand, an advantage of this study is that it was conducted at a highly instrumented research farm emulating modern suckler beef production. As such, results pertaining to carriage biology may be more reflective of UK farms than they would be from studies using fewer animals in highly controlled settings.

Few studies in cattle using live attenuated vaccines have been conducted to investigate viral-bacterial interactions. One study investigating the effect of temperature and humidity on nasal and tracheal bacterial flora of 12-week-old calves, remarked on a significantly higher total bacterial colony count 7 days after intranasal vaccination with a live attenuated IBR vaccine containing thermosensitive BHV-1 [137]. No further details were provided on the effect of viral infection on particular bacterial species other than that for *M. haemolytica*, but so few animals were colonised with this bacterium that conclusions could not be drawn. Some conflicting evidence exists following deliberate exposure to wild-type BHV-1 in cattle – one study reported no effect on tonsil or nasal colonisation with *M. haemolytica* [138], whilst another reported induction of *M. haemolytica* nasal shedding; however, shedding was induced in only 4 of 8 calves studied [310]. Thus, the present study has helped bridge an important knowledge gap on the influence of live attenuated respiratory viral vaccination on bacterial colonisation.

Stepped wedge studies are inherently confounded by calendar time. To account for this confounding, the basic Hussey and Hughes mixed effect model assumes a homogeneous secular trend across clusters and is specified as a fixed effect. However, effects of time may not be linear and misspecification of time trends may lead to biased treatment effects or biased standard errors [311]. Varying secular trends over time were accounted for in

mixed model analysis by including a random effect of time within cluster [303] [312]. This random effect is an example of a crossed random effect because every cluster is observed at every time point and therefore represents a kind of interaction between time and cluster. A limitation to the model implemented in this study was that it assumed no correlation structure. In reality, this assumption may not be true, and it may be more likely that observations further apart in time are indeed less correlated [311]. As such, autoregressive correlation structures at the cluster (or individual within cluster) level may be more appropriate. Currently there are no published examples of closed cohort stepped wedge studies implementing autoregressive correlation structures, but both Hooper and Hemming have acknowledged their potential [303] [311].

Although the vertical, between-cluster analysis approach did not account for confounding on the response by time (i.e. different intervention rollout times) the horizontal mixed effect models included a random effect for time within cluster to account for this; consequently, the horizontal analysis can be seen to strengthen vertical comparisons. The rationale for performing both analyses is further strengthened by Davey et al. who highlighted the need to identify an efficient vertical analysis and compare this to the results of a mixed effects analysis, as has been done in this study [287]. In addition to these two analysis approaches, data from both the 1st and 2nd crossover points were combined into one single analysis, effectively treating the first two crossover points as experimental replicates. This allowed a greater number of observations to be modelled thereby giving greater statistical power, but ignored differences with respect to the timing of vaccination.

Throughout the study animals remained generally healthy. No *Dictyocaulus viviparous* larvae were detected and the nutritional plane of animals was similar among the different farmlet treatments, both at pasture and when housed (see Appendix D). One animal (ID: 177) presented with signs of pneumonia (increased respiration rate, elevated temperature, and dry adventitious lung sounds detected on auscultation). However, no nasal discharge was observed. Paired serum samples collected from this animal at the time of illness provided evidence of a rising titre to BRSV. These serological results should be treated with caution; at Week 0 this animal already had high levels of serum antibody to BRSV and it was later vaccinated at Week 4 with Rispoval RS+PI3 IntraNasal, seven weeks prior to signs of disease onset. Accordingly rising antibody titres may not have resulted

exclusively from natural exposure to circulating BRSV. It is possible that vaccination reduced the severity of this illness. Of note, carriage patterns for this animal were unremarkable compared to others housed in the same barn.

A limitation to this study is that detection of respiratory viruses was not undertaken during its course. PCR assays capable of detecting wild-type virus and vaccine strains could have been employed. Such information could have been used to look for association between viral infection and bacterial carriage and provide insight into the duration of viral-infection following vaccination. Moreover, it could provide evidence for viral-infection due either to vaccination or a circulating natural infection. Virus isolation could also have been employed to provide evidence of active viral infection [283] [278]. Instead, this study used serology to provide evidence of exposure to naturally circulating respiratory viruses (Table 6.2). Bloods were collected prior to vaccination at the start of the study (Week 0), and after vaccination at the last sampling occasion (Week 12). Seroconversion for any of the five agents tested (BRSV, BPIV-3, BHV-1, BVDV and *Mycoplasma bovis*) was investigated. Ideally, if resources permitted an additional blood sample collected at the study mid-point would have been informative.

Seroconversion to both BRSV and BPIV-3 was observed (Table 6.2), a reassuring result given vaccination was against these agents; however, it was not likely to have been associated with natural infection as animals remained generally healthy during the study. In addition, at Week 12, the number of animals with detectable antibodies to both these viruses was lowest in the Green Barn. This may reflect that this cluster was last in sequence to be vaccinated, just two weeks previously, whereas the Red and Blue Barn animals were respectively vaccinated four and six weeks previously and therefore had longer for antibody responses to develop. As such, there was no serological evidence to suggest that outcomes observed in this study were influenced by wild-type viral infection.

At Week 0, detectable antibody titres to BVDV (Blue Barn: 2/26; Green Barn: 1/28) and BHV-1 (Blue Barn: 2/26; Green Barn: 2/28; Red Barn: 1/28) occurred in younger calves aged 5.0–6.4 months (and thus may represent maternal antibody [313]. Two of the five calves positive for BHV-1 at Week 0 also had detectable antibodies to BVDV. Seroconversion for both BVDV (one calf in the Red Barn and one calf in the Green Barn) and BHV-1 (one calf in the Green Barn) was observed and implies that a natural infection

may have been circulating on the NWFP before the start of the study given - this could have occurred through bought-in breeding stock. The relatively high proportion of animals seroconverting (11/24) to *M. bovis* in the Red Barn is interesting and raises the question whether this was a stochastic event or the due to a barn effect. The Red Barn is situated centrally and could be more sheltered and hence be less well ventilated (despite identical building design) compared with the Blue and Green barns on either side. Consistent with this hypothesis was that the Blue and Green barns were highly correlated with each other in terms of both temperature ($r = 0.97$) and humidity ($r = 0.92$), more so than either were with the Red Barn (correlations Red with Blue and Green: $r_{temperature} = 0.10$, $r_{humidity} \approx 0.2$; Figure 6.6).

As discussed previously, RCTs are robust research designs [285]. This study uses a variant of an RCT - the stepped wedge design. This allowed every animal to act as its own control and permitted phased implementation of vaccination to clusters (barns). Concerns about possible transmission of live-vaccine virus shed in nasal secretions of vaccinated animals to co-housed controls militated against possible alternative study designs with rollout of vaccination to clusters within each barn; for example, three clusters of ten animals in each barn, with rollout of vaccine following a stepped wedge design to one cluster in each barn simultaneously. Instead, a pragmatic approach was taken to administer treatment at the barn level to avoid such risk of cross-contamination. To some extent the statistical power of the study was limited by the small number of clusters (three barns), and that only one cluster was randomised to receive the treatment at each crossover point, but the minimum number of clusters required for reasonable estimation of the intervention effect in stepped wedge studies is under-explored [312].

The study was strengthened through its randomisation strategy: animals were individually randomised to clusters following covariate-based constrained randomisation. This procedure ensured that covariates (breed, sex, sire, age, weaning weight, average daily growth rate) were balanced across clusters (Table 6.1). The advantage of such a rigorous randomisation procedure is that variation in covariates among groups is minimised as much as possible, thus decreasing the likelihood of confounding by these nuisance variables. Interestingly, Haines and Hemming recently recommended restricted randomisation procedures (e.g. covariate based randomisation, stratification, matching) for balancing cluster level covariates across intervention and

condition phase arms of stepped wedge studies [314]. It can be argued that for infectious disease studies where the outcome of interest is an infectious agent readily detectable by rapid molecular techniques, then the outcome of interest could itself be incorporated as a covariate in restricted randomisation, provided that samples can be collected and assayed quickly, or as Moulton proposed, baseline prevalence data which is already available at the outset could be taken and used as a constraining variable in the randomisation procedure. This approach then avoids the need to adjust for any initial differences at the time of analysis [170]. A further study strength was the implementation of administering placebo to clusters at the same time as those randomised to receive the intervention. This allowed for any changes in the measured outcomes to occur as a result of the intervention and not from the intranasal procedure. It also allowed the study to be blinded, minimising bias. The blinding was achieved through masking the contents of the syringe (Figure 6.3), which was highly effective.

In conclusion, this study demonstrates that following intranasal vaccination with attenuated BRSV and BPIV-3, rates of nasal carriage of *H. somni*, *M. haemolytica* and *P. multocida* were reduced in healthy cattle, but there was little evidence to suggest an effect on nasal carriage density. To my knowledge this is the first example of implementing a trial of stepped wedge design in veterinary research. Although the stepped wedge study is not necessarily difficult to implement, it is complicated and challenging to analyse whilst methods of analysis and reporting are still a rapidly developing field. Targeted approaches such as qPCR can be used to assess for species-specific changes following respiratory viral infection. Collectively, this work provides a platform for further investigation of viral-bacterial interactions in the upper respiratory tract of cattle using live attenuated vaccination and molecular detection techniques as tools for future work. These approaches may be useful for studying viral-bacterial interactions in other host species and/or with different target microorganisms.

Chapter 7 General Discussion

The work presented in this thesis attempts to provide insights into carriage of respiratory pathobionts in the bovine upper airways and how this might be affected by transient respiratory viral infection. Key findings of these studies described are highlighted and discussed, and recommendations provided for further work in this area.

The methodological approaches for detecting *Pasteurellaceae* from bovine nasal swabs presented in Chapter 3 have provided a valuable platform for further carriage studies. The three qPCR assays developed and optimised offer advantages over culture - they are rapid, reliable and are capable of quantifying bacterial DNA over a large range. While combining the three qPCR assays into a multiplex assay would be ideal, this is unachievable with the current annealing temperature of the *M. haemolytica* assay (69°C), which is higher than that of the *H. somni* and *P. multocida* assays (60°C). As discussed previously in Chapter 3, obtaining full genome sequences of *Mannheimia* spp. could aid in future design of primers allowing for an optimised assay with a lower annealing temperature. An alternative approach to qPCR for nucleic acid detection and quantification is the emerging technique of digital PCR (dPCR) [315]. In analogue qPCR, the amplification single is logarithmic and the quantification is based on external calibration [316]. In contrast, dPCR offers linear and digital quantification, based on the number of positive and negative reactions [316]. The digital format of the reaction may be divided into i) hundreds or thousands of chambers on a single plate or array (microfluidic-based approach), or ii) into thousands or millions of droplets (droplet-based approach) [316]. Prior to PCR amplification, the sample is partitioned – each reaction chamber receives at random either 0 or ≥1 copies of the target DNA. Poisson statistics can be used to measure DNA quantities, providing there are negative partitions. Compared to qPCR, dPCR is reportedly more tolerant to some PCR inhibitors, sequence variations, and different types of DNA template and master mixes. In addition, dPCR performs better when measuring low DNA concentrations (enhanced repeatability compared to qPCR), but has a restricted reaction volume, which may yield lower analytical sensitivity [315] [317].

Before the work presented in this thesis was conducted, there were few recent studies investigating upper respiratory tract (URT) carriage with *H. somni*, *M. haemolytica* or

P. multocida in cattle within the UK. Only one study has reported nasal carriage rates using culture-amplified PCR, which was conducted in Scotland in 2010 and reported rates of *P. multocida* carriage in beef and dairy calves [149]. The lack of carriage studies is surprising given that BRD continues to present a significant economic and welfare burden to the UK cattle industry. The work presented in Chapters 4, 5 and 6 has helped to bridge this knowledge gap. In these studies using qPCR, the three pathobiont species, *H. somni*, *M. haemolytica* and *P. multocida*, exhibited remarkably different carriage rates and density profiles, both in early life and when cattle were older. Rates of carriage were highest at the start of winter housing for all pathobiont species over the two years of study (Chapters 4 and 6), but rates did differ between years and the two cohorts. Although carriage rates differed between years, general trends in carriage rates of the three pathobionts were similar: *P. multocida* was carried at the highest rates, followed by *H. somni* and *M. haemolytica*. Furthermore, the density profiles were similar between years for the three bacterial species: *M. haemolytica* and *P. multocida* were carried over a wide range of densities (2–6 $\log_{10}$ genome copies/ml), with *H. somni* carried over a narrower range (1–2 $\log_{10}$ genome copies/ml). This was also true in early life for *H. somni* when colonisation was detected as early as 1 week of age, with similar density profiles seen at 1 week and 2, 3 and 7 months of age (Chapter 5, Figure 5.4). Obtaining distinct, consistent density profiles for each bacterium across different study years, with different animals, and at different ages suggests that these profiles are not due to sampling error and reflect real distributions of carriage density. Neither *M. haemolytica* nor *P. multocida* were detected in calves until 7 months of age, with the exception of two calves which were colonised with *P. multocida* at 3 months of age. Changes in colonisation patterns as calves age may have implications for later respiratory health and also for developing vaccination strategies [160].

A well-known limitation of the technique used is that PCR will detect DNA from non-viable organisms that persist in the respiratory tract even when viable organisms are no longer present or cannot be detected by culture. It can be argued that specific detection of DNA from these unculturable organisms provides evidence of either current or recent colonisation and is thus of biological interest. In studies in humans it has often been found that samples are positive by culture and negative by PCR [171] perhaps reflecting that, on occasion, culture has the potential to be more sensitive than PCR when there are very small numbers of organisms present. Interestingly, this phenomenon was not encountered

in the study presented in Chapter 4, perhaps reflecting the poor sensitivity of culture for these bacterial species. Of particular interest is that *H. somni* was only isolated from one of 60 nasal swabs cultured, but it was commonly detected by PCR. Sequencing of PCR products from PCR-amplified nasal swab samples determined positive for *H. somni* confirmed their identity, strengthening confidence in this assay's ability to detect *H. somni* reliably.

Moraxella bovoculi was isolated from one nasal swab (10-month-old heifer, Chapter 3) with a further 5 out of 60 swabs identified as either *Moraxella* or *Pasteurella* based on biochemical testing of isolates (10-month-old cattle, Chapter 3). Other authors have reported isolation of *Moraxella*-like organisms from calves suffering from respiratory disease. These findings prompted further investigation using PCR and confirmed the presence of *M. ovis* in bronchoalveolar lavages and nasopharyngeal swabs collected from calves suffering with respiratory disease on separate farms [318]. More recently, using 16S rRNA sequencing, the presence of *Moraxella* in bovine URT samples has been highlighted by other investigators. Lima et al. reported a significantly increased mean relative abundance of *Moraxella* in the nasal passages of dairy calves diagnosed with pneumonia, otitis or a combination of both compared to healthy calves at 14 days of age [264]. Sequencing of maternal vaginal and calf URT microbiota has also revealed a high abundance of *Moraxella* in both of these sites – the second most abundant genus identified after *Mannheimia* [268]. *Moraxella catarrhalis* is frequently carried in the nasal passages of healthy children [171] and is recognised as a significant human bacterial pathogen involved with respiratory disease and otitis media [220] [221]; similarly, *Moraxella* may be carried in the nasal passages of healthy cattle and contribute towards respiratory disease. Further work is needed to test this hypothesis, and to this end PCR or sequencing could be performed on collected nasal swabs from healthy and diseased cattle, and/or pneumonic lung tissue collected from cattle at post mortem.

Short nasal swabs were employed in Chapters 4–6 to sample nasal flora. Short swabs were advantageous compared to deep-guarded swabs in that the procedure was quick and less invasive. It is not known with certainty whether and to what extent the bacteria are evenly distributed within the upper respiratory tract of colonised animals, but one study did detect *M. haemolytica* from 15 different anatomical locations within the nasal cavity. Notably, the authors reported no differences between nasal passages [9], a finding

supported by others [310]. While some authors have suggested *M. haemolytica* preferentially colonises the palatine tonsil [139] [158], in this work deep-guarded swabs performed no better than short swabs for detection of *M. haemolytica* (Chapter 4). In fact, *M. haemolytica* was not detected from any short or deep swab collected from the same animal. Future studies investigating different sites of colonisation should consider larger sample sizes, as this study comparing 30 paired swabs was inconclusive. In common with all studies of mucosal colonisation, the studies presented in this thesis are subject to sampling error – colonisation will have remained undetected on occasion by obtaining the swabs from the wrong place, at the wrong time or insufficiently frequently and, indeed, the choice of the nasal cavity may not have been optimal for detection for one or more of these organisms. Accordingly, the results are likely to be underestimates and there is a need to develop sufficiently non-invasive techniques which will permit more frequent or even continuous sampling with due consideration to animal welfare. More broadly, these are studies in healthy cattle, and it cannot be certain whether and to what extent the strains of bacteria carried in the nasal passages have the potential to cause or contribute to outbreaks of disease or how specific virulence factors may vary among the same bacterial species.

Longitudinal studies characterising bacterial carriage in humans are common but veterinary medicine has lagged behind; emphasis has been placed on studies identifying the aetiological agents involved with disease outbreaks or risk factors contributing towards those outbreaks [10] [24] [147]. As such, there is little knowledge on the natural history of respiratory pathobionts of cattle. In Chapter 4 the association between density and duration of carriage was investigated using interval-censored survival analysis. In this study it was observed that density of *P. multocida* carriage was significantly associated with carriage duration, and that the highest density category investigated ($\geq$4.77 $\log_{10}$ genome copies/ml) was associated with the longest carriage duration (hazard ratio: 0.414 per day; $CI_{95\%}$: 0.197 – 0.868). This observation could have implications for the transmission of pathobionts within a susceptible population – animals with higher density carriage above a critical threshold could potentially be more infectious due to increased bacterial load and remaining infectious for longer periods of time; therefore, increasing opportunities for transmission events [251].

Exploring the complexity of infectious disease systems can be achieved through mathematical models. Mathematical models could be used to enhance basic understanding of infectious diseases, for example, to determine transmission routes, to predict disease outbreaks, or to test the effects of prevention strategies. Epidemiological surveys are important sources of data for parametrizing models [319]. Similarly, the studies in this thesis reporting rates of carriage and clearance rates could be used to provide initial parameter estimates for transmission models of BRD, for example, either SIS (susceptible-infectious-susceptible) or SIR (susceptible-infectious-recovered) compartmental models. Transmission models could then be used to inform prevention and control strategies, for example, investigating timing of vaccination (considering age and environmental influences) and/or optimising stocking densities.

To investigate the effect of respiratory viral vaccination on bacterial carriage patterns, a rigorous randomised controlled trial was conducted (Chapter 6). The results suggested that following vaccination, carriage of clinically important bacterial species in the bovine URT decreased. This observation supports the hypothesis that respiratory viral infection can alter the respiratory microbiota and suggests that strategic vaccination schedules could be used to favourably manipulate microbiota, as well as to generate immunity to respiratory viruses. Future work focusing on elucidation of the immunological mechanisms associated with the non-specific effects of vaccination described in Chapter 6 and comparison of these mechanisms with wild-type infection could be highly rewarding. In addition to non-specific effects of vaccination on bacterial species, effects may be serotype specific. The qPCR assays employed did not discriminate between the different serotypes of bacteria targeted. Of the capsular serotypes of *M. haemolytica*, A2 is frequently isolated from healthy cattle, whilst A1 and A6 are associated with BRD [113]. Consequently, there is a knowledge gap relating to long-term carriage dynamics of specific serotypes. Longitudinal carriage studies could be employed to characterise serotype-specific carriage and the influence of respiratory viral infection and/or respiratory viral vaccination on bacterial serotypes. Moreover, this work indicates that vaccines have the potential to have broader impacts than that relating to either a reduction of the disease caused by or prevalence/transmission of the target organism of the vaccines. This may have implications for future studies evaluating the effects of vaccines – should vaccine studies be broadening investigations to consider effects on the microbiome, and how will this impact on defining the outcomes of studies?

The three bacterial species investigated in Chapter 6 exhibited remarkably different carriages rates and dynamics of carriage. The strongest evidence for an effect of respiratory viral infection on bacterial carriage rate was observed for *M. haemolytica*. For this bacterium, carriage was often transient and overall rates observed (25.5%) were in-between that for *H. somni* (18.0%) and *P. multocida* (66.1%). If, indeed, vaccination does interfere with colonisation, differences in colonisation patterns among bacterial species could determine whether an effect of attenuated respiratory viral infection was observed within the study design implemented. Moreover, the ability of the study to detect an effect depends on the size of the effect, the size of the study and the heterogeneity of the population with regard to bacterial carriage rates and density of carriage. Thus, results from this study can be used to inform design of future studies to elucidate the unexpected inhibitory effects of attenuated respiratory viral vaccination on bacterial carriage dynamics. It would be rewarding to explore whether this phenomenon is related to an effect on the likelihood of acquisition, abundance of carriage and/or duration of carriage. For example, future work could employ interval-censored survival analysis, as demonstrated in Chapter 4 to investigate this. There was no evidence of an interaction between prior carriage and vaccination in any of the log-linear analyses conducted in Chapter 6; however, it is likely these analyses were underpowered. Further experiments powered to detect an interaction between prior carriage and vaccination may help elucidate whether effects of vaccination are on acquisition of bacterial colonisation or on bacteria already colonised or both.

The randomised controlled trial with stepped wedge design presented in Chapter 6 is unique in several ways. Firstly, to my knowledge, it is the first application of a stepped wedge design in veterinary research. Accordingly this study lays a foundation for further trials where phased implementation of an invention at the group level in veterinary settings may be beneficial, for example, at the farm level within a national setting. Secondly, it is unusual in that the investigator had control over designating participants to clusters, to which the intervention was then delivered. More commonly, in cluster randomised controlled trials the clusters are predetermined, for example, general practices, schools, hospitals, or villages or other communities [170]. Thirdly, the intervention in Chapter 6 (vaccination) was not maintained after its introduction. This differs to the stepped wedge trials most commonly employed in healthcare settings, where once introduced, the intervention is typically maintained, for example, staff

training/education on hand-hygiene or a school breakfast programme [320] [321] [322]. Possible transient effects of vaccination were explored through mixed effects models. There was evidence to suggest that, for *M. haemolytica*, the effect of vaccination on bacterial carriage rates was strongest 2 weeks post administration and waned thereafter.
The animals studied in this thesis were bred and housed at the North Wyke Farm Platform, Rothamsted Research. This provided a unique opportunity to work with a largely closed herd, on an operational farm, within a research setting. This was advantageous as the farm is highly instrumented and extensively monitored for running long-term experiments involving grazing livestock. If the studies had been conducted on a commercial farm then changes to the study environment or animals may have been more frequent, potentially introducing confounders. Future studies conducted at Rothamsted offer great potential as the herd studied at the Farm Platform will soon be comprised mainly of the Stabiliser suckler beef breed – a genetically stable composite breed expected to have less animal to animal variability, as is currently seen with the cross-bred beef breeds on the farm [323]. In addition, all cattle will be genotyped. The calf cohort involved in the stepped wedge study presented in Chapter 6 were the first cohort to have 50,000 single nucleotide polymorphisms genotyped, and these results are currently being compiled into a database of respective phenotypes and genotypes. It would of interest to return to these genotypes to look for possible associations with the bacterial carriage patterns described for these animals.

Recent advances using genetics to help control BRD include genome-editing resistance to *M. haemolytica* leukotoxin (Lkt) [324]. Binding of Lkt to the signal peptide of ruminant specific CD18, the β subunit of β_2 integrins, expressed on the surface of ruminant leukocytes results in cell lysis. It has been demonstrated that Lkt binds to the amino acids 5–17 of signal peptide of CD18 [109]. Cleavage of the CD18 signal peptide in ruminants is inhibited by the signal peptide sequence encoding glutamine. Using gene editing glutamine was substituted for glycine, which in non-ruminants induces cleavage of the signal peptide. This substitution produced leukocytes that expressed the signal peptide-less CD18 on their surface, in turn resisting leukotoxin-induced cytolysis. Genome-editing technologies could play an important role in breeding livestock resistant to disease.

Manipulating the respiratory microbiome might prove to be useful to support respiratory health and management of BRD, but the success of this approach would hinge partly on better defining the role of respiratory microbiota and its interplay with the immune system [325]. Historically, emphasis has been placed on investigating bovine respiratory pathobionts as pathogens; for example, much work has been conducted on elucidating virulence factors, such as the leukotoxin of *M. haemolytica* [85] [326] [327]. However, it is equally important to consider whether and how pathobionts may contribute towards respiratory health [328]. Development of technologies such as high-throughput sequencing, metabolomics and transcriptomics has allowed investigation of complex microbial communities and their interaction with the host [209]. This has led to a paradigm shift in how we view determinants of disease, and instead of attributing one pathogen to a disease, we can now consider disease as a consequence of several specific interactions within the microbial environment [329]. As discussed in Chapter 1, management events such as transport, weaning and social reorganisation may predispose cattle to BRD. These events have been investigated in relation to URT microbiota using sequencing, for example, at weaning and arrival at the feedlot [178], and before versus after transport to the feedlot [330]. In addition, emphasis has been placed on characterising the URT microbiota from healthy versus diseased animals within feedlots [177]. Of note, all of these studies have been conducted in US feedlot settings and none to date have focused on extensive or intensive beef production systems in the UK. Future work employing such technologies could investigate changes in the respiratory microbial ecosystem before and after respiratory viral infection, or indeed following other stressors, such as transportation or weaning [160] [264]. Moreover, using such technologies, livestock offer a unique opportunity to study the transmission of microbiomes within closed herd settings, a topic of recent interest in human medicine [331].

In summary, this thesis has provided novel perspectives and insights into bovine respiratory disease within a UK setting. Three real-time PCR assays were evaluated, optimised and validated on collected bovine nasal swabs, providing a platform for studying carriage dynamics with *H. somni*, *M. haemolytica* and *P. multocida*. The longitudinal carriage studies conducted have provided unique and detailed information on the natural history of these three bacterial species in healthy cattle: at early life, during winter housing and following respiratory viral infection. Moreover, this work has drawn parallels between human and veterinary fields to address challenges in livestock farming;

pioneering the use of live attenuated vaccines as model infection systems in cattle to enhance understanding of empirical associations between host-pathogen interactions. Consequently, outputs are applicable to both livestock and human health.

References

1. de Haan C, Steinfeld H, Blackburn H. Livestock and the environment. Finding a balance.: European Commission Directorate General for Development.; 1997.

2. FAO STAT. Production - Live Animals - Number of heads 2015

3. Thomson DU, White BJ. Backgrounding beef cattle. Vet Clin North Am Food Anim Pract. 2006;22(2):373.

4. USDA. Cattle and Beef, Sector at a Glance 2019 [Available from: https://www.ers.usda.gov/topics/animal-products/cattle-beef/sector-at-a-glance/.

5. Mintert J. Beef feedlot industry. Vet Clin North Am Food Anim Pract. 2003;19(2):387.

6. Martin SW, Meek AH, Davis DG, Thomson RG, Johnson JA, Lopez A, et al. Factors associated with mortality in feedlot cattle - Bruce County Beef Cattle Project. Can J Comp Med. 1980;44(1):1-10.

7. Macartney JE, Bateman KG, Ribble CS. Health performance of feeder calves sold at conventional auctions versus special auctions of vaccinated or conditioned calves in Ontario. Journal of the American Veterinary Medical Association. 2003;223(5):677-83.

8. White BJ, Blasi D, Vogel LC, Epp M. Associations of beef calf wellness and body weight gain with internal location in a truck during transportation. J Anim Sci. 2009;87(12):4143-50.

9. Pass DA, Thomson RG. Wide distribution of Pasteurella haemolytica type-1 over nasal mucosa of cattle. an J Comp Med. 1971;35(3):181.

10. Hay KE, Barnes TS, Morton JM, Clements ACA, Mahony TJ. Risk factors for bovine respiratory disease in Australian feedlot cattle: Use of a causal diagram-informed approach to estimate effects of animal mixing and movements before feedlot entry. Prev Vet Med. 2014;117(1):160-9.

11. Allen JW, Viel L, Bateman KG, Rosendal S. Changes in the bacterial flora of the upper and lower respiartory tracts and bronchoalveolar lavage differential cell counts in feedlot calves treated for respiratory diseases Can J Comp Med. 1992;56(3):177-83.

12. National Beef Association N. Beef statisitics 2015 [Available from: https://www.nationalbeefassociation.com/resources/beef-statistics/.

13. Gates MC. Evaluating the reproductive performance of British beef and dairy herds using national cattle movement records. Vet Rec. 2013;173(20):499.

14. AHDB. Better returns from pure dairy-bred male calves. 2015.

15. Eisler MC, Lee MRF, Tarlton JF, Martin GB, Beddington J, Dungait JAJ, et al. Steps to sustainable livestock. Nature. 2014;507(7490):32-4.
16. Barrett DC. A Serological Survey of Viral Respiratory Pathogens in Growing Calves on a Multi-system Cattle Unit 1997.
17. Edwards TA. Control Methods for Bovine Respiratory Disease for Feedlot Cattle. Vet Clin North Am Food Anim Pract. 2010;26(2):273.
18. Dabo SM, Taylor JD, Confer AW. *Pasteurella multocida* and bovine respiratory disease. Anim Health Res Rev. 2007;8(02):129.
19. Panciera RJ, Confer AW. Pathogenesis and pathology of bovine pneumonia. Vet Clin North Am Food Anim Pract. 2010;26(2):191-214.
20. Frank GH, Smith PC. Prevalence of *Pasteurella haemolytica* in transported calves. Am J Vet Res. 1983;44(6):981-5.
21. Autio T, Pohjanvirta T, Holopainen R, Rikula U, Pentikainen J, Huovilainen A, et al. Etiology of respiratory disease in non-vaccinated, non-medicated calves in rearing herds. Vet Microbiol. 2007;119(2-4):256-65.
22. Srikumaran S, Kelling CL, Ambagala A. Immune evasion by pathogens of bovine respiratory disease complex. Anim Health Res Rev. 2007;8(2):215-29.
23. Taylor JD, Fulton RW, Lehenbauer TW, Step DL, Confer AW. The epidemiology of bovine respiratory disease: What is the evidence for predisposing factors? Can Vet J. 2010;51(10):1095-102.
24. Klima CL, Zaheer R, Cook SR, Booker CW, Hendrick S, Alexander TW, et al. Pathogens of bovine respiratory disease in North American feedlots conferring multidrug resistance via integrative conjugative elements. J Clin Microbiol. 2014;52(2):438-48.
25. Cernicchiaro N, White BJ, Renter DG, Babcock AH, Kelly L, Slattery R. Associations between the distance traveled from sale barns to commercial feedlots in the United States and overall performance, risk of respiratory disease, and cumulative mortality in feeder cattle during 1997 to 2009. J Anim Sci. 2012;90(6):1929-39.
26. Sporer KRB, Xiaoc L, Tempelmanc RJ, Burtonc JL, Earley B, Crowe MA. Transportation stress alters the circulating steroid environment and neutrophil gene expression in beef bulls. Vet Immunol Immunopathol. 2008;121(3-4):300-20.
27. Taylor JD, Holland BP, Step DL, Payton ME, Confer AW. Nasal isolation of Mannheimia haemolytica and Pasteurella multocida as predictors of respiratory disease in shipped calves. Res Vet Sci. 2015;99:41-5.

28. Sanderson MW, Dargatz DA, Wagner BA. Risk factors for initial respiratory disease in United States' feedlots based on producer-collected daily morbidity counts. Can J Vet Res. 2008;49(4):373-8.
29. Weaver DM, Tyler JW, VanMetre DC, Hostetler DE, Barrington GM. Passive transfer of colostral immunoglobulins in calves. J Vet Intern Med. 2000;14(6):569-77.
30. Ackermann MR, Derscheid R, Roth JA. Innate Immunology of Bovine Respiratory Disease. Vet Clin North Am Food Anim Pract. 2010;26(2):215.
31. Aich P, Potter AA, Griebel PJ. Modern approaches to understanding stress and disease susceptibility: A review with special emphasis on respiratory disease. Int J Gen Med. 2009;2:19-32.
32. Miles DG. Overview of the North American beef cattle industry and the incidence of bovine respiratory disease (BRD). Anim Health Res Rev. 2009;10(2):101-3.
33. Alsultan, II, Aitken ID. The tonsillar carriage of Pasteurella haemolytica in lambs. J Comp Pathol. 1985;95(2):193-201.
34. Orr JP. Haemophilus somnus infection - a retrospective analysis of cattle necropsied at the western college of veterinary medicine from 1970 to 1990. Can J Vet Res. 1992;33(11):719-22.
35. Hodgins DC, Conlon JA, Shewen PE. Respiratory viruses and bacteria in cattle. Polymicrobial Diseases. 2002:213-29.
36. Wisconsin Uo. Calf Respiratory Scoring Chart [Calf Respiratory Scoring Chart].
37. Love WJ, Lehenbauer T, Kass PH, Van Eenennaam AL, Aly SS. Development of a novel clinical scoring systemfor on-farm diagnosis of bovine respiratory disease in pre-weaned dairy calves. PeerJ. 2014;2.
38. Thompson PN, Stone A, Schultheiss WA. Use of treatment records and lung lesion scoring to estimate the effect of respiratory disease on growth during early and late finishing periods in South African feedlot cattle. J Anim Sci. 2006;84(2):488-98.
39. Griffin D. Economic impact associated with respiratory disease in beef cattle. Vet Clin North Am Food Anim Pract. 1997;13(3):367-77.
40. Gardner BA, Dolezal HG, Bryant LK, Owens FN, Smith RA. Health of finishing steers: Effects on performance, carcass traits, and meat tenderness. J Anim Sci. 1999;77(12):3168-75.
41. Buhman MJ, Perino LJ, Galyean ML, Wittum TE, Montgomery TH, Swingle RS. Association between changes in eating and drinking behaviors and respiratory tract disease in newly arrived calves at a feedlot. Am J Vet Res. 2000;61(10):1163-8.

42. Eysker M. The sensitivity of the Baermann method for the diagnosis of primary Dictyocaulus viviparus infections in calves. Veterinary Parasitology. 1997;69(1-2):89-93.

43. Klewer AM, Forbes A, Schnieder T, Strube C. A survey on Dictyocaulus viviparus antibodies in bulk milk of dairy herds in Northern Germany. Prev Vet Med. 2012;103(2-3):243-5.

44. Catry B, Dewulf J, Maes D, Pardon B, Callens B, Vanrobaeys M, et al. Effect of Antimicrobial Consumption and Production Type on Antibacterial Resistance in the Bovine Respiratory and Digestive Tract. PLoS One. 2016;11(1).

45. Caswell JL, Hewson J, Slavic D, DeLay J, Bateman K. Laboratory and Postmortem Diagnosis of Bovine Respiratory Disease. Vet Clin North Am Food Anim Pract. 2012;28(3):419.

46. Fulton RW, Confer AW. Laboratory test descriptions for bovine respiratory disease diagnosis and their strengths and weaknesses: Gold standards for diagnosis, do they exist? Can J Vet Res. 2012;53(7):754-61.

47. Horwood PF, Mahony TJ. Multiplex real-time RT-PCR detection of three viruses associated with the bovine respiratory disease complex. J Virol Methods. 2011;171(2):360-3.

48. Alexander TW, Cook SR, Yanke LJ, Booker CW, Morley PS, Read RR, et al. A multiplex polymerase chain reaction assay for the identification of Mannheimia haemolytica, Mannheimia glucosida and Mannheimia ruminalis. Vet Microbiol. 2008;130(1-2):165-75.

49. Fulton RW, Briggs RE, Payton ME, Confer AW, Saliki JT, Ridpath JF, et al. Maternally derived humoral immunity to bovine viral diarrhea virus (BVDV) 1a, BVDV1b, BVDV2, bovine herpesvirus-1, parainfluenza-3 virus bovine respiratory syncytial virus, Mannheimia haemolytica and Pasteurella multocida in beef calves, antibody decline by half-life studies and effect on response to vaccination. Vaccine. 2004;22(5-6):643-9.

50. Salt JS, Thevasagayam SJ, Wiseman A, Peters AR. Efficacy of a quadrivalent vaccine against respiratory diseases caused by BHV-1, PI3V, BVDV and BRSV in experimentally infected calves. Veterinary Journal. 2007;174(3):616-26.

51. Rice JA, Carrasco-Medina L, Hodgins DC, Shewen PE. *Mannheimia haemolytica* and bovine respiratory disease. Anim Health Res Rev. 2007;8(2):117-28.

52. Hjerpe CA. Bovine vaccines and herd vaccination programs. Vet Clin North Am Food Anim Pract. 1990;6(1):169.

53. Portis E, Lindeman C, Johansen L, Stoltman G. A ten-year (2000-2009) study of antimicrobial susceptibility of bacteria that cause bovine respiratory disease complex *Mannheimia haemolytica*, *Pasteurella multocida*, and *Histophilus somni* in the United States and Canada. J Vet Diagn Invest. 2012;24(5):932-44.

54. AHDB. Use of vaccines in dairy and beef cattle production 2011–2017 2018 [Available from: https://ahdb.org.uk/knowledge-library/use-of-vaccines-in-dairy-and-beef-cattle-production-2011-17.

55. UK-Statutory-Instrument. Veterinary Medicines Regulations 2013. 2013.

56. NOAH. Annual Review 2015/2016 2018 [Available from: https://www.noah.co.uk/wp-content/uploads/2016/08/NOAH-Review-2015-16-HR.pdf.

57. NOAH. Industry Facts and Figures 2018 [Available from: https://www.noah.co.uk/about/industry-facts-and-figures/.

58. Cresswell E, Brennan ML, Barkema HW, Wapenaar W. A questionnaire-based survey on the uptake and use of cattle vaccines in the UK. Vet Rec Open. 2014;1(1).

59. Agency) AAPH. Cattle Dashboard 2018 [Available from: https://public.tableau.com/profile/siu.apha#!/vizhome/CattleDashboard/Overview.

60. Agency) AAPH. Veterinary Investigation Diagnosis Analysis (VIDA) 2019 [Available from: http://apha.defra.gov.uk/vet-gateway/surveillance/scanning/vida.htm.

61. National Animal Disease Information Service N. Bovine Viral Diarrhoea 2019 [Available from: https://www.nadis.org.uk/disease-a-z/cattle/bovine-viral-diarrhoea-bvd/.

62. Scottish-Government. May 2017 - Forward look from Scotland's Chief Veterinary Officer 2019 [Available from: https://www2.gov.scot/Topics/farmingrural/Agriculture/animal-welfare/Diseases/disease/bvd/whatsnew.

63. Agency) AAPH. GB Emerging Threats Quarterly Report Cattle Diseases: Quartely Report; Vol 20; Q1. 2016.

64. Kilian M, Frederiksen, W., Biberstein, E. L. Haemophilus, Pasteurella and Actinobacillus: Academic Press Inc. (London) Ltd, 24/28 Oval Road, London NW1 7DX; 1980.

65. Adlam RJM. Pasteurellosis of Cattle (Frank G.H); In Pasteurella and Pasteurellosis. United States ed: Academic Press Inc.; 1989.
66. Blackall PJ, Miflin JK. Identification and typing of Pasteurella multocida: a review. Avian Pathol. 2000;29(4):271-87.
67. Olsen I, Dewhirst FE, BJ P. Family Pasteurellaceae. In: Bergey's manual of systematic bacteriology. Part B ed. New York, NY: Springer; 2005.
68. Christensen H, Kuhnert P, Busse H-J, Frederiksen WC, Bisgaard M. Proposed minimal standards for the description of genera, species and subspecies of the Pasteurellaceae. Int J Syst Evol Microbiol. 2007;57:166-78.
69. Angen O, Quirie M, Donachie W, Bisgaard M. Investigations on the species specificity of Mannheimia (Pasteurella) haemolytica serotyping. Vet Microbiol. 1999;65(4):283-90.
70. Angen O, Ahrens P, Kuhnert P, Christensen H, Mutters R. Proposal of Histophilus somni gen. nov., sp nov for the three species incertae sedis 'Haemophilus somnus', 'Haemophilus agni' and 'Histophilus ovis'. Int J Syst Evol Microbiol. 2003;53:1449-56.
71. Smith GR. Characteristics of 2 types of Pasteurella haemolytica associated with different pathological conditions in sheep Journal of Pathology and Bacteriology. 1961;81(2):431.
72. Angen O, Mutters R, Caugant DA, Olsen JE, Bisgaard M. Taxonomic relationships of the Pasteurella haemolytica complex as evaluated by DNA-DNA hybridizations and 16S rRNA sequencing with proposal of Mannheimia haemolytica gen. nov., comb, nov., Mannheimia granulomatis comb, nov., Mannheimia glucosida sp. nov., Mannheimia ruminalis sp. nov., and Mannheimia varigena sp. nov. Int J Syst Evol Microbiol. 1999;49:67-86.
73. Mutters R, Ihm P, Pohl S, Frederiksen W, Mannheim W. Reclassification of the genus Pasteurella trevisan 1887 on the basis of deoxyribonucleic acid homology, with proposals for the new species Pasteurella dagmatis, Pasteurella canis, Pasteurella stomatis, Pasteurella anatis, and Pasteurella langaa. Int J Syst Evol Microbiol. 1985;35(3):309-22.
74. Capitini CM, Herrero IA, Patel R, Ishitani MB, Boyce TG. Wound infection with Neisseria weaveri and a novel subspecies of Pasteurella multocida in a child who sustained a tiger bite. Clin Infect Dis. 2002;34(12):E74-E6.

75. Heddlest.Kl, Rebers PA, Gallaghe.Je. Fowl cholera gel diffusion preciptitaion test for serotyping Pasteurella multocida from avian species. Avian Dis. 1972;16(4):925.
76. Harper M, Boyce JD, Adler B. Pasteurella multocida pathogenesis: 125 years after Pasteur. FEMS Microbiol Lett. 2006;265(1):1-10.
77. Shivachandra SB, Viswas Kn Fau - Kumar AA, Kumar AA. A review of hemorrhagic septicemia in cattle and buffalo. 2011(1475-2654 (Electronic)).
78. Bonaventura MPD, Lee EK, Desalle R, Planet PJ. A whole-genome phylogeny of the family Pasteurellaceae. Mol Phylogenet Evol. 2010;54(3):950-6.
79. Robinson J. Colonization and infection of the respiratory tract: What do we know? Paediatrics & child health. 2004;9(1):21-4.
80. Oxford-English-Dictionary. Definition of carriage in English 2019 [Available from: https://en.oxforddictionaries.com/definition/carriage.
81. van Cleef B, van Benthem BHB, Verkade EJM, van Rijen MML, Kluytmans-van den Bergh MFQ, Graveland H, et al. Livestock-Associated MRSA in Household Members of Pig Farmers: Transmission and Dynamics of Carriage, A Prospective Cohort Study. PLoS One. 2015;10(5).
82. Bogaert D, van Belkum A, Sluijter M, Luijendijk A, de Groot R, Rumke HC, et al. Colonisation by *Streptococcus pneumoniae* and *Staphylococcus aureus* in healthy children. Lancet. 2004;363(9424):1871-2.
83. Finn A, Morales-Aza B, Sikora P, Giles J, Lethem R, Marlais M, et al. Density Distribution of Pharyngeal Carriage of Meningococcus in Healthy Young Adults New Approaches to Studying the Epidemiology of Colonization and Vaccine Indirect Effects. J Pediatric Infect Dis Soc. 2016;35(10):1080-5.
84. van Belkum A, de Vogel Corné P, Boelens Hélène A, Verbrugh Henri A, Nouwen Jan L, Verveer J, et al. Reclassification of Staphylococcus aureus Nasal Carriage Types. J Infect Dis. 2009;199(12):1820-6.
85. Singh K, Ritchey JW, Confer AW. Mannheimia haemolytica: Bacterial-Host Interactions in Bovine Pneumonia. Vet Pathol. 2011;48(2):338-48.
86. Weiser JN, Ferreira DM, Paton JC. Streptococcus pneumoniae: transmission, colonization and invasion. Nat Rev Microbiol. 2018;16(6):355-67.
87. Khamesipour F, Momtaz H, Mamoreh MA. Occurrence of virulence factors and antimicrobial resistance in Pasteurella multocida strains isolated from slaughter cattle in Iran. Front Microbiol. 2014;5.

88. Kisiela DI, Czuprynski CJ. Identification of Mannheimia haemolytica Adhesins Involved in Binding to Bovine Bronchial Epithelial Cells. Infect Immun. 2009;77(1):446-55.

89. Tagawa Y, Sanders JD, Uchida I, Bastida-Corcuera FD, Kawashima K, Corbeil LB. Genetic and functional analysis of Haemophilus somnus high molecular weight-immunoglobulin binding proteins. Microbial Pathogenesis. 2005;39(5-6):159-70.

90. Behling-Kelly E, Vonderheid H, Kim KS, Corbeil LB, Czuprynski CJ. Roles of cellular activation and sulfated glycans in Haemophilus somnus adherence to bovine brain microvascular endothelial cells. Infect Immun. 2006;74(9):5311-8.

91. Bosch A, Biesbroek G, Trzcinski K, Sanders EAM, Bogaert D. Viral and Bacterial Interactions in the Upper Respiratory Tract. PLoS Pathog. 2013;9(1).

92. Mosier DA. Bacterial pneumonia. Vet Clin North Am Food Anim Pract. 1997;13(3):483.

93. Corbeil LB. Histophilus somni host-parasite relationships. Anim Health Res Rev. 2007;8(2):151-60.

94. Headley SA, Alfieri AF, Oliveira VHS, Beuttemmueller EA, Alfieri AA. Histophilus somni is a potential threat to beef cattle feedlots in Brazil. Vet Rec. 2014;175(10).

95. O'Toole D, Allen T, Hunter R, Corbeil LB. Diagnostic Exercise: Myocarditis Due to Histophilus somni in Feedlot and Backgrounded Cattle. Vet Pathol. 2009;46(5):1015-7.

96. Brown WW, Griner LA, R J. Infectious embolic meningo-encephalitis in cattle. (0003-1488 (Print)).

97. Kennedy PC, Biberstein EL, Howarth JA, Frazier LM, Dungworth DL. Infectious meningo-encephalitis in cattle, caused by a haemophilus-like organism. Am J Vet Res. 1960;21(82):403-9.

98. Bailie WE, Anthony HD, Weide KD. Infectious thromboemboic meningoencephalomyelitis (sleeper syndrome) in feedlot cattle. Journal of the American Veterinary Medical Association. 1966;148(2):162.

99. O'Toole D, Hunter R, Allen T, Zekarias B, Lehmann J, Kim KS, et al. Effect of Histophilus somni on Heart and Brain Microvascular Endothelial Cells. Vet Pathol. 2017;54(4):629-39.

100. Inzana TJ, Gogolewski RP, Corbeil LB. Phenotypic phase variation in Haemophilus somnus lipooligosaccharide during bovine pneumnia and after invitro passage. Infect Immun. 1992;60(7):2943-51.
101. Elswaifi SF, Scarratt WK, Inzana TJ. The role of lipooligosaccharide phosphorylcholine in colonization and pathogenesis of Histophilus somni in cattle. Veterinary Research. 2012;43.
102. Kuckleburg CJ, Elswaifi SF, Inzana TJ, Czuprynski CJ. Expression of phosphorylcholine by Histophilus somni induces bovine platelet aggregation. Infect Immun. 2007;75(2):1045-9.
103. Andrews JJ, Anderson TD, Slife LN, Stevenson GW. Microscopic lesions associated with the isolation of Haemophilus somnus from pneumonic bovine lungs. Vet Pathol. 1985;22(2):131-6.
104. Gogolewski RP, Leathers CW, Liggitt HD, Corbeil LB. Experimental haemophilus-somnus pneumonia in calves and immunoperoxidase localization of bacteria. Vet Pathol. 1987;24(3):250-6.
105. Krismer B, Weidenmaier C, Zipperer A, Peschel A. The commensal lifestyle of Staphylococcus aureus and its interactions with the nasal microbiota. Nat Rev Microbiol. 2017;15(11):675-87.
106. Prado ME, Prado TM, Payton M, Confer AW. Maternally and naturally acquired antibodies to Mannheimia haemolytica and Pasteurella multocida in beef calves. Vet Immunol Immunopathol. 2006;111(3-4):301-7.
107. Devenish J, Rosendal S, Johnson R, Hubler S. Immunoserological comparison of 104-kilodalton proteins associated with hemolysis and cytolysis in Actinobacillus pleuropneumoniae, Actinobacillus suis, Pasteurella haemolytica, and Escherichia coli. Infect Immun. 1989;57(10):3210-3.
108. Shewen PE, Wilkie BN. Evidence for the Pasteurella haemolytica cytotoxin as a product of actively growing bacteria. Am J Vet Res. 1985;46(5):1212-4.
109. Shanthalingam S, Srikumaran S. Intact signal peptide of CD18, the beta-subunit of beta(2)-integrins, renders ruminants susceptible to Mannheimia haemolytica leukotoxin. Proceedings of the National Academy of Sciences of the United States of America. 2009;106(36):15448-53.
110. Czuprynski CJ, Noel EJ, Ortizcarranza O, Srikumaran S. Activation of bovine neutrophils by partially purified Pasteurella haemolytica leukotoxin. Infect Immun. 1991;59(9):3126-33.

111. Atapattu DN, Czuprynski CJ. Mannheimia haemolytica leukotoxin induces apoptosis of bovine lymphoblastoid cells (BL-3) via a caspase-9-dependent mitochondrial pathway. Infect Immun. 2005;73(9):5504-13.

112. Czuprynski CJ. Host response to bovine respiratory pathogens. Anim Health Res Rev. 2009;10(2):141-3.

113. Griffin D, Chengappa MM, Kuszak J, McVey DS. Bacterial Pathogens of the Bovine Respiratory Disease Complex. Vet Clin North Am Food Anim Pract. 2010;26(2):381.

114. Leite F, Sylte MJ, O'Brien S, Schultz R, Peek S, van Reeth K, et al. Effect of experimental infection of cattle with bovine herpesvirus-1 (BHV-1) on the ex vivo interaction of bovine leukocytes with Mannheimia (Pasteurella) haemolytica leukotoxin. Vet Immunol Immunopathol. 2002;84(1-2):97-110.

115. Gagea MI, Bateman KG, van Dreumel T, McEwen BJ, Carman S, Archambault M, et al. Diseases and pathogens associated with mortality in Ontario beef feedlots. J Vet Diagn Invest. 2006;18(1):18-28.

116. Dabo SM, Confer AW, Murphy GL. Outer membrane proteins of bovine Pasteurella multocida serogroup A isolates. Vet Microbiol. 1997;54(2):167-83.

117. Kumar AA, Shivachandra SB, Biswas A, Singh VP, Srivastava SK. Prevalent serotypes of Pasteurella multocida isolated from different animal and avian species in India. Vet Res Commun. 2004;28(8):657-67.

118. Rimler RB, Rhoades KR. Serogroup F, a new capsule serogroup of *Pasteurella multocida*. J Clin Microbiol. 1987;25(4):615-8.

119. Harmon BG, Glisson JR, Latimer KS, Steffens WL, Nunnally JC. Resistance of *Pasteurella multocida* A-3,4 to phaggocytosis by turkey macrophages and heterophils. Am J Vet Res. 1991;52(9):1507-11.

120. Chung JY, Wilkie I, Boyce JD, Townsend KM, Frost AJ, Ghoddusi M, et al. Role of capsule in the pathogenesis of fowl cholera caused by Pasteurella multocida serogroup A. Infect Immun. 2001;69(4):2487-92.

121. Chung JY, Wilkie I, Boyce JD, Adler B. Vaccination against fowl cholera with acapsular Pasteurella multocida A : 1. Vaccine. 2005;23(21):2751-5.

122. Horadagoda NU, Hodgson JC, Moon GM, Wijewardana TG, Eckersall PD. Development of a clinical syndrome resembling haemorrhagic septicaemia in the buffalo following intravenous inoculation of Pasteurella multocida serotype B : 2 endotoxin and the role of tumour necrosis factor-alpha. Res Vet Sci. 2002;72(3):194-200.

123. Galdiero M, Folgore A, Nuzzo I, Galdiero E. Neutrophil adhesion and transmigration through bovine endothelial cells in vitro by protein H and LPS of Pasteurella multocida. Immunobiology. 2000;202(3):226-38.

124. Harper M, Boyce JD, Cox AD, Michael FS, Wilkie IW, Blackall PJ, et al. Pasteurella multocida expresses two lipopolysaccharide glycoforms simultaneously, but only a single form is required for virulence: Identification of two acceptor-specific heptosyl I transferases. Infect Immun. 2007;75(8):3885-93.

125. Caswell JL, Middleton DM, Sorden SD, Gordon JR. Expression of the neutrophil chemoattractant interleukin-8 in the lesions of bovine pneumonic pasteurellosis. Vet Pathol. 1998;35(2):124-31.

126. Morsey MA, Popowych Y, Kowalski J, Gerlach G, Godson D, Campos M, et al. Molecular cloning and expression of bovine interleukin-8. Microbial Pathogenesis. 1996;20(4):203-12.

127. Guzman E, Taylor G. Immunology of bovine respiratory syncytial virus in calves. Molecular Immunology. 2015;66(1):48-56.

128. McGill JL, Rusk RA, Guerra-Maupome M, Briggs RE, Sacco RE. Bovine Gamma Delta T Cells Contribute to Exacerbated IL-17 Production in Response to Co-Infection with Bovine RSV and Mannheimia haemolytica. PLoS One. 2016;11(3).

129. Gresham CN, Confer AW, Bush LJ, Rummage JA. Serum and colostrum antibody to Pasteurella species in dairy cattle. Am J Vet Res. 1984;45(11):2227-30.

130. Roth JA. How cattle defend themselves against Pasteurella haemolytica. Veterinary Medicine. 1988;83(10):1067.

131. Lee CW, Shewen PE. Evidence of bovine immunoglobulin G(1) (IgG(1)) protease activity in partially purified culture supernate of Pasteurella haemolytica A1. Can J Comp Med. 1996;60(2):127-32.

132. Butler JE. Bovine immunoglobulins - an augmented review. Vet Immunol Immunopathol. 1983;4(1-2):43-152.

133. Gentry MJ, Confer AW, Panciera RJ. Serum neuralization of cytotoxin from Pasteurella haemolytica, serotype 1 and resistance to experimental bovine pneumonic pasteurellosis Vet Immunol Immunopathol. 1985;9(3):239-50.

134. Gioia J, Qin X, Jiang HY, Clinkenbeard K, Lo R, Liu YM, et al. The genome sequence of Mannheimia haemolytica A1: Insights into virulence, natural competence, and Pasteurellaceae phylogeny. J Bacteriol. 2006;188(20):7257-66.

135. DeRosa DC, Mechor GD, Staats JJ, Chengappa MM, Shryock TR. Comparison of Pasteurella spp. simultaneously isolated from nasal and transtracheal swabs from cattle with clinical signs of bovine respiratory disease. Journal of Clinical Microbiology. 2000;38(1):327-32.
136. Fulton RW, Cook BJ, Step DL, Confer AW, Saliki JT, Payton ME, et al. Evaluation of health status of calves and the impact on feedlot performance: assessment of a retained ownership program for postweaning calves. Can J Comp Med. 2002;66(3):173-80.
137. Woldehiwet Z, Mamache B, Rowan TG. The effects of age, environmental temperature and relative humidity on the bacterial flora of the upper respiratory tract in calves. . British Veterinary Journal. 1990;146(3):211-8.
138. Frank GH, Briggs RE. Colonization of the tonsils of calves with Pasteurella haemolytica. Am J Vet Res. 1992;53(4):481-4.
139. Frank GH, Briggs RE, Debey BM, editors. Bovine tonsils as reservoirs for *Pasteurella haemolytica* colonisation, immune response, and infection of the nasopharynx Workshop on Pasteurellosis in Production Animals; 1993 Aug 10-13; Bali, Indonesia.
140. Ellis JA. Update on viral pathogenesis in BRD. Anim Health Res Rev. 2009;10(2):149-53.
141. Murray GM, O'Neill RG, Lee AM, McElroy MC, More SJ, Monagle A, et al. The bovine paranasal sinuses: Bacterial flora, epithelial expression of nitric oxide and potential role in the in-herd persistence of respiratory disease pathogens. PLoS One. 2017;12(3).
142. Timsit E, Christensen H, Bareille N, Seegers H, Bisgaard M, Assie S. Transmission dynamics of Mannheimia haemolytica in newly-received beef bulls at fattening operations. Vet Microbiol. 2013;161(3-4):295-304.
143. Murphy GL, Robinson LC, Burrows GE. Restriction endonuclease analysis and ribotyping differentiate Pasteurella haemolytica serotype A1 isolates from cattle within a feedlot. J Clin Microbiol. 1993;31(9):2303-8.
144. Taylor JD, Fulton RW, Dabo SM, Lehenbauer TW, Confer AW. Comparison of genotypic and phenotypic characterization methods for Pasteurella multocida isolates from fatal cases of bovine respiratory disease. J Vet Diagn Invest. 2010;22(3):366-75.
145. Magwood SE, Barnum DA, Thomson RG. Nasal bacterial flora of calves in healthy and in pneumonia prone herds. an J Comp Med. 1969;33(4):237-43.

146. Allen JW, Viel L, Bateman KG, Rosendal S, Shewen PE, Physicksheard P. The microbial flora of the respiratory tract in feedlot calves: associations between nasopharyngeal and bronchoalveolar lavage cultures. Can J Comp Med. 1991;55(4):341-6.

147. Catry B, Decostere A, Schwarz S, Kehrenberg C, de Kruif A, Haesebrouck F. Detection of tetracycline-resistant and susceptible Pasteurellaceae in the nasopharynx of loose group-housed calves. Veterinary Research Communications. 2006;30(7):707-15.

148. Angen O, Thomsen J, Larsen LE, Larsen J, Kokotovic B, Heegaard PMH, et al. Respiratory disease in calves: Microbiological investigations on trans-tracheally aspirated bronchoalveolar fluid and acute phase protein response. Vet Microbiol. 2009;137(1-2):165-71.

149. Hotchkiss EJ, Dagleish MP, Willoughby K, McKendrick IJ, Finlayson J, Zadoks RN, et al. Prevalence of *Pasteurella multocida* and other respiratory pathogens in the nasal tract of Scottish calves. Vet Rec. 2010;167(15):555-60.

150. Townsend KM, Frost AJ, Lee CW, Papadimitriou JM, Dawkins HJS. Development of PCR assays for species- and type-specific identification of Pasteurella multocida isolates. J Clin Microbiol. 1998;36(4):1096-100.

151. Guenther S, Schierack P, Grobbel M, Luebke-Becker A, Wieler LH, Ewers C. Real-time PCR assay for the detection of species of the genus *Mannheimia*. J Microbiol Methods. 2008;75(1):75-80.

152. Angen O, Ahrens P, Tegtmeier C. Development of a PCR test for identification of *Haemophilus somnus* in pure and mixed cultures. Vet Microbiol. 1998;63(1):39-48.

153. Noyes NR, Benedict KM, Gow SP, Booker CW, Hannon SJ, McAllister TA, et al. *Mannheimia haemolytica* in feedlot cattle: prevalence of recovery and associations with antimicrobial use, resistance, and health outcomes. J Vet Intern Med. 2015;29:705 - 13.

154. Klima CL, Alexander TW, Hendrick S, McAllister TA. Characterization of *Mannheimia haemolytica* isolated from feedlot cattle that were healthy or treated for bovine respiratory disease. Can J Comp Med. 2014;78(1):38-45.

155. How Mannheimia haemolytica defeats host defence through a kiss of death mechanism.

156. Katsuda K, Kamiyama M, Kohmoto M, Kawashima K, Tsunemitsu H, Eguchi M. Serotyping of *Mannheimia haemolytica* isolates from bovine pneumonia: 1987-2006. Veterinary Journal. 2008;178(1):146-8.

157. Liu DY, Lawrence ML, Austin FW. Specific PCR identification of Pasteurella multocida based on putative transcriptional regulator genes. J Microbiol Methods. 2004;58(2):263-7.
158. Frank GH, Briggs RE, Gillette KG. Colonization of the nasal passages of calves with Pasteurella haemolytica serotype 1 and regeneration of colonization after experimentally induced viral infection of the respiratory tract. Am J Vet Res. 1986;47(8):1704-7.
159. Corbeil LB, Woodward W, Ward ACS, Mickelsen WD, Paisley L. Bacterial interactions in bovine respiratory and reproductive infections J Clin Microbiol. 1985;21(5):803-7.
160. Biesbroek G, Tsivtsivadze E, Sanders EAM, Montijn R, Veenhoven RH, Keijser BJF, et al. Early respiratory microbiota composition determines bacterial succession patterns and respiratory health in children. Am J Respir Crit Care Med. 2014;190(11):1283-92.
161. McCullers JA. Insights into the interaction between influenza virus and pneumococcus. Clin Microbiol Rev. 2006;19(3):571.
162. Francis T, Detorregrosa MV. Combine infection of mice with H. influenzae and Influenza virus by the intransal route. Journal of Infectious Diseases. 1945;76(1):70-7.
163. Mars MH, Bruschke CJM, van Oirschot JT. Airborne transmission of BHV1, BRSV, and BVDV among cattle is possible under experimental conditions. Vet Microbiol. 1999;66(3):197-207.
164. Orr RJ, Murray PJ, Eyles CJ, Blackwell MSA, Cardenas LM, Collins AL, et al. The North Wyke Farm Platform: effect of temperate grassland farming systems on soil moisture contents, runoff and associated water quality dynamics. Eur J Soil Sci. 2016;67(4):374-85.
165. Clancy M J WRK, editor Development and application of a new chemical method for predicting the digestibility and intake of herbage samples. 10th International Grasslands Congress; 1966; Helsinki.
166. Alderman G CBR. Energy and Protein Requirements of Ruminants. Oxfordshire: CABI Publishing; 1993.
167. McAuliffe GA, Takahashi T, Orr RJ, Harris P, Lee MRF. Distributions of emissions intensity for individual beef cattle reared on pasture-based production systems. J Clean Prod. 2018;171:1672-80.

168. Hawkins J. Data quality and summary statistics. Annual Report 2016: meterological data. 2019.
169. Hawkins J. Data quality and summary statistics. Annual Report 2017: meterological data. 2019.
170. Moulton LH. Covariate-based constrained randomization of group-randomized trials. Clinical trials (London, England). 2004;1(3):297-305.
171. Thors V, Morales-Aza B, Pidwill G, Vipond I, Muir P, Finn A. Population density profiles of nasopharyngeal carriage of 5 bacterial species in pre-school children measured using quantitative PCR offer potential insights into the dynamics of transmission. Hum Vaccin Immunother. 2016;12(2):375-82.
172. Chochua S, D'Acremont V, Hanke C, Alfa D, Shak J, Kilowoko M, et al. Increased nasopharyngeal density and concurrent carriage of *Streptococcus pneumoniae*, *Haemophilus influenzae*, and *Moraxella catarrhalis* are associated with pneumonia in febrile children. PLoS One. 2016;11(12).
173. Wang Y, Qian PY. Conservative Fragments in Bacterial 16S rRNA Genes and Primer Design for 16S Ribosomal DNA Amplicons in Metagenomic Studies. PLoS One. 2009;4(10).
174. Lane DJ. 16S/23S rRNA Sequencing. . New York Wiley; 1991.
175. Crawley MJ. The R Book: Wiley; 2012.
176. Agresti A. An introduction to categorical data analysis. New York Wiley; 1996.
177. Holman DB, McAllister TA, Topp E, Wright A-DG, Alexander TW. The nasopharyngeal microbiota of feedlot cattle that develop bovine respiratory disease. Vet Microbiol. 2015;180(1-2):90-5.
178. Timsit E, Workentine M, Schryvers AB, Holman DB, van der Meer F, Alexander TW. Evolution of the nasopharyngeal microbiota of beef cattle from weaning to 40 days after arrival at a feedlot. Vet Microbiol. 2016;187:75-81.
179. Gaeta NC, Lima SF, Teixeira AG, Ganda EK, Oikonomou G, Gregory L, et al. Deciphering upper respiratory tract microbiota complexity in healthy calves and calves that develop respiratory disease using shotgun metagenomics. J Dairy Sci. 2017;100(2):1445-58.
180. Moseley SL, Huq I , Alim AR, So M, Samadpour-Motalebi M, M F. Detection of enterotoxigenic Escherichia coli by DNA colony hybridization. J Infect Dis. 1980;142:892-8.

181. Engleberg NC, Eisenstein BI. Detection of microbial nucleic acids for diagnostic purposes. Annual Review of Medicine. 1992;43:147-55.
182. Yang S, Rothman RE. PCR-based diagnostics for infectious diseases: uses, limitations, and future applications in acute-care settings. Lancet Infect Dis. 2004;4(6):337-48.
183. Higuchi R, Fockler C, Dollinger G, Watson R. Kinetic PCR analysis real-time monitoring of DNA amplification reactions. Nat Biotechnol. 1993;11(9):1026-30.
184. Gilliland G, Perrin S Fau - Blanchard K, Blanchard K Fau - Bunn HF, Bunn HF. Analysis of cytokine mRNA and DNA: detection and quantitation by competitive polymerase chain reaction. (0027-8424 (Print)).
185. Diviacco S, Norio P, Zentilin L, Menzo S, Clementi M, Biamonti G, et al. A novel procedure for quantitative polymerase chain reaction by coamplification of competitive templates. Gene. 1992;122(2):313-20.
186. Paabo S, Higuchi RG, Wilson AC. Ancient DNA and the polymerase chain reaction - the emerging field of molecular archaeology. J Biol Chem. 1989;264(17):9709-12.
187. Tyagi S, Kramer FR. Molecular beacons: Probes that fluoresce upon hybridization. Nat Biotechnol. 1996;14(3):303-8.
188. Nagy A, Vitaskova E, Cernikova L, Krivda V, Jirincova H, Sedlak K, et al. Evaluation of TaqMan qPCR System Integrating Two Identically Labelled Hydrolysis Probes in Single Assay. Sci Rep. 2017;7.
189. Pfaffl MW. A new mathematical model for relative quantification in real-time RT-PCR. Nucleic Acids Research. 2001;29(9).
190. Butler JM. Chapter 3 - DNA Quantitation. In: Butler JM, editor. Advanced Topics in Forensic DNA Typing: Methodology. San Diego: Academic Press; 2012. p. 49-67.
191. Bustin S, Huggett, J. qPCR primer design revisited. Biomol Detect Quantif. 2017;14:19 - 28.
192. Forootan A, Sjöback R, Björkman J, Sjögreen B, Linz L, Kubista M. Methods to determine limit of detection and limit of quantification in quantitative real-time PCR (qPCR). Biomol Detect Quantif. 2017;12:1-6.
193. Satzke C, Turner P, Virolainen-Julkunen A, Adrian PV, Antonio M, Hare KM, et al. Standard method for detecting upper respiratory carriage of Streptococcus pneumoniae: Updated recommendations from the World Health Organization Pneumococcal Carriage Working Group. Vaccine. 2013;32(1):165-79.

194. Coughtrie AL, Whittaker RN, Begum N, Anderson R, Tuck A, Faust SN, et al. Evaluation of swabbing methods for estimating the prevalence of bacterial carriage in the upper respiratory tract: a cross sectional study. Bmj Open. 2014;4(10).

195. Horwood PF, Mahony TJ. Rapid detection of bovine respiratory disease pathogens. North Sydney: Meat & Livestock Australia Limited; 2007

196. Miflin JK, Blackall PJ. Development of a 23S rRNA-based PCR assay for the identification of Pasteurella multocida. Lett Appl Microbiol. 2001;33:216-21.

197. Lichtensteiger CA, Steenbergen SM, Lee RM, Polson DD, Vimr ER. Direct PCR analysis for toxigenic Pasteurella multocida. J Clin Microbiol. 1996;34(12):3035-9.

198. Townsend KM, Frost AJ, Lee CW, Papadimitriou JM, Dawkins HJS. Genetic Organization of Pasteurella multocida cap Loci and Development of a Multiplex Capsular PCR Typing System. J Clin Microbiol. 2001;39(3):924-9.

199. Sievers F, Wilm A, Dineen D, Gibson TJ, Karplus K, Li WZ, et al. Fast, scalable generation of high-quality protein multiple sequence alignments using Clustal Omega. Mol Syst Biol. 2011;7.

200. Korczak B, Christensen H, Emler S, Frey J, Kuhnert P. Phylogeny of the family Pasteurellaceae based on rpoB sequences. Int J Syst Evol Microbiol. 2004;54:1393-9.

201. Dassanayake RP, Call DR, Sawant AA, Casavant NC, Weiser GC, Knowles DP, et al. *Bibersteinia trehalosi* inhibits the growth of *Mannheimia haemolytica* by a proximity-dependent mechanism. Appl Environ Microbiol. 2010;76(4):1008-13.

202. Bavananthasivam J, Dassanayake RP, Kugadas A, Shanthalingam S, Call DR, Knowles DP, et al. Proximity-dependent inhibition of growth of *Mannheimia haemolytica* by *Pasteurella multocida*. Appl Environ Microbiol. 2012;78(18):6683-8.

203. Sweeney MT, Quesnell R, Tiwari R, Lemay M, Watts JL. In vitro activity and rodent efficacy of clinafloxacin for bovine and swine respiratory disease. Front Microbiol. 2013;4.

204. Rodrigues F, Foster D, Nicoli E. Relationships between rhinitis symptoms, respiratory viral infections and nasopharyngeal colonization with *Streptococcus pneumoniae*, *Haemophilus influenzae* and *Staphylococcus aureus* in children attending daycare. J Pediatric Infect Dis Soc. 2013;32(3):227-32.

205. Tegtmeier C, Angen O, Ahrens P. Comparison of bacterial cultivation, PCR, in situ hybridization and immunohistochemistry as tools for diagnosis of *Haemophilus somnus* pneumonia in cattle. Vet Microbiol. 2000;76(4):385-94.

206. Angen O, Ahrens P, Bisgaard M. Phenotypic and genotypic characterization of *Mannheimia* (*Pasteurella*) haemolytica-like strains isolated from diseased animals in Denmark. Vet Microbiol. 2002;84(1-2):103-14.

207. Quinn P J, Markley F C, Leonard E S, FitzPatrick E S, Fanning S, J HP. Veterinary Microbiology and Microbial Disease Second ed: Blackwell Publishing Ltd. ; 2011.

208. Sprouffske K, Wagner A. Growthcurver: an R package for obtaining interpretable metrics from microbial growth curves. BMC Bioinformatics. 2016;17.

209. Bailey M, Thomas A., Francis O., Stokes C., Smidt, H. The dark side of technological advances in analysis of microbial ecosystems. Journal of Animal Science and Biotechnology. 2019.

210. Janda JM, Abbott SL. 16S rRNA gene sequencing for bacterial identification in the diagnostic laboratory: Pluses, perils, and pitfalls. J Clin Microbiol. 2007;45(9):2761-4.

211. Rosselli R, Romoli O, Vitulo N, Vezzi A, Campanaro S, de Pascale F, et al. Direct 16S rRNA-seq from bacterial communities: a PCR-independent approach to simultaneously assess microbial diversity and functional activity potential of each taxon. Sci Rep. 2016;6.

212. Bustin SA, Benes V, Garson JA, Hellemans J, Huggett J, Kubista M, et al. The MIQE Guidelines: Minimum Information for Publication of Quantitative Real-Time PCR Experiments. Clinical Chemistry. 2009;55(4):611-22.

213. Christensen H, Angen O, Olsen JE, Bisgaard M. Revised description and classification of atypical isolates of Pasteurella multocida from bovine lungs based on genotypic characterization to include variants previously classified as biovar 2 of Pasteurella canis and Pasteurella avium. JMM Case Rep. 2004;150:1757-67.

214. Scherrer S, Frei D, Wittenbrink MM. A novel quantitative real-time polymerase chain reaction method for detecting toxigenic Pasteurella multocida in nasal swabs from swine. Acta Vet Scand. 2016;58.

215. Caraguel CGB, Stryhn H, Gagne N, Dohoo IR, Hammell KL. Selection of a cutoff value for real-time polymerase chain reaction results to fit a diagnostic purpose: analytical and epidemiologic approaches. J Vet Diagn Invest. 2011;23(1):2-15.

216. Fryer JF, Heath AB, Minor PD, Collaborative Study G. A collaborative study to establish the 1st WHO International Standard for human cytomegalovirus for nucleic acid amplification technology. Biologicals. 2016;44(4):242-51.

217. Hotchkiss EJ, Hodgson JC, Schmitt-van de Leemput E, Dagleish MP, Zadoks RN. Molecular epidemiology of *Pasteurella multocida* in dairy and beef calves. Vet Microbiol. 2011;151(3-4):329-35.

218. Campbell F, Strang C, Ferguson N, Cori A, Jombart T. When are pathogen genome sequences informative of transmission events? PLoS Pathog. 2018;14(2).

219. Angelos JA. Moraxella bovoculi and Infectious Bovine Keratoconjunctivitis: Cause or Coincidence? Vet Clin North Am Food Anim Pract. 2010;26(1):73.

220. Berner R, Schumacher RF, Brandis M, Forster J. Colonization and infection with Moraxella catarrhalis in childhood. European Journal of Clinical Microbiology & Infectious Diseases. 1996;15(6):506-9.

221. Broides A, Dagan R, Greenberg D, Givon-Lavi N, Leibovitz E. Acute Otitis Media Caused by Moraxella catarrhalis: Epidemiologic and Clinical Characteristics. Clin Infect Dis. 2009;49(11):1641-7.

222. Dassanayake RP, Shanthalingam S, Herndon CN, Subramaniam R, Lawrence PK, Bavananthasivam J, et al. Mycoplasma ovipneumoniae can predispose bighorn sheep to fatal Mannheimia haemolytica pneumonia. Vet Microbiol. 2010;145(3-4):354-9.

223. Fablet C, Marois-Crehan C, Simon G, Grasland B, Jestin A, Kobisch M, et al. Infectious agents associated with respiratory diseases in 125 farrow-to-finish pig herds: A cross-sectional study. Vet Microbiol. 2012;157(1-2):152-63.

224. Kock RA, Orynbayev M, Robinson S, Zuther S, Singh NJ, Beauvais W, et al. Saigas on the brink: Multidisciplinary analysis of the factors influencing mass mortality events. Sci Adv. 2018;4(1).

225. Lima SF, Teixeira AGV, Higgins CH, Lima FS, Bicalho RC. The upper respiratory tract microbiome and its potential role in bovine respiratory disease and otitis media. Sci Rep. 2016;6:12.

226. Brugger SD, Bomar L, Lemon KP. Commensal-pathogen interactions along the human nasal passages. PLoS Pathog. 2016;12(7).

227. Krismer B, Liebeke M, Janek D, Nega M, Rautenberg M, Hornig G, et al. Nutrient Limitation Governs Staphylococcus aureus Metabolism and Niche Adaptation in the Human Nose. PLoS Pathog. 2014;10(1).

228. Wald ER, DeMuri GP. The Group A Streptococcal Carrier State Reviewed: Still an Enigma. Journal of the Pediatric Infectious Diseases Society. 2014;3(4):336-42.

229. Wolter N, Tempia S, Cohen C, Madhi SA, Venter M, Moyes J, et al. High Nasopharyngeal Pneumococcal Density, Increased by Viral Coinfection, Is Associated With Invasive Pneumococcal Pneumonia. Journal of Infectious Diseases. 2014;210(10):1649-57.

230. Siegel SJ, Weiser JN. Mechanisms of Bacterial Colonization of the Respiratory Tract. Annual Review of Microbiology, Vol 69. 2015;69:425-44.

231. Murphy TF, Bakaletz LO, Smeesters PR. Microbial Interactions in the Respiratory Tract. J Pediatric Infect Dis Soc. 2009;28(10):S121-S6.

232. Caruana EJ, Roman M, Hernandez-Sanchez J, Solli P. Longitudinal studies. Journal of Thoracic Disease. 2015;7(11):E537-E40.

233. Radke BR. A demonstration of interval-censored survival analysis. Prev Vet Med. 2003;59(4):241-56.

234. Abdullahi O, Karani A, Tigoi CC, Mugo D, Kungu S, Wanjiru E, et al. Rates of acquisition and clearance of Pneumococcal serotypes in the nasopharynges of children in Kilifi district, Kenya. J Infect Dis. 2012;206(7):1020-9.

235. Sherman M, leCessie S. A comparison between bootstrap methods and generalized estimating equations for correlated outcomes in generalized linear models. Commun Stat Simul Comput. 1997;26(3):901-25.

236. Clark TG, Bradburn MJ, Love SB, Altman DG. Survival analysis part IV: Further concepts and methods in survival analysis. Br J Cancer. 2003;89(5):781-6.

237. Ampe B, Goethals K, Laevens H, Duchateau L. Investigating clustering in interval-censored udder quarter infection times in dairy cows using a gamma frailty model. Prev Vet Med. 2012;106(3-4):251-7.

238. Weber MF, Kogut J, de Bree J, van Schaik G, Nielen M. Age at which dairy cattle become Mycobacterium avium subsp. paratuberculosis faecal culture positive. Prev Vet Med. 2010;97(1):29-36.

239. Gibbens JC, Pascoe SJS, Evans SJ, Davies RH, Sayers AR. A trial of biosecurity as a means to control Campylobacter infection of broiler chickens. Prev Vet Med. 2001;48(2):85-99.

240. Anderson-Bergman C. icenReg: regression models for interval censored data in R. J Stat Softw. 2017;81(12):1-23.

241. McGuirk SM. Disease management of dairy calves and heifers. Vet Clin North Am Food Anim Pract. 2008;24(1):139-53.

242. Newcombe RG. Two-sided confidence intervals for the single proportion: Comparison of seven methods. Stat Med. 1998;17(8):857-72.
243. Newcombe RG. Interval estimation for the difference between independent proportions: Comparison of eleven methods. Stat Med. 1998;17(8):873-90.
244. Brown LD, Cai TT, DasGupta A, Agresti A, Coull BA, Casella G, et al. Interval estimation for a binomial proportion. Stat Sci. 2001;16(2):101-33.
245. Tueller SJ, Van Dorn RA, Bobashev GV. Visualization of categorical longitudinal and times series data. Methods Rep RTI Press. 2016;2016:MR-0033-1602.
246. Agency) AAPH. Veterinary Investigation Diagnosis Analysis (VIDA) report. Yearly trends 2009 to 2016: Cattle 2016 [Available from: https://www.gov.uk/government/publications/veterinary-investigation-diagnosis-analysis-vida-report-2016.
247. Uttenthal A, Larsen LE, Philipsen JS, Tjornehoj K, Viuff B, Nielsen KH, et al. Antibody dynamics in BRSV-infected Danish dairy herds as determined by isotype-specific immunoglobulins. Vet Microbiol. 2000;76(4):329-41.
248. Stott EJ, Thomas LH, Collins AP, Crouch S, Jebbett J, Smith GS, et al. A survey of virus-infections of the respiratory tract of cattle and their association with disease. J Hyg (Lond). 1980;85(2):257-70.
249. Graham DA, McShane J, Mawhinney KA, McLaren IE, Adair BM, Merza M. Evaluation of a single dilution ELISA system for detection of seroconversion to bovine viral diarrhea virus, bovine respiratory syncytial virus, parainfluenza-3 virus, and infectious bovine rhinotracheitis virus: comparison with testing by virus neutralization and hemagglutination inhibition. J Vet Diagn Invest. 1998;10(1):43-8.
250. Wang LM, McMahan CS, Hudgens MG, Qureshi ZP. A flexible, computationally efficient method for fitting the proportional hazards model to interval-censored data. Biometrics. 2016;72(1):222-31.
251. Kenkre VM, Kuperman MN. Applicability of the Fisher equation to bacterial population dynamics. Phys Rev E. 2003;67(5).
252. Mina MJ, McCullers JA, Klugman KP. Live attenuated influenza vaccine enhances colonization of *Streptococcus pneumoniae* and *Staphylococcus* aureus in mice. MBio. 2014;5(1).
253. Thors V, Christensen H, Morales-Aza B, Vipond I, Muir P, Finn A. The effects of live attenuated influenza vaccine on nasopharyngeal bacteria in healthy 2 to 4 year olds a randomized controlled trial. Am J Respir Crit Care Med. 2016;193(12):1401-9.

254. Cho I, Blaser MJ. Applications of next-generation sequencing.The human microbiome: at the interface of health and disease. Nature Reviews Genetics. 2012;13(4):260-70.

255. Cox LM, Yamanishi S, Sohn J, Alekseyenko AV, Leung JM, Cho I, et al. Altering the Intestinal Microbiota during a Critical Developmental Window Has Lasting Metabolic Consequences. Cell. 2014;158(4):705-21.

256. Pettigrew MM, Gent JF, Pyles RB, Miller AL, Nokso-Koivisto J, Chonmaitree T. Viral-Bacterial Interactions and Risk of Acute Otitis Media Complicating Upper Respiratory Tract Infection. J Clin Microbiol. 2011;49(11):3750-5.

257. Taschuk R, Griebel PJ. Commensal microbiome effects on mucosal immune system development in the ruminant gastrointestinal tract. Anim Health Res Rev. 2012;13(1):129-41.

258. Aagaard K, Ma J, Antony KM, Ganu R, Petrosino J, Versalovic J. The Placenta Harbors a Unique Microbiome. Science Translational Medicine. 2014;6(237).

259. Lauder AP, Roche AM, Sherrill-Mix S, Bailey A, Laughlin AL, Bittinger K, et al. Comparison of placenta samples with contamination controls does not provide evidence for a distinct placenta microbiota. Microbiome. 2016;4.

260. Yanez-Ruiz DR, Abecia L, Newbold CJ. Manipulating rumen microbiome and fermentation through interventions during early life: a review. Front Microbiol. 2015;6.

261. Chen YH, Oba M, Guan LL. Variation of bacterial communities and expression of Toll-like receptor genes in the rumen of steers differing in susceptibility to subacute ruminal acidosis. Vet Microbiol. 2012;159(3-4):451-9.

262. Lewis MC, Inman CF, Patel D, Schmidt B, Mulder I, Miller B, et al. Direct experimental evidence that early-life farm environment influences regulation of immune responses. Pediatric Allergy and Immunology. 2012;23(3):265-9.

263. Dowling A, Hodgson JC, Schock A, Donachie W, Eckersall PD, McKendrick IJ. Pathophysiological and immune cell responses in calves prior to and following lung challenge with formalin-killed Pasteurella multocida biotype A:3 and protection studies involving subsequent homologous live challenge.

264. Lima SF, Teixeira AGV, Higgins CH, Lima FS, Bicalho RC. The upper respiratory tract microbiome and its potential role in bovine respiratory disease and otitis media. Sci Rep. 2016;6.

265. Widders PR, Paisley LG, Gogolewski RP, Evermann JF, Smith JW, Corbeil LB. Experimental abortion and the systemic immune response to Haemophilus somnus in cattle. Infect Immun. 1986;54(2):555-60.
266. Corbeil LB, Gogolewski RP, Kacskovics I, Nielsen KH, Corbeil RR, Morrill JL, et al. Bovine IgG2a antibodies to Haemophilus somnus and allotype expression. Can J Comp Med. 1997;61(3):207-13.
267. Yeoman CJ, Ishaq SL, Bichi E, Olivo SK, Lowe J, Aldridge BM. Biogeographical Differences in the Influence of Maternal Microbial Sources on the Early Successional Development of the Bovine Neonatal Gastrointestinal tract. Sci Rep. 2018;8.
268. Lima SF, Bicalho MLD, Bicalho RC. The Bos taurus maternal microbiome: Role in determining the progeny early-life upper respiratory tract microbiome and health. PLoS One. 2019;14(3).
269. Neu J, Rushing J. Cesarean Versus Vaginal Delivery: Long-term Infant Outcomes and the Hygiene Hypothesis. Clinics in Perinatology. 2011;38(2):321.
270. Magnus MC, Haberg SE, Stigum H, Nafstad P, London SJ, Vangen S, et al. Delivery by Cesarean Section and Early Childhood Respiratory Symptoms and Disorders The Norwegian Mother and Child Cohort Study. American Journal of Epidemiology. 2011;174(11):1275-85.
271. Siegel SJ, Roche AM, Weiser JN. Influenza Promotes Pneumococcal Growth during Coinfection by Providing Host Sialylated Substrates as a Nutrient Source. Cell Host & Microbe. 2014;16(1):55-67.
272. McCullers JA, McAuley JL, Browall S, Iverson AR, Boyd KL, Normark BH. Influenza Enhances Susceptibility to Natural Acquisition of and Disease due to Streptococcus pneumoniae in Ferrets. Journal of Infectious Diseases. 2010;202(8):1287-95.
273. Larsen LE, Tjornehoj K, Viuff B. Extensive sequence divergence among bovine respiratory syncytial viruses isolated during recurrent outbreaks in closed herds. J Clin Microbiol. 2000;38(11):4222-7.
274. Ellis JA. Bovine Parainfluenza-3 Virus. Vet Clin North Am Food Anim Pract. 2010;26(3):575.
275. Woodbine KA, Medley GF, Moore SJ, Ramirez-Villaescusa AM, Mason S, Green LE. A four year longitudinal sero-epidemiological study of bovine herpesvirus

type-1 (BHV-1) in adult cattle in 107 unvaccinated herds in south west England. BMC Vet Res. 2009;5.

276. Sacco RE, McGill JL, Pillatzki AE, Palmer MV, Ackermann MR. Respiratory Syncytial Virus Infection in Cattle. Vet Pathol. 2014;51(2):427-36.

277. Gale C. Role of Parainfluenza-3 in Cattle. J Dairy Sci. 1970;53(5):621-5.

278. Vangeel I, Antonis AFG, Fluess M, Riegler L, Peters AR, Harmeyer SS. Efficacy of a modified live intranasal bovine respiratory syncytial virus vaccine in 3-week-old calves experimentally challenged with BRSV. Veterinary Journal. 2007;174(3):627-35.

279. Ellis JA, Philibert H, West K, Clark E, Martin K, Haines D. Fatal pneumonia in adult dairy cattle associated with active infection with bovine respiratory syncytial virus. Can J Vet Res. 1996;37(2):103-5.

280. Thors V, Christensen H, Morales-Aza B, Oliver E, Sikora P, Vipond I, et al. High-density Bacterial Nasal Carriage in Children Is Transient and Associated With Respiratory Viral Infections-Implications for Transmission Dynamics. 2019(1532-0987 (Electronic)).

281. Mitchell JA, Brownlie J. The challenges in developing effective canine infectious respiratory disease vaccines. Journal of Pharmacy and Pharmacology. 2015;67(3):372-81.

282. Karron RA. 55 - Respiratory syncytial virus and parainfluenza virus vaccines. In: Plotkin SA, Orenstein WA, Offit PA, editors. Vaccines (Sixth Edition). London: W.B. Saunders; 2013. p. 1146-53.

283. Vangeel I, Ioannou F, Riegler L, Salt JS, Harmeyer SS. Efficacy of an intranasal modified live bovine respiratory syncytial virus and temperature-sensitive parainfluenza type 3 virus vaccine in 3-week-old calves experimentally challenged with PI3V. Veterinary Journal. 2009;179(1):101-8.

284. NOAH. Rispoval RS+PI3 Intranasal Spec 2019 [Available from: http://www.noahcompendium.co.uk/?id=-458257.

285. Mdege ND, Man MS, Taylor CA, Torgerson DJ. Systematic review of stepped wedge cluster randomized trials shows that design is particularly used to evaluate interventions during routine implementation. J Clin Epidemiol. 2011;64(9):936-48.

286. Hemming K, Haines TP, Chilton PJ, Girling AJ, Lilford RJ. The stepped wedge cluster randomised trial: rationale, design, analysis, and reporting. Bmj-British Medical Journal. 2015;350.

287. Davey C, Hargreaves J, Thompson JA, Copas AJ, Beard E, Lewis JJ, et al. Analysis and reporting of stepped wedge randomised controlled trials: synthesis and critical appraisal of published studies, 2010 to 2014. Trials. 2015;16.

288. Copas AJ, Lewis JJ, Thompson JA, Davey C, Baio G, Hargreaves JR. Designing a stepped wedge trial: three main designs, carry-over effects and randomisation approaches. Trials. 2015;16.

289. Martin J, Taljaard M, Girling A, Hemming K. Systematic review finds major deficiencies in sample size methodology and reporting for stepped-wedge cluster randomised trials. Bmj Open. 2016;6(2).

290. Group TGHS. The Gambia hepatitis intervention study. Cancer Research. 1987;47(21):5782-7.

291. Leontjevas R, Gerritsen DL, Smalbrugge M, Teerenstra S, Vernooij-Dassen M, Koopmans R. A structural multidisciplinary approach to depression management in nursing-home residents: a multicentre, stepped-wedge cluster-randomised trial. Lancet. 2013;381(9885):2255-64.

292. Hemming K, Lilford R, Girling AJ. Stepped-wedge cluster randomised controlled trials: a generic framework including parallel and multiple-level designs. Stat Med. 2015;34(2):181-96.

293. Hussey MA, Hughes JP. Design and analysis of stepped wedge cluster randomized trials. Contemp Clin Trials. 2007;28(2):182-91.

294. Brown C, Lilford R. The stepped wedge trial design: a systematic review. BMC Med Res Methodol. 2006;6(54).

295. Twisk JWR. Applied Longitudinal Data Analysis for Epidemiology: A Practical Guide. 2 ed. Cambridge: Cambridge University Press; 2013.

296. McDermott JJ, Schukken YH. A review of methods used to adjust for cluster effects in explantory epidemiological studies of animal populations Prev Vet Med. 1994;18(3):155-73.

297. Hemming K, Girling A. A menu-driven facility for power and detectable-difference calculations in stepped-wedge cluster-randomized trials. Stata J. 2014;14(2):363-80.

298. Baio G, Copas A, Ambler G, Hargreaves J, Beard E, Omar RZ. Sample size calculation for a stepped wedge trial. Trials. 2015;16.

299. Hemming K. Power and Sample size for Cluster Randomised Trials 2018 [Sample size calculation with R shiny app]. Available from: https://clusterrcts.shinyapps.io/rshinyapp/.

300. Mead A., Thomas A C., Evans J., Griffiths B., Eisler MC., editors. An application of covariate-based constrained randomisation in livestock research. 29th International Biometric Conference; 2018; Spain, Barcelona.

301. Thomas A C. FAHR, Eisler M C. Unblinding protocol and data from a blinded randomised controlled trial investigating carriage of bovine respiratory pathogens. Bristol Data Repository; 2018.

302. Stryhn H CJ. Confidence intervals by the profile likelihood methods, with applications in veterinary epidemiology. Proceedings of 10th Symposium of the International Society for Veterinary Epidemiology and Economics; 17/11/03; Vina Del Mar2003.

303. Hooper R, Teerenstra S, de Hoop E, Eldridge S. Sample size calculation for stepped wedge and other longitudinal cluster randomised trials. Stat Med. 2016;35(26):4718-28.

304. Morpeth SC, Munywoki P, Hammitt LL, Bett A, Bottomley C, Onyango CO, et al. Impact of viral upper respiratory tract infection on the concentration of nasopharyngeal pneumococcal carriage among Kenyan children. Sci Rep. 2018;8.

305. Pulendran B. Learning immunology from the yellow fever vaccine: innate immunity to systems vaccinology. Nature Reviews Immunology. 2009;9(10):741-7.

306. Bystrom J, Al-Adhoubi N, Al-Bogami M, Jawad AS, Mageed RA. Th17 Lymphocytes in Respiratory Syncytial Virus Infection. Viruses-Basel. 2013;5(3):777-91.

307. Hoorens PR, Rinaldi M, Li RW, Goddeeris B, Claerebout E, Vercruysse J, et al. Genome wide analysis of the bovine mucin genes and their gastrointestinal transcription profile. BMC Genomics. 2011;12.

308. Linden SK, Sutton P, Karlsson NG, Korolik V, McGuckin MA. Mucins in the mucosal barrier to infection. Mucosal Immunology. 2008;1(3):183-97.

309. Mantis NJ, Forbes SJ. Secretory IgA: Arresting Microbial Pathogens at Epithelial Borders. Immunological Investigations. 2010;39(4-5):383-406.

310. Frank GH, Nelson SL, Briggs RE. Infection of the middle nasal meatus of calves with Pasteurella haemolytica serotype-1. Am J Vet Res. 1989;50(8):1297-301.

311. Hemming K, Taljaard M, Forbes A. Analysis of cluster randomised stepped wedge trials with repeated cross-sectional samples. Trials. 2017;18.
312. Barker D, McElduff P, D'Este C, Campbell MJ. Stepped wedge cluster randomised trials: a review of the statistical methodology used and available. BMC Med Res Methodol. 2016;16.
313. Chamorro MF, Walz PH, Haines DM, Passler T, Earleywine T, Palomares RA, et al. Comparison of levels and duration of detection of antibodies to bovine viral diarrhea virus 1, bovine viral diarrhea virus 2, bovine respiratory syncytial virus, bovine herpesvirus 1, and bovine parainfluenza virus 3 in calves fed maternal colostrum or a colostrum-replacement product. Can J Comp Med. 2014;78(2):81-8.
314. Haines TP, Hemming K. Stepped-wedge cluster-randomised trials: level of evidence, feasibility and reporting. Journal of Physiotherapy. 2018;64(1):63-6.
315. Sanders R, Huggett JF, Bushell CA, Cowen S, Scott DJ, Foy CA. Evaluation of Digital PCR for Absolute DNA Quantification. Analytical Chemistry. 2011;83(17):6474-84.
316. Pavsic J, Zel J, Milavec M. Assessment of the real-time PCR and different digital PCR platforms for DNA quantification. Anal Bioanal Chem. 2016;408(1):107-21.
317. Huggett JF. OGJ, Bustin S. qPCR, dPCR, NGS - A journey. Biomol Detect Quantif. 2015:A1 - A5.
318. Catry B, Boyen F, Baele M, Dewulf J, de Kruif A, Vaneechoutte M, et al. Recovery of Moraxella ovis from the bovine respiratory tract and differentiation of Moraxella species by tDNA-intergenic spacer PCR. Vet Microbiol. 2007;120(3-4):375-80.
319. Ellis AM, Garcia AJ, Focks DA, Morrison AC, Scott TW. Parameterization and Sensitivity Analysis of a Complex Simulation Model for Mosquito Population Dynamics, Dengue Transmission, and Their Control. American Journal of Tropical Medicine and Hygiene. 2011;85(2):257-64.
320. Horner C, Wilcox M, Barr B, Hall D, Hodgson G, Parnell P, et al. The longitudinal prevalence of MRSA in care home residents and the effectiveness of improving infection prevention knowledge and practice on colonisation using a stepped wedge study design. Bmj Open. 2012;2(1).
321. Mhurchu CN, Gorton D, Turley M, Jiang YN, Michie J, Maddison R, et al. Effects of a free school breakfast programme on children's attendance, academic

achievement and short-term hunger: results from a stepped-wedge, cluster randomised controlled trial. Journal of Epidemiology and Community Health. 2013;67(3):257-64.

322. Fuller C, Michie S, Savage J, McAteer J, Besser S, Charlett A, et al. The Feedback Intervention Trial (FIT)-Improving Hand-Hygiene Compliance in UK Healthcare Workers: A Stepped Wedge Cluster Randomised Controlled Trial. PLoS One. 2012;7(10).

323. Stabiliser-Cattle-Company. Driving beef profitability through innovation 2019 [Available from: http://www.bigbeef.co.uk.

324. Shanthalingam S, Tibary A, Beever JE, Kasinathan P, Brown WC, Srikumaran S. Precise gene editing paves the way for derivation of Mannheimia haemolytica leukotoxin-resistant cattle. Proceedings of the National Academy of Sciences. 2016;113(46):13186.

325. Hooper LV, Littman DR, Macpherson AJ. Interactions Between the Microbiota and the Immune System. Science. 2012;336(6086):1268-73.

326. Saadati M, Gibbs HA, Parton R, Coote JG. Characterisation of the leukotoxin produced by different strains of Pasteurella haemolytica. J Med Microbiol. 1997;46(4):276-84.

327. Larsen J, Pedersen AG, Davies RL, Kuhnert P, Frey J, Christensen H, et al. Evolution of the leukotoxin promoter in genus Mannheimia. Bmc Evolutionary Biology. 2009;9.

328. Price LB, Hungate BA, Koch BJ, Davis GS, Liu CM. Colonizing opportunistic pathogens (COPs): The beasts in all of us. PLoS Pathog. 2017;13(8).

329. Vayssier-Taussat M, Albina E, Citti C, Cosson JF, Jacques MA, Lebrun MH, et al. Shifting the paradigm from pathogens to pathobiome: new concepts in the light of meta-omics. Frontiers in Cellular and Infection Microbiology. 2014;4.

330. Holman DB, Hallewell J, Alexander TW. The nasopharyngeal microbiota of beef cattle before and after transport to a feedlot. J Anim Sci. 2017;95:29-.

331. Brito IL, Gurry T, Zhao S, Huang K, Young SK, Shea TP, et al. Transmission of human-associated microbiota along family and social networks. Nature Microbiology. 2019;4(6):964-71.

332. Quinn P J, Markley F C, Leonard E S, FitzPatrick E S, Fanning S, J HP. *Histophilus somni, Haemophilus parasuis* and *Avibacterium paragallinarum*. Second ed: Blackwell Publishing Ltd. ; 2011.

333. Hunt Gerardo S, Citron DM, Claros MC, Fernandez HT, Goldstein EJ. Pasteurella multocida subsp. multocida and P. multocida subsp. septica differentiation by PCR fingerprinting and alpha-glucosidase activity. J Clin Microbiol. 2001;39(7):2558-64.

Appendices

Appendix A

Management of farmlet swards

Inorganic fertiliser is applied annually to the Green farmlet permanent pasture system, no field has been reseeded for at least 20 years [167]. Blue farmlet pastures are supplemented with low levels of inorganic fertiliser, fertiliser is replaced predominately by nitrogen fixation capacity of clover, emulating the driving principles of organic farming. Farmlet fields were progressively reseeded in 2013 – 2015, achieving sufficient productivity levels for future self-sufficiency. Initial sowings were 25kg AberMagic (high sugar perennial ryegrass, *Lolium perenne*) per ha plus 3.5kg AberHerald (white clover, *Trifolium repens*) per ha. The Red farmlet undergoes regular planned periodic reseeding with innovative varieties of grasses. From June onwards, grass is cut and harvested for silage. A lactobacillus additive is included to improve fermentation in the silage clamps.

Bull details

Table A.1: History and details of bulls at the North Wyke Farm Platform 2015–2017

Official Tag	Date of Birth	Breed	Additional Information
UK 142911 303178	09/04/15	ST	Serving cows/heifers for 2017 spring calving
UK 380678 601707	24/03/15	ST	Serving cows/heifers for 2017 spring calving
UK 303596 501955	28/04/12	ST	Serving cows/heifers for 2017 spring calving
UK 701354 700138	21/08/08	CH	Serving cows/heifers for 2017 spring calving
UK 141011 400520	29/11/07	CH	Serving cows/heifers for Spring 2015 & 2016 calving.
UK 362915 500228	04/04/10	HE	Serving cows/heifers for Spring 2015 calving.
UK 365879 100867	Unknown	LIM	Sired cows/heifers that have been bought in (naturally or AI). Calves born 2016.
UK 104665 600203	Unknown	CH	Sired cows/heifers that have been bought in (naturally or AI). Calves born 2016.
UK 123916 112296	Unknown	ST	Sired cows/heifers that have been bought in (naturally or AI). Calves born 2016.

Media recipes: 1% agarose gel

For 150 ml of agarose, 1.5 g of agarose powder is dissolved (Sigma Aldrich) in 150 ml of Tris-acetate-EDTA (TAE buffer used at 1x (Fluka Analytical Science). Microwave on full power for 3 minutes. Cool under running water. Add 7.5 µl ethidium bromide solution, swirl and pour into a prepared gel electrophoreses cartridge.

Appendix B

Bacteriological characteristics of *Pasteurellaceae*

Table B.1: Characteristics of *Histophilus somni*, *Mannheimia haemolytica* and *Pasteurella multocida*

Characteristic	*P. multocida*	*M. haemolytica*	*H. somni*
Colony morphology	Regular, smooth, 0.5–2mm, grey, no ß-haemolysis	Regular, smooth, 1–2mm, greyish, ß-haemolysis	Raised, circular, smooth, yellow-ish, 0.2–0.6mm
Gram stain	Gram-negative cocco-bacilli, short chains, singularly or in pairs	Gram-negative small bacilli and cocco-bacilli	Gram-negative, small, pleomorphic, sometimes filaments
Haemolysis	-	+	v
Catalase	+	+	-
Oxidase	+	+	+
Urease	v	-	-
Indole	+	-	+
X factor	-	-	-
V factor	v	-	-
D- Galactose	+	+	-
D- Glucose	+	+	+
Acid from D-Mannose	+	-	
Acid from lactose	-	+	-
Acid from mannitol	+		+
Acid from sucrose			-
Acid from trehalose	v	-	

V: variable

Data compiled from several sources [72] [332] [206] [333] [207]

In silico alignment of candidate primers to target bacterial species

Candidate primers for *H. somni*, *M. haemolytica* and *P. multocida* were aligned against available sequences in the Genbank library. For *H. somni* and *M. haemolytica* amplicon homology to available reference genome sequences was 100%. For *P. multocida* amplicon homology ranged to available genome sequences was between 97–100%. Data are available at the University of Bristol data repository, data.bris, at https://doi.org/10.5523/bris.nyqkgnysra9q2ic5dok0swnbg.

Sequencing bacterial strains

Table B.2: 16S rRNA gene sequence data from short bovine nasal swabs collected from healthy cattle on the North Wyke Farm Platform in January 2016 and cultured for the presence of *Pasteurellaceae*: identity given from BLAST identification of sequences, bacteriological biochemistry (API test strips) and final identification.

Isolate no.	BLAST identification output	Identity (% homology)	API 20NE	API NH	Final ID
V1-71-1 (11)	*Mannheimia haemolytica* strain NIVEDI/MHS-4 16S ribosomal RNA gene, partial sequence	99	*Mannheimia haemolytica*	*Haemophilus paragallinarum*	*Mannheimia haemolytica*
V1-53-2	*Mannheimia haemolytica* NIVEDI/MHS-4 16S ribosomal RNA gene, partial sequence	98	*Mannheimia haemolytica*		*Mannheimia haemolytica*
V1-71-1 (19)	*Mannheimia haemolytica* NIVEDI/MHS-4 16S ribosomal RNA gene, partial sequence	99	*Mannheimia haemolytica*		*Mannheimia haemolytica*
V1-37-1	*Mannheimia haemolytica* strain NIVEDI/MHS-4 16S ribosomal RNA gene, partial sequence	99	*Mannheimia haemolytica*		*Mannheimia haemolytica*
V1-26-1	*Moraxella bovoculi* strain 57922, complete genome	99	*Moraxella spp.* (82.3%), *Pasteurella* (4%)		*Moraxella bovoculi*
V1-65-1	*M. haemolytica* strain NIVEDI/MHS-4 16S ribosomal RNA gene, partial sequence	99	*Mannheimia haemolytica*		*Mannheimia haemolytica*
V1-27-1	*Arcobacter skirrowii* strain VPH/V129/2014 16S ribosomal RNA gene, partial sequence	99	Unidentified by culture, API not performed		*Arcobacter spp.*
V1-38-5	*Pasteurella multocida* subsp. *multocida* PMTB2.1, complete genome	99	*Pasteurella multocida*		*Pasteurella multocida*
V1-52-2	*Pasteurella multocida* subsp. *multocida* PMTB2.1, complete genome	99	*Pasteurella multocida*		*Pasteurella multocida*
V1-41-1	*Pasteurella multocida* subsp. *multocida* PMTB2.1, complete genome	99	*Pasteurella multocida*		*Pasteurella multocida*

Table B.2 continued

Isolate no.	BLAST identification output	Identity (% homology)	API 20NE	API NH	Final ID
V1-66-2	*Rhodococcus equi* strain FY1 16S ribosomal RNA gene, partial sequence	100	*Pasteurella* spp. (66.65)		*Rhodococcus* sp.
V1-25-1	*Jeotgalicoccus huakuii* strain Nc5RA-2 16S ribosomal RNA gene, partial sequence	98	*Morexella* spp. (82.3%), *Pasteurella* spp. (4%)		*Jeotgalicoccus* sp.
V1-72-1 (11)	*Mannheimia ruminalis* strain HPA98; CCUG38466 16S ribosomal RNA gene, partial sequence	99		*Haemophilus paragallinarum*	*Mannheimia* sp.
	Mannheimia ruminalis strain HPA98; CCUG38466 16S ribosomal RNA gene, partial sequence	99			
V1-72-1 (23)	*Mannheimia* sp. MCCM 00145 16S ribosomal RNA gene, partial sequence	100	*Pasteurella multocida*	*Haemophilus paragallinarum*	Inconclusive
	Mannheimia ruminalis strain HPA98; CCUG38466 16S ribosomal RNA gene, partial sequence	98		*Haemophilus paragallinarum*	Inconclusive
V1-85-2	*Mannheimia* sp. MCCM 00145 16S ribosomal RNA gene, partial sequence	98		*Haemophilus paragallinarum*	Inconclusive
	Haemophilus parasuis strain SC1401, complete genom	99			
V1-67-1	*Achromobacter xylosoxidans* strain S3A 16S ribosomal RNA gene, partial sequence	100	*Achrobacter dentrificens* (78.3%), *Bordetella bronchohioseptica* (18.3%)		*Achromobacter* sp.
	Achromobacter denitrificans strain 1104 16S ribosomal RNA gene, partial sequence	100			
V1-27-2	*Mannheimia* sp. MCCM 00145 16S ribosomal RNA gene, partial sequence	100	*Pasteurella* spp. (47.9%), *Morexella* spp. (25.6%), *M. haem*/*B. trehalosi* (12.1%)		*Mannheimia* sp.
	Mannheimia ruminalis strain HPA98; CCUG38466 16S ribosomal RNA gene, partial sequence	99			

Table B.3: Variable region 16S rRNA gene sequence data from strains supplied by APHA for use in specificity panel testing. Sequences amplified using primer pair 337F & 907R

APHA Strain ID	Sequence*	Length (bp)	BLAST identity	Identity (%)
Mannheimia glucosida APHA IS14-07997	TGATGCAGCCATGCCGCGTGAATGAAGAAGGCCTTCGGGTTGTAAAGTTCTTTCGGTGACGAGGAAGGCGATTGTT TTAATAGAACAGTCGATTGACGTTAATCACAGAAGAAGCACCGGCTAACTCCGTGCCAGCAGCCGCGGTAATACG GGGGGTGCGAGCGTTAATCGGAATAACTGGGCGTAAAGGGCACGCAGGCGGTTGTTTAAGTGAGGTGTGAAAGCC CCGGGCTTAACCTGGGAATTGCATTTCAGACTGAACAACTAGAGTACTTTAGGGAGGGGTAGAATTCCACGTGTAG CGGTGAAATGCGTAGAGATGTGGAGGAATACCGAAGGCGAAGGCAGCCCCTTGGAAATGTACTGACGCTCATGTG CGAAAGCGTGGGGAGCAAACAGGATTAGATACCCTGGTAGTCCACGCCGTAAACGCTGTCGATTTGGGGATTGGG GTTTAACTCTGGTGCCCGTAGCTAACGTGATAAATCGACCGCCTGGGGAGTACGGCCGCAAGGTTAAAACTCAAA	527	*Mannheimia haemolytica*	100
Mannheimia granulomatis APHA IS14-1386	GATGCAGCCATGCCGCGTGAATGAAGAAGGCCTTCGGGTTGTAAAGTTCTTTCGGTGACGAGGAAGGCGATTGTTT TAATAGAACAGTCGATTGACGTTAATCACAGAAGAAGCACCGGCTAACTCCGTGCCAGCAGCCGCGGTAATACGG GGGGTGCGAGCGTTAATCGGAATAACTGGGCGTAAAGGGCACGCAGGCGGTTGTTTAAGTGAGGTGTGAAAGCCC CGGGCTTAACCTGGGAATTGCATTTCAGACTGGACAACTAGAGTACTTTAGGGAGGGGTAGAATTCCACGTGTAGC GGTGAAATGCGTAGAGATGTGGAGGAATACCGAAGGCGAAGGCAGCCCCTTGGGAATGTACTGACGCTCATGTGC GAAAGCGTGGGGAGCAAACAGGATTAGATACCCTGGTAGTCCACGCCGTAAACGCTGTCGATTTGGGGATTGGGG TTTAACTCTGGTGCCCGTAGCTAACGTGATAAATCGACCGCCTGGGGAGTACGGCCGCAAGGTTAAAACTCAAG	526	*Mannheimia haemolytica*	100
Mannheimia varigena APHA IS12-04533	TGATGCAGCCATGCCGCGTGAATGAAGAAGGCCTTCGGGTTGTAAAGTTCTTTCGGTAGCGAGGAAGGCAGACTTG TTAATAGCAAGTTTGATTGACGTTAACTACAGAAGAAGCACCGGCTAACTCCGTGCCAGCAGCCGCGGTAATACGG GGGGTGCAAGCGTTAATCGGAATAACTGGGCGTAAAGGGCACGCAGGCGGACTTTTAAGTGAGATGTGAAAGCCC CGGGCTTAACCTGGGAATTGCATTTCAGACTGGGAGTCTAGAGTACTTTAGGGAGGGGTAGAATTCCACGTGTAGC GGTGAAATGCGTAGAGATGTGGAGGAATACCGAAGGCGAAGGCAGCCCCTTGGGAATGTACTGACGCTCATGTGC GAAAGCGTGGGGAGCAAACAGGATTAGATACCCTGGTAGTCCACGCCGTAAACGCTGTCGATTTGGGGATTGGGC TTTAAGCTTGGTGCCCGTAGCTAACGTGATAAATCGACCGCCTGGGGAGTACGGCCGCAAGGTTAAAACTCAAA	527	*Mannheimia varigena*	100
Mannheimia ruminalis APHA IS23-01503	GATGCAGCCATGCCGCGTGAATGAAGAAGGCCTTCGGGTTGTAAAGTTCTTTCGGTGACGAGGAAGGCGATTGTTT TAATAGAACAGTCGATTGACGTTAATCACAGAAGAAGCACCGGCTAACTCCGTGCCAGCAGCCGCGGTAATACGG GGGGTGCGAGCGTTAATCGGAATAACTGGGCGTAAAGGGCACGCAGGCGGTTGTTTAAGTGAGGTGTGAAAGCCC CGGGCTTAACCTGGGAATTGCATTTCAGACTGAACAACTAGAGTACTTTAGGGAGGGGTAGAATTCCACGTGTAGC GGTGAAATGCGTAGAGATGTGGAGGAATACCGAAGGCGAAGGCAGCCCCTTGGAAATGTACTGACGCTCATGTGC GAAAGCGTGGGGAGCAAACAGGATTAGATACCCTGGTAGTCCACGCCGTAAACGCTGTCGATTTGGGGATTGGGG TTTAACTCTGGTGCCCGTAGCTAACGTGATAAATCGACCGCCTGGGGAGTACGGCCGCAAGGTTAAAACTCAAAGA	528	*Mannheimia haemolytica*	100

Table B.3 continued

APHA Strain ID	Sequence*	Length (bp)	BLAST identity	Identity (%)
Bibersteinia trehalosi APHA IS21-03264	TGATGCAGCCATGCCGCGTGAATGAAGAAGGCCTTCGGGTTGTAAAGTTCTTTCGGTGATGAGGAAGGCGGTTGTT TTAATAGAACAATCGATTGACGTTAGTCACAGAAGAAGCACCGGCTAACTCCGTGCCAGCAGCCGCGGTAATACG GAGGGTGCGAGCGTTAATCGGAATAACTGGGCGTAAAGGGCACGCAGGCGGATTGTTAAGTGGGATGTGAAAGCC CCGGGCTTAACCTGGGAATTGCATTTCAGACTGGCAATCTAGAGTATTTTAGGGAGGGGTAGAATTCCACGTGTAG CGGTGAAATGCGTAGAGATGTGGAGGAATACCGAAGGCGAAGGCAGCCCCTTGGGAATATACTGACGCTCATGTG CGAAAGCGTGGGGAGCAAACAGGATTAGATACCCTGGTAGTCCACGCTGTAAACGATGTTGATTTGGGGATTGGG CTTTAAGCTTGGTGCCCGTAGCTAACGTGATAAATCAACCGCCTGGGGAGTACGGCCGCAAGGTTAAAACTCAAA	527	*Biberstenia trehalosi*	99
Actinobacillus suis APHA IS14-13758	GATGCAGCCATGCCGCGTGAATGAAGAAGGCCTTCGGGTTGTAAAGTTCTTTCGGTAGCGAGGAAGGTGGTTGATT TTAATAGATTTGTCAATTGACGTTAACTACAGAAGAAGCACCGGCTAACTCCGTGCCAGCAGCCGCGGTAATACGG AGGGTGCGAGCGTTAATCGGAATAACTGGGCGTAAAGGGCACGCAGGCGGTTGATTAAGTGAGATGTGAAAGCCC CGGGCTTAACCTGGGAATTGCATTTCATACTGGTCAACTAGAGTACTTTAGGGAGGGGTAGAATTCCACGTGTAGC GGTGAAATGCGTAGAGATGTGGAGGAATACCGAAGGCGAAGGCAGCCCCTTGGGAATGTACTGACGCTCATGTGC GAAAGCGTGGGGAGCAAACAGGATTAGATACCCTGGTAGTCCACGCTGTAAACGCTGTCGATTTGGGGATTGGAC TTTAAGTCTGGTGCCCGAAGCTAACGTGATAAATCGACCGCCTGGGGAGTACGGCCGCAAGGTTAAAACTCAAAG	528	*Actinobacillus equuli subsp. equuli*	99
Salmonella dublin APHA R07571	CCTGATGCAGCCATGCCGCGTGTATGAAGAAGGCCTTCGGGTTGTAAAGTACTTTCAGCGGGGAGGAAGGGAGTA AAGTTAATACCTTTGCTCATTGACGTTACCCGCAGAAGAAGCACCGGCTAACTCCGTGCCAGCAGCCGCGGTAATA CGGAGGGTGCAAGCGTTAATCGGAATTACTGGGCGTAAAGCGCACGCAGGCGGTTTGTTAAGTCAGATGTGAAAT CCCCGGGCTCAACCTGGGAACTGCATCTGATACTGGCAAGCTTGAGTCTCGTAGAGGGGGGTAGAATTCCAGGTGT AGCGGTGAAATGCGTAGAGATCTGGAGGAATACCGGTGGCGAAGGCGGCCCCCTGGACGAAGACTGACGCTCAGG TGCGAAAGCGTGGGGAGCAAACAGGATTAGATACCCTGGTAGTCCACGCCGTAAACGATGTCGACTTGGAGGTTG TGCCCTTGAGGCGTGGCTTCCGGAGCTAACGCGTTAAGTCGACCGCCTGGGGAGTACGGCCGCAAGGTTAAAACTC	528	*Escherichia coli*	100
Fusobacterium necrophorum necrophorum APHA C977	GATCCAGCAATTCTGTGTGCACGATGACGTTTTTCGGAATGTAAAGTGCTTTCAGTCGGGAAGAAGTCAGTGACGG TACCGACAGAAGAAGCGACGGCTAAATACGTGCCAGCAGCCGCGGTAATACGTATGTCGCAAGCGTTATCCGGAT TTATTGGGCGTAAAGCGCGTCTAGGCGGCAAGGAAAGTCTGATGTGAAAATGCGGAGCTCAACTCCGTATGGCGTT GGAAACTGCCTTACTAGAGTACTGGAGAGGTAGGCGGAACTACAAGTGTAGAGGTGAAATTCGTAGATATTTGTA GGAATGCCGATGGGGAAGCCAGCCTACTGGACAGATACTGACGCTAAAGCGCGAAAGCGTGGGTAGCAAACAGG ATTAGATACCCTGGTAGTCCACGCTGTAAACGATGATTACTAGGTGTTGGGGGTCAAACCTCAGCGCCCAAGCTAA CGCGATAAGTAATCCGCCTGGGGAGTACGTACGCAAGTATGAAACTCAAAG	503	*Fusobacterium necrophorum necrophorum*	100

Table B.3 continued

APHA Strain ID	Sequence*	Length (bp)	BLAST identity	Identity (%)
Streptococcus suis APHA 25	ACCTGACCGAGCACGCCGCGTGAGTGAAGAAGGTTTTCGGATCGTAAAGCTCTGTTGTAAGAGAAGAACGTGTGA GAGAGTGGAAAGTTCTCACAGTGACGGTATCTTACCAGAAAGGGACGGCTAACTACGTGCCAGCAGCCGCGGTAA TACGTAGGTCCCGAGCGTTGTCCGGATTTATTGGGCGTAAAGCGAGCGCAGGCGGTTTCGTAAGTCTGAAGTAAAA GGCTGTGGCTTAACCATAGTACGCTTTGGAAACTGCGGAACTTGAGTGCAGAAGGGGAGAGTGGAATTCCATGTGT AGCGGTGAAATGCGTAGATATATGGAGGAACACCGGTGGCGAAAGCGGCTCTCTGGTCTGTAACTGACGCTGAGG CTCGAAAGCGTGGGTAGCGAACAGGATTAGATACCCTGGTAGTCCACGCCGTAAACGATGAGTGCTAGGTGTTGG GTCCTTTCCGGGACTCAGTGCCGCAGCTAACGCATTAAGCACTCCGCCTGGGGAGTACGGCCGCAAGGCTGAAACT CAAAGG	534	*Streptococcus suis*	99
Mannheimia glucosida APHA IS14-07997	GTTTTCGGATCGTAAAGCTCTGTTATAAGCGAAGAACGGGAGTAAGAGTGGAAAGTTTACTCTGTGACGGTAGCTT ATCAGAAAGGGACGGCTAACTACGTGCCAGCAGCCGCGGTAATACGTAGGTCCCGAGCGTTGTCCGGATTTATTGG GCGTAAAGCGAGCGCAGGTGGTTTAATAAGTCTGAAGTTAAAGGCATTGGCTCAACCAATGTACGCTTTGGAAACT GTTAAACTTGAGTGCAGAAGGGGAGAGTGGAATTCCATGTGTAGCGGTGAAATGCGTAGATATATGGAGGAACAC CGGTGGCGAAAGCGGCTCTCTGGTCTGTAACTGACACTGAGGCTCGAAAGCGTGGGTAGCGAACAGGATTAGATA CCCTGGTAGTCCACGCCGTAAACGATGAGTGCTAGGTGTTGGGTCCTTTCCGGGACTCAGTGCCGCAGCTAACGCA TTAAGCACTCCGCCTGGGGAGTACGACCGCAAGGTTGAAACTCAAAGG	502	*Streptococcus pluranimalium*	100

* Sequences shown are cleaned of primers and anomalies identified according to visualisation of chromatograms

Table B.4: Variable region 16S rRNA gene sequence data from strains supplied by APHA for use in specificity panel testing. Sequences amplified using primer pair 785F & 1100R

APHA Strain ID	Sequence*	Length (bp)	BLAST identity	Identity (%)
Mannheimia glucosida APHA IS14-07997	TTTGGGGATTGGGGTTTAACTCTGGTGCCCGTAGCTAACGTGATAAATCGACCGCCTGGGGAGTACGGC CGCAAGGTTAAAACTCAAATGAATTGACGGGGGCCCGCACAAGCGGTGGAGCATGTGGTTTAATTCGA TGCAACGCGAAGAACCTTACCTACTCTTGACATCCATGGAATCTTGTAGAGATATGAGAGTGCCTTCGG GAACCATGAGACAGGTGCTGCATGGCTGTCGTCAGCTCGTGTTGTGAAATGTTGGGTTAAGTCCCGCAA CGAGCGCAACCCC	288	*Mannheimia haemolytica*	99
Mannheimia granulomatis APHA IS14-1386	GGGGTTTAACTCTGGTGCCCGTAGCTAACGTGATAAATCGACCGCCTGGGGAGTACGGCCGCAAGGTT AAAACTCAAATGAATTGACGGGGGCCCGCACAAGCGGTGGAGCATGTGGTTTAATTCGATGCAACGCG AAGAACCTTACCTACTCTTGACATCCATGGAATCTTGTAGAGATATGAGAGTGCCTTCGGGAACCATGA GACAGGTGCTGCATGGCTGTCGTCAGCTCGTGTTGTGAAATGTTGGGTTAAGTCCCGCAACGAGCGCA ACCC	277	*Mannheimia haemolytica*	100
Mannheimia varigena APHA IS12-04533	GGGGATTGGGCTTTAAGCTTGGTGCCCGTAGCTAACGTGATAAATCGACCGCCTGGGGAGTACGGCCG CAAGGTTAAAACTCAAATGAATTGACGGGGGCCCGCACAAGCGGTGGAGCATGTGGTTTAATTCGATG CAACGCGAAGAACCTTACCTACTCTTGACATCCAGAGAATCTTGTAGAGATACGAGAGTGCCTTCGGG AACTCTGAGACAGGTGCTGCATGGCTGTCGTCAGCTCGTGTTGTGAAATGTTGGGTTAAGTCCCGCAAC GAGCGCAACCC	284	*Mannheimia varigena*	100
Mannheimia ruminalis APHA IS23-01503	GGGGTTTAACTCTGGTGCCCGTAGCTAACGTGATAAATCGACCGCCTGGGGAGTACGGCCGCAAGGTT AAAACTCAAATGAATTGACGGGGGCCCGCACAAGCGGTGGAGCATGTGGTTTAATTCGATGCAACGCG AAGAACCTTACCTACTCTTGACATCCATGGAATCTTGTAGAGATATGAGAGTGCCTTCGGGAACCATGA GACAGGTGCTGCATGGCTGTCGTCAGCTCGTGTTGTGAAATGTTGGGTTAAGTCCCGCAACGAGCGCA ACCC	277	*Mannheimia haemolytica*	100
Bibersteinia trehalosi APHA IS21-03264	GGGCTTTAAGCTTGGTGCCCGTAGCTAACGTGATAAATCAACCGCCTGGGGAGTACGGCCGCAAGGTT AAAACTCAAATGAATTGACGGGGGCCCGCACAAGCGGTGGAGCATGTGGTTTAATTCGATGCAACGCG AAGAACCTTACCTACTCTTGACATCCATGGAATCTTGTAGAGATACGAGAGTGCCTTCGGGAACCATGA GACAGGTGCTGCATGGCTGTCGTCAGCTCGTGTTGTGAAATGTTGGGTTAAGTCCCGCAACGAGCGC	272	*Bibersteinia trehalosi*	100
Actinobacillus suis APHA IS14-13758	TTTAAGTCTGGTGCCCGAAGCTAACGTGATAAATCGACCGCCTGGGGAGTACGGCCGCAAGGTTAAAA CTCAAATGAATTGACGGGGGCCCGCACAAGCGGTGGAGCATGTGGTTTAATTCGATGCAACGCGAAGA ACCTTACCTACTCTTGACATCCATGGAATCTTGTAGAGATACGAGAGTGCCTTCGGGAACCATGAGACA GGTGCTGCATGGCTGTCGTCAGCTCGTGTTGTGAAATGTTGGGTTAAGTCCCGCAACGAGCGCAA	270	*Actinobacillus suis*	100

Table B.4 continued

APHA Strain ID	Sequence*	Length (bp)	BLAST identity	Identity (%)
Salmonella dublin APHA R07571	GCCCTTGAGGCGTGGCTTCCGGAGCTAACGCGTTAAGTCGACCGCCTGGGGAGTACGGCCGCAAGGTTAAAACTCAAATGAATTGACGGGGGCCCGCACAAGCGGTGGAGCATGTGGTTTAATTCGATGCAACGCGAAGAACCTTACCTGGTCTTGACATCCACAGAACTTTCCAGAGATGGATTGGTGCCTTCGGGAACTGTGAGACAGGTGCTGCATGGCTGTCGTCAGCTCGTGTTGTGAAATGTTGGGTTAAGTCCCGCAACGAGCGCAACCC	277	*Escherichia coli*	100
Fusobacterium necrophorum necrophorum APHA C977	GTTGGGGGTCAAACCTCAGCGCCCAAGCTAACGCGATAAGTAATCCGCCTGGGGAGTACGTACGCAAGTATGAAACTCAAAGGAATTGACGGGGACCCGCACAAGCGGTGGAGCATGTGGTTTAATTCGACGCAACGCGAGGAACCTTACCAGCGTTTGACATCCTACGAACGGAGCAGAGATGCGCCGGTGCCCTTTCGGGGGAACGTAGTGACAGGTGGTGCATGGCTGTCGTCAGCTCGTGTCGTGAGATGTTGGGTTAAGTCCCGCAACGAGCGCAA	281	*Fusobacterium necrophorum*	100
Streptococcus suis APHA 25	GTTGGGTCCTTTCCGGGACTCAGTGCCGCAGCTAACGCATTAAGCACTCCGCCTGGGGAGTACGGCCGCAAGGCTGAAACTCAAAGGAATTGACGGGGGCCCGCACAAGCGGTGGAGCATGTGGTTTAATTCGAAGCAACGCGAAGAACCTTACCAGGTCTTGACATCCCAGTGACCGCCCTAGAGATAGGGTTTCTCTTCGGAGCACTGGTGACAGGTGGTGCATGGTTGTCGTCAGCTCGTGTCGTGAGATGTTGGGTTAAGTCCCGCAACGAGCGCAA	281	*Streptococcus suis*	100
Streptococcus pluranimalium APHA C06551	NA†	NA†	NA†	NA†

* Sequences shown are cleaned of primers and anomalies identified according to visualisation of chromatograms. † Read not clean, chromatogram messy, unable to use.

Sequencing the Mhae-SGR primer binding region of the *Mannheimia* spp. *sodA* gene

Table B.5: DNA sequences relating to the reverse primer binding region of Mhae-SGR within the *Mannheimia sodA* gene

Strain	Sequence*
M. haemolytica 33396	CAGGCGTTTCAGGCTATCCGATTTTAGTCTT
M. haemolytica V1-53-2	CAGGCGTTTCAGGCTATCCGATTTTAGTCTT
M. haemolytica V1-71-1	CAGGCGTTTCAGGCTATCCGATTTTAGTCTT
M. haemolytica V1-37-1	CAGGCGTTTCAGGCTATCCGATTTTAGTCTT
M. varigena APHA	CAGGCTACCCAATTTTAGGTTTAGACGTGTG
M. granulomatis CCUG 45422 T	CAGGCTACCCAATTTTAGGTTTAGATGTTTG
M. ruminalis CCUG 38470 T	CAGGCTATCCGATTTTAGGCTTAGACGTTTG
M. glucosida CCUG 38457 T	CAGGCTACCCAATTTTAGGCTTAGACGTTTG
M. glucosida CCUG 38459	CAGGCTACCCAATTTTAGGCTTAGATTGGGA
M. glucosida CCUG 38460	CAGGCTACCCGATTTTAGGCTTAGACGTTTG
M. glucosida CCUG 38467	CAGGCTATCCGATTTTAGGCTTAGACGTTTG

*Sequences highlighted in yellow relate to the reverse compliment of the Mhae-SGR primer described by Guenther et al. [151] located within the *Mannheimia sodA* gene. Nucleotides highlighted in green correspond to differences between the *M. haemolytica* type strain (33396) and other species of *Mannheimia* assessed.

Growth curves and best fit logistic curves for bacterial species in liquid culture

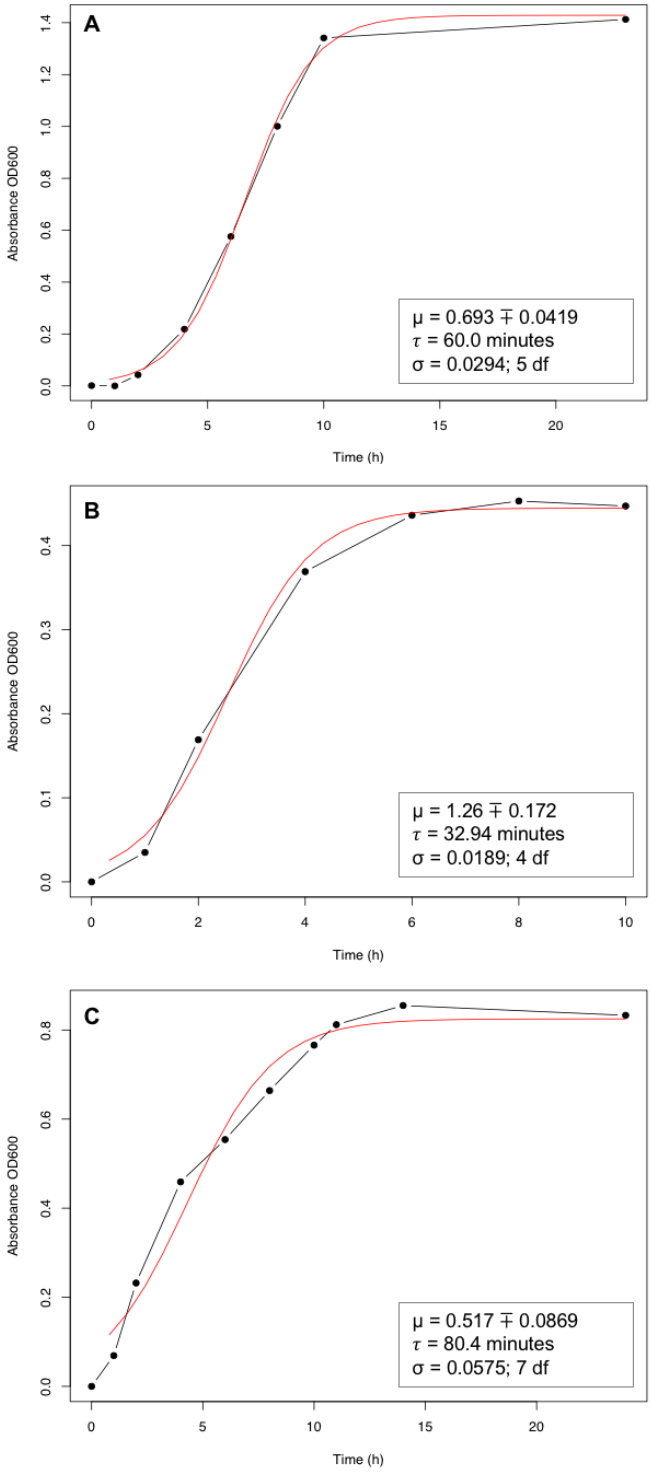

Figure B.1: Growth curves in liquid culture for (A) *H. somni,* (B) *M. haemolytica* and (C) *P. multocida*. Observed points are shown as black circles. The best fit logistic curve for each species is shown in red. Estimated growth rates (μ) ∓ standard error, generation times (τ), goodness of fit (σ) and degrees of freedom (df) are given for each species. Two points were removed during model fitting for *M. haemolytica* at 14 and 24 hours in late stationary phase, points not shown.

Inter- and intra-assay reproducibility: qPCR development

For the three qPCR assays detecting *H. somni*, *M. haemolytica* and *P. multocida* the inter and intra-assay variability was calculated. Data are available at the University of Bristol data repository, data.bris, at https://doi.org/10.5523/bris.nyqkgnysra9q2ic5dok0swnbg.

Table B.6: Within- and between-assay variance: PCR standard curves.

Species	Dilution	%CV (w)*	%CV (b)†
P. multocida	1	3.78	0.00
	2	2.53	0.00
	3	2.23	1.63
	4	1.23	1.40
	5	1.34	0.00
	6	1.67	1.26
M. haemolytica	1	1.39	0.95
	2	0.82	1.62
	3	0.51	1.61
	4	0.82	1.24
	5	0.00	0.00
	6	1.57	2.58
H. somni	1	1.81	1.86
	2	2.46	1.01
	3	0.48	2.33
	4	1.49	0.59
	5	1.00	0.88
	6	1.07	0.00
	7	1.75	0.23

* Within-assay variance: coefficient of variation between C_q values of 5 technical replicates at each dilution on the same day of testing. † Between-assay variance: coefficient of variation between C_q values of biological replicates performed on different days (duplicate for *H. somni*, triplicate for *P. multocida* and *M. haemolytica*)

Sequencing PCR products from *H. somni*, *M. haemolytica* and *P. multocida* PCR assays

Table B.7: 16S rRNA sequencing of PCR products from *H. somni*, *M. haemolytica* and *P. multocida* PCR assays

Sample ID	Sequence*	Sequence length	BLAST identity	Identity (%)
P. multocida ATCC® 43137 10^{-1} dilution†	TGGCTTGGCTGAGTTCGCTCGTAGAACAGCATGTGAACTATGTAAAACAGCTGAAGAG CGCCA	63	*P. multocida*	100
P. multocida ATCC® 43137 10^{-2} dilution†	TGAGTTCGCTCGTAGAACAGCATGTGAACTATGTAAAACAGCTGAAGAGCGCCA	54	*P. multocida*	100
H. somni ATCC® 43625 10^{-1} dilution†	GGATTAACGATATAAGAAGAGCACCGGCTAACTCCGTGCCAGCAGCCGCGGTAATACG GAGGGTGCGAGCGTTAATCGGAATGACTGGGCGTAAAGGGCACGCAGGTGGTGACTTA AGTGAGGTGTGAATATCTATAGTGACG	143	*H. somni*	96
H. somni ATCC® 43625 10^{-2} dilution†	GGACGTCGACGCCAGTCTTCCGATTAACGCTCGCACCCTCCGTATTACCGCGGCTGCTG GCACGGAGTTAGCCGGTGCTTCTTCTGTGATTATCGTCAATCAATTAATCTCTTAAACTA ATCGCCTTCCTTGATTAGGCCCAGAACGTACCAACCGACCCGCCTTCATACGCGGAGGA GAAAAATAAGGGCTTTCCCGCACTCTTTTAGTTTAAACGAGAAA	222	*H. somni*	98
H. somni ATCC® 43625 10^{-2} dilution‡	TATGCATAGATTTACTTACGTGAGGTGCAGAGGCTAACTCCGTGCCAGCAGCCGCGGTA ATACGGAGGGTGCGAGCGTTAATCGGAATGACTGGGCGTAAAGGGCACGCAGGTGGTG ACTTAAGTGAGGTGTGAATGAAA	140	*H. somni*	100
H. somni ATCC® 43625 10^{-4} dilution‡	GACCGGACTACGCAGTCGCCCTGATACACAGCTCGCACCCTCCGTATTACCGCGGCTGC TGGCACGGAGTTAGCCGGTGCTTCTTCTGTGATTATCGTCAATCAATTAATCTCTTAAAC TAATCGCCTTCCTTGATTCCAACCAT	145	*H. somni*	100
M. haemolytica ATCC® 33396 10^{-1} dilution†	GCTGGACGTCTAGTATTAGAGAGGGTAATTAGCCGTTGTTTCAACCGCTAACCAGGACA ACCCACTAATGGGTAAAGAAGTGGCAGGCGTTTCAGGCTATCCGATTTTAGTCAAGTCC AGCGAAAGCAATCCTATTCTTATCATACTATCCGATTTTACTCTTGGACCCAGCCAGGG GTTCACGCCAAAAC	191	*M. haemolytica*	98

Table B.7 continued

Sample ID	Sequence*	Sequence length	BLAST identity	Identity (%)
H. somni, UoB, V1-48§	ACGTGACTAACTCCGTGCCAGCAGCCGCGGTAATACGGAGGGTGCGAGCGTTAATCGGAATGACTGGGCGTAAAGGGCACGCAGGTGGTGACTTAAGTGAGGTGTGAATAAA	112	*H. somni*	100
H. somni, UoB, V1-42§	ACGGAGGGTGCGAGCGTTAATCGGAATGACTGGGCGTAAAGGGCACGCAGGTGGTGACTTAAGTGAGGTGTGAAGACTTATTG	83	*H. somni*	100
H. somni, UoB, V1-45§	CTTGCTACTCCGTGCCAGCAGCCGCGGTAATACGGAGGGTGCGAGCGTTAATCGGAATGACTGGGCGTAAAGGGCACGCAGGTGGTGACTTAAGTGAGGTGTGAACACCTTGTC	114	*H. somni*	98
H. somni, UoB, V1-50§	CGCTCGCACCCTCCGTATTACCGCGGCTGCTGGCACGGAGTTAGCCGGTGCTTCTTCTGTGATTATCGTCAATCAATTAATCTCTTAAACTAATCGCCTTCCTGATCG	108	*H. somni*	99
H. somni, UoB, V1-9§	GTTTCTTCTGTGATTATCGTCAATCAATTAATCTCTTAAACTAATCGCCTTCCTCGTA	58	*H. somni*	100
H. somni ATCC® 43625 10^{-2} dilution‡	GCTACGCACCCTCCGTATTACCGCGGCTGCTGGCACGGAGTTAGCCGGTGCTTCTTCTGTGATTATCGTCAATCAATTAATCTCTTAAACTAATCGCCTTCCTGATT	107	*H. somni*	98
H. somni ATCC® 43625 10^{-3} dilution‡	AGCTCGCACCCTCCGTATTACCGCGGCTGCTGGCACGGAGTTAGCCGGTGCTTCTTCTGTGATTATCGTCAATCAATTAATCTCTTAAACTAATCGCCTTCCTCGAC	107	*H. somni*	100
H. somni ATCC® 43625 10^{-4} dilution‡	ATTGCGCTCGCACCCTCCGTATTACCGCGGCTGCTGGCACGGAGTTAGCCGGTGCTTCTTCTGTGATTATCGTCAATCAATTAATCTCTTAAACTAATCGCCTTCCTCGAT	111	*H. somni*	100

***** Sequences shown are cleaned of anomalies identified according to visualisation of chromatograms

† Reference strain dilution of qPCR standard curve

‡ Reference strain dilution of overnight culture used to generate qPCR positive controls

§ Bovine nasal swabs collected from healthy calves on the North Wyke Farm Platform and determined *H. somni* positive by the qPCR assays described in this chapter

Appendix C

Effect of pen and barn on bacterial carriage rates

Differences in the carriage of *Histophilus somni* and *Pasteurella multocida* between animals in pens within two barns was investigated prior to combination of animals into one cohort (n = 60) for survival analyses. For both bacterial species, datasets were constructed by counting the number of calves positive and negative for carriage (response) for each pen within each barn. General linear models with a Poisson error distribution and log-link function were fitted using the base 'glm' function of R version 3.5.0.

A sequence of nested multi-level models were built from the baseline model (M0); response of carriage plus main effect of barn and nested effect of pen within barn. Two additional models were considered: M1 = baseline (M0) plus the effect of barn on carriage; and M2 = model M1, plus the effect of pen nested within barn on carriage. The impact of additional terms included in a more complex model was assessed by comparing the change in residual deviance from a nested, simpler model with the upper-tailed critical value ($p < 0.05$) of the appropriate chi-squared distribution (as identified by the change in the residual degrees of freedom between the models).

There was no evidence for differences in carriage rates between barns for *P. multocida* on any sampling occasion (Day 0, p = 0.549; Day 33, p = 0.487; Day 47, p = 0.824; Day 62, p = 0.0617; Day 75, p = 0.174). No evidence for barn differences were found for *H. somni* on Day 0 (p = 0.0693) or day 47 (p = 0.0979), but evidence was found on Day 33 (p = 0.001), Day 62 (p < 0.001) and Day 75 (p < 0.001). Differences in carriage rates between pens were found on two occasions only: *H. somni* on Day 47 (p = 0.0178) and *P. multocida* on Day 62 (p = 0.0199).

Interval-censored survival analysis

Rules to define carriage episodes

Interval-censored survival analysis was used to estimate the rate ('hazard') of clearance of bacterial carriage and the median duration of carriage. Models were fitted in R (version 3.5.0) using the package icenReg [240].

The following definitions, rules and assumptions were applied:

I) Carriage episode: a period where a calf is positive for *H. somni* or *P. multocida*. A period may span multiple visits/observations if carriage is detected consecutively without interruption. If carriage is interrupted, i.e. lost and then re-acquired, the period following re-acquisition of carriage constitutes a new carriage episode.

II) The covariates, sex and density when first positive, were assumed to be time-invariant.

III) The maximum possible duration of carriage was from the first carriage-positive visit to the day before the first following carriage-free visit.

IV) The minimum possible duration of carriage was set from the first to the last positive visit in the series, assuming carriage was uninterrupted between visits.

V) If the episode was interrupted by one or more missed visit's then the minimum duration was up to the last positive visit *before* the first missed one.

VI) If the last positive visit was the calves last visit in the study, then the duration was right-censored at 365 days (otherwise it would have been infinite).

Follow-up was interrupted by one missed visit for one calf (ID 23, Day 47). This missed visit interrupted a carriage-free episode and therefore it was not necessary to define a carry-free interval. Recurrent-episodes of carriage and non-carriage were distinguished for each calf when observed, for example episode 1, 2 and 3. No more than 3 episodes could be experienced by one calf. Carriage rates for *M. haemolytica* were too low to model.

Dataset construction

Datasets were constructed prior to analysis in R. Briefly, minimum and maximum carriage intervals were defined for each possible carriage permutation using the rules outlined above and inputted into a VLOOKUP table in Microsoft® Excel. There were 32 different carriage scenarios possible.

Carriage or no carriage for each animal at each visit was coded as either 1 or 0 respectively. This resulted in each animal having a five-digit binary number representing their carriage on each visit of the study. Similarly, all possible carriage permutations (n = 32) were coded as a five-digit binary number, with each binary number corresponding to its decimal number (from 0 to 31); creating a code. This decimal code was inputted into the same VLOOKUP table and corresponded to a defined carriage interval, allowing future lookup of any given carriage permutation from an animal.

Support for underlying exponential distribution

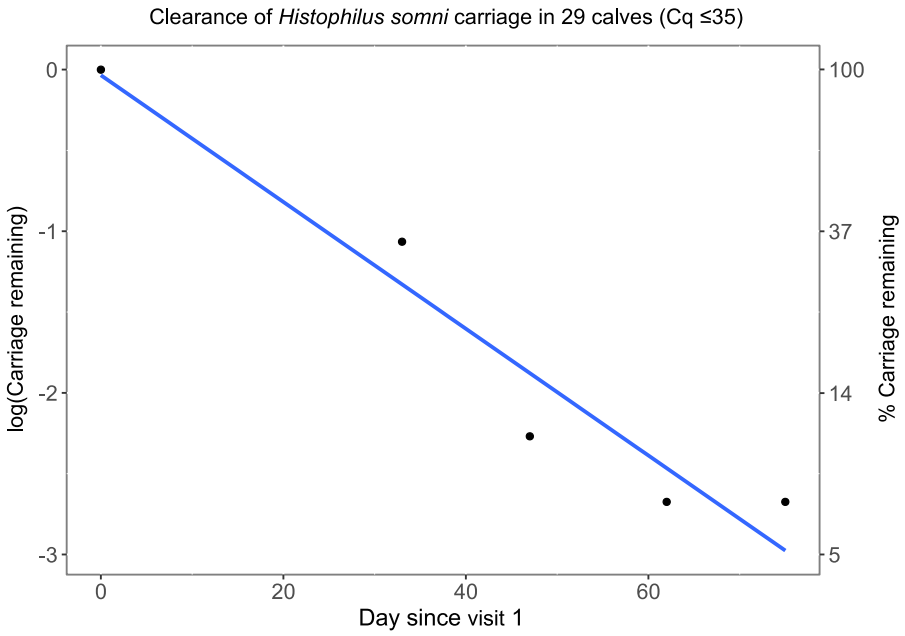

Figure C.1: Clearance of *Histophilus somni* carriage in the nasal passages of 29 calves completing 5 visits, carriage determined by qPCR on collected short nasal swabs (Cq ≤ 35). Nasal swabs collected at days 0, 33, 47, 62 and 75 (Day 0 = visit 1). The natural logarithm of the proportion of calves remaining positive at each visit was plotted and checked for linearity (Adjusted $R^2 = 0.913$).

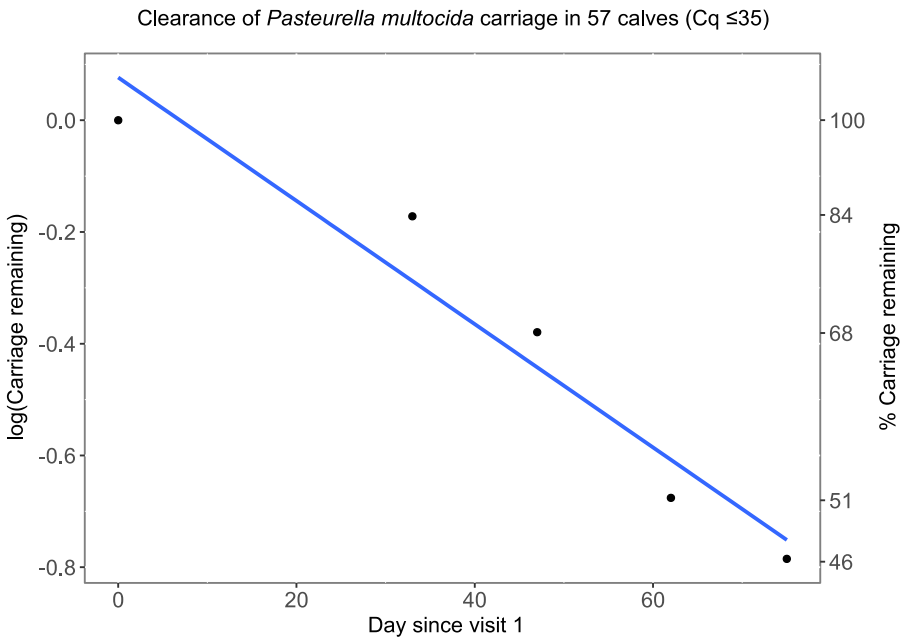

Figure C.2: Clearance of *Pasteurella multocida* carriage in the nasal passages of 29 calves completing 5 visits, carriage determined by qPCR on collected short nasal swabs (Cq ≤ 35). Nasal swabs collected at days 0, 33, 47, 62 and 75 (Day 0 = visit 1). The natural logarithm of the proportion of calves remaining positive at each visit was plotted and checked for linearity (Adjusted $R^2 = 0.912$).

Assessment of pasture and silage quality: 2015 born cohort

To investigate the similarity of feed type between the three barns (farmlets) forage quality assessments for each farmlet were compared. Although the study in this chapter reports bacterial carriage for animals housed in the Green and Red barn, the Blue is presented for completeness. The metabolisable energy (ME) and crude protein (CP) of pasture and silage samples collected in 2015–2016 for each farmlet is shown in Table . ME and CP were similar between farmlets for both forage types with small numerical differences observed. ME was higher in pasture (12.1–12.2) compared to silage (10.1–10.3). Similarly, CP was higher in pasture (17.4–20.7) compared to silage (8.7–12.8) and was observed over a greater range compared to ME.

Table C.1: Mean metabolisable energy and crude protein of pasture and silage samples collected between April 2015 to March 2016 on the North Wyke Farm Platform

Sample type	Variable	Farmlet	N	Mean	Standard deviation
Pasture	**ME**	Blue	33	12.2	0.69
		Green	42	12.2	0.49
		Red	33	12.1	0.57
	CP	Blue	33	20.1	3.13
		Green	42	20.7	1.25
		Red	33	17.4	1.73
Silage	**ME**	Blue	29	10.1	0.20
		Green	29	10.3	0.27
		Red	29	10.1	0.31
	CP	Blue	29	8.7	0.58
		Green	29	12.8	0.70
		Red	29	12.4	0.55

ME was similar between farmlets for pasture samples ($p = 0.444$; Figure C.3 panel a and b), but it did differ significantly for silage ($p = 0.008$): ME of silage was significantly higher in the Green farmlet compared to the Blue ($p = 0.018$) and Red ($p = 0.042$) (Figure C.4, panel a). CP was significantly lower ($p < 0.001$) in the Red compared to Blue ($p = 0.003$) and Green ($p < 0.001$) farmlet pasture samples (Figure C.3, panel c); temporal trends were similar up August 2015, thereafter greater differences between farmlets were observed (Figure C.3, panel d). Conversely, for silage, CP was consistently lower in the Blue farmlet (Figure C.4, panel c and d) and differed significantly from both Green and Red farmlets ($p < 0.001$).

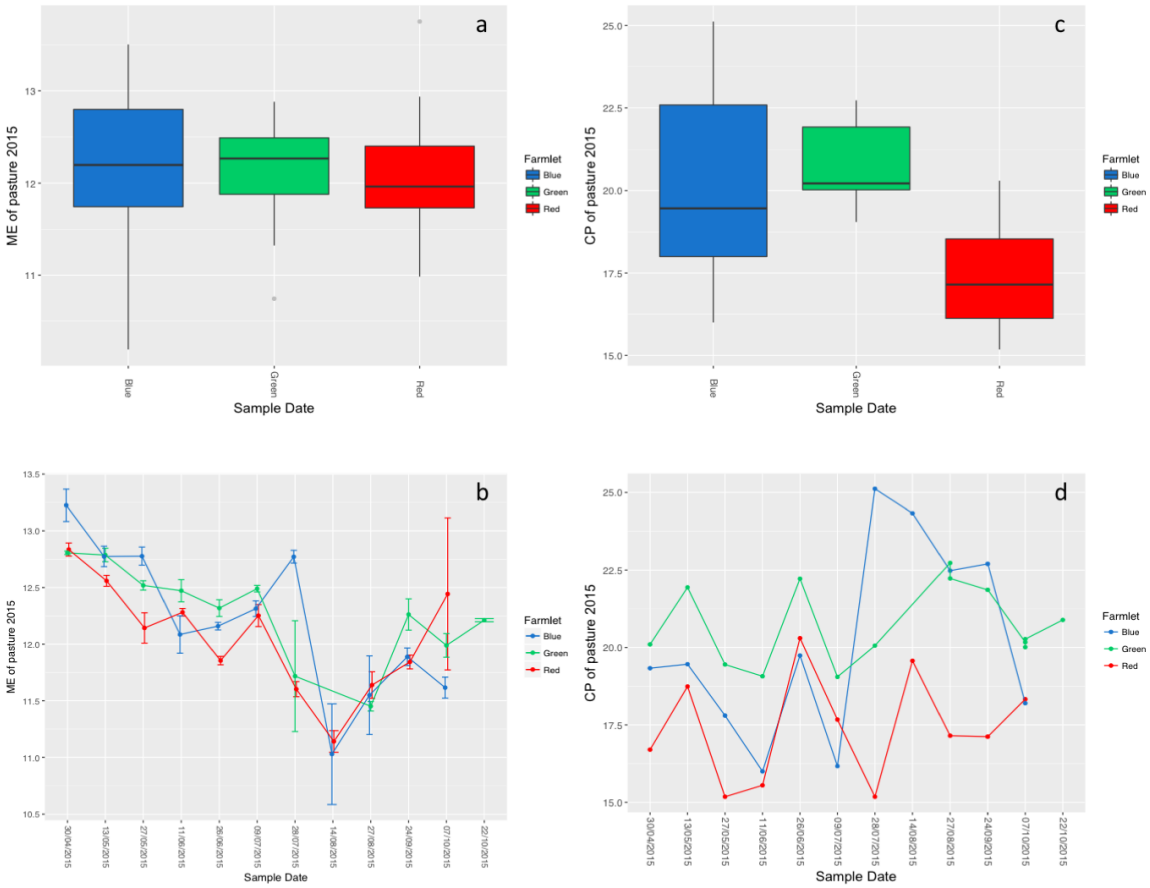

Figure C.3: Analysis of pasture samples collected between April 2015 to October 2015 for Blue, Green and Red farmlets. Metabolisable energy shown in panels a and b; crude protein is shown in panels c and d. Outlier samples are shown by grey dots (panel a). Error bars represent standard error of the mean.

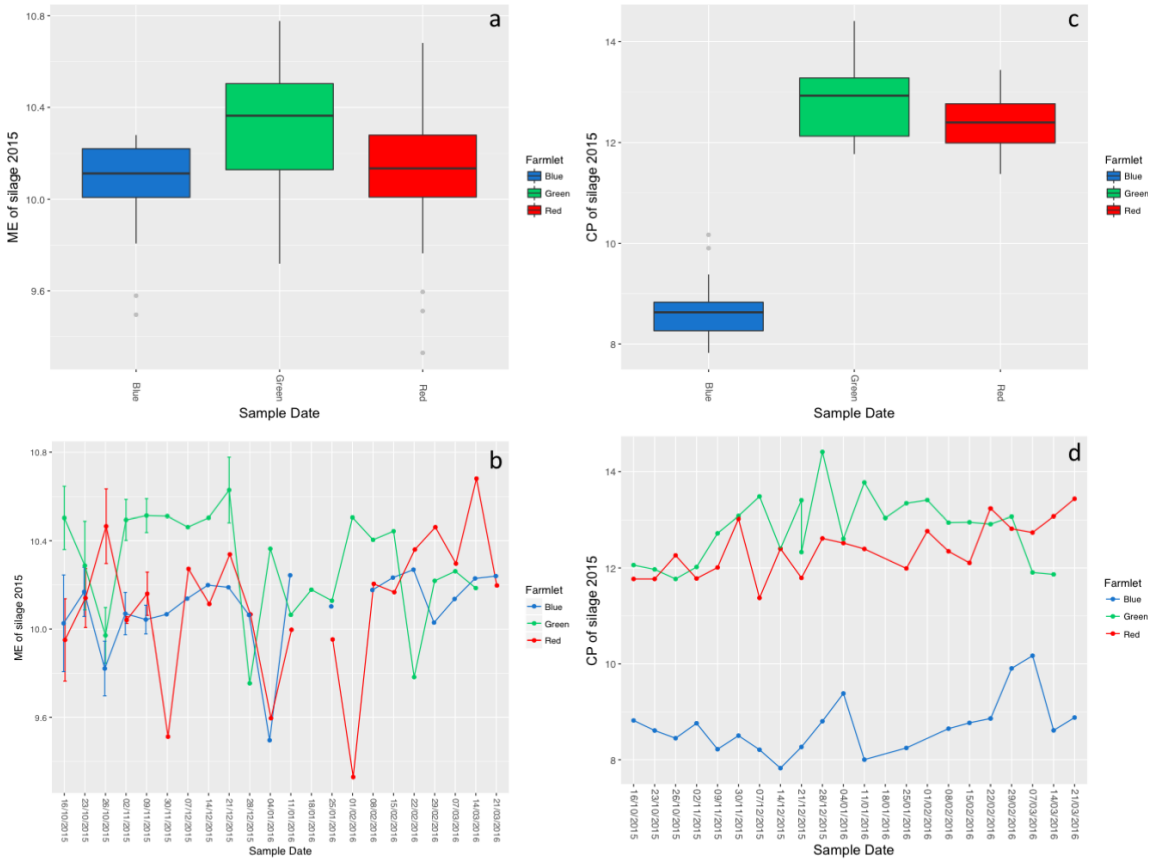

Figure C.4: Analysis of silage samplescollected between October 2015 to March 2016 for Blue, Green and Red farmlets. Metabolisable energy is shown in panels a and b; crude protein is shown in panels c and d. Outlier samples are shown by grey dots (panel a and c). Error bars represent standard error of the mean.

Carriage rates of *Histophilus somni*, *Mannheimia haemolytica* and *Pasteurella multocida*

Table C.2: *Histophilus somni*, *Mannheimia haemolytica* and *Pasteurella multocida* nasal carriage rates determined by qPCR

	***Histophilus somni* carriage**		***Mannheimia haemolytica* carriage**		***Pasteurella multocida* carriage**	
Day	**n/N**	**$CI_{95\%}$***	**n/N**	**$CI_{95\%}$***	**n/N**	**$CI_{95\%}$***
0	29/60	0.354 – 0.615	8/60	0.063 – 0.251	57/60	0.852 – 0.987
33	22/60	0.249 – 0.502	6/60	0.041 – 0.212	50/60	0.710 – 0.913
47	13/59	0.127 – 0.351	2/59	0.006 – 0.127	44/59	0.613 – 0.846
62	8/60	0.063 – 0.251	0/60	0.000 – 0.075	37/60	0.482 – 0.736
75	8/60	0.063 – 0.251	1/60	0.001 – 0.101	39/60	0.515 – 0.766

* Confidence intervals for single proportions calculated using the Wilson score

Co-carriage rates of *Pasteurellaceae*

Table C.3: Co-carriage of *Pasteurellaceae* in the nasal passages of healthy calves determined by qPCR

	***H. somni* and *P. multocida* carriage**		***M. haemolytica* and *P. multocida* carriage**		***M. haemolytica* and *H. somni* carriage**		***H. somni, M. haemolytica* and *P. multocida* carriage**	
Day	**n/N**	**$CI_{95\%}$***	**n/N**	**$CI_{95\%}$***	**n/N**	**$CI_{95\%}$***	**n/N**	**$CI_{95\%}$***
0	28/60	0.339–0.599	8/60	0.0634–0.251	3/60	0.0130–0.148	3/60	0.0130–0.148
33	20/60	0.220–0.468	6/60	0.0413–0.212	1/60	0.000871–0.101	1/60	0.000871–0.101
47	9/59	0.0763–0.275	2/59	0.00589–0.127	0/59	0–0.0762	0/59	0–0.0762
62	7/60	0.0521–0.232	0/60	0–0.0750	0/60	0–0.0750	0/60	0–0.0750
75	5/60	0.0311–0.191	1/60	0.000871–0.101	0/60	0–0.0750	0/60	0–0.0750

* Confidence intervals for single proportions calculated using the Wilson score

Appendix D

Covariate based constrained randomisation

Allocation of calves to three clusters (barns) involved balancing three categorical variables (breed, sex and sire) and three continuous covariates (age, weaning weight, average daily growth rate) across the three clusters. Given the 2016 calf crop characteristics, 7 groups of breed/sex/sire combinations were possible: -

1. 6 ST Steers - 2 to each farmlet
2. 7 LIMX Steers - 3 to one farmet, 2 to the other two
3. 5 LIMX Heifers - 1 to one farmlet (linked to 3 above), 2 to the other two
4. 28 CHX (Other) Heifers - (10, 9, 9) allocation to farmlets
5. 16 CHX (Other) Steers - (5, 6, 5) allocation to farmlets
6. 10 CHX (400250) Heifers - (3, 3, 4) allocation to farmlets
7. 15 CHX (400250) Steers - 5 to each farmlet

Log-linear models for vertical analysis of bacterial carriage

Construction and sequence of log-linear models

A sequence of nested models was built by adding explanatory variables to the baseline model until the saturated model, which included all explanatory variables and the interactions between them was reached. The baseline model consisted of the response (count of calves with bacterial carriage) plus the combinations of explanatory variables. To this baseline model, the explanatory variables of prior carriage at day of vaccination, treatment (vaccine/control), and farmlet nested within treatment were added. Dependence and independence between explanatory variables was assessed by inclusion of an interaction term, or lack of, respectively. The sequence of nested models and the comparisons between competing models is shown in Table D. D.1.

Log-linear model selection for evaluation of the association between carriage and explanatory variables

The effect of vaccination and prior carriage was estimated from either Model 1, 2 or 3 based on comparisons between nested models. The impact of additional terms between competing models was assessed by comparing the change in residual deviance with the

upper-tailed critical value ($p < 0.05$) of the appropriate chi-squared distribution (as identified by the change in the residual degrees of freedom between the models). If the impact of additional of terms was significant, then the coefficients relating to explanatory terms from the complex model were evaluated. If additional terms were not significant, the simpler, parsimonious model was evaluated i.e. Model 1 for prior carriage and Model 2 for treatment. To assess for differences in the level of carriage between clusters in the same intervention phase, Model 5 was compared to Model 2 (Table D.1) Model fit was assessed by comparing the fitted counts to observed counts and observing the residual deviance in relation to the residual degrees of freedom.

Table D.1: Sequence of log-linear models used for vertical analysis of bacterial carriage at each crossover point of the stepped wedge trial

Model	**Model structure**	**Description**	**Model Comparison**
M0	Count ~ R + P * (T1/T2)	Baseline: Defines overall structure of the data	
M1	M0 + R * P	Does carriage depend on prior carriage?	M1 vs M0
M2	M0 + R * T1	Does carriage depend on treatment?	M2 vs M0
M3	M0 + R * P + T1	Does carriage depend on prior carriage and vaccination, but independently?	M3 vs M1; M3 vs M2
M4	M0 + R * P * T1	Does carriage depend on prior carriage and vaccination, but dependently?	M4 vs M3
M5	M0 + R * (T1/T2)	Does carriage depend on variation between the two clusters in the same treatment phase?	M5 vs M2
M6	M0 + R * P + (T1/T2)	Does carriage depend on prior carriage and the additional, independent effect of variation between the two clusters in the same treatment phase?	M6 vs M5
M7	M0 + R * (P+T1/T2) + (P * T1)	Combines models 4 and 6 to provide the saturated model	M7 vs M4; M7 vs M6
M8	M0 + R * P * (T1/T2)	Saturated: describes perfectly any set of expected frequencies	M8 vs M7

Notation: -
R: response of carriage either 2- or 4-weeks post vaccination; P: prior carriage at day of vaccination; T1: treatment (vaccine/control); T2: cluster (blue/green/red)
+ denotes an additive effect
* denotes an interaction effect

Assessment of pasture and silage quality: 2016 born cohort

The metabolisable energy (ME) and crude protein (CP) of pasture and silage samples collected in 2016–2017 for each farmlet is shown in Table D.2. For both pasture and silage samples ME and crude protein CP values were similar between farmlets (Table D.2). Silage fed to animals housed during the stepped wedge study was divided based on its storage, either in a bale or clamp. ME was similar between bales and clamp storage; however, CP was higher in bales. ME was marginally higher in pasture compared to silage. Similarly, CP was higher in pasture compared to silage.

There was little evidence to suggest a difference between ME of farmlet pasture samples (Figure D.1a; $p = 0.060$). However, there was strong evidence to suggest that the CP of pasture was significantly different (Figure D.1c; $p = 0.00387$) between farmlets, with both Blue ($p = 0.0206$) and Green ($p = 0.0075$) significantly higher than Red; however, numerically differences were small (Table D.2). Greater temporal variation was seen for pasture ME compared to CP (Figure D1b and D.1d). Over the summer months CP increased and peaked in August (Figure D.1d). There was moderate evidence to suggest a difference in ME of bale silage samples (Figure D.2a, top panel; $p = 0.0430$) between farmlets, with Blue significantly higher than Green ($p = 0.0193$). There was strong evidence to suggest a difference in the ME of clamp silage samples (Figure D.2a, bottom panel, $p < 0.001$), with the mean ME of each farmlet significantly different from each other ($p < 0.001$). There was evidence to suggest a difference in CP of bale silage samples ($p = 0.0337$), with Blue higher than Green ($p = 0.0674$) and Red ($p = 0.218$). For clamp silage samples, there was strong evidence for a difference in CP between farmlets ($p < 0.001$), with the mean CP of each farmlet significantly different from each other ($p < 0.001$). Mean CP for the Blue and Red farmlets was higher in silage from bales compared to the clamp (Table D.2).

Table D.2: Mean metabolisable energy and crude protein of pasture and silage samples collected between May 2016 to April 2017 on the North Wyke Farm Platform

Farmlet	Sample	Variable *	Mean	Standard deviation	N
Blue	Pasture	ME	12	0.407	20
Green	Pasture	ME	11.8	0.243	20
Red	Pasture	ME	11.7	0.356	20
Blue	Pasture	CP	22.8	3.45	10
Green	Pasture	CP	23.1	3.17	10
Red	Pasture	CP	20.5	3.98	10
Blue	Silage (Bale)	ME	10.8	0.320	9
Green	Silage (Bale)	ME	10.6	0.320	14
Red	Silage (Bale)	ME	10.7	0.00952	7
Blue	Silage (Bale)	CP	17.6	3.8	9
Green	Silage (Bale)	CP	15.2	1.14	14
Red	Silage (Bale)	CP	14.4	0.567	7
Blue	Silage (Clamp)	ME	10.8	0.187	23
Green	Silage (Clamp)	ME	11.2	0.072	18
Red	Silage (Clamp)	ME	10.6	0.206	25
Blue	Silage (Clamp)	CP	11.1	1.27	23
Green	Silage (Clamp)	CP	15.82	0.383	18
Red	Silage (Clamp)	CP	12.9	0.548	25

* Metabolisable energy (MJ/kg DM); † Crude protein (g/kg DM)

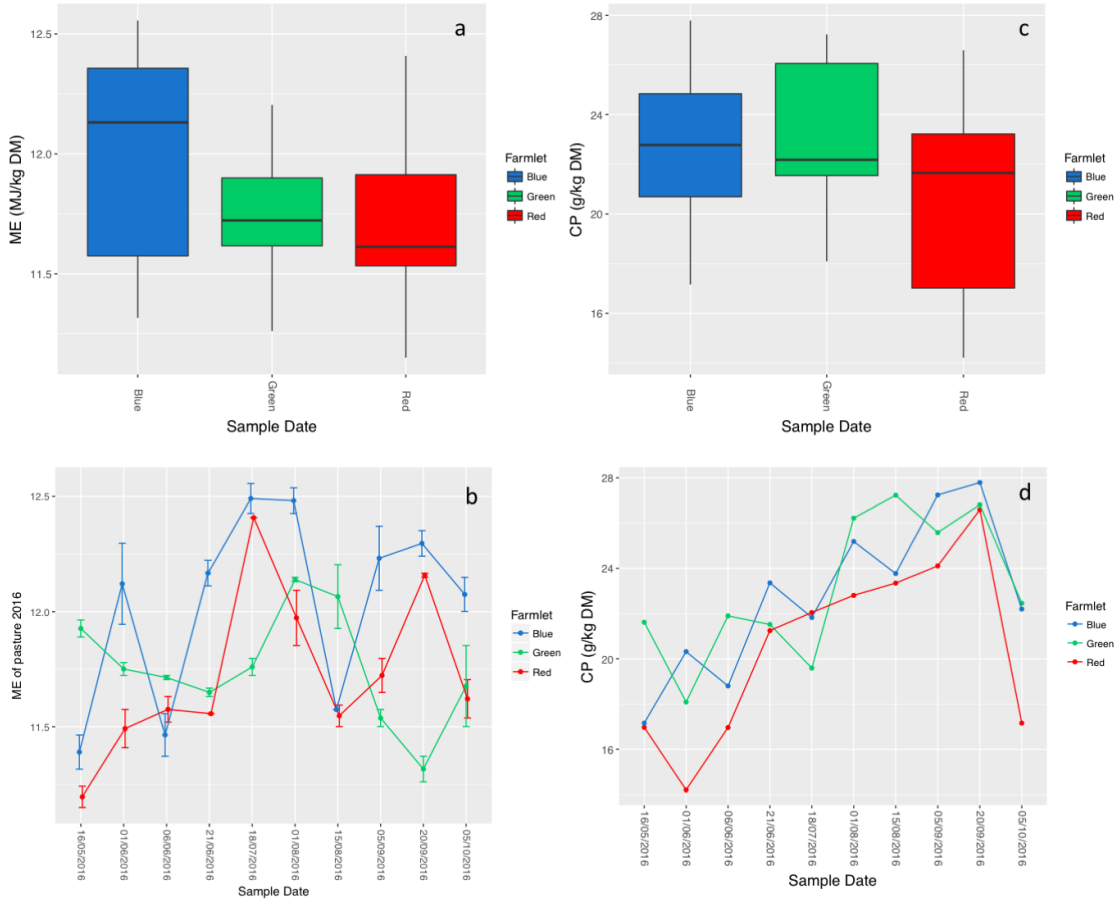

Figure D.1: Analysis of pasture samples collected between May to October 2016 for Blue, Green and Red farmlets. Metabolisable energy is shown in panels a and b; crude protein is shown in panels c and d. Error bars represent standard error of the mean between two technical replicates.

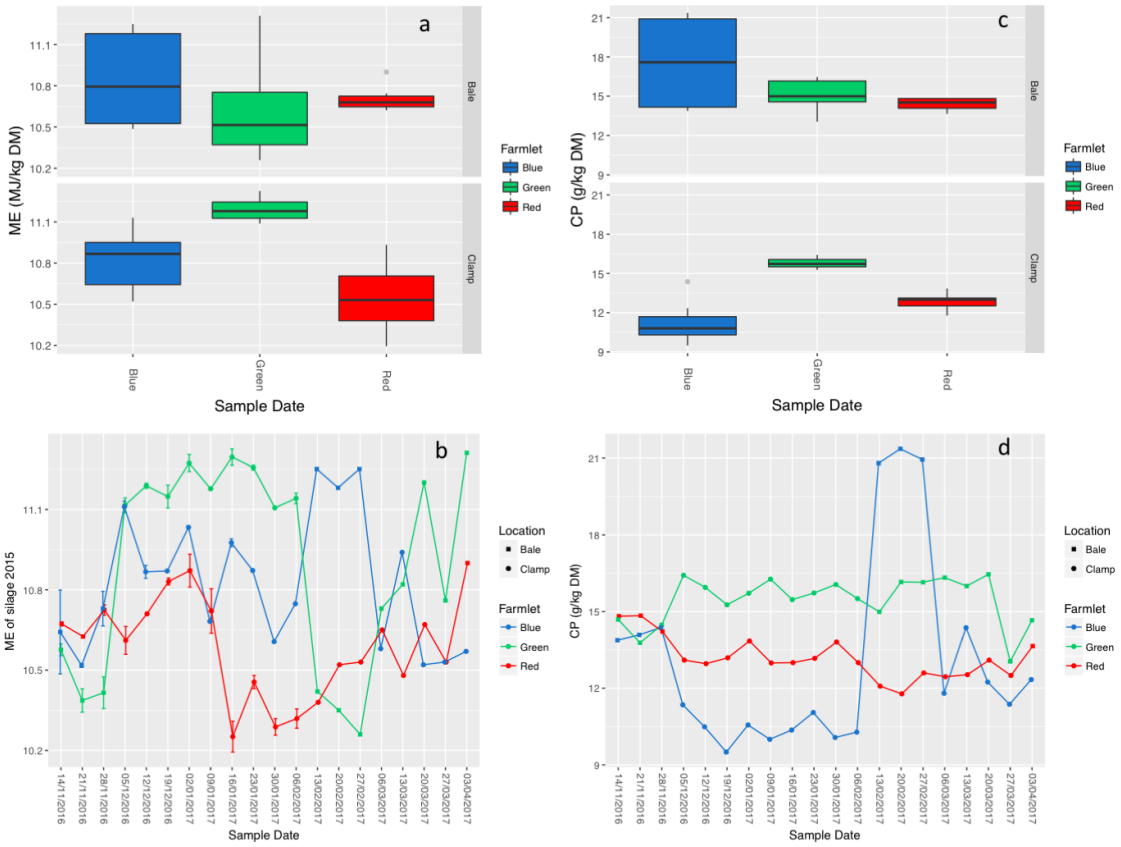

Figure D.2: Analysis of silage samples collected between September 2016 to April 2017 for Blue, Green and Red farmlets. Metabolisable energy is shown in panels a and b; crude protein is shown in panels c d. Outlier samples are shown by grey dots (panel a and c). Error bars represent standard error of the mean between two technical replicates. Silage was held either in a bale or clamp as indicated.

Appendix E

List of publications and presentations

Publications

Thomas A.C., Bailey M., Lee M.R.F., Mead A., Morales-Aza B., Reynolds R., Vipond B., Finn A., Eisler M.C., Insights into *Pasteurellaceae* carriage dynamics in the nasal passages of healthy beef calves., Sci Rep., 2019;9(1):11943.

Conferences

Thomas A.C., Lee M.R., Bailey M., Finn A., Eisler M.C., (2017, August). Characterisation and development of the bovine respiratory microbiome. European Federation of Animal Science (EAAP) 68th Annual Meeting, Tallinn, Estonia. Oral presentation.

Thomas A.C., Bailey M., Lee M.R., Finn A., Eisler M.C., (2017, October). Bacterial colonisation dynamics and development of the bovine respiratory microbiome. British Cattle Veterinary Association, Southport, UK. Poster.

Thomas A.C., Bailey M., Finn A., Fleming H.R., Lee M.R., Mead A., Morales-Aza B. Vipond B., Eisler M.C., (2018, January). Attenuated vaccines as model respiratory viral infection systems: from human to bovine. Veterinary Vaccinology Conference, Stirling, UK. Oral presentation.

Mead A., Thomas A C., Evans J., Griffiths B., Eisler MC,. (2018, July). An application of covariate-based constrained randomisation in livestock research., 29th International Biometric Conference, Barcelona, Spain. Poster.